Inhibition of Group I Metabotropic Glutamate Receptors (mGluR1 and mGluR5) Protects Against Prion-Induced Toxicity

Dissertation*

zur

Erlangung der naturwissenschaftlichen Doktorwürde

(Dr. sc. nat.)

vorgelegt der

Mathematisch-naturwissenschaftlichen Fakultät

der

Universität Zürich

von

Despoina Goniotaki

aus

Griechenland

Promotionskomitee

Prof. Dr. Adriano Aguzzi (Vorsitz und Leitung der Dissertation)

Prof. Dr. Lukas Sommer

Prof. Dr. Frijhof Helmchen

Prof. Dr. Charles Weissmann

Dr. Silvia Sorce

Zürich, October 2016

ABSTRACT

Prion infections cause inexorable, progressive neurological dysfunction and neurodegeneration. Expression of the cellular prion protein PrP^C is required for toxicity, suggesting the existence of deleterious PrP^C-dependent signaling cascades. Because Group-I metabotropic glutamate receptors (mGluR1 and mGluR5) can form complexes with the cellular prion protein (PrP^C), we investigated the impact of mGluR1 and mGluR5 inhibition on prion toxicity *ex vivo* and *in vivo*. We found that pharmacological inhibition of mGluR1 and mGluR5 antagonized dose-dependently the neurotoxicity triggered by prion infection and by exposure to prion-mimetic anti-PrP^C antibodies in organotypic brain slices. Prion-mimetic antibodies increased mGluR5 cell surface expression and clustering around dendritic spines mimicking a mechanism of toxicity documented for Aβ oligomers, whereas prion-protective antibodies prevented mGluR5 clustering. Oral treatment with the mGluR5 inhibitor, MPEP, delayed the onset of motor deficits and prolonged survival of prion-infected mice. Although Group-I mGluR inhibition was not curative, these results suggest that it may alleviate the neurological dysfunctions induced by prion diseases.

ABSTRAKT

Prionen-Infektionen verursachen unaufhaltsame, progressive neurologische Dysfunktionen und Neurodegeneration. Die Expression des zellulären Prionproteins PrP^C ist für die Toxizität unabdingbar, was auf schädliche PrP^C abhängige Signalwege hindeutet. Weil Gruppe-I metabotropen Glutamatrezeptoren (mGluR1 und mGluR5) Komplexen mit den zellulären Prionproteinen (PrP^C) bilden können, wurde der Einfluss von mGluR1 und mGluR5-Hemmung auf die Prion Toxizität ex vivo und in vivo untersucht. Gefunden wurde, dass, wenn mGluR1 und mGluR5 pharmakologisch und dosisabhängig gehemmt wurde, die Neurotoxizität, die durch Prionen-Infektion antagonisiert wurde. Des Weiteren werden wurde die Neurotoxizität von prionenmimetischen anti-PrP^C Antikörper in Hirnschnitten, ebenfalls antagonisiert. Der prionmimetische Antikörper erhöhte dabei die mGluR5 Zellober-flächenexpression sowie die Clusterbildung um die dendritischen Dornen. Dieser imitiert einen Mechanismus der Toxizität, der bereits für Aß-Oligomere bestätigt ist. Indes verhindert der prion-schützende Antikörper mGluR5 die Clusterbildung. Die orale Behandlung mit dem mGluR5-Inhibitor, MPEP, verzögert den Beginn der motorischen Defizite und verlängert das Überleben von

prioninfizierten Mäusen. Obwohl die Behandlung mit dem Gruppe-1 mGluR Hemmer nicht kurativ war, legen diese Ergebnisse nichtsdestotrotz nahe, dass diese Behandlung neurologische Funktionsstörungen von prionen-induzierten Erkrankungen lindern kann.

Preface

The following work was performed at the Institute of Neuropathology, University Hospital Zurich, Switzerland during the years 2011-2016, under the supervision of Prof. Dr. Adriano Aguzzi (Director of the Institute of Neuropathology, University Hospital Zurich, CH).

Declaration

The experimental work described in this thesis was performed by myself as part of the Molecular Life Sciences (MLS) PhD program in the laboratory headed by Prof. Adriano Aguzzi [*Institute of Neuropathology, University Hospital, Zurich, CH*]. This thesis has not been submitted in whole or in part for a degree or diploma or other qualification at any other University.

This thesis includes work done in collaboration with Dr. Silvia Sorce, Dr. Asvin Lakkaraju, Ms. Pamela Bakirci, Dr. Amulya Shrivastava, Dr. Fabrizio Gasparini, Dr. Ladan Egolf and Dr. Linda Madisen. Specifically, Dr. Silvia Sorce from the laboratory headed by Prof. Adriano Aguzzi [*Institute of Neuropathology, University Hospital, Zurich, CH*] assisted in the design of slice and *in vivo* mouse experiments, performed the RML6 and NBH inoculations and helped with data analysis. Dr. Asvin Lakkaraju from the laboratory headed by Prof. Adriano Aguzzi [*Institute of Neuropathology, University Hospital, Zurich, CH*] assisted in the design of biochemical experiments as well as in the data analysis. Ms. Pamela Bakirci from the laboratory headed by Prof. Adriano Aguzzi [*Institute of Neuropathology, University Hospital, Zurich, CH*] assisted in the design of the mGluR1 slice experiments and contributed to the Immunoprecipitation (IP) and Interaction domain mapping experiments. Dr. Shrivastava from the laboratory of Dr. Antoine Triller [*Institut de Biologie de l'ENS (IBENS) INSERM CNRS PSL Research University, Paris, France*] performed Photoactivated Localization Microscopy (PALM) in cultured neurons. Dr. Ladan Egolf from the laboratory headed by Prof. Fritjof Helmchen [*Brain Research Institute, University of Zurich, Switzerland*] and Dr. Linda Madisen from the laboratory headed by Dr. Hongkui Zeng [*Allen Institute for Brain Sciences, Seattle, WA, USA*] assisted in the RCaMP1.07 transgenic mouse breeding and the production of the ES cells with a targeted insertion of the TITL-RCaMP1.07 calcium indicator in the TIGRE locus respectively as part of the Synergia grant consortium. Last but not least, Dr. Fabrizio Gasparini and his team [Novartis Institutes for Biomedical Research] assisted in the design of the *in vivo* mouse experiments and performed the pharmacokinetic/pharmakodynamic measurements of the MPEP-treated brain and blood samples.

Special reference should be made to the contributions of the following colleagues from the laboratoty of Prof. Adriano Aguzzi [*Institute of Neuropathology, University Hospital, Zurich, CH*]:

Rita Moos, Petra Schwarz, Ahmet Valor, Irina Abakumova, Isaac Barwon and Delic Mirzet for technical help, M. Bieri, N. Wey and A. Wethmar for imaging and software development, Dr. Mario Nuvolone for assistance with the analysis of the SNP data, Dr. Assunta Senatore for discussion about the IP and the Cell Surface Biotinylation experiments and for sharing protocols. Also, services from the transgenic facility of the University of Zurich significantly assisted the completion of this thesis. More specifically Dr. Pawel Pelczar performed the revitalization of *Grm5*$^{+/-}$ embryos and Dr. Johannes vom Berg and Ms. Monika Tarnowska performed the blastocyst injections of the ES cell expressing RCaMP1.07.

……..
Despoina G. Goniotaki
PhD Candidate
Molecular Life Sciences (MLS) PhD program
University of Zurich

The following thesis was accepted by the Faculty of Science at the University of Zurich in the **Fall semester 2016.**

Doctoral committee:

Prof.Dr. Adriano Aguzzi (Leitung der Dissertation) ……..

Prof. Dr. Lukas Sommer (Vorsitz) ……..

Prof. Dr. Frijhof Helmchen ……..

Prof. Dr. Charles Weissmann ……..

Dr. Silvia Sorce ……..

SUMMARY

Prion infections cause fatal, progressive neurological dysfunction and neurodegeneration. Expression of the cellular prion protein PrP^C is required for toxicity, suggesting the existence of deleterious PrP^C-dependent signaling cascades. But how can PrP^C, an extracellular GPI-linked protein, initiate toxicity? Most likely this process requires interactions with transmembrane constituents, and indeed PrP^C was shown to interact with membrane proteins that initiate intracellular signaling cascades. Among these proteins are group I metabotropic glutamate receptors (mGluR1 and mGluR5).

We first attempted to characterize the interaction domain of PrP^C and group I metabotropic glutamate receptors on PrP^C by utilizing an array of amino-proximal deletion mutants of the cellular prion protein (PrP^C). The interaction domain for mGluR1 and mGluR5 on PrP^C seems to span amino acid residues 51 to 90 and 32 to 134, respectively. Control experiments in which we probed for selected group II and III mGluRs in PrP^C immunoprecipitates further confirm the specificity of the interaction. We next investigated the impact of mGluR1 and mGluR5 inhibition on prion toxicity *ex vivo* and *in vivo*. We found that pharmacological inhibition of mGluR1 and mGluR5, as well as mGluR5 genetic ablation, antagonized dose-dependently the neurotoxicity triggered by prion infection and by exposure to prion-mimetic anti-PrP^C antibodies in organotypic brain slices.

We further assessed the effect of toxic (POM1) versus protective (POM2) anti PrP^C antibodies on the cell surface expression of mGluR5 using biotinylation of organotypic slice cultures with a cell impermeable reagent. At 2hr, scPOM1 treatment induced an increase in surface mGluR5 as well as surface PrP^C, indicating fixation of the PrP^C and mGluR5 in stable, immobile complexes on the membrane. In contrast, blocking of scPOM1 with scPOM2 or parallel treatment with MPEP rescued the surface mGluR5s clustering.

In primary hippocampal cultures, treatment with prion-mimetic antibodies (POM1) induced PrP^C and mGluR5 redistribution in dendritic spines and accumulation in spine heads; mimicking a mechanism of toxicity documented for Aβ oligomers. The observed clustering of mGluR5s in dendritic spines was prevented by protective anti PrP^C antibodies (POM2). In contrast, the cluster size of NMDA and AMPA receptors was not modified by addition of anti-PrP antibodies. In prion-infected mice, oral treatment with the mGluR5 inhibitor MPEP delayed the onset of motor deficits, reduced the vacuole size and the extent of astrogliosis and prolonged survival. Although genetic ablation of mGluR5

rescued POM1- or RML6-induced neuronal death in organotypic brain slices, it did not exert a similar statistically significant disease modifying effect *in vivo*.

We conclude that formation of POM1/PrP^{Sc}-PrP^{C}-mGluR5 complexes on the neuronal membrane mobilizes mGluR5 to alter the normal neuronal activity; resulting in toxicity. Although Group-I mGluR inhibition was not curative, these results suggest that it may have the potential to alleviate – at least temporarily – the neurological dysfunctions induced by prion diseases.

Keywords: *group I metabotropic glutamate receptors (mGluRs), mGluR1, mGluR5, prion diseases, PrP^{C}, organotypic slice cultures, prion mouse models, prion mimetic antibodies (POMs), MPEP, Grm5ko, rotarod, mouse primary neurons.*

ACKNOWLEDGEMENTS

I would like to thank my supervisor Professor Adriano Aguzzi (Director of the Institute of Neuropathology, University Hospital Zurich, CH) for his scientific guidance during my PhD study, his advice and encouragement. I am also grateful to Dr. Silvia Sorce and Dr. Asvin Lakkaraju (Institute of Neuropathology, University Hospital Zurich, CH) who supervised my work, guided me in the last five years in the development of my thesis project and contributed to my scientific advancement. Their scientific guidance, support and patience were decisive for the project completion.

I am also grateful to my current and former colleagues (Tiziana Sonati, Sine Yaganoglu, Uli Herrmann, Paolo Dametto, Chandrasekar Vijay, Sergey Yakusev, Lau Agnes, Bakirci Pamela, Hermann Mario, Melanie Einsiedler) whose precious friendship, help, scientific advices and support made every day pleasant in the lab. I would also like to thank the slice culture team (Regina Reimann, Karl Frontzek, Assunta Senatore, Marie-Angela Wulf, Liu Yingjun, Katrin Frauenknecht) for their help and support. Special thanks to the current and former member of the lab technical team (Abakumova Irina, Cedric Doucerain, Ahmet Varol, Clemence Tournaire, Lisa Caflisch, Arroyo Karina, Rita Moos, Petra Schwarz, Takacs Livia, Marpakwar Rajlakshmi, Cinzia Tiber-Schmidt), the histology technical team (Svetlana Kayser, Marianne König, Fröhlich Cecile, Brigitte), the IT team (Monika Bieri, Norbert Wey and André Wethmar) and the animal technical team (Delic Mirzet, Sturzenegger Christine, Petra Schwarz, Laura Cervantes Jimenez and Isaac Barwon) for their constant assistance and support. A special thanks to the administration team (Meike Nau Lüber, Isabella Jianella and Jacqueline Wiedler) for their regular support and assistance. To all the other members of the lab (Claudia Scheckel, Assunta Senatore, Mario Nuvolone, Daniel Kischenbaum, Airich Kristina, Daniel Heinzer, Eckhardt Valeria, Emmenegger Marc, Epskamp Mirka, Hamid Ahmad Kamal, Keller Annika, Li Bei, Pease Daniel Patrick, Pfammatter Manuela, Henning Leske, Zarb Yvette, Orsolya Török, Valerio Berardi and Zhu Caihong) thank you for the help and discussions and for making the lab an enjoyable place to be.

Finally, I would like to thank Stiftung Neuropath for founding my research project.

At the end, a very special thanks to my family - words cannot express how grateful I am. Thank you for every sacrifice you have made on my behalf, for your love and for always being there for me. I could not have done this without your support.

Table of Contents

LIST OF TABLES

LIST OF FIGURES

ABBREVIATIONS

aa: aminoacid

a1: alpha-helix 1

a2: alpha-helix 2

a3: alpha-helix 3

Aβ: Amyloid β

AC: adenylate cyclase

a7nAChR: a7 nicotinic acetylcholine receptor

AD: Alzheimer's disease

AEQ: aequorin

AHPs: afterhyperpolarization potentials

ALS: amyotropic lateral sclerosis

AMPA: a-amino-3-hydroxy-5-methyl-4-isoxazolepropionic acid

AMPAR: AMPA receptor

ATD: amino-terminal domain

BSE: bovine spongiform encephalopathy

CaM: calmodulin

CamKIIα: calcium/calmodulin-dependent protein kinase type II alpha chain

cAMP: cyclic adenosine monophosphate

CC1: charged cluster 1

CC2: charged cluster 2

CDP: chronic demyelinating polyneuropathy

CGNs: cerebellar granular neurons

CJD: Creutzfeldt-Jakob's disease

CNS: Central Nervous System

COCS: Cerebellar organotypic cultures slices

CRD: cysteine-rich domain

CTD: carboxy-terminal domain

CWD: chronic wasting disease

DAG: 1,2-diacylglycerol

DHPG: (S)-3,5-Dihydroxyphenylglycine

DRM: detergent resistant membranes

EAA: excitatory amino acid

EAATs: excitatory amino acid transporters

ERs: estrogen receptors

ER: endoplasmic reticulum

ERK: extracellular regulated kinases

fCJD: familial CJD

FFI: fatal familial insomnia

FMRP: fragile-X mental retardation protein

FSE: feline spongiform encephalopathy

FXS: Fragile X syndrome

HR: hydrophobic core

GABA: gamma-aminobutyric acid

GDL: globular domain ligand

GDP: guanosine 5/- diphosphate

GFAP: glial fibrillary acidic protein

GTP: guanosine 5/-triphosphate

Glu: Glutamate

GluR: glutamate receptor

GPCRs: G-protein coupled receptors

GPI: glycosylphosphatidylinositol

GSS: Gerstmann-Straüssler-Scheinker

HD: heptahelical domain

HD: Huntington's disease

HOCS: Hippocampal organotypic cultures slices

HSPG: heparan-sulphate proteoglycan

iCJD: iatrogenic CJD

iGluR: ionotropic glutamate receptor

IP_3: inositol 1,4,5-trisphosphate

IP_3Rs: inositol triphosphate receptors

KAR: kainate receptor

KBPs: kainate binding proteins

LBD: ligand-binding domain

Ln γ1: laminin γ chain

LTD: long-term depression

LTP: long-term potentiation

MAPK: mitogen-activated protein kinases

MPEP: 2-Methyl-6-(phenylethynyl)pyridine

MPTP: 1-methyl-4-phenyl-1,2,3,6-tetrahydropyridine

MTEP: 3-((2-Methyl-4-thiazolyl)ethynyl)pyridine

mGluR: metabotropic glutamate receptor

NCAM: neural cell adhesion molecule

NMDA: *N*-methyl-D-aspartate

NMDARs: NMDA receptors

VGCCs: N-type voltage-gated Ca^{2+} channels

OGD: oxygen/glucose deprivation

OR: octapeptide repeat

ORF: open reading frame

PALM: Photoactivated Localization Microscopy

PCD: programmed cell death

PD: Parkinson's disease

PFA: paraformaldehyde

PI: phosphoinositide

PI3K: phosphatidylinositol-4,5-biphosphate 3-kinase

PIKE: PI3K enhancer

PK: proteinase K

PKA: protein kinase A

PKC: protein kinase C

PLC-β1: phospholipase C-β1

PLC1: 4,5-bisphosphate phosphodiesterase 1

PM: plasma membrane

PNS: peripheral nervous system

PrP^{C}: normal cellular prion protein

PrP^{Sc}: scrapie prion

PRNP: prion protein gene

PSDs: post-synaptic densities

PSD95: postsynaptic density protein 95

PVDF: Polyvinylidene difluoride

rPrP: recombinant prion protein

ROS: reactive oxygen species

sCJD: sporadic CJD

Scrg1: scrapie regulated gene 1

SERCA: sarco/endoplasmic reticulum calcium ATPase

SOD: superoxide dismutase

SP: signal peptide

Stip 1: stress-inducible protein 1

TMD: transmembrane domain

TME: transmissible mink encephalopathy

TSEs: transmissible spongiform encephalopathies

UPR: unfolded protein response

UV: ultraviolet

vCJD: variant CJD

VFT: venus fly trap domain

Vn: vitronectin

VTA: ventral tegmental area

XBP-1: X-box-binding protein-1

Chapter 1: INTRODUCTION

1.1 Common Features of Neurodegenerative Diseases

Neurodegenerative diseases are a phenotypically heterogenous group of diseases that have unique characteristics. Diseases including prion diseases, Alzheimer's disease (AD), Parkinson's disease (PD) and Huntington's disease (HD) target different subsets of neurons and thus exhibit a range of pathological and molecular features. For example, prion diseases can initially target neurons of various brain areas, cortex, cerebellum and/or thalamus (Farlow *et al.*, 1989; Reder *et al.*, 1995). The specific anatomical region of the brain that is targeted is dependent on several factors including the etiology and the prion strain. However, the exact mechanism for such variation remains unknown (Mallucci and Collinge, 2005). The latter accentuates the phenotypic and pathologic heterogeneity of these diseases. As a result, depending on the affected brain region, initial symptoms can vary from dementia, ataxia and psychological problems or insomnia. In turn, cholinergic neurons of the cerebral cortex and hippocampus are targeted in AD and lead to progressive dementia (Babic, 1999). Dopaminergic neurons of the substantia nigra are targeted in PD and cause aberrant function in movement (Sulzer and Surmeier, 2013), while GABAergic medium-sized spiny neurons of the striatum are targeted in HD which leads to the development of dementia, motor and psychiatric problems (Graveland *et al.*, 1985). Although these neurodegenerative diseases affect different regions of the brain, they are all caused by the misfolding of specific cellular proteins that results in the formation of intracellular and/or extracellular aggregates as disease progresses (**Figure 1.1**). Remarkably, the earliest pathological alteration observed in all of these diseases [reviewed in (Martin, 1999)] is disruption of synapses followed by spine loss and dendrite retraction. It can therefore be speculated that a similar molecular mechanism is responsible for driving neurodegeneration downstream of protein misfolding in all these diseases. Consequently, identifying cellular processes involved in neurodegeneration in one of these diseases may prove helpful for understanding degeneration in others.

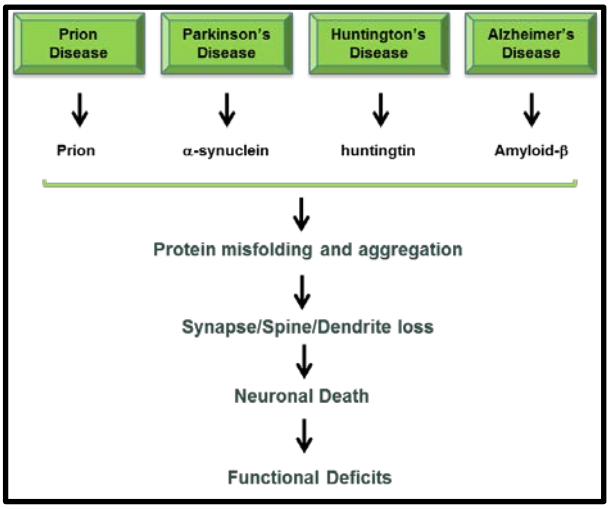

Figure 1.1. Common features of major neurodegenerative diseases. The degeneration process starts with the misfolding of the normal form of protein. Misfolded isoforms accumulate and aggregate intracellularly and/or extracellularly. As a consequence, neuronal death is observed, proceeded by synaptic dysfunction and dendritic loss.

The neuronal cell loss observed in neurodegenerative disorders is generally restricted to cell bodies and dendrites of glutamatergic neurons. For example, in AD, the highest damage is observed to neurons in layers III and IV of the neocortex. Damage is also observed to glutamatergically-innervated cortical and hippocampal neurons (Albin and Greenamyre, 1992). Axons, terminal buttons, glia, endothelial and ependymal cells are relatively spared (Choi, 1992). The observed pathological phenotypes are attributed to toxic glutamatergic signaling, due to continuous stimulation of the glutamate receptors. Detailed information about the different types of glutamate receptors, as well as their roles in physiology and pathology, will be presented in the following paragraphs.

1.2. Glutamate and Glutamate receptors

Glutamate (Glu) is the primary excitatory neurotransmitter in the central nervous system (CNS) participating in a wide range of neural functions such as learning and memory, long-term potentiation and synaptic plasticity (Fairman and Amara, 1999). The observation that increased amounts of Glu can trigger excitotoxicity and neuronal death established the research interest on the role of Glu in neurodegeneration. Extensive study of Glu signaling mechanisms has promoted the development of

treatments for Glu-related neurodegeneration.

Glutamate exerts its effects through the activation of several glutamate receptor (GluR) subtypes. GluRs are divided into two families: ionotropic (iGluR) and metabotropic (mGluR) depending on the mechanism of postsynaptic current generation (Conn and Pin, 1997; Julio-Pieper *et al.*, 2011; Traynelis *et al.*, 2010). The ionotropic receptor family comprises of *N*-methyl-D-aspartate (NMDA), a-amino-3-hydroxy-5-methyl-4-isoxazolepropionic acid (AMPA), and kainate receptor subtypes; so named by the pharmacological agonist that selectively binds to each subtype. Researchers have also identified another subgroup in vertebrates (the orphan delta receptors, δ_1 and δ_2) and another subfamily, the kainate binding proteins (KBPs), in non–mammalian vertebrates. Although each receptor subtype serves a distinct function, they all share a common voltage-gated ion channel function and serve as the main mediators of fast excitatory synaptic transmission (Mayer, 2006). The metabotropic glutamate receptor (mGluR) family on the other hand, comprises of three subfamilies: group I, group II and group III; subdivided based on sequence homology, pharmacology and second messenger association. They are all G-protein coupled receptors (GPCRs) consisting of a seven transmembrane domain structure. Upon Glu binding, they initiate signaling cascades, modulate or fine tune synaptic activity (Conn and Pin, 1997). Advancing our understanding of the specific roles of iGluRs and mGluRs could significantly benefit the development of novel treatment strategies for a variety of neurologic disorders.

1.2.1. Ionotropic Glutamate Receptors (iGluRs)

The glutamate-receptor ion channels (iGluRs), namely NMDA, AMPA and kainate, are typically classified by the synthetic agonists that mimic the effects of L-Glu and are the primary mediators of excitatory synaptic transmission in the CNS (Collingridge and Lester, 1989).

IGluRs are integral membrane proteins consisting of four large subunits (> 900 residues), which form the central ion channel pore. Each of the four subunits that form the channel shares a common structure of four well-conserved domains: a. the extracellular amino-terminal domain (ATD), b. the ligand-binding domain (LBD), c. the transmembrane domain (TMD) and d. the intracellular carboxy-terminal domain (CTD). The CTM region is unique to iGluRs and is involved, via protein interactions, in synaptic anchoring, trafficking and receptor-mediated signaling (Chen *et al.*, 1999).

Upon Glu or agonist binding to the LBD a conformation shift occurs which changes the angle of the TMD regions. The latter induces opening of a pore in the membrane where influx of sodium, potassium and/or calcium takes place.

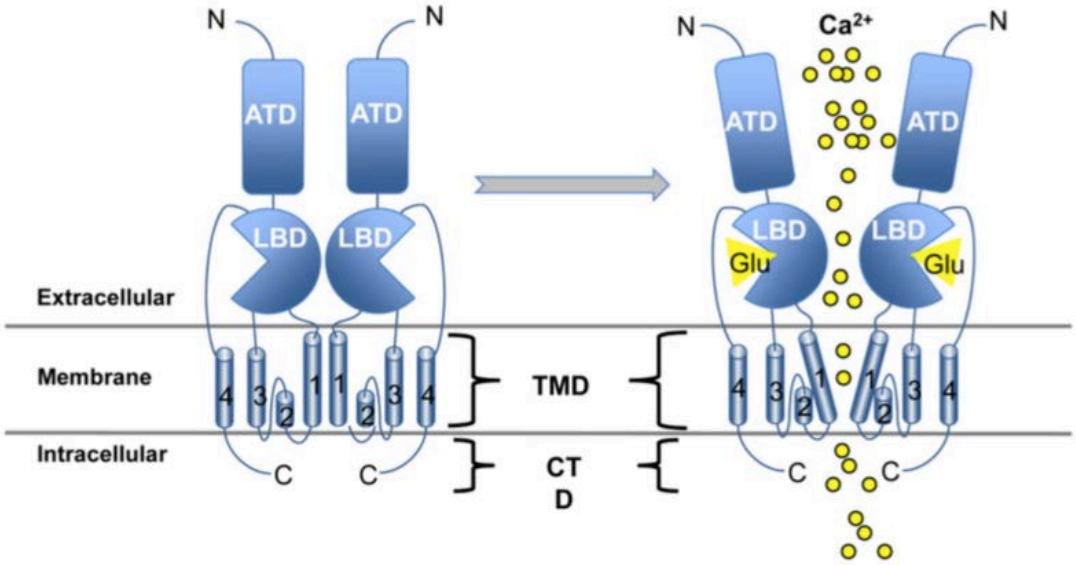

Figure 1.2. Structure and activation mechanism of iGluRs

iGluRs share the same basic structure comprising of four well-conserved domains: a. the extracellular amino-terminal domain (ATD), b. the ligand-binding domain (LBD), c. the four transmembrane domains (TMDs; numbered 1-4) and d. the intracellular carboxy-terminal domain (CTD). The schematic on the left illustrates the native resting conformation of iGluRs. Although only two subunits are depicted, the entire molecule naturally consists of four subunits arranged in such a way as to create a channel through the plasma membrane. Upon glutamate binding (schematic on the right), a conformational change in TDM region I occurs triggering the opening of the channel and allowing the influx of Ca^{2+} into the cell by diffusion [modified by (Willard and Koochekpour, 2013)].

If a sufficient amount of iGluRs is simultaneously stimulated, high concentrations of cation influx will trigger an action potential – the fastest type of excitatory synaptic transmission throughout the central and peripheral nervous systems (CNS, PNS) and the retina. The signal is received by the target cell and induces the activation of excitatory amino acid transporters (EAATs; also known as glutamate transporters). EAATs are mainly expressed on postsynaptic and supporting glial cells. They serve to empty the synaptic cleft of Glu, to effectively turn off the signal and to reset the system for generation

and propagation of new action potentials (Traynelis *et al.*, 2010). Sustained stimulation and overactivation of iGluRs allows high levels of calcium ions to enter the cell and initiates a pathological process, known as excitotoxicity. Even though physiological increases in intracellular Ca^{2+} levels are salient to normal cell functioning, the excessive influx of Ca^{2+} in addition to any Ca^{2+} release from intracellular compartments can overwhelm Ca^{2+}-regulatory mechanisms, induce aberrant over-activation of proteases and caspases as well as the production of reactive oxygen species (ROS) and lead to cell death (Dong *et al.*, 2009).

An AMPA receptor was the first iGluR to be identified by expression cloning (Hollmann *et al.*, 1989). The same method also resulted in identification of the first NMDA receptor subunit and the first metabotropic glutamate receptor (mGluR) (Nakanishi and Masu, 1994). Sequence information on the cloned receptors prompted the identification of the various members of the iGluR family. To date, 18 genes belonging to the iGluR family have been identified in mammals. Of the eighteen subunits, 7 belong to the NMDA subtype (NR1 or GluN1, NR2 or GluN2 (A-D), NR3 or GluN3 (A-B)), 4 to the AMPA (GluR1-4/GluRA-D) subtype and 5 to the kainate (GluR5-7, KA1-2) subtype. The remaining two, δ1 and δ2, share high sequence similarity with the other iGluR subunits and are called orphan receptors because there is no evidence that they form functional glutamate-gated receptors (Hollmann and Heinemann, 1994; Hollmann *et al.*, 1993).

Each iGluR subtype has a unique role. NMDA receptors (NMDARs) are glutamate-gated ion channels that monitor changes in membrane potential and presence of glutamate in the synaptic cleft (Collingridge and Bliss, 1995). They are located not only at synapses but also at extrasynaptic sites (Clark *et al.*, 1997). As a result, they play key roles in synapse development, consolidation and plasticity, as well as in learning and memory. NMDARs exist in different forms, defined by the different combinations of subunits that can assemble into a functional reporter; they form a tetramer consisting of at least one GluN1 and combinations of GluN2 and GluN3 subunits. The so-called classical NMDARs contain two GluN1 and two GluN2 subunits, are highly permeable to Ca^{2+} and accumulate at post-synaptic densities (PSDs). Owing to their permeability to calcium, they relay not only physiological signals to neurons, but also trigger intracellular signalling cascades that can ultimately lead to cell death. Thus, they are also involved in excitatory amino acid (EAA)-mediated neuronal toxicity (Hynd *et al.*, 2004).

NMDA receptors are found in most CNS neurons (Petralia *et al.*, 1994a; Petralia *et al.*, 1994b) and

mediate Ca^{2+}-influx in response to coincident agonist binding (Seeburg, 1993). Two agonists bind to activate them: glutamate (L-Glu), which binds to the S1 and S2 regions of the GluN2 subunit and glycine which binds to the S1 and S2 regions of the GluN1 subunit. Activation of these receptors also requires synchronous post-synaptic depolarization. The latter facilitates extrusion of Mg^{2+} ions, which normally block the ion pore at resting membrane potentials, and thus allow Ca^{2+} influx (Paoletti *et al.*, 2013). NMDARs can identify coincident presynaptic and postsynaptic activity, connect it to Ca^{2+}-activated signalling pathways and induce permanent synaptic changes, such as changes in "functional" [long-term potentiation (LTP) or long-term depression (LTD)] or "structural" plasticity (synapse enlargement and stabilization) (Malenka and Nicoll, 1999; Matsuzaki *et al.*, 2004).

Potentiation of NMDA channels happens dose-dependently and is characterized by increase in peak channel open probability and peak channel current duration (Araneda *et al.*, 1993).

AMPA receptors (AMPARs) are believed to be the most common type of neurotransmitter receptor in the CNS. They are tetrameric, cation-permeable ionotropic glutamate receptors, expressed throughout the brain (Beneyto and Meador-Woodruff, 2004). They are assembled as two identical heterodimers, formed by combinations of the GluR1-4 subunits. They reside at extrasynaptic sites of the soma or the dendrites and travel to dendritic spines via lateral diffusion (Traynelis *et al.*, 2010). GluA1/2 is the predominant AMPAR subtype in hippocampal pyramidal neurons, followed by GluA2/3 (Lu *et al.*, 2009). Upon Glu binding, the pore opens and allows the influx of Na^{+} ions (along with K^{+} efflux) to depolarize the postsynaptic compartment. However, depending on the subunit composition and the RNA editing, AMPARs also permit Ca^{2+}-influx, which has important consequences for receptor trafficking and synaptic plasticity (Henley *et al.*, 2011; Kessels and Malinow, 2009). AMPARs primarily vary in their intracellular C-terminal domains. These domains contain regulatory elements that interact with scaffold proteins and signalling molecules and are subjected to multiple post-translational modifications. Therefore, they are crucial for the regulation of the receptors' functions, such as channel gating, trafficking and stabilization at synapses (Shepherd and Huganirl, 2007). Due to the rapid nature of both AMPAR desensitization and resensitization kinetics, AMPARs are considered to be the primary mediators of fast excitatory synaptic transmission in the mammalian brain, through sodium and potassium conductance, with nominal permeability to calcium (Gouaux, 2004). The trafficking of AMPARs into and out of synapses is highly dynamic and regulates activity-dependent changes in synaptic transmission. It is controlled by subunit specific AMPAR-interacting

proteins as well as by various post-translational modifications that occur on their C-terminal domains. Practically, increased AMPAR activity at synapses results in the long-term potentiation (LTP) of synaptic strength, whereas removal of synaptic AMPARs leads to long-term depression (LTD) (Shepherd and Huganirl, 2007).

Kainate receptors (KARs), on the other hand, are tetrameric assemblies of subunits that share structural similarities with the subunits of the other iGluRs. The resultant receptors contain combinations of low-affinity GluK1-3 (formerly named GluR5-7) and high-affinity GluK4 and GluK5 (formerly KA-1 and KA-2) subunits (Ayalon and Stern-Bach, 2001). Similar to both NMDA and AMPA receptors, KARs are widely distributed throughout the brain. Unlike other receptors, studies of KARs proved out to be complicated, due to the lack of specific compounds to activate or block them. For example, kainite (the principal KAR agonist) can also activate AMPARs. Moreover, the prototypic AMPAR agonist, AMPA, can also activate KARs. Contrary to NMDARs and AMPARs, the activation of postsynaptic KARs produces small amplitude excitatory post-synaptic currents (EPSCs), with slow activation and de-activation kinetics (Castillo *et al.*, 1997). The slow kinetics of $EPSP_{KAR}$ is a distinct feature that separates KARs and highlights their role in integrating exclusive information transfer (Pinheiro *et al.*, 2013). Also, while NMDARs and AMPARs are found at the PSDs of most glutamatergic brain synapses, KARs are only found in certain central synapses (Lerma and Marques, 2013). Therefore, based on their electrophysiological and distribution profile it has been suggested that KARs, rather than being direct mediators of synaptic plasticity, they play a modulatory role. KARs are also reported to contribute to the development of early neuronal connectivity by driving the formation and guidance of the early synaptic contacts and tracks (Goda and Davis, 2003; Lanore *et al.*, 2012). The disparate actions of kainate receptors as well as their unique functions are supported by the variety shown in their subcellular localization and the interaction with multiple proteins, some of which are shown to be true ancillary proteins.

Although glutamate signaling is of utmost importance for synaptic plasticity and transmission throughout the CNS, continuous application of L-Glu could result in the death of post-synaptic neurons. Also, application of glutamate agonists could induce neurotoxicity. Based on the later observations, the term “excitotoxicity”, the pathological process by which neurons are either damaged or killed as a result of excessive stimulation by EAAs, was coined (Olney, 1989; Olney *et al.*, 1990; Rothman and Olney, 1995). Excitotoxicity induces entering of excessive amounts of Ca^{2+} at the post-

synaptic neuron. The latter triggers the activation of many nucleolytic and proteolytic pathways (Zundorf and Reiser, 2011). As a result, with continuous L-Glu stimulation and concomitant Ca^{2+}-influx, the neuron undergoes cellular degeneration. This includes cellular DNA, RNA and protein degradation along with disassembling of the cell membrane and the cytoskeleton (Olney *et al.*, 1986; Whetsell and Shapira, 1993).

Excitotoxicity is considered a major contributing factor to a multitude of neurodegenerative disorders, such as traumatic brain injury (Luo *et al.*, 2011), amyotropic lateral sclerosis (ALS) (Grosskreutz et al., 2010), multiple sclerosis (Frigo et al., 2012), epilepsy (Czuczwar, 2000) and chronic neurodegenerative disorders like AD (Woods and Padmanabhan, 2012), PD (Surmeier *et al.*, 2010) and HD (Raymond *et al.*, 2011).

For many years, iGluRs were thought to be the sole regulators of glutamatergic signaling and the culprits of excitotoxicity-mediated neuronal death. Recent research, however, has also implicated glutamate receptors coupled to second messenger systems via GTP-binding proteins, denoted metabotropic glutamate receptors (mGluRs) (Conn and Pin, 1997).

1.2.2. Metabotropic Glutamate Receptors (mGluRs)

Metabotropic Glutamate receptors (mGluRs) are members of the G-protein-coupled receptor (GPCR) superfamily, the largest receptor gene family in the human genome. The GPCR family contains several subfamilies. The classical neurotransmitter GPCRs, known as rhodopsin-like GPCRs, belong to subfamily A. They are structurally common, containing an extracellular N-terminal domain, seven transmembrane-spanning domains, and an intracellular C-terminal domain. In contrast to family A receptors, mGluRs as well as gamma-aminobutyric acid B (GABAB) receptors, calcium-sensing receptors, pheromone receptors, and taste receptors belong to class C GPCRs. These receptors differ from the family A receptors in the presence of a large extracellular N-terminal domain that contains the endogenous ligand-binding site (Conn and Pin, 1997). GPCRs are membrane-bound proteins activated by multiple extracellular ligands, such as light, peptides, and neurotransmitters, and transduce intracellular signals via interactions with G proteins. Ligand binding triggers a conformational change of the GPCRs, which further activates a receptor-bound G protein. Each G-protein is composed of a heterotrimeric complex of α, β, and γ subunits. In their inactive state, G proteins bind guanosine 5/- diphosphate (GDP). However, activation of the G protein induces the

exchange of GDP for guanosine 5/-triphosphate (GTP), causing the α-subunit dissociation from the βγ-subunit. Activated G protein subunits subsequently change the function of various effector molecules (such as enzymes, ion channels, and transcription factors) and induce changes in intracellular signalling. Inactivation of the G protein occurs when the bound GTP is hydrolyzed to GDP, resulting in reassembly of the heterotrimer (Niswender and Conn, 2010). Two independent groups cloned the first mGluR cDNA (mGluR1a) by using the same functional expression assay (Houamed *et al.*, 1991; Masu *et al.*, 1991). MGluR1 amino acid sequence revealed that this receptor shared no sequence homology with any other GPCR, suggesting that it could be a member of a new receptor gene family. The search for mGluR-related cDNA resulted in the isolation of seven more genes (known as mGluR1-8), many with several splice variants, which are differentially expressed throughout the CNS (Conn and Pin, 1997). These receptors are subclassified into three groups based on sequence homology, ligand selectivity and G-protein coupling. Group I consists of mGluR1 and 5, Group II includes mGluR2 and 3, and group III includes mGluR4, 6, 7 and 8.

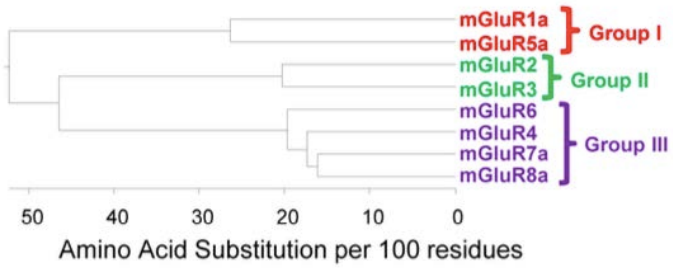

Figure 1.3. Relationship between the three mGluR subgroups

The phenogramshows the relationship between the three mGluR subgroups (Group I, II and III) as well as the individual receptors within each group. Branch length indicates the amino acid identity between the protein sequences [modified by (Willard and Koochekpour, 2013)].

Activation of group I mGluRs results in coupling to heterotrimeric G_q/G_{11} proteins (Conn and Pin, 1997). G_q activation promotes phospholipase C-β1 (PLC-β1) stimulation, which triggers the hydrolysis of phosphoinositide (PI). The latter results in the formation of 1,2-diacylglycerol (DAG), an activator of protein kinase C (PKC), and inositol 1,4,5-trisphosphate (IP_3), which initiates calcium release from intracellular stores. Conversely, group II and group III mGluRs, couple primarily to $G_{i/o}$ proteins, which inhibit adenylate cyclase (AC) and indirectly adjust ion channel activity (Table (Conn and Pin, 1997;

Niswender and Conn, 2010).

Group	Receptor/splice variants	CNS expression	Synaptic localization	Signaling pathways of group
Group I	mGluR1 a,b,c,d,e,f Taste mGluR1	Widespread in neurons Taste buds	Predominantly postsynaptic	Phospholipase C stimulation Stimulation of adenylyl cyclase (some systems) MAP kinase phosphorylation
	mGluR5 a,b	Widespread in neurons, astrocytes		
Group II	mGluR2	Widespread in neurons	Presynaptic and postynaptic	Inhibition of adenylyl cylcase Activation of K^+ channels Inhibition of Ca^{++} channels
	mGluR3 GRM3A2 GRM3A4 GRM3A2A3	Widespread in neurons, astrocytes		
Group III	mGluR4 Taste mGluR4	Widespread in neurons, High in cerebellum Taste buds	Predominantly presynaptic	Inhibition of adenylyl cylcase Activation of K^+ channels Inhibition of Ca^{++} channels
	mGluR6 a,b,c	Retina	Postsynaptic in ON-bipolar retinal cells	Stimulation of cGMP phosphodiesterase (mGluR6)
	mGluR7 a,b,c,d,e	Widespread in neurons	Active zone of presynaptic terminals	
	mGluR8 a,b,c	Lower and more restricted expression than mGluR4/7	Predominantly presynaptic	

Table 1.1. Key features of mGluRs (Niswender and Conn, 2010)

1.3. Group I mGluRs: structure and signalling

Group I share the same basic mGluR structure; they consist of: a. a large bi-lobed extracellular N-terminal domain (known as amino-terminal domain (ATD)) - also referred to as the venus fly trap domain (VFT), due to its unique shape, b. the cysteine-rich domain (CRD) that is critical for dimerization and activation of the receptors, c. the classic seven alpha-helical transmembrane

domains (TMD) and d. an intracellular carboxy-terminal domain (CTD) (Seebahn *et al.*, 2013).

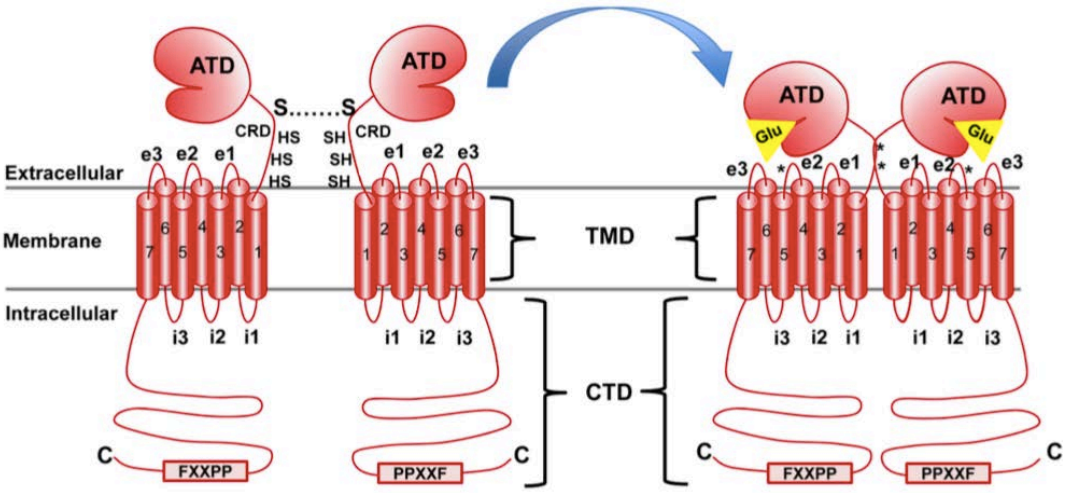

Figure 1.4. Structure and activation mechanism of mGluRs

mGluRs share the same basic structure comprising of four well-conserved domains: a. the amino terminal domain (ATD) at the N-terminus (N) is followed by the cysteine rich domain (CRD), the seven transmembrane domains (TMD; numbered) and the C-terminal domain (CTD). At the native resting conformation of mGluRs (schematic on the left side), cysteine residues aid the receptor dimerization, as indicated by the formation of the S-S bond. Upon, Glu binding (schematic on the right), a conformational change at the ATD region, involving the CRD region – stars indicate the disulfide bridges created by Glu binding- induces activation of the receptor-bound G-proteins.

Note: i1,i2, etc. indicate intracellular loops between transmembrane regions, while e1, e2, etc. indicate extracellular loops. The stars (*) at the right schematic indicate cysteine residues that are important in transmitting activation information to the docked G-protein complex [modified by (Willard and Koochekpour, 2013)]

Their particularly large N-terminal domain allows for extracellular ligand recognition and protein interactions. Ligand binding occurs at the neighboring VFD region. Induction and propagation of signals via the VFD regions partly depends on the presence of a disulfide bridge between the ninth cysteine residue of the CRD region and the cysteine on lobe 2 of the VRD region (Jingami *et al.*, 2003; Muto *et al.*, 2007; Rondard *et al.*, 2006). Upon ligand binding, a conformational change occurs that is relayed to the heptahelical domain (HD) of the intracellular C-terminus (Liu *et al.*, 2006). The

VFD has also been known to bind auxiliary ligands such as divalent cations, which both activate and intensify receptor activity (Francesconi and Duvoisin, 2004; Kubo *et al.*, 1998). Depending on the presence of an agonist or an antagonist, VDF can exist in three conformational states: a. the open-open conformation (an inactive state induced by antagonist treatment), b. the open-closed conformation and c. the closed-closed conformation (both induced by ligand or agonist binding). Upon stable ligand (glutamate) binding on both monomers, the two lobes of each VFD come together and form a cleft; acquiring a closed-closed state conformation (Tsuchiya *et al.*, 2002) (Kunishima *et al.*, 2000).

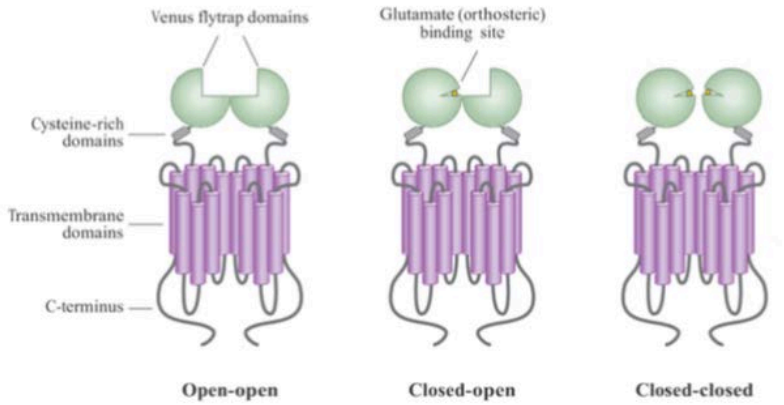

Figure 1.5. Activity-dependent states of mGluR5 dimers

A schematic representation of the mGluR5 dimeric structures in different activity-dependent states. The mGluR5 dimers contain two extracellular domains called the Venus flytrap domains (VFDs), which bind glutamate and other orthosteric ligands. The open-open state (left) is the inactive conformation of the receptor and can be stabilized by treatment with antagonists. Either one or two VFDs can then bind glutamate, resulting in the closed-open (middle) or the closed-closed (right) active receptor conformations [modified by (Niswender and Conn, 2010)].

The dimerization hypothesis is further supported by functional studies showing that group I mGluRs behave as constitutive, covalently linked homodimers (Jingami *et al.*, 2003; Kunishima *et al.*, 2000). It has been reported that group I mGluRs will perform at maximum activity only when both dimer subunits are occupied (Kammermeier and Yun, 2005). The significance of receptor dimerization however is still unknown. The main function of the intracellular C-terminal domain is to modulate G-

protein coupling. It also takes part in protein-protein interactions and is the major site of post-translational modifications, such as regulatory phosphorylation and alternative splicing (Niswender and Conn, 2010). Activation of the C-terminal region of the mGluR induces the stimulation of the coupled $G_{q/11}$- protein. GDP is then exchanged for GTP causing α-subunit dissociation from the ßγ-subunit, which induced PLC and various downstream effector molecules' activation (Pin *et al.*, 2003). In addition to well-established coupling to G_q-type G-proteins, group I mGluRs can also couple to $G_{i/o}$, G_S and G-protein independent pathways (Hermans and Challiss, 2001) so as to activate alternative downstream effector molecules including adenylate cyclase (AC), tyrosine kinases, and mitogen-activated protein kinases (MAPK) (Balazs *et al.*, 1997; Boxall, 2000).

1.4. Group I mGluRs: expression patterns and distribution

Group I mGluRs are differentially expressed throughout the mammalian central CNS and PNS in a diverse array of neuronal subpopulations (Pin *et al.*, 2003). Both receptor subtypes are highly expressed at the postsynaptic densities (PSDs) of excitatory glutamatergic synapses. Nonetheless, there is also evidence for presynaptic localization of group I mGluRs as well as of presynaptic-targeted actions via endogenous retrograde signalling (Maejima *et al.*, 2001; Niswender and Conn, 2010). In early developmental stages high expression of both mGlu1 and 5 receptors has been reported in multiple brain areas, including the cortex, hippocampus and cerebellum (Catania *et al.*, 1994; Lopez-Bendito *et al.*, 2002; Romano *et al.*, 1996a). In adult brain, mGluR1 is most abundant in the Purkinje neurons of the cerebellum (Shigemoto *et al.*, 1992), while mGluR5 is most abundant in the strata oriens and radiatum of the hippocampus (Lopez-Bendito *et al.*, 2002; Lujan *et al.*, 1996). The hippocampus is a region of differential group I mGluR expression; mGluR1 predominates in CA3, while mGluR5 in CA1 pyramidal cells (Fotuhi et al., 1994). Within the hippocampus, mGluR1 is mainly localized in cell bodies whereas mGluR5 in the dendritic regions. Apart from the hippocampus mGluR5 is also highly expressed in the cerebral cortex, subiculum, olfactory bulb, nucleus accumbens, lateral septal nucleus and in the medium spiny projection neurons of the striatum (Fotuhi *et al.*, 1994; Luscher and Huber, 2010; Romano *et al.*, 1996a). mGluR1 is additionally expressed in the mitral cells of the olfactory bulb, the lateral septum, the pallidum, and in the thalamus (Luscher and Huber, 2010). Both group I mGluRs are also expressed in the PNS in peripheral sensory

unmyelinated afferent terminals (Bhave *et al.*, 2001). At the subcellular level, mGluR1 and 5 are localized in the extrasynaptic regions of dendritic spines, where they are anchored to NMDARs via scaffolding proteins, such as Homer, Shank, and postsynaptic density protein 95 (PSD95) (Baude *et al.*, 1993; Lujan *et al.*, 1996; Tu *et al.*, 1999). Their localization profile supports their role as mediators of synaptic strength, by modulating the activity and distribution of ionotropic and GABA(A) receptors (Xiao *et al.*, 2006). The knowledge about the distinct expression profiles of mGluR1 and mGluR5 and their roles in modulating glutamate and GABA(A) neurotransmission can provide a basis for identifying the physiological and pathological factors that can contribute to changes in group I mGluR's activity, expression and interaction profile and thus for understanding and treating many CNS diseases.

1.5. Group I mGluRs: roles in Physiology and Pathology

In the nervous system, Glu is the primary fast excitatory neurotransmitter participating in a wide range of neural functions such as learning and memory, long-term potentiation and synaptic plasticity (Fairman and Amara, 1999; Meldrum, 2000). Although glutamatergic signalling is considered fast, mGluRs are classified as slow-acting, neuromodulators (Pin *et al.*, 2003). Group I mGluRs, due to their diverse expression profile and their role in modulating signalling pathways (Coutinho and Knopfel, 2002), have been linked to modulation of multiple processes, such as neuronal development, synaptic plasticity (Le Duigou and Kullmann, 2011) and induction of reactive astrocytes (Ferraguti *et al.*, 2008). The principal function of group I mGluRs is the modulation of excitatory neuronal signalling, mainly by inhibition of potassium conductance and activation of selective cationic transmissions (Guerineau *et al.*, 1994). However, mGluR1/5 can also induce inhibitory hyperpolarizing responses (Crepel *et al.*, 1994). For example, mGluR1 generates inhibitory hyperpolarizing signals in midbrain dopamine neurons (Valenti *et al.*, 2002). Moreover, pharmacological inhibition studies have shown that regulation of CA1 pyramidal cell excitability is executed by mGluR1, while mGluR5 generates the slow after hyperpolarization potential (Mannaioni *et al.*, 2001). This illustrates that, in spite of high sequence homology between mGluR1 and mGluR5 (Abe *et al.*, 1992), each receptor subtype exerts specific physiological effects even at the same neuronal population (Valenti *et al.*, 2002).

Neurodevelopmental processes are considerably influenced by aberrant group I mGluR signaling. This notion is finely demonstrated in the rodent barrel cortex. In *Grm5*$^{-/-}$ mice, despite fractional segregation of thalamic afferents, the barrel cortex fails to develop, most probably due to lack of mGluR5-stimulated PLC-β1 signalling, which is important in the early development of the region (Hannan *et al.*, 2001). Additional studies have highlighted a role of mGluR1 in the regression of climbing fibers from cerebellar Purkinje neurons. In normal development, innervations of Purkinje neurons cease so that most climbing fibers regress and only one strong excitatory input remains. The climbing fibers of transgenic mice expressing reduced levels of mGluR1 fail to regress (Aiba *et al.*, 1994; Levenes *et al.*, 1997; Sachs *et al.*, 2007). Another distinctive feature of mGluR1$^{-/-}$ mice is ataxia, a common hallmark of many neurological disorders (Conti *et al.*, 2006; Sachs *et al.*, 2007). Additionally, ataxia, a common hallmark of many neurological disorders, has been linked to mutants in the mGluR1 locus (Sachs *et al.*, 2007). A role of group I mGluRs in neuronal differentiation was additionally demonstrated. PrP^C and laminin γ chain (PrP^C-Ln γ1) were identified as group I mGluR interaction partners (Graner *et al.*, 2000). Beraldo and colleagues showed that upon formation of the group I mGluRs -PrP^C -Ln γ1 complex, group I mGluRs are activated and transduce signals for neuritogenesis (Beraldo *et al.*, 2011).

Furthermore, group I mGluRs are key regulators of synaptic plasticity. Both receptor subtypes have been associated with hippocampal long-term potentiation (LTP), long-term depression (LTD), spatial learning and memory formation (Balschun *et al.*, 1999; Salinska and Stafiej, 2003). In agreement with these observations, *Grm1*$^{-/-}$ mice lack induction of hippocampal LTP (Lapointe *et al.*, 2004), whereas antagonism of both mGluR1 *and* mGluR5 is required to fully suppress cortico-striatal LTP (Gubellini *et al.*, 2003).

The localization of group I mGluRs significantly influences their role in pathology. Both mGlu1 and 5 receptors reside in the extrasynaptic region of the dendritic spines, interacting with the NMDARs through a group of scaffolding proteins, such as Homer, Shank and PSD95 (Tu *et al.*, 1999). Group I mGluRs promote the activation of NMDARs by either relieving the Mg^{2+}-ion blockage of the NMDA channel or by other mechanisms (Attucci *et al.*, 2001; Doherty *et al.*, 1997; Mannaioni *et al.*, 2001; Pisani *et al.*, 2001). Thus, it was expected that the activation of mGlu1/5 receptors induces neuronal damage by the activating NMDA receptor. However, activation of mGluR1/5 receptors by addition of

(S)-3,5-Dihydroxyphenylglycine (DHPG) was reported to either amplify or reduce excitotoxic neuronal death, depending on the neurodegeneration models used (Bruno *et al.*, 2001; Nicoletti *et al.*, 2011). The idea that group I mGluRs either promote or attenuate neuronal damage depending on their functional state was supported by multiple *in vitro* and *in vivo* studies. For example, in mixed primary cortical cultures DHPG amplifies NMDA toxicity when applied only once (either before or during the NMDA pulse). However, it turns neuroprotective when applied for the second time after a brief pre-exposure, due to an activity-dependent switch in group I mGluR activity triggered by hydrolysis of phosphatidylinositol 4,5-bisphosphate (PtdIns-4,5-P) and a subsequent inhibition of voltage-sensitive Ca^{2+} channels (Herrero *et al.*, 1998; Sistiaga and Sanchez-Prieto, 1998). Another study showed that mGluR1a could both stimulate intracellular Ca^{2+} release and activate phosphatidylinositol-4,5-biphosphate 3-kinase (PI3K) signalling only when the C-terminal region (main interaction domain) of the receptor is intact. This favours the toxic activation of NMDARs and a sustained Ca^{2+}-influx, which induce a calpain-mediated cleavage of the C-terminus of mGluR1a. The latter prevents activation of the PI3K pathway and instead promotes stimulation of the PtdIns-4,5-P hydrolysis, which results in the production of a neurotoxic signal and ultimately in neuronal cell death (Xu *et al.*, 2007). Conversely, prevention of calpain-mediated truncation of the C-terminus of mGluR1a protects hippocampal slices against oxygen/glucose deprivation (OGD). It also protects neonatal rats from hypoxia/ischemia-induced neuronal damage (Zhou *et al.*, 2009). In cultured cerebellar granule cells, mGluR1 promotes cell survival in the presence of glutamate, but causes apoptotic death in the absence of bound ligand (Pshenichkin *et al.*, 2008), due to an interaction of the mGluR1a C-terminal domain with intracellular targets that regulate the activation of pro- and anti- apoptotic signals (Pshenichkin *et al.*, 2011). On the other hand, mGluR1a-mediated neuroprotection involves a G-protein independent pathway, driven by β-arrestin1 dependent activation of the mitogen-activated protein kinase (MAPK) pathway (Emery *et al.*, 2010; Pshenichkin *et al.*, 2011). Pharmacological studies further suggest the existence of a "ligand bias". Glutamate binding can induce both neuroprotective and neurotoxic signals, whereas quisqualate (an mGluR1 orthosteric agonist) can only stimulate PtdIns-4,5-P hydrolysis and neurotoxicity. Interestingly, mGluR1 antagonists can block PtdIns-4,5-P hydrolysis, but not the pro-survival signals triggered by glutamate. The mechanism of action is still elusive (Emery *et al.*, 2011).

Contrary to receptor agonists, mGlu1 and mGlu5 receptor antagonists or negative allosteric modulators (NAMs) are repeatedly neuroprotective, independently of the context and the nature of the toxic insult. Both *in vitro* and *in vivo* studies have shown that selective mGlu1 receptor antagonists are neuroprotective by enhancing GABA release (Battaglia *et al.*, 2001; Cozzi *et al.*, 2002). Group I mGluRs have also been studied in mechanisms of ischemic tolerance. In organotypic hippocampal slices, treatment with mGluR1, but not mGluR5, antagonists abrogated a non-lethal 10min pre-exposure to OGD, a paradigm of "ischemic preconditioning". A subsequent lethal exposure to OGD, a paradigm of pharmacological preconditioning, was rescued by pre-exposure to DHPG (Werner *et al.*, 2007). Conversely, when hippocampal slices were subjected to a protocol of "ischemic post-conditioning", in which a brief (3 min) period of OGD was delivered 5 min after a lethal episode of OGD, neuroprotection was suppressed by both mGluR1 and mGluR5 antagonists, due to stimulation of the phosphatidylinositide 3-kinase/ Protein kinase B/ Glycogen synthase kinase (3PI3K/Akt/GSK3β pathway) (Scartabelli *et al.*, 2008). A recent study shows that mGluR1/5 and also highly expressed on oligodendrocytes during development and their modulation is protective in a rodent model of periventricular leukomalacia (Jantzie *et al.*, 2010).

mGluR5 has been critically linked to a wide spectrum of disorders including neurodegenerative disorders, fragile X and autism spectrum disorder (Caraci *et al.*, 2012; Krueger and Bear, 2011). Intracellular mGluR5 has been shown to induce an increase of dendritic Ca^{2+}, with amplitude that differs from activation of the cell surface variant (Purgert *et al.*, 2014). Intracellular mGluR5 was additionally shown to mediate protein-synthesis-dependent LTD, whereas cell-surface mGluR5 mediated both LTD and LTP (Purgert *et al.*, 2014). Increases in the levels of mGlu5 and β-arrestin immunoreactivity have been reported in the putamen of PD patients as well as in the frontal cortex, hippocampus and putamen of patients with Lewy Body Dementia (Price *et al.*, 2010). Levels of mGlu5 receptors were also increased in α-synuclein transgenic mice (Price *et al.*, 2010). In parkinsonian disease models in mice and monkeys (animals were challenged with 1-methyl-4-phenyl-1,2,3,6-tetrahydropyridine (MPTP) compound), systemic treatment with mGluR5 inhibitor [2-Methyl-6-(phenylethynyl)pyridine (MPEP) and 3-((2-Methyl-4-thiazolyl)ethynyl)pyridine (MTEP), respectively) protected nigro-striatal neurons against degeneration (Battaglia *et al.*, 2004; Masilamoni *et al.*, 2011). Moreover, in a 6-hydroxydopamine model of PD, pharmacological inhibition or genetic deletion of

mGluR5 attenuated motor deficits and prevented the loss of nigrostriatal neurons (Armentero *et al.*, 2006; Black *et al.*, 2010).

In Fragile X syndrome (FXS), aberrant signaling via group 1 metabotropic glutamate receptors (mGluRs) is suggested to trigger the observed pathophysiology. The first connection between the fragile-X mental retardation protein (FMRP) and mGluR pathways was described by Weiler *et al.*, who observed that DHPG-mediated activation of group I mGluRs stimulated protein synthesis (including the expression of FMRP) in synaptoneurosomes (Weiler *et al.*, 1997). Studies in *Fmr1* knockout (KO) mouse models demonstrated that the absence of FMRP leads to increased protein synthesis and altered synaptic plasticity, including enhanced long-term depression (LTD) (Huber *et al.*, 2002). These observations set the basis for the formulation of the mGluR theory. The latter states that the absence of FMRP in FXS induces excessive glutamatergic signaling via mGluR5 (Bear, 2005). In the absence of FMRP, increased local mRNA translation as well as a high rate of AMPAR internalization, and then degradation occurs at the synapse and gradually weakens it. Increased internalization of AMPARs influences the maturation of dendritic spines, resulting in an increased number of immature dendritic spines and thus intellectual disability (Portera-Cailliau, 2012).

In Alzheimer's disease (AD), PrP^C and mGluR5 were considered to directly contribute to disease manifestation and toxicity of Amyloid β (Aβ) aggregates. Aβ oligomers can bind to PrP^C at the cell surface (Lauren *et al.*, 2009) and form complexes that contain mGluR5 (Haas *et al.*, 2014). In a mouse model of Aβ deposition, cognitive decline and synaptic alterations were rescued by mGluR5 inhibition (Um *et al.*, 2013). Furthermore, PrP^C-mGluR5 coupling is involved in Aβ-mediated inhibition of LTP and Aβ-facilitated LTD *in vivo* (Hu *et al.*, 2014), and genetic ablation of mGluR5 reverses disease-related memory deficits in a murine model of AD (APPswe/PS1ΔE9) (Hamilton A. *et al.*, 2014). In another study, exposure of cortical APPswe/PS1ΔE9 neuronal cultures to Aβ oligomers upregulated mGluR1 and PrP^C α-cleavage, whereas activation of group-I mGluRs increased PrP^C shedding from the membrane (Ostapchenko *et al.*, 2013). In primary hippocampal neurons, membrane-bound Aβ oligomers induce toxicity by promoting clustering of mGluR5 in synapses, resulting in elevated intracellular calcium and synaptic failure (Renner *et al.*, 2010). All these studies speak in favor of an involvement of group-I mGluRs in the pathogenesis of AD. On the other hand,

others have reported that neither PrP^C ablation nor overexpression had any effect on neurotoxicity in AD models (Balducci *et al.*, 2010; Calella *et al.*, 2010; Cisse *et al.*, 2011; Kessels *et al.*, 2010). As a possible explanation for these discrepancies, it has been suggested that only a defined oligomeric fraction of Aβ (Kostylev *et al.*, 2015) interacts with mGluR5 (Haas *et al.*, 2016). These findings are particularly interesting because mGluR5 inhibitors are under clinical development for the treatment of PD, AD and FXS.

The role of mGluR5 in neurodegeneration/neuroprotection-related mechanism should also be examined in the context of glia-neuron crosstalk. Cultured astrocytes express mGlu5 receptors and its expression is increased with culturing conditions promoting a reactive-like phenotype in astrocytes. Conversely, thrombin treatment, which reverses the reactive-like phenotype of cultured astrocytes, reduces the mGluR5 expression (Balazs *et al.*, 1997; Miller *et al.*, 1995; Miller *et al.*, 1996). Pharmacological inhibition of mGluR5 reduces excitotoxic death of cultured spinal motor neurons grown in cultures enriched of reactive astrocytes (D'Antoni *et al.*, 2011) and delays the onset of motor symptoms in transgenic mice expressing a mutated form of human superoxide dismutase (SOD) (Rossi *et al.*, 2008); models of ALS.

To conclude, group I mGluRs possess a variety of physiological functions owing to their distribution, localization, structural variants and protein- interaction partners. However, finr tuning of the receptor activity is required so as not to exert their neurotoxic function.

1.6. Group I mGluRs: Interaction partners

Group I mGluRs are mainly located at the PSD, a specialized region of the post-synapses that concentrates and organizes multiple signalling molecules and thus serves as a signalling apparatus. Their localization and their interactions with neighboring molecules frequently specify their functions.

The most well-established interaction partners are members of the Homer family adaptor proteins (Shiraishi *et al.*, 2004). Homer proteins are postsynaptic scaffolding proteins that interact with the C-terminal region of mGluR1a and mGluR5a/b through their PDZ domains and couple the latter with intracellular inositol triphosphate receptors (IP_3Rs). They are an integral component of the postsynaptic mGluR signalling complex (Duncan *et al.*, 2005; Xiao *et al.*, 1998). Long forms of Homer,

harbor a distinct dimerization domain that allows them to function both as scaffolds for multiprotein complex formation at PSDs and as mediators of mGluR signalling. Long homer protein dimerization assists recruitment of PI3K enhancer (PIKE) to mGluR5. PIKE is a small GTPase molecule, which binds PI3K to trigger its endogenous lipid kinase activity (Rong *et al.*, 2003). For example, the interaction of mGluR1-Homer is necessary for mGluR1-LTD and reversal of cocaine-induced plasticity *in vivo* in the ventral tegmental area (VTA) (Mameli *et al.*, 2009), whereas disruption of this interaction in hippocampal slices antagonizes mGluR-LTD (Ronesi and Huber, 2008). In contrast, short forms of Homer, such as Homer1a, lack the dimerization domain and behave as dominant negatives (Xiao *et al.*, 1998).

Multiple studies have shown that mGlu1 receptors interact with membrane estrogen receptors (ERs) in hypothalamic neurons. This interaction is integral for the regulation of the estrous cycle (Mermelstein, 2009; Micevych and Mermelstein, 2008). In cortical neurons, the same interaction occurs. In these cultures, the protective effect of 17-β-estradiol treatment against β-amyloid is prevented by addition of mGluR1 inhibitors. Also, the protective effect of DHPG application is prevented by the pharmacological inhibition of ER [Spampinato *et al.*, 2012). However, the mechanism of interaction still remains unknown.

NMDARs are also known functional interaction partners of group I mGluRs. Homer proteins facilitate the physical association of group I mGluRs with the NR2 subunit of the NMDARs. Homer proteins act as scaffolds and recruit PSD95 and Shank to the complex to stimulate group I mGluRs (Tu *et al.*, 1999). The latter promote the activation of NMDARs by either relieving the Mg^{2+}-ion blockage of the NMDA channel or by other mechanisms (Attucci *et al.*, 2001; Doherty *et al.*, 1997; Mannaioni *et al.*, 2001; Pisani *et al.*, 2001). Pharmacological agonists of either mGluR1 or mGluR5 also enhance NMDA receptor function (Collett and Collingridge, 2004; Pisani *et al.*, 2001). For example, exposure to DHPG potentiated NMDA toxicity in cultured cortical cells (Bruno *et al.*, 1995). Sustained activation of group I mGluRs promotes the toxic stimulation of NMDARs and a sustained Ca^{2+}-influx, which induce a calpain-mediated cleavage of the C-terminus of mGluR1a. The latter prevents activation of the PI3K pathway and instead promotes stimulation of the PtdIns-4,5-P hydrolysis, which further supports the production of a neurotoxic signal and ultimately causes neuronal cell death (Xu *et al.*, 2007).

In line with this, Jin and colleagues have showed that the interaction of calcium/calmodulin-dependent protein kinase type II alpha chain (CamKIIα), NMDAR GluN2B subunit and mGluR5 at the synapse, regulates excitatory synaptic transmission. The binding of CaMKIIa to the proximal C-terminal region of mGluR5 is Ca^{2+}-sensitive. Ca^{2+} activates calmodulin (CaM) and CaMKIIa and thus induces the dissociation of CamKIIa from mGluR5 *in vitro* and in striatal neurons. Also, treatment with an mGluR5 agonist triggers the activation of CaMKIIa and its subsequent binding to the GluN2B subunit of the NMDAR. This enables CaMKIIa to phosphorylate GluN2B at position S1303 and activate NMDARs. To sum up, Jin and colleagues described a model of functional interaction between mGlu5 and NMDA receptors via the mGluR5- and Ca^{2+}- regulated CamKIIa activation (Jin *et al.*, 2013).

Another interactor of mGluR5 is Calmodulin (CaM). CaM binding actively regulates the cell surface expression of mGluR5. In rat hippocampal neurons, CaM was shown to compete with E3 ligase seven in absentia homolog (Siah-1A) to regulate the trafficking of mGluR5 in a phosphorylation-dependent manner. More specifically, phosphorylation of mGluR5 at position S901 by protein kinase C (PKC) displaces CaM and favors Siah-1A binding. Siah-1A binding decreases the surface expression and increases endosomal trafficking and lysosomal degradation of mGluR5 (Ko *et al.*, 2012).

A balanced trafficking of the mGluRs is essential so as to ensure attenuation, preclude overstimulation and cell damage and maintain a healthy cellular milieu (Lipton, 2007). A known regulator of mGluR localization and activity, through phosphorylation and subsequent desensitization, is the G-protein-coupled receptor kinase 2 (GRK2). GRK2 is primarily regulated by inflammation in several cell types (Dale *et al.*, 2000). Inflammation-induced neuronal sensitization triggers GRK2 down-regulation and over-activation of group I mGluRs. The latter promotes continuous calcium mobilization from intracellular stores; mimicking the sensitizing effect of inflammation on excitotoxic neurodegeneration. The same effect was observed upon genetic deletion of GRK2 gene (Degos *et al.*, 2013). Thus, GRK2 at the molecular level links sensitizing inflammation with group I mGluR activation and excitotoxicity; highlighting group I mGluRs as potential therapeutic targets.

1.7. Group I mGluRs and PrP^C

The normal cellular prion protein (PrP^C) has also recently emerged as an interaction partner of group I mGluRs. PrP^C together with laminin γ chain (Ln γ1) were identified as group I mGluR interaction partners (Graner *et al.*, 2000). Beraldo and colleagues showed that the formation of the group I mGluRs -PrP^C -Ln γ1 complex, stimulates group I mGluRs to transduce signals for neuritogenesis (Beraldo *et al.*, 2011). However, PrP^C-group I mGluR interaction can also contribute to neuronal toxicity and pathology.

In AD, binding of Aβ oligomers to PrP^C induces its interation with mGluR5 (Lauren *et al.*, 2009). The Aβ-PrP^C-mGluR5 complex fomation, (Haas *et al.*, 2014) activates mGluR5s, which act as the effectors of the Aβ-toxicity. In a mouse model of Aβ deposition, cognitive decline and synaptic alterations were rescued by mGluR5 inhibition (Um *et al.*, 2013). Furthermore, PrP^C-mGluR5 coupling has been shown to be involved in Aβ-mediated inhibition of LTP and Aβ-facilitated LTD *in vivo* (Hu *et al.*, 2014), and genetic ablation of mGluR5 reversed disease-related memory deficits in a murine model of AD (APPswe/PS1ΔE9) (Hamilton A. *et al.*, 2014). In another study, exposure of cortical APPswe/PS1ΔE9 neuronal cultures to Aβ oligomers upregulated mGluR1 and PrP^C α-cleavage, whereas activation of group-I mGluRs increased PrP^C shedding from the membrane (Ostapchenko *et al.*, 2013). In primary hippocampal neurons, membrane-bound Aβ oligomers induced toxicity by promoting clustering of mGluR5 in synapses, resulting in elevated intracellular calcium and synaptic failure (Renner *et al.*, 2010). All these studies speak in favor of a role of group-I mGluRs in the pathogenesis of AD. A role of PrP^C-mGluR1 interaction has additionally been suggested in prion diseases. Impairment of the mGluR1/1-phosphatidylinositol 4,5-bisphosphate phosphodiesterase 1 (PLC1)/protein kinase C (PKC) signaling pathway has been observed in a murine model of BSE; abnormal mGluR1 signaling correlated with PrP^{Sc} deposition, histological changes, and clinical scores (Rodriguez *et al.*, 2006). Another study proposed that PrP^C functioned as a receptor to mediate the deleterious effects of Aβ oligomers. This interaction did not require the infectious PrP^{Sc} conformation. This proposition was further supported by the binding of Aβ-oligomers to a neurodegeneration-linked domain of PrP^C as well as by the isolation of PrP^C as an Aβ-oligomer interaction partner in an unbiased, genome-wide screen (Lauren *et al.*, 2009). PrP^C has also been shown to interact with the 2D subunit of NMDARs

and to modulate its function (Khosravani *et al.*, 2008; Senatore *et al.*, 2012); suggesting a potential role of PrP^{C} as a regulator of glutamatergic signalling, by fine-tuning mGluR5-NMDA interaction. Detailed information about PrP^{C} and its role in physiology and in prion diseases will be presented in the following paragraphs.

1.8. Introduction to Prion Diseases

Prion diseases, also known as transmissible spongiform encephalopathies (TSEs), are a group of rare, progressive, neurodegenerative disorders of sporadic genetic or infectious origin that are invariably fatal. They affect human and a wide variety of animals. TSEs include scrapie, bovine spongiform encephalopathy (BSE), disease in humans (Aguzzi and Calella, 2009; Collinge, 2001). Although quite rare in the human population, industrial (*i.e.* cattle) and wild-life (*i.e.* deer and elk) animal populations have been affected by prion diseases at a much larger scale. Indeed, it was prion-infected cattle in the 1990s that brought the disease to light for the general public as a potentially serious public health concern (Aguzzi and Weissmann, 1996; Ghani *et al.*, 2002). Currently, CJD is the most common human prion disease, affecting approximately 1-2 people per million per year (Ladogana *et al.*, 2005). There are 4 major forms of CJD: sporadic (sCJD), familial (fCJD) or otherwise known as genetic or inherited, iatrogenic (iCJD) and variant (vCJD). The most common is sCJD, which accounts for approximately 85% of the total incidence of CJD and arises from a spontaneous somatic mutation within the prion protein gene (*PRNP*) or through a random structural change of the prion protein itself (Colby and Prusiner, 2011).

Prions have attracted the attention of the scientific community because they challenged the central dogma of molecular biology; that the biological information flows from nucleic acid to proteins and not the other way round. Indeed, according to the 'prion hypothesis' the infectivity is completely protein-mediated. The infectious agent is an unconventional pathogen: a self-propagating, proteinaceous particle devoid of nucleic acids, known as scrapie prion (PrP^{Sc}) (Prusiner, 1982). PrP^{Sc} is a misfolded conformational variant of the host-encoded cellular prion protein (PrP^{C}) (Prusiner, 1998); a glycosylphosphatidylinositol (GPI)-anchored protein that is highly abundant in the central nervous system. The presence and accumulation of PrP^{Sc} in the affected brains is the unifying hallmark of prion disorders.

Prion diseases are unique in many pathological and phenotypic traits, such as their long incubation periods, infectious nature, characteristic mode of propagation within and between species as well as the distinctive spongiform changes associated with neuronal loss and a failure to induce inflammatory response, but share several key features with other neurodegenerative disorders on the subcellular level (Aguzzi and Calella, 2009). Similar to Alzheimer's, Parkinson's and Huntington's disease (AD, PD and HD respectively), prions are neurodegenerative disorders caused by the misfolding of normal cellular proteins. One of the earliest changes is synaptic dysfunction, followed by neuronal spine loss. These pathologies accumulate progressively within the brain tissue such that extensive damage typically precedes clinical symptom manifestation and neuronal loss.

The clinical and histopathological phenotypes of prion diseases are highly heterogeneous. Signs include neurodegeneration, astrogliosis in the absence of inflammatory reaction, and, in some cases, spongiosis (due to neuronal vacuolation) and deposition of amyloid plaques. Clinical symptomatology is also variable; in humans dominant clinical features are fatigue, insomnia, dementia, weight loss, headaches and ill-defined pain sensations, whereas key neurological features include myoclonus, cerebellar ataxia, dysautonomia, pyramidal and extrapyramidal signs and in some cases cortical blindness and psychiatric features (Kubler *et al.*, 2003).

Despite significant advances in our understanding of prion diseases and the role of the infectious agent, many key questions concerning the nature of the prion, the mechanism of its replication and the underlying molecular events remain unanswered. The focus of the following paragraphs will be on the unresolved issues pertaining to early pathogenic events at the synapse and the role of PrP^{C}-interacting partners.

1.9. Prion Protein - two main conformational isoforms

Alper and Griffith first proposed that prion diseases are caused by an infectious agent devoid of nucleic acids; i.e. a protein (Alper *et al.*, 1967; Griffith, 1967). Years later, this protein was isolated and termed "prion" due to its properties as a "proteinaceous infection particle" (Prusiner, 1982). The prion protein exists in two major conformational isoforms, the normal form termed cellular PrP (PrP^{C}) and the infectious, misfolded form termed scrapie PrP (PrP^{Sc}).

PrP^C is a glycoprotein anchored to the external surface of cells by a glycosylphosphatidylinositol (GPI) anchor (Stahl *et al.*, 1987). Major elements of the protein are highly conserved among species suggesting an important biological role of PrP^C (Wopfner *et al.*, 1999). It consists of a flexible and unstructured N-terminal domain [23-120 amonicacids (aa)] and a structured C-terminal globular domain (121-131 aa) (Zahn *et al.*, 2000). At the N-terminus, a 22 aa signal domain drives transport of the protein to the Golgi apparatus where it is glycosylated and further transported to the cellular membrane. Four octapeptide domains (PHGGGWGQ) are located within the octapeptide repeat (OR) region and favor binding to metal ions (Zn^{2+}, Cu^{2+}, Ni^{2+}, Mn^{2+}) (Jackson *et al.*, 2001). The C-terminus includes two glycosylation sites (181N and 197N) that can be un-, mono- and di-glycosylated and a signal sequence for a GPI anchor. Biochemical analysis of PrP^C showed that it is sensitive to chemical treatments and digestion by cellular proteases (e.g. Proteinase K (PK)) and is inactivated by either heat or ultraviolet (UV) radiation (Meyer *et al.*, 1986). PrP^C is typically tethered to the cell membrane by its GPI anchor and located in the lipid raft microdomains of the plasma membrane (Linden *et al.*, 2008). Like other GPI-linked proteins, it is suggested to play a functional role in signal transduction and intracellular trafficking (Kasahara *et al.*, 1999) (**Figure 1.6.**).

(A)

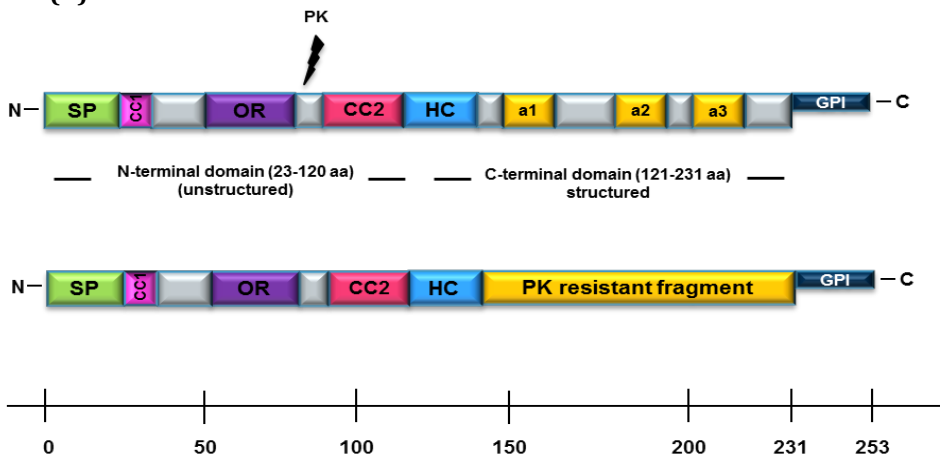

(B)

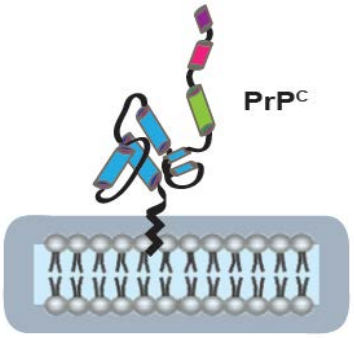

Figure 1.6. The normal cellular Prion Protein (PrP^C)

(A) Linear representation of the unprocessed human PrP depicting several features of the normal cellular prion protein (PrP^C). It is a 253 amino acid (aa) residues in length and includes a signal peptide (SP) (aa 1-22), charged cluster 1 (CC1) (aa 23-30), four octapeptide repeats (OR) (aa 59-90), charged cluster 2 (CC2) (aa 101-110), hydrophobic core (HR) (aa 114-121), alpha-helix 1 (a1) (aa 145-153), alpha helix 2 (a2) (aa 166-194), alpha helix 3 (a3) (aa 200-226) and glycosylphosphatidylinositol (GPI) anchor (aa 232-253), proteinase K (PK). A linear representation of the PK resistance region is presented below [modified by: (Aguzzi and Heikenwalder, 2006)].

(B) Schematic representation of the cellular prion protein (PrP^C) anchored in the membrane.

The infectious prion protein (PrP^{Sc}) was first discovered to co-purify in brain extracts from rodents infected with prions. In contrast to PrP^C, proteinase K (PK) digestion of PrP^{Sc} results in a protease-resistance fragment, 27-30kDa in size, called PrP27-30, which is the canonical biochemical hallmark of PrP^{Sc}. This fragment usually presents three different glycoforms (diglycosylated, monoglycosylated and unglycosylated) that can be easily identified in immunoblot analysis (Bolton *et al.*, 1984; McKinley *et al.*, 1991; Prusiner *et al.*, 1982) (**Figure 1.3.**).

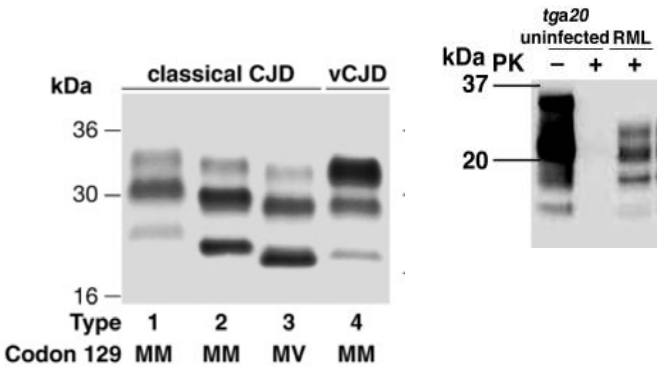

Figure 1.7. Proteinase K (PK) digestion immunoblots

Immunoblot of proteinase K digested brain homogenate from cases of classical CJD and variant CJD (vCJD) [modified by (Nuvolone *et al.*, 2016)] (left side). Immunoblot of proteinase K digested brain homogenate from RML6-infected, *Tga20* mice and uninfected controls [modified by (Raeber *et al.*, 1997)] (right side).

Although the two isoforms have the same amino acid sequence and main post-translational modifications (glycosylations, GPI anchor), their biochemical properties differ. PrP^{C} is α-helical, whereas PrP^{Sc} is at least 40% β–pleated sheet; PrP^{C} is soluble in nondenaturing detergents, whereas PrP^{Sc} is insoluble; PrP^{C} is completely degraded by proteases, whereas PrP^{Sc} has a relative resistance to proteases (Caughey *et al.*, 1991; Meyer *et al.*, 1986; Pan *et al.*, 1993; Stahl *et al.*, 1993) (**Table1.1.**)

Prion isoforms	*α-helix content*	*β-sheet content*	*Proteinase resistance/ aggregation*	*Form*	*Cellular Localization*	*Infectivity*	*Effect of wt PrP*
PrP^{C}	high	low	-	Monomer	Plasma membrane/ Rafts	-	N/A
PrP^{Sc}	low	high	++	Multimer	Plasma membrane/ Endosomes	+	Required for toxicity

Table 1.2. The main properties of the normal and the infectious prion protein isoforms

The high β-sheet conformation of PrP^{Sc} exposes parts of the protein normally buried inducing a higher degree of "stickiness" between these proteins (Nelson *et al.*, 2005). As a result, PrP^{Sc} is susceptible to aggregate into prion fibrils that consist of trimeric, left-handed β-pleated sheet units (Govaerts *et al.*, 2004; Wille *et al.*, 2002). Oligomers, protofibrils and fibrils [reviewed in (Caughey and Lansbury, 2003)] are commonly observed in prion-infected brain tissue, yet, the soluble oligomers (sizes ranging from 17-27nm) exhibit the highest infectivity and activity of structural conversion (Silveira *et al.*, 2005) (Silveira *et al.*, 2005). These oligomeric entities are of equivalent mass to 14-28 PrP molecules, are composed solely of PrP^{Sc} and cause toxicity in neurons (Simoneau *et al.*, 2007).

1.10. The "protein-only" hypothesis

Alper and co-workers with a series of well-designed experiments were the first to demonstrate that the infectious agent was not a nucleic acid. The use of procedures that eliminate nucleic acids, such as high doses of inonizing radiation and UV, did not destroy the prion infectious material (Chaffin *et al.*, 1990). The same group also identified the minimum molecular weight of the unit that maintained infectivity (2 *10^5 Da), which was too small to be a virus or another microorganism (Rockman *et al.*, 2014). Based on this observations and the identification of the two conformational isoforms the "protein-only" hypothesis of prions was formed. The latter postulates that the infectious agent is a protein (PrP^{Sc}), which self-replicates in the absence of nucleic acids. Two models have been proposed to explain PrP^{Sc} propagation (**Figure 1.8.**). The "refolding or template-assisted model" which states that PrP^{Sc} exists in a monomeric state, thermodynamically more stable than PrP^{C}. According to this model PrP^{Sc} binds to PrP^{C} and induces the formation of an heteromeric PrP^{C}-PrP^{Sc} unit and the subsequent conformational conversion of PrP^{C} by lowering the energy barrier that separates the two states (Cohen, 1999). The model suggests that the conversion is rare (unless catalyzed by pre-existing PrP^{Sc} units) and that the infectious unit is a monomer of PrP^{Sc}. This model was questioned by Caughey and colleagues who showed that small oligomers (<6 units of PrP^{Sc}) were non-infectious in Syrian hamsters. Actually, small, non-fibrillar oligomers (14-28 units of PrP^{Sc}) exhibited the highest infectivity (Silveira *et al.*, 2005).

The second model, the "nucleated polymerization model" postulates that PrP^{C} and PrP^{Sc} are in reversible thermodynamic equilibrium, shifted towards the normal PrP^{C} conformer under normal conditions. The formation of an ordered stable oligomer is the limiting step for the "de novo" production of PrP^{Sc} units. These units act as nucleation seeds that recruit PrP^{C} and incorporate it, after misfolding, into this amyloid-like oligomeric-structure. Fragmentation of these structures generates new nucleation seeds inducing the propagation of the infectious agent (Jarrett and Lansbury, 1993). Thus, in a self-propagating process, more disease-associated molecules accumulate, aggregate and are deposited in the brain. According to this model, PrP^{Sc} is only infectious as a highly ordered aggregate. Both mechanisms are considered credible, since they can explain the different aetiology of prion diseases –infectious or sporadic origin. However, experimental evidence from the yeast prion model favors the "seeded nucleation" hypothesis (Serio *et al.*, 2000).

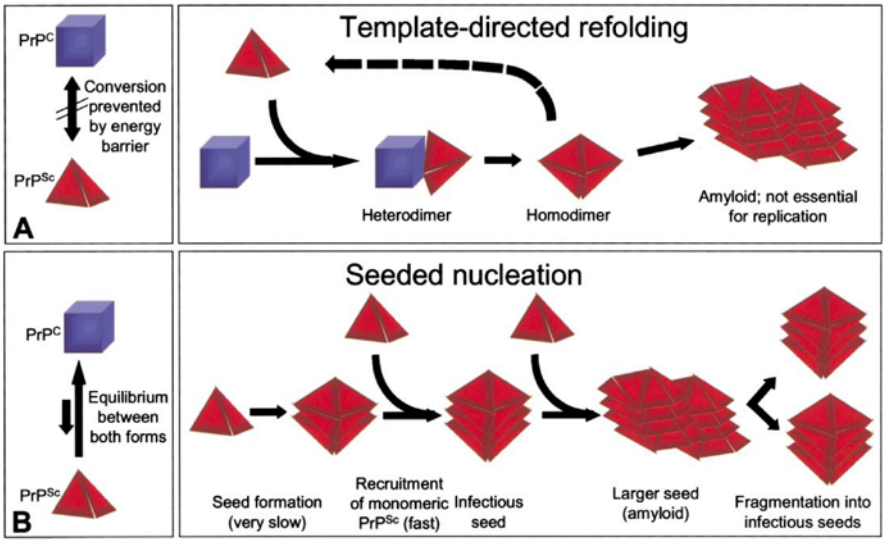

Figure 1.8. Models for the conformational conversion of PrP^{C} into PrP^{Sc}

(A) The **"refolding or template-assisted model"** proposes an interation between exogenously introduced PrP^{Sc} and endogenous PrP^{C} that induced the transformation of the latter into PrP^{Sc}. A high-energy barrier could hinder the spontaneous conversion of PrP^{C} to PrP^{Sc}.

(B) The **"seeding or nucleation-polymerization model"** suggests that PrP^{C} and PrP^{Sc} are in a reversible thermodynamic equilibrium. Only if several monomeric PrP^{Sc} units form a stable, highly-ordered seed, further monomeric PrP^{Sc} molecules can be recruited and eventually form an amyloid-like aggregate. Fragmentation of PrP^{Sc} aggregated seeds increases the number of seeding nuclei, which can recruit more PrP^{Sc} units and thus induce the propagation of the infectious agent [modified by (Aguzzi and Polymenidou, 2004)].

Efficient conversion requires the donor PrP^{Sc} to come from the same species as the host PrP^{C}. This is called the 'species barrier', it affects cross-species transmission time of prion diseases and is attributed to differences in the primary structure of PrP^{C} amongst species (Collinge and Clarke, 2007). PrP^{Sc} prions, unlike their normal counterparts, have a long half-life, cannot be broken down and cluster in brain tissue forming aggregates. This leads to synaptic & dendrite loss, spongiform degeneration, brain inflammation and neuronal death – the hallmarks of prion disease (Aguzzi and O'Connor, 2010; Soto and Satani, 2011) (**Figure 1.9.**).

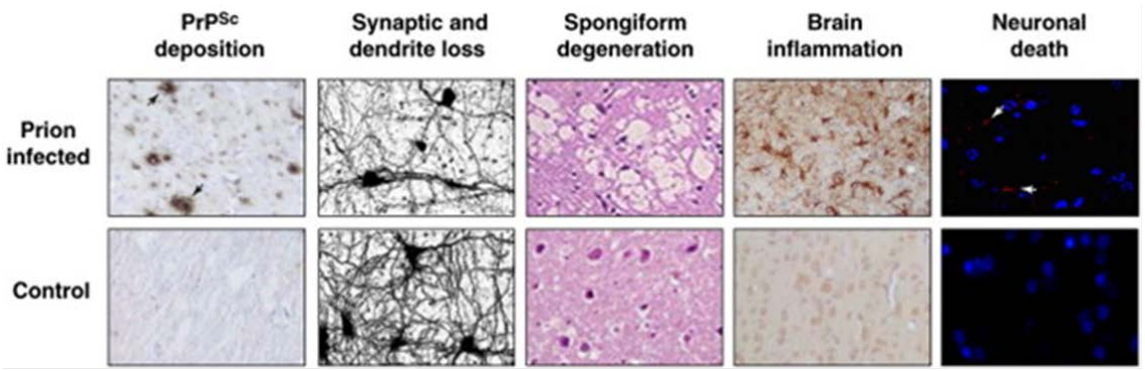

Figure 1.9. Neurodegenerative pathways implicated in prion diseases

Abnormalities in the brain of individuals infected with prions include deposition of PrP^{Sc} aggregates, synaptic damage and dendrite loss, spongiform degeneration, brain inflammation and neuronal death. Dendrite degeneration was evaluated by Golgi-silver staining, spongiform degeneration was evaluated by hematoxylin and eosin staining, astrogliosis was detected by immunological staining of reactive astrocytes with an anti-GFAP (Glial fibrillary acidic protein) antibody and apoptosis was detected by caspase-3 antibody immunostaining (red indicated by white arrows). Control stainings are presented below [modified from (Soto and Satani, 2011)].

A key assumption of the protein-only hypothesis was that PrP expression by the host is essential for scrapie multiplication and disease progression. The advent of homologous recombination and molecular cloning techniques [cloning of the cDNA coding the entire open reading frame (ORF) of the mouse Prnp was published in 1986 (Locht *et al.*, 1986)] favored the generation of Prnp-knockout ($Prnp^{-/-}$) animals. The first $Prnp^{-/-}$ mice were produced by the Weissmann group. Mice developed normally and displayed no overt abnormalities in size, weight, fertility, behavior and appearance of brain, skeletal muscles and visceral organs (Bueler *et al.*, 1992). The only remarkable findings were absence of prion propagation and resistance to scrapie infection (Bueler *et al.*, 1993); confirming the initial hypothesis. Further support was provided by showing that pre-existing PrP^{Sc} can catalyze conversion of PrP^{C} into PrP^{Sc}. This was achieved in a cell-free system, where [^{35}S]methionine-labeled PrP^{C} was converted into PrP^{Sc} in the presence of unlabelled purified PrP^{Sc} (Kocisko *et al.*, 1994). It was also shown that the conversion rate relied on the initial concentration of PrP^{Sc} and was associated only with aggregates and not monomers; in compliance with the nucleated polymerization mechanism (Caughey *et al.*, 1995). However, the efficiency of this first cell-free conversion system

was low, as the amount of newly converted protein was significantly less compared to the initial concentration of PrP^{Sc} needed to trigger the conversion reaction. Recently, the *in vitro* PMCA (protein misfolding cyclic amplification) conversion system, confirmed another crucial prediction of the prion hypothesis – that prion replication is a cyclic process, in which the production of new PrP^{Sc} units induces further misfolding (Castilla *et al.*, 2006; Saborio *et al.*, 2001).

Despite the compelling evidence in favor of the prion hypothesis, arguments against remained. First, prion strains were believed to arise from mutations or polymorphisms in the DNA (Manuelidis, 2003). This claim was debated by Bassen *et al.* who showed that each prion strain constitutes a different conformational state of PrP^{Sc} and can propagate only in the presence of host PrP^{C} (Bessen *et al.*, 1995). Second, the presence and the quantity of PK-resistant PrP^{Sc} correlate with infectivity. This argument was debated by reports showing that infectivity is propagated even in the absence of detectable PK-resistant PrP^{Sc} (Hill *et al.*, 2000; Lasmezas *et al.*, 1997). It was further shown that there are infectious PrP^{Sc} forms that are not protease resistant (Safar *et al.*, 1998).

The main premise of the prion hypothesis that needed to be tested, which would also explain familial prion diseases, was that “de novo” mutations can induce the production of PrP^{Sc} units by icreasing the probability of a misfolding event. In order to determine whether familial PrP mutations can spantaneously give rise to infectivity, unique *in vitro* and animal models of prion disease were created. Transgenic mice over-expressing the P101L substitution, which is homologous to the human P102L GSS-related mutation, were generated and spontaneously developed neurological symptoms similar to those of prion diseases. Also, brain homogenates from these mice were reported to be infectious (Hsiao *et al.*, 1990; Telling *et al.*, 1996). However, these experiments were severily criticized due to the fact that brain homogenates from these mice were used to inoculate trangenic mice (expressing the same mutation) and not wt mice. Therefore, the most plausible interpretation of the former experiments would be that the inocula from the PrP-P101L over-expressing mice accelerated a pre-existing disease process and did not cause “de novo” prion infection (Nazor *et al.*, 2005).

Additional, transgenic mice were generated expressing the D177N substitution, the mouse equivalent of the human FFI-associated mutation. These mice showed neurological symptoms resembling the ones reported for FFI patients. Inocula from these mice caused prion disease in *Tga20* mice, but failed to propagate the disease in $Prnp^{-/-}$ mice (Jackson *et al.*, 2009).

The most irrefutable evidence in support of the revolutionary "protein-only" hypothesis would be to produce prions "de novo" *in vitro*. Legname *et al.* generated amyloid fibers by in vitro polymerization of the recombinant PrP fragment (rPrP89-230) and used them to inoculate TG9949 (PrP89-230 overexpressing) transgenic mice. Inoculated mice got sick and their brain tissue was used to induce TSE in wild-type mice. However, "*in vitro prions*" induced disease in Tg9949 mice after a very long incubation-time (much longer compared to the "natural" prion strains). Also these "*synthetic prion fibrils*" did not cause TSE to wild-type mice (Legname *et al.*, 2004). It was suggested that the "*synthetic prion fibrils*" were either not "bona fide" infectious, and just accelerated a spontaneous, pre-existing neurodegenerative process, or that they were many orders of magnitude less infectious than "natural" prion strains (Caughey *et al.*, 2009; Weissmann, 2005). Further evidence in favor of the "protein-only" hypothesis were acquired when the infectious prion particles were produced in a test tube by experimental manipulation of recombinant or synthetic PrP in the absence of nucleic acids (Castilla *et al.*, 2008). In a recent publication, full-length rPrP (converted to cross-□-sheet amyloid structure and subjected to annealing) was serially transmitted and inoculated to Syrian hamsters. It gave rise to prion disease, with neuropathological and clinical features resembling human TSEs (Makarava *et al.*, 2010).

An alternative approach for the generation of "synthetic infectious prions" was the protein misfolding cyclic amplification (PMCA) assay (Saborio *et al.*, 2001). Crude brain homogenates were used as a substrate for the production of infectious material. These "synthetic prions" were inoculated to wt hamsters and induced a scrapie disease identical to the one produced by "natural prions" (Castilla *et al.*, 2005). "De novo" generation of PrP^{Sc} *in vitro* was further achieved, using a modified PMCA procedure, from brain homogenate substrate without PrP^{Sc} seeds. Yet, poly (A) RNA was present in the preparation (Barria *et al.*, 2009; Deleault *et al.*, 2007). A bit later, infectious "*bona fide*" synthetic prions were produced by PMCA using purified rPrP as template together with a synthetic anionic lipid and liver RNA (Wang *et al.*, 2010). Recently, infectious "synthetic PrP" generated by PMCA assay, caused TSE in wild-type mice that intracerebrally inoculated with these (Zhang *et al.*, 2013). The fact that infectious synthetic prions were generated and caused disease in wt mice strongly supports the prion hypothesis. Whether cofactors, such as RNA or lipids, are important parts of the infectious unit or just catalyze the formation of prions (formed solely out of PrP) needs to be further clarified.

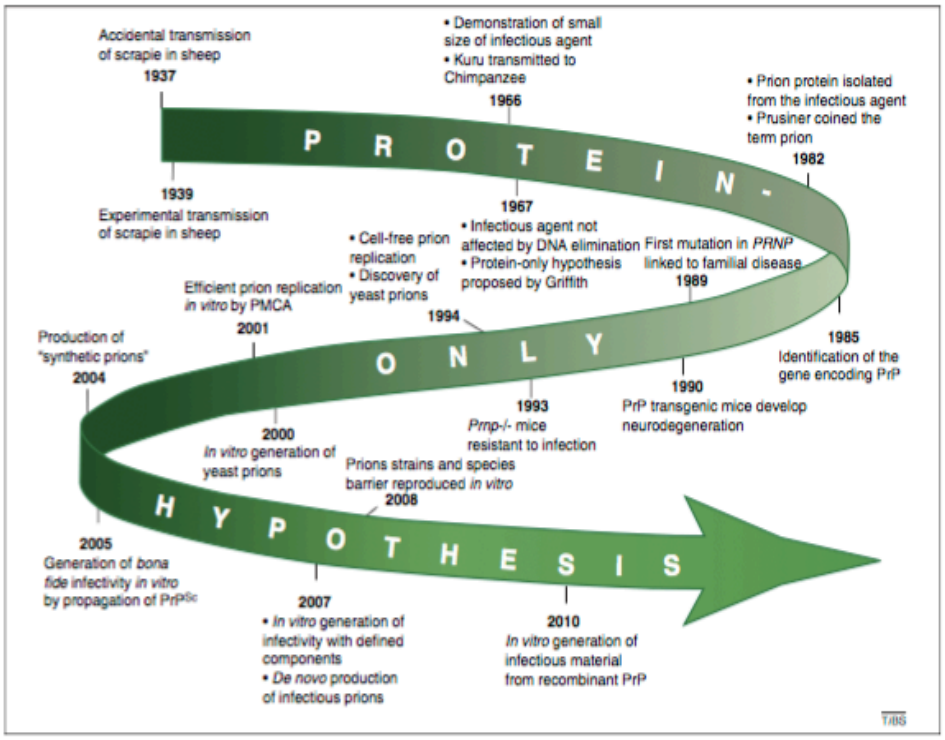

Figure 1.10. Timeline representation of the major milestones in the protein-only hypothesis [modified from (Kim *et al.*, 2007)].

1.11. Cellular biology of PrP^C: structure, biosynthesis and localization

PrP^C is encoded by the *PrP* gene (PRNP in human, Prnp in mouse and PrP gene in other species) (Basler *et al.*, 1986). The gene is expressed in all mammals and many vertebrates (Lee *et al.*, 1998; Wopfner *et al.*, 1999). It is first expressed early in embryogenesis and in the adult it is highly expressed in the neuronal and glial cells of the CNS as well as in a number of peripheral cell types (Ford *et al.*, 2002; Harris *et al.*, 1993b; Manson *et al.*, 1992; Moser *et al.*, 1995). The PrP gene is located on chromosome 20 in humans and chromosome 2 in mice (Puckett *et al.*, 1991a; Sparkes *et al.*, 1986) (Figure 1.2). Only a single exon (exon 2 in human and exon 3 in mice respectively) is coding for the open reading frame (ORF) and the 3' untranslated mRNA region of PrP^C (Maas *et al.*, 2007; Puckett *et al.*, 1991a).

PRNP expression is regulated by sequences within the 5'-flanking region, the first intron and the 3'-untranslated sequences. *Prnp* is considered a housekeeping gene, due to the absence of a TATA

box, presence of CpG islands, and the identification of several Sp1 binding sites (Basler *et al.*, 1986; Puckett *et al.*, 1991b) (**Figure 1.11.**).

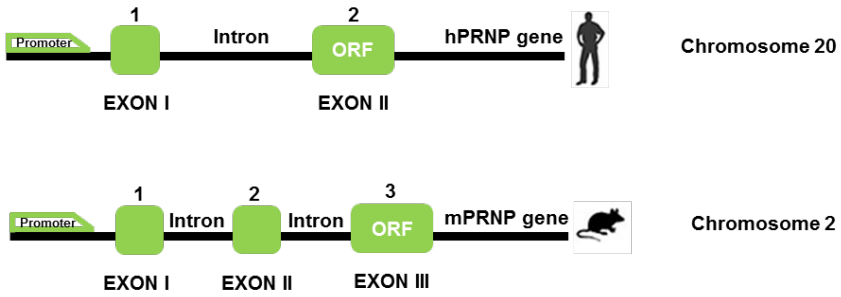

Figure 1.11. The prion gene

Schematic diagram of the human PRNP and the mouse prnp genes - ORF: open reading frame (PrP coding region), hPRNP: human prion gene, mPRNP: mouse prion gene.

The resulting protein, PrP^C, is a protein of ~250 amino acids (aa) in length and 30-35kDa in size. The primary structure of PrP^C is conserved across mammals and contains distinct domains: the N-terminal signal peptide, the octapeptide region (OR), a central domain (spanning amino acids 105-125 in the mouse polypeptide chain), and a C-terminal hydrophobic region (a detailed representation can be found in Figure 1.2.A). PrP^C is synthesized in the endoplasmic reticulum (ER), transits the Golgi and reaches the cell surface. In the ER, the signal peptide at the N-terminus (22 amino acids) is cleaved soon after translation and the hydrophobic signal at the C-terminus (23 amino acids) is removed upon addition of the GPI anchor (Stahl *et al.*, 1987; Turk *et al.*, 1988). Also, the protein obtains N-linked glycosylation at residues 182 and 198 and a disulphide bond is formed between residues 180 and 215 (Caughey *et al.*, 1989). During transit to the Golgi, sialic acid residues are added to the oligosaccharides. At the steady state of the protein unglycosylated, monoglycosylated and fully glycosylated forms coexist and can be detected by Western blot analysis. PrP^C is anchored to cell membrane by a GPI moiety and is preferentially localized in specialized domains of the cell membrane, rich in sphingolipids and cholesterol, known as lipid rafts. Lipid rafts mediate important physiological processes, such as signal transduction and transcytosis (Simons and Toomre, 2000). They are biochemically defined as detergent resistant membranes (DRM) because of their Triton X-

100 detergent insolubility at 4°C. They are considered crucial for the PrP^{C}-to-PrP^{Sc} conversion process (Naslavsky *et al.*, 1997; Taraboulos *et al.*, 1995). After reaching the cell surface, PrP^{C} does not reside permanently in raft domains. In contrast, it is regularly transfered between the plasma membrane and the endocytic compartment. The internalization is induced by copper ions, which bind the octapeptide region (Shyng *et al.*, 1993; Taylor *et al.*, 2005).

PrP^{C} undergoes different post-translational modifications as part of its normal metabolism. These are mainly directed clevages. A first cleavage takes place within and very near the GPI-anchor by a cell surface phospholipase and by a metalloprotease and promotes the release of the polypeptide chain in the extracellular milieu (Borchelt *et al.*, 1993; Harris *et al.*, 1993a; Parkin *et al.*, 2004). PrP^{C} further undergoes two distinct endoproteolytic cleavages (Hooper, 2005), the α- and the β- cleavage. The α-cleavage of PrP^{C} occurs inside the highly conserved hydrophobic region of the protein by the members of the ADAM (a disintegrin and metalloprotease) family (Shyng *et al.*, 1993; Taylor *et al.*, 2009; Vincent *et al.*, 2001) leading to the formation of a 9 kDa soluble N-terminal fragment (N1) and a 17 kDa C-terminal fragment (C1), still attached to the cell membrane through the GPI-anchor. The α-cleavage can occur either in DRM (Taraboulos *et al.*, 1995), or in a raft-independent manner within a late compartment of the secretory pathway (Walmsley *et al.*, 2009). The β-cleavage of PrP^{C} occurs within or adjacent to the octapeptide repeats and produces a 7 kDa N-terminal fragment (N2) and the complementary 19 kDa GPI-anchored C-terminal fragment (C2) that typically accumulates in prion-infected cells and brains (Caughey *et al.*, 1989; Mange *et al.*, 2004). The β-cleavage is mediated by reactive oxygen species and could play a role in cellular resistance to oxidative stress (Watt *et al.*, 2005). Apart from the GPI-anchored form, that is fully extracellular, two additional, topologically distinct PrP variants have been reported: ^{Ntm}PrP (transmembrane segment of PrP, N-terminus on the exofacial surface) and ^{Ctm}PrP (transmembrane segment of PrP, C-terminus on the exofacial surface). These forms have opposite orientations with respect to the lumen of the ER and are normally present in minute amounts in the absence of predisposing mutations (Hegde *et al.*, 1998; Stewart and Harris, 2001). Nuclear forms of PrP carrying stop-mutations at codon 145 and 160 have also been described (Lorenz *et al.*, 2002; Zanusso *et al.*, 1999).

1.12. Antibodies against the prion protein PrP^C

Active and passive immunotherapy can promote the clearance of pathological aggregates and thus represent legitimate therapeutic strategies in protein aggregation diseases (Aguzzi and O'Connor, 2010). Preclinical studies in transgenic mouse models have illustrated the potency of active immunotherapy in the prevention of both AD and TSEs (Wisniewski and Boutajangout, 2010; Wisniewski and Goni, 2015). However, active immunotherapeutic strategies in prion diseases had neither significantly improved the survival time of prion inoculated mice (Magri *et al.*, 2005; Sigurdsson *et al.*, 2003) nor induced high-affinity immune responses to PrP^C in wt mice (Polymenidou *et al.*, 2004). Passive immunotherapy turned out to be more efficient. Trangenic mice, expressing the heavy chain of an anti-PrP^C antibody were protected from peripheral prion infection (Heppner *et al.*, 2001). A later study showed that passive intraperitoneal immunization with the ICSM18 and ICSM35 anti-prion antibodies prevented peripheral infection with Rocky Mountain Laboratory (RML) strain (mouse adapted) scrapie prions. Unfortunately, the same antibody treatment did not induce any advantageous response against inracerebral inoculation with RML prions (White *et al.*, 2003). Likewise, peripheral administration of the 31C6, 110 and 44B1 anti-prion antibodies increased survival of mice inoculated with the Chandler and Obihiro prion strains (Ohsawa *et al.*, 2013). Intraventricular administration of the 31C6 anti-prion antibody through osmotic mini pumps also prolonged survival of prion inoculated mice (Song *et al.*, 2008). A summary of the active or passive immunization preclinical studies are presented in the table below (**Table 1.4.**).

Study design	Antibody	Outcome
Transgenic expression of antiprion antibodies	6H4	Protection against i.p. RML prion inoculation
Active immunization with PrP peptides	$PrP_{131–150}$	Immunogenic response and reduction of PrP^{Sc} in tumor transplants
	$PrP_{211–250}$	
Active vaccination with recombinant mouse prion protein	Full length rPrP	Prolonged latency and clinical course after i.p. 139A prion inoculation
Passive immunization with antiprion holoantibodies	ICSM18 ICSM35	Protection against i.p. RML prion inoculation
Active immunization with PrP peptides	$PrP_{105–128}$	Increased survival in a hamster model of TSE
	$PrP_{119–146}$	
	$PrP_{142–179}$	
Passive immunization with holoantibodies and $F(ab)_1$ fragments delivered by osmotic minipumps	4H11	Severe untoward effects with neuronal cell loss, astrogliosis and microglia activation
Passive immunization with holoantibodies delivered by osmotic minipumps	110	Partial prolongation of survival after intracerebral inoculation with the Chandler and Obihiro prion strains
	31C6	
	44B1	
Passive immunization with holoantibodies injected into the tail vein	31C6	Minimal prolongation of survival time

Table 1.3. Summary of the active and passive immunization preclinical trials in prion diseases (Reimann *et al.*, 2016)

However, certain antibodies against PrP^C have also been reported to induce brain damage. Chronic intracerebral administration of the antiprion antibody 4H11 led to severe neuronal loss, gliosis, and microglial activation (Lefebvre-Roque *et al.*, 2007). Likewise, stereotaxic injection of various anti-PrP^C antibodies, such as POM, targeting the globular domain of PrP^C, triggered neuronal apoptosis (Solforosi *et al.*, 2004; Sonati *et al.*, 2013).

Toxic anti-PrP^C antibodies induce damage by stimulating pathways similar to the *bona fide* prion infections, such as activation of calpains and PERK pathway and production of reactive oxygen species (Doolan and Colby, 2015; Falsig *et al.*, 2012; Herrmann *et al.*, 2015; Sonati *et al.*, 2013). The proposed mechanism of action postulates that the amino-terminal, flexible tail of PrP^C mediates the toxicity of antiprion antibodies by binding to the globular domain of PrP^C (Sonati *et al.*, 2013). Administration of the D13 anti-prion antibody, which also binds to the globular domain of PrP^C, was also shown to induce neurotoxicity in *Tga20* mice (Bueler *et al.*, 1992; Fischer *et al.*, 1996). However, Klöhn and co-authors did not replicate the reported neurotoxic effects of D13. Moreover, no acute toxicity of *in vivo* administration of ICSM18 and ICSM35 anti-prion antibodies was reported (Klohn *et*

al., 2012). Therefore, D13 and ICSM18, surprisingly, unlike the other globular-domain neurotoxic ligands were reported to be innocuous. The aforementioned discrepancy was recently addressed by Reimann *et al.* POM1, D13 and ICSM18 (all antiprion antibodies against a set of epitopes at the globular domain of PrP^{C}) induced acute, dose-dependent neurotoxicity both *ex vivo* and *in vivo* (Reimann *et al.*, 2016).

Nevertheless, not all antiprion antibodies are intrinsically toxic. Out of 12 POM antibodies tested (Polymenidou *et al.*, 2008), 5 were reported to be innocuous *ex vivo* in organotypic slice cultures. The innocuousness of POM2 (an octapeptide repeat ligand) was further confirmed *in vivo* in *Tga20* mice (Sonati *et al.*, 2013).

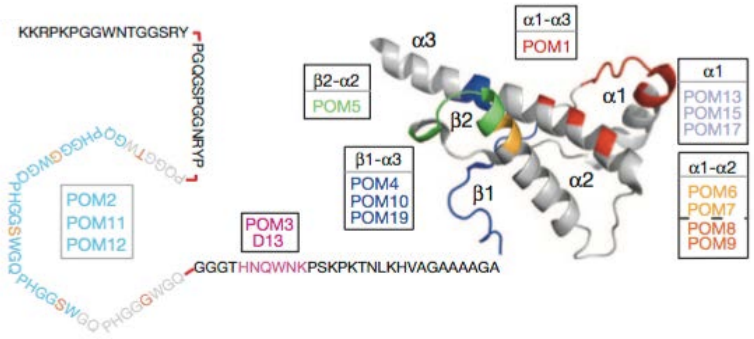

Figure 1.12. POM antibodies

Schematic diagram of the binding sites of POM, anti-PrP^{C}, antibodies. POM6–9, 13, 15 and 17 bind helix a1 and compete with the toxic POM1 antibody. POM6 and POM7 (light orange) show additional binding sites at helix a2 (dark orange), whereas POM5 recognizes a unique epitope at the b2–a2 transition (green). Innocuous antibodies (POM2, POM11, POM2; light blue) bind to the globular domain of PrP^{C} [modified by (Sonati *et al.*, 2013)].

Likewise, 31C6, 44B1 and 110 antiprion antibodies did not show neurotoxicity at high doses in preclinical efficacy experiments (Ohsawa *et al.*, 2013; Song *et al.*, 2008).

Altogether, the efficacy of antiprion antibodies seems to rely on both intrinsic factors (the targeting epitope on PrP^{C}) and extrinsic factors (the route of administration and dosage). Despite the potential of immunotherapeutic studies for prion diseases, these issues need to be seriously taken into

consideration before conducting any human clinical trials.

1.13. The physiological function of PrP^C - insights gained from transgenic mice and interaction partners

Like other GPI-linked proteins, PrP^C is located on the extra-cytoplasmic milieu of the lipid bilayer and is mostly associated with membrane lipid rafts (Harris, 1999; Taraboulos *et al.*, 1992). Despite decades of research the exact function of PrP^C and its role in prion diseases remains unclear. However, the remarkable conservation of the Prnp gene (>85% homology between mouse and human sequences) and its ubiquitous expression in vertebrates indicate that the gene executes an essential function (Cotto *et al.*, 2005; Wopfner *et al.*, 1999). There is little doubt that the formation and progressive accumulation of PrP^{Sc} in the brain is the triggering factor of neurodegeneration and disease. However, the mechanism by which PrP^{Sc} is involved in the disease pathogenesis and what is the role of PrP^C remains largerly unknown. A better understanding of the function of PrP^C in homeostasis could assist the evolutionary interpretation of the Prnp gene conservation, annotate its role in pathogenesis and hightlight the molecular pathways of prion diseases. The localization of PrP^C at the membrane and the insertion of the GPI-anchor are suggestive of three potential functions: capture of an exogenous ligand, adhesion to cells or to the extracellular matrix and signalling. But how can PrP^C, an extracellular GPI-linked protein, initiate intracellular signaling modifications? Most likely this process requires mediation by transmembrane constituents, and indeed many studies aimed at the identification of the elusive ‘protein X’; considered being an integral part of the pathogenic conformational conversion mechanism and pathology (Prusiner, 1998; Telling *et al.*, 1995). In order to elucidate the normal function of PrP^C researchers have utilized multiple techniques: deletion or knockout models in mice and other animals, human genetics, over/ectopic expression, biochemical techniques to identify critical PrP^C-dependent cellular processes and interaction partners (Bosque *et al.*, 1995). The techniques used and the putative functions will be discussed in detail in the following paragraphs.

1.13.1. Generation and properties of Prnp$^{-/-}$ mice

In order to elucidate the normal function of PrP^{C} researchers sought to produce animals in which the Prnp gene was deleted. The advent of homologous recombination and molecular cloning techniques [cloning of the cDNA coding the entire open reading frame (ORF) of the mouse Prnp was published in 1986 (Locht *et al.*, 1986)] favored the generation of Prnp-knockout (Prnp$^{-/-}$) animals. The first Prnp$^{-/-}$ mice, designated Zurich I (ZrchI) were produced by the Weissmann group in a mixed C57BL/6J x 129/Sv(ev) background, by replacing codons 4-187 (insertion into the only coding exon of Prnp) with a neomycin phosphotransferase (neo) expression cassette. Mice developed normally and displayed no overt abnormalities in size, weight, fertility, behavior and appearance of brain, skeletal muscles and visceral organs. Behavioral tests, such as Morris' water maze, Y maze discrimination and a test scoring for the efficiency of distinct problem solving strategies, showed no defects in behavior or learning (Bueler *et al.*, 1992). A second line of Prnp$^{-/-}$ mice under 129/Ola background, known as Npu or Prnp$^{-/-}$ Edinburgh (Edbg), was produced soon after by interruption of the Prnp ORF at position 93 and insertion of the neo cassette after the splice acceptor site. Similar to the ZrchI, the Edbg mice did not present any overt developmental defects (Manson *et al.*, 1994). The absence of any apparent phenotype in these Prnp$^{-/-}$ lines suggested that the function of PrP^{C} is redundant or inert. The only remarkable finding was that host expression of PrP^{C} is necessary to maintain prion replication and induce prion toxicity; since Prnp$^{-/-}$ lines show complete resistance to prion infections (Bueler *et al.*, 1993). In contrast, the next Prnp$^{-/-}$ mouse lines: the Nagasaki, (Katamine et al., 1998; Sakaguchi et al., 1996), the Rcm0 (Moore *et al.*, 1999) and the Zurich II (Rossi *et al.*, 2001) lines, generated with extensive deletions in the Prnp gene, displayed Purkinje cell loss and cerebellar ataxia. The striking phenotypic differences between the former and the latter group of Prnp$^{-/-}$ mouse lines were attributed to the deletion strategy (Weissmann *et al.*, 1996), which drove the ectopic, chimeric and over-expression of a PrP^{C} paralogue gene (Prnd) encoding Doppel (Dpl) (Li *et al.*, 2000; Moore *et al.*, 1999). This was later confirmed by the re-introduction of Prnp in Prnd overexpressing mice. Prnp re-introduction rescued the phenotypic alterations caused by ectopic expression of Dpl in thr brain, suggesting that it was the ectopic expression of Dpl in the absence of PrP^{C}, rather than the absence of PrP^{C} per se, that caused the phenotypic abnormalities (Moore *et al.*, 2001; Nishida *et al.*, 1999). An overview of the knock-out strategies for the generation of the above mentioned lines is presented below (**Figure 1.13.**).

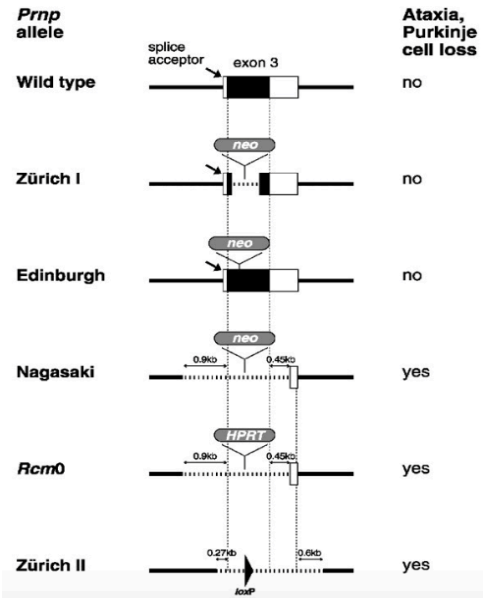

Figure 1.13. Overview of the know-out strategies for the generation of Prnp$^{-/-}$ mouse lines

Schematic diagram of the various strategies used to target the Prnp locus by homologous recombination for the generation of Prnp$^{-/-}$ mouse lines. The black boxes represent PrP ORFs; white boxes, non-coding Prnp regions; grey boxes, inserted sequences; dotted line, deleted regions; neo, neomycin phosphotransferase; HPRT, hypoxanthine phosphoribosyltransferase; loxP (black arrowhead), a 34-bp recombination site from phage P1 [modified by (Montrasio *et al.*, 2000)].

The recent advent of site-specific recombination technology allowed the generation of conditional PrP knockout NFH-Cre/tg37 mice, to study the effects of PrP depletion on neuronal survival and function in the adult brain (Mallucci *et al.*, 2002). These bigenic mice were generated by breeding a floxed PrP transgenic mouse with a NFH-Cre transgenic mouse [expressing the phage P1 enzyme Cre recombinase using the control elements of the murine neurofilament (NFH) gene]. Cre-mediated ablation of PrP in neurons was initiated at week nine. For up to 15 months post knock-out, no overt phynotype (signs of histopathological changes or neurodegeneration) was reported. Only subtle electrophysiological abnormalities [significant reduction of afterhyperpolarization potentials (AHPs)] in hippocampal CA1 cells were observed; suggesting a role of PrP^{C} in the modulation of neuronal excitability.

Multiple functions for PrP^C have been proposed based on the phenotyped of $Prnp^{-/-}$ mice. However, all the aforementioned $Prnp^{-/-}$ mouse lines were generated in embryonic stem cells from the 129 mouse strain and crossed to non-129 strains. This resulted in Prnp-linked polymorphic loci between 129 and backcrossing strain. As an effect, erroneous conclusions were drawn due to insufficient accounting for systematic genetic confounders. Recently, TALEN-mediated genome editing techniques were used to generate the Zurich-3 (ZH3) Prnp-ablated allele on a pure C57BL/6J background (Nuvolone *et al.*, 2016). Profound (genomic, transcriptional and phenotypic) characterization of these mice was performed and failed to identify any of the phenotypes reported in non-co-isogenic $Prnp^{-/-}$ mouse lines. Of note, aged Prnp (ZH3/ZH3) mice developed chronic demyelinating peripheral neuropathy supporting the described role of PrP^C in peripheral myelin maintenance (Bremer *et al.*, 2010; Kuffer *et al.*, 2016).

1.13.2. Generation and properties of PrP deletion mutant mice

Although the physiological and molecular functions of PrP^C still remain elusive, new insights were gained by the expression of partially deleted Prnp variants in cultured cells and transgenic mice. The main aim for the production of these constructs was to identify the essential domains for restoring prion susceptibility. But, these mice rather permitted the identification of functionally relevant domains within PrP^C. Investigators reported that specific domain expression, in $Prnp^{-/-}$ background, induced spontaneous neurodegeneration [as reviewed in the figure below, (**Figure1.14.**)]. Often, these phenotypes were partially or fully rescued by co-expression of wt PrP^C (Aguzzi *et al.*, 2008).

1.13.2.1 Amino-terminal deletion mutants of PrP

Transgenic mice harboring deletions between residues 32-121 (PrP Δ32-121) or 32-134 (PrP Δ32-134), on a PrP-deficient genetic background, exhibited a spontaneous neurodegenerative illness (severe apoptosis of cerebellar granular neurons and ataxia) even without inoculations with scrapie prions (Shmerling *et al.*, 1998). In these mice widespread white matter disease (severe demyelination and axonal loss in the spinal cord and the cerebellar white matter) was additionally observed, which could be rescued by expression of endogenous PrP^C in both neurons and glia (Radovanovic *et al.*, 2005).

PrPΔ32-134 and Dpl both lack the flexible N-terminal domain and have a similar structure. Therefore they could also share the same mechanisms of neurodegeneration (Weissmann and Aguzzi, 1999). Indeed, it was shown that PrPΔ32-134 expression targeted to Purkinje cells of ZrchI *Prnp*$^{-/-}$ mice led to their selective degeneration, whereas the granule cell layer was unaffected (Flechsig et al., 2003). Mice with shorter deletions [32-80 (PrPΔ32-80), 32-93 (PrPΔ32-93), 32-106 (PrPΔ32-106) had a normal phenotype, suggesting an important role for amino acids distal to residue 106. Transgenic mice expressing truncated PrPΔ94-134, but not those expressing a smaller deletion PrPΔ114-121 (residues spanning the HC domain), also showed extensive central and peripheral myelin degeneration and early ataxia (Baumann *et al.*, 2007b). Yet, transgenic animals expressing an even smaller truncation, PrPΔ105-125 (residues spanning the CC domain) showed a more acute pathology (Li *et al.*, 2007). These mice developed a severe illness within two weeks of birth and died within one month. Pathological signs inlcuded: decreased body size and weight, immobility, impaired righting reflexes, myoclonus and tremor. Histopathological stainings revealed severe loss of cerebellar granule cells, cerebellar atrophy, gliosis and astrocytic hypertrophy. Notably, all the above mentioned degenerative phenotypes can be rescued by re-introduction of the wt PrP allele (Baumann *et al.*, 2007b; Li *et al.*, 2007; Shmerling *et al.*, 1998).

1.13.2.2 Carboxy-terminal deletion mutants of PrP

Transgenic mice harboring deletions at the C-terminal of PrP^{C} also showed altered phenotypes.

Mice expressing PrP mutants with deletions pertaining Helix 2 (PrPΔ177-200), Helix 3 (PrPΔ201-217) or both helices 2 and 3 (PrPΔ141-221), together with a deletion spanning the octapeptide region (residues 23-88) that is per se innocuous, exhibited neuronal storage disease associated with neurodegeneration, ataxia and features of cerebellar disorder (Muramoto *et al.*, 1997). Contrary to the group of delection mutants affecting the CC and HC domains, none of C-terminal deletion associated diseases were transmissible to normal wt mice. Also, presence or absence of wt PrP didn't affect manifestation and progression of the disease.

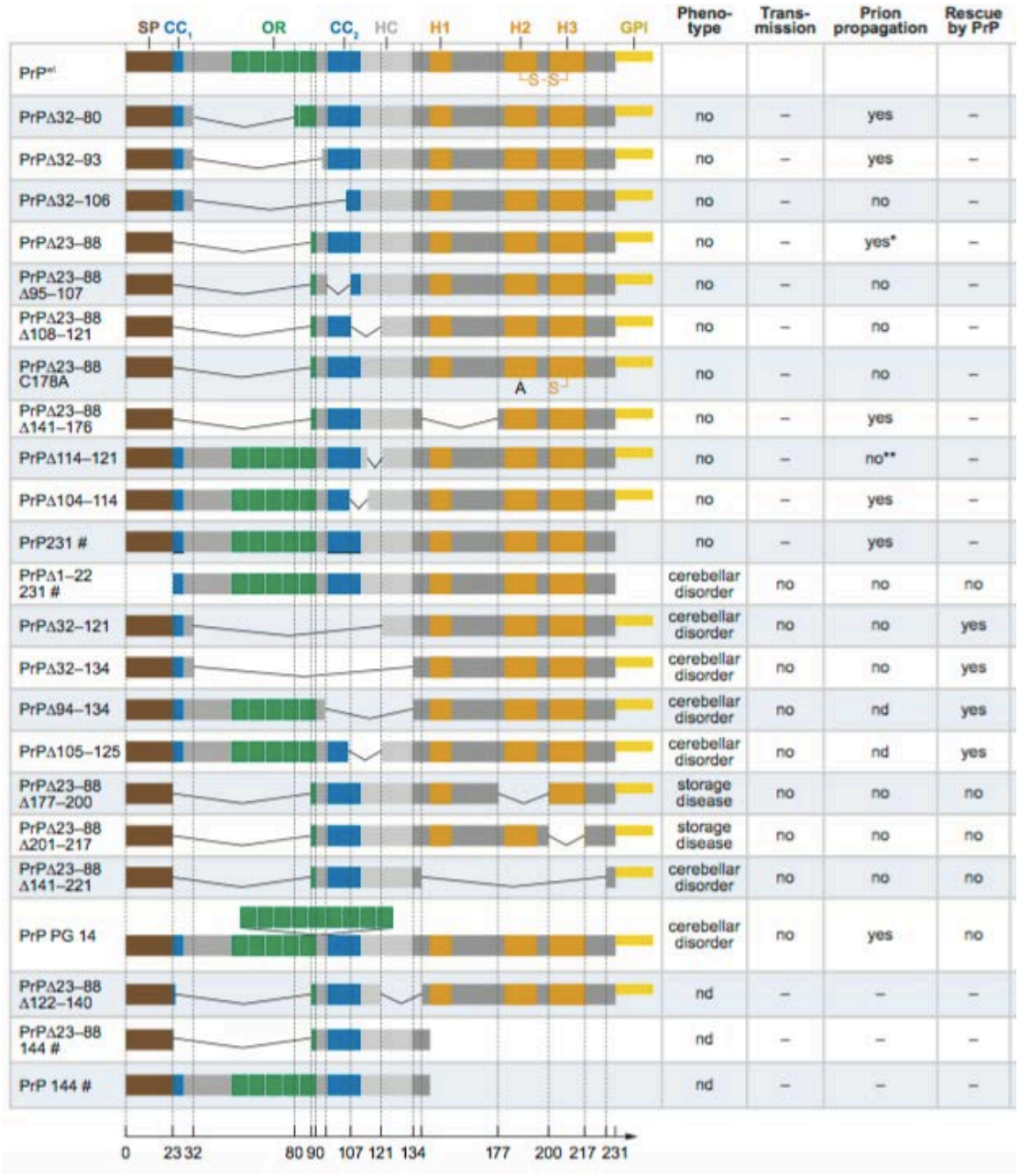

	Pheno-type	Trans-mission	Prion propagation	Rescue by PrP
PrP[C]				
PrPΔ32–80	no	–	yes	–
PrPΔ32–93	no	–	yes	–
PrPΔ32–106	no	–	no	–
PrPΔ23–88	no	–	yes*	–
PrPΔ23–88 Δ95–107	no	–	no	–
PrPΔ23–88 Δ108–121	no	–	no	–
PrPΔ23–88 C178A	no	–	no	–
PrPΔ23–88 Δ141–176	no	–	yes	–
PrPΔ114–121	no	–	no**	–
PrPΔ104–114	no	–	yes	–
PrP231 #	no	–	yes	–
PrPΔ1–22 231 #	cerebellar disorder	no	no	no
PrPΔ32–121	cerebellar disorder	no	no	yes
PrPΔ32–134	cerebellar disorder	no	no	yes
PrPΔ94–134	cerebellar disorder	no	nd	yes
PrPΔ105–125	cerebellar disorder	no	nd	yes
PrPΔ23–88 Δ177–200	storage disease	no	no	no
PrPΔ23–88 Δ201–217	storage disease	no	no	no
PrPΔ23–88 Δ141–221	cerebellar disorder	no	no	no
PrP PG 14	cerebellar disorder	no	yes	no
PrPΔ23–88 Δ122–140	nd	–	–	–
PrPΔ23–88 144 #	nd	–	–	–
PrP 144 #	nd	–	–	–

Figure 1.14. Overview of the PrP deletion mutants

Schematic drawing of full-length murine PrP^{C}, including the signal peptide of the precursor protein (SP; brown box). All the major domains are also included: charged cluster 1 (CC1), charged cluster 2 (CC2), octarepeat region (OR), hydrophobic core (HC) and alpha helixes 1-3 (H1-H3). Mouse PrP also contains a disulphide bond (S-S) and a GPI-anchor. The first column denotes the individual mutants (defined as deletions of specific residues, e.g. the construct which harbors the deletion of residues 32-80 is defined as PrPΔ32-80). The four columns on the right indicate presence or absence of phenotypic abnormalities in transgenic mice when expressed on a PrP-deficient genetic background, transmissibility of the phenotype to recipient mice, rescue of the phenotype by co-

expression of wt PrP and susceptibility of transgenic mice to prions after intracerebral inoculation with a mouse adapted strain of scrapie prions [modified by (Aguzzi *et al.*, 2008)].

1.13.3. PrP^C and divalent ions

One of the first suggestions was that PrP^C plays a role in copper metabolism. This hypothesis was supported by the identification of two copper binding domains (at residues 96 and 111) as well as copper (Cu^{2+}) ion binding at the histidine-containing octapeptide repeat region of PrP^C (Brown *et al.*, 1997a). Therefore, it was hypothesized that PrP^C could function as a transporter for copper. This was tested in an inducible cell system, where the levels of PrP^C correlated with the amount of Cu^{2+} binding to the membranes, but not with its transportation rate (Rachidi *et al.*, 2003). In addition the transportation of Cu^{2+} ions to synaptosomes was reported to be independent of the expression of PrP^C (Giese *et al.*, 2005). Additionally, the binding of copper to PrP^C seemed to protective against oxidative stress by preventing reactive oxygen species (ROS) generation via free Cu^{2+}-mediated redox reactions. Cultured $Prnp^{-/-}$ neurons were more vulnerable than wt to high levels of Cu^{2+}. This was blocked by treatment with a synthetic PrP^C 59–91 peptide (Brown *et al.*, 1998). Likewise, brain tissue from PrP knockout mice exhibited biochemical changes indicative of oxidative stress, such as increased levels of protein carbonyls and lipid peroxidation products (Wong *et al.*, 2001). In addition, $Prnp^{-/-}$ mice were more susceptible to brain lesions induced by hypoxia and ischemia (Sakurai-Yamashita *et al.*, 2005; Spudich *et al.*, 2005). The exact mechanism by which copper and PrP^C are functionally related is still not clear. Three different mechanisms were suggested: a) PrP^C exerts a copper-dependent superoxide dismutase (SOD) activity, b) Cu^{2+}-induced endocytosis of PrP^C induces an antioxidative defence signal (Brown *et al.*, 2001; Brown *et al.*, 1999) and c) a PrP-dependent increase in the expression of antioxidant enzymes, such as catalase and glutathione reductase (Klamt *et al.*, 2001; White *et al.*, 1999) . Yet, a couple of other studies failed to confirm an effect of PrP^C on SOD level or an intrinsic dismutase activity of PrP^C (Hutter *et al.*, 2003; Waggoner *et al.*, 2000).

Alterations in copper transport and homeostasis, leading to CNS dysfunction, have been documented in humans and animals in multiple neurodegenerative diseases. The evidence that PrP^C plays a role in copper metabolism may be important in understanding the pathogenesis of prion diseases, since loss of this copper-related function (as a result of conversion to PrP^{Sc}) could be accountable for certain phenotypes. Interestingly, early studies reported that cuprizone, a copper-chelating agent,

induces neuropathological changes in mice similar to those found in prion diseases (Waggoner *et al.*, 1999), suggesting a role for copper in these disorders.

Apart from copper, PrP^{C} was shown to bind to other divalent ions, such as manganese (Mg^{2+}), iron (Fe^{2+}) and zink (Zn^{2+}). Using the PMCA technique, Kim *et al.*, showed that manganese, like copper, can bind to PrP^{C} and induce the generation of PrP^{Sc} (Kim *et al.*, 2005). Also, mice infected with PrP^{Sc} exhibit significant differences in the content of metal ions in blood, muscle and brain, compared to non-infected mice. Interestingly, the PrP^{Sc} infected mice had increased Mg^{2+} and decrease Cu^{2+} content, suggesting a role of altered metal content in the disease manifestation and progression (Thackray *et al.*, 2002). Last but not least, the presence of Mg^{2+} has also been shown to favor the formation of PK resistant forms of PrP^{C} (Brown *et al.*, 2000). With regards to iron, Fernaus *et al.* showed that PrP^{Sc} infection disrupted the normal regulation and processing of iron, resulting in increased levels of the labile iron pool (LIP), decreased levels of ferittin and the formation of ROS, in mouse neuroblastoma N2a cells. These findings suggest scrapie infection results in cell death by altering iron metabolism and reducing the cell's capacity to counteract the presence of excessive iron (Fernaeus *et al.*, 2005a; Fernaeus and Land, 2005; Fernaeus *et al.*, 2005b). Zinc on the other hand, similar to Cu^{2+}, induces transfer of the prion protein from the plasma membrane to a subset of early endosomes and the Golgi (Brown and Harris, 2003). Also Cu^{2+} and/or Zn^{2+} binding mediate the aggregation and the neurotoxic properties of the PrP106-126 peptide (Jobling *et al.*, 2001).

1.13.4. Anti-oxidative and anti-apoptotic activity of PrP^{C}

Several lines of evidence indicated that PrP^{C} might have a cytoprotective activity. Multiple experimental systems, including cultured mammalian cells, yeast and mice have been used to test this hypothesis. Immortalized hippocampal neurons (HpL3-4 cells) derived from $Prnp^{-/-}$ mice were highly sensitive to serum deprivation compared to their wt counterparts (Kuwahara *et al.*, 1999). The ability of PrP^{C} to counteract cell death was shown by transfection of knockout cells with *Prnp*. The mechanism seemed to involve Bax, a pro-apoptotic member of the Bcl-2 family, that plays a major role in postmitotic neurons of the central nervous system (Yuan and Yankner, 2000). The ability of PrP^{C} to counteract Bax-dependent apoptotic pathway was documented in multiple experimental systems, but the molecular pathways involved remain largely unknown (Roucou and LeBlanc, 2005).

Additionally, primary cultures of cortical and cerebellar granular neurons from ZrchI $Prnp^{-/-}$ mice undergo cell death faster compared to their wt counterparts upon oxidative stress (Brown *et al.*, 2002; Brown *et al.*, 1997c). Oxidation of both proteins and lipids was documented to contribute to the observed phenotype (Brown *et al.*, 2002). Moreover, $Prnp^{-/-}$ mice were reported to be more sensitive to seizures caused by kainic acid (Walz *et al.*, 1999).

An additional function attributed to PrP was its role in myelin maintenance in adult mice (Shmerling et al., 1998). Bremer *et al* elegantly demonstrated the association in 2010. In three independently targeted PrP strains (ZrchI, GFP and Edbg) (Bremer *et al.*, 2010) and later a forth (ZH3) (Nuvolone et al., 2016) ablation of PrP^C, specifically in neurons, triggered progressive chronic demyelinating polyneuropathy (CDP) associated with reduced grip strength and nociception. The fact that this phenotype persisted on four genetic backgrounds (C57BL6/6, 129, Balb/c and mixed) further supports the initial hypothesis. Mechanistic insights into the nature of axonal PrP^C's role in the maintenance of peripheral nervous system (PNS) myelin, were recently provided by the same group. PrP^C was reported to act as an agonistic ligand of the G protein-coupled receptor Adgrg6, causing a reduction of the cAMP concentration levels of the sciatic nerves from PrP^C-deficient mice (Kuffer *et al.*, 2016).

Unlike mice, the knockdown of the Prnp horthologs (PrP1 and PrP2) in zebrafish resulted in a loss of function phenotype. Knockdown of PrP1 cuased impairment of E-cadherin-mediated cell adhesion and signaling in the zebrafish embryos as well as arrested gastrulation, whereas knockdown of PrP2 had an effect on later developmental stages (impairing proliferation and differentiation of developing neurons) (Malaga-Trillo *et al.*, 2009).

1.13.5. Functional roles of PrP^C in neuronal excitability and synaptic activity

PrP^C is thought to play a role in synaptic structure, function and maintenance. Experiments on the localization of the PrP-EGFP tagged protein, as well as data from light and electron microscopy studies, indicated that PrP^C is enriched along axons and in pre-synaptic terminals (Herms *et al.*, 1999; Medrano *et al.*, 2008; Mironov *et al*., 2003) and subject to anterograde and retrograde axonal transport (Borchelt *et al.*, 1994; Moya *et al.*, 2004). Yet, PrP^C is also present in postsynaptic densities (Haeberle *et al.*, 2000). The presence of PrP^C at both pre- and post-synaptic sites advocates that it

plays a role in synaptic plasticity and neuronal communication. Consistent with this, synaptic pathology is often a prominent feature of prion diseases (Jeffrey *et al.*, 2000).

Electrophysiological recordings from hippocampal slices of $Prnp^{-/-}$ mice (ZrchI and Edbg lines), showed impaired long-term potentiation (LTP) at physiological temperature, associated with reduced $GABA_A$ receptor mediated fast inhibition (Collinge *et al.*, 1994; Manson *et al.*, 1995). This was rescued by addition of a transgene encoding PrP^C (Whittington *et al.*, 1995). In contrast, no deficits in cell excitability, synaptic inhibition, reversal potential or LTP were reported in another study, in which hippocampal slices from $Prnp^{-/-}$ mice (three different genetic backgrounds) were examined at room temperature (Lledo *et al.*, 1996). Also, no changes in the activity of $GABA_A$ receptors were reported in outside-out membrane patches of cerebellar Purkinje cells from $Prnp^{-/-}$ mice (Herms *et al.*, 1995). However, recently it was shown that post-tetanic potentiation and LTP were significantly reduced in the CA1 hippocampal region of aged $Prnp^{-/-}$ mice (ZrchI and Edbg lines), when compared with younger animals, possibly due to increased levels of oxidative stress during aging (Curtis *et al.*, 2003). Further studies also supported a positive correlation between the expression level of PrP^C and the facilitation of the excitatory synaptic transmission. Experiments in PrP-over-expressing mice showed supra-physiological responses (Carleton *et al.*, 2001); due to more efficient recruitment of pre-synaptic fibers.

A consistent electrophysiological phenotype in $Prnp^{-/-}$ mice is a reduction in the slow (late) afterhyperpolarization potential (AHP) (Asante *et al.*, 2004; Colling *et al.*, 1996; Fuhrmann *et al.*, 2006; Mallucci *et al.*, 2002; Powell *et al.*, 2008). Slow AHP is a property of many neurons. It is triggered by a series of repetitive action potentials, is mediated by an unknown Ca^{2+}-dependent K^+ channel and controls the post action potential firing. Although the absence of PrP^C was reported to influence Ca^{2+} homeostasis in cerebellar granular cells (Herms *et al.*, 2000), it did not alter the K^+ channels directly. It indirectly influences them by reducing Ca^{2+} influx through L-type voltage gated calcium channels (VGCCs) in CA1 hippocampal neurons (Fuhrmann *et al.*, 2006) or by changing the maximal amplitude of Ca^{2+}-activated K^+ currents in cerebellar Purkinje cells (Herms *et al.*, 2001). Alternatively, the observed reduced slow AHP in $Prnp^{-/-}$ neurons could be attributed to an increased Ca^{2+} buffering at the endoplasmic reticulum (ER), due to an increased activity of the sarco/endoplasmic reticulum calcium ATPase (SERCA) (Powell *et al.*, 2008). Conditional PrP^C ablation in adult neurons led to reduced AHP and thus increased neuronal excitability , due to loss of PrP^C function (Mallucci *et al.*,

2002). A few years later, re-introduction of PrP^C rescued the impairment of Ca^{2+}-activated K^+ currents in Purkinje cells from $Prnp^{-/-}$ mice (Herms *et al.*, 2001).

Further evidence on the role of PrP^C in neuronal excitability is provided by studies of $Prnp^{-/-}$ mice which show lower threshold to proconvulsant drug-induced seizures (Rangel *et al.*, 2007; Walz *et al.*, 1999) as well as by studies in *Tga20* mice which show that PrP^C over-expression is associated with increased susceptibility to kainate-induced seizures (Rangel *et al.*, 2009). Consistent with the aforementioned neuronal excitability data in $Prnp^{-/-}$ mice, anatomical changes within the hippocampus were reported, suggesting a re-organization of the neuronal circuitry resembling the "epileptic neuronal network" (Colling *et al.*, 1997). The observed susceptibility to neuronal damage in $Prnp^{-/-}$ mice correlated with altered expression of AMPA/kainate and NMDA glutamate receptors (Maglio *et al.*, 2004; Rangel *et al.*, 2007). More specifically, it was shown that PrP^C suppressed NMDA receptor activation and blocked excitotoxic Ca^{2+} influx by binding to NMDA receptors containing NR2D subunit (Khosravani *et al.*, 2008; Senatore *et al.*, 2012). Although PrP^C ablation increased neuronal excitability in the hippocampus, juvenile (up to 25 days of age) $Prnp^{-/-}$ mice showed defective neuronal excitability and synaptic plasticity in the cerebellar granular layer and thus impaired motor control. The phenotype was associated with a delayed maturation of cerebellar granule cells and dissipated P40–P50 along with the recovery of normal motor behaviour; indicating a role of PrP^C in motor control and formation of the cerebellum (Prestori *et al.*, 2008).

Despite the numerous studies indicating a role of PrP^C in synaptic plasticity and neuronal excitability, the precise molecular mechanisms remain largerly unknown. It was proposed that PrP^C acts as a copper uptake protein and buffers Cu^{2+} levels in the synaptic cleft so as to reduce Ca^{2+} influx via VGCCs, regulate synaptic calcium homeostasis and neurotransmission (Vassallo and Herms, 2003) and protect synapses from oxidative damage (Brown, 2001b).

Altogether, these studies identify a role of PrP^C in modulating various neuronal processes. PrP^C seems to affect not only neuronal proliferation and differentiation but also essential mechanisms of neuronal function: excitability and synaptic transmission. The observed experimental discrepancies could be attributed to differences in the genetic background of the knockout lines that were used in the studies. Further experiments are needed to clarify the issue.

1.14. PrP^C-interactors mediated effects

An alternative method for resolving the physiological function of PrP^C would be to identify other cellular proteins with which PrP^C interacts. These interactors are likely to be units of the physiological pathways in which PrP^C plays a role (Linden *et al.*, 2008; Oesch *et al.*, 1990).

There are certain structural features within PrP^C that could allow it to interact with other proteins; such as a copper binding domain (58-110 aa), an amphipathic helix near the middle of the molecule and the GPI anchor which may internalize and deliver signals. Multiple potential PrP^C-interacting partners have been detected so far using conventional yeast two-hybrid screens, co-immunoprecipitation, crosslinking as well as other methods. Quite a few groups have reported that PrP^C binds and internalizes copper ions (Brown *et al.*, 1997b; Hornshaw *et al.*, 1995; Viles *et al.*, 1999). This action enhances the activity of superoxide dismutase (SOD) enzymes and thus increases the resistance against oxidative stress (Brown and Besinger, 1998; Brown *et al.*, 1997c).

The localization of PrP^C at the the plasma membrane additionally regulates its neuroprotective effects. For example, in four different cell lines (GT1-7 neurohypothalamic cells, 1C11 neuroectodermal precursor, 1C11 differentiated neuronal cells and BW5147 lymphoid cells) antibody-mediated dimerization of PrP triggered rapid phosphorylation of extracellular regulated kinases (ERK) 1 and 2, supporting neuronal survival. Especially in 1C11 differentiated neuronal cells, Fyn kinase activation triggers the ERK1/2 stimulation (Grewal *et al.*, 1999; Mouillet-Richard *et al.*, 2000; Schneider *et al.*, 2003a). In these studies, PrP^C is considered a cellular redox homeostasis regulator. Interaction of PrP with the plasma membrane stress-inducible protein 1 (Stip 1) also triggers neuroprotection (Zanata *et al.*, 2002). In another study, mouse primary cerebellar granular neurons seeded onto a PrP^C-expressing substrate (either PrP-coated dishes or Chinese hamster ovary cells overexpressing PrP^C at their cell surface) exhibit increased neurite outgrowth and neuronal survival. The related mechanisms include activation of the phosphatidyl-inositol-3-kinase/Akt and the mitogen-activated protein kinase/ERK kinases pathways (Chen *et al.*, 2003; Graner *et al.*, 2000).

A well-established neuroprotective function of PrP^C is mediated through its connection with laminin receptor precursor 37LRP/67LR (Rieger *et al.*, 1997). The latter is a membrane-associated protein, which interacts with laminins and triggers a range of dynamic events (filopodia formation, directional motility and changes in gene expression). PrP^C also acts as specific, high affinity receptor for laminin; their interaction domain residing at the carboxy-terminal decapeptide (RNIAEIIKDI) of the laminin γ-1

chain (Graner *et al.*, 2000). The PrP^C-laminin complex also binds to the heparan-sulphate proteoglycan (HSPG) and in competition with 37LRP/67LR (Hundt *et al.*, 2001; Warner *et al.*, 2002). Interestingly, PrP^C-interaction with integrins (also laminin receptors) was reported to form a cluster that promotes neurotrophic signalling (Tzu and Marinkovich, 2008). Moreover, the PrP^C-vitronectin (Vn) binding was shown to stimulate axonal growth during embryogenesis as well as during cerebellar development (Hajj *et al.,* 2007; Hajj *et al.*, 2009).

Given that PrP^C binds to both laminin and vitronectin, it was suggested that it could be involved in the development of the cerebellum. The hypothesis was supported by data from $Prnp^{-/-}$ mice. During development, $Prnp^{-/-}$ mice exhibited altered excitability of cerebellar granular neurons and impaired synaptic transmission associated with motor abnormalities; due to a delay in granule cell maturation (Prestori *et al.*, 2008).

The neuroprotective role of PrP^C was further supported by studies showing that PrP^C -binding to astrocyte-secreted stress-induced protein 1 (STI1), promoted neuritogenesis, neuronal survival as well as memory formation and consolidation (Coitinho *et al.*, 2007; Lima *et al.*, 2007). PrP^C contacts STI1 through interaction with the "co-chaperone Hsp70/Hsp90 protein/STI1 (hop/STI1)" organizing complex. PrP^C-hop/STI1 interaction controls protein synthesis in neurons via the PI3K-Akt-mTOR and ERK1/2 pathways. The data were further validated in PrP^{Sc}-infected cells where protein synthesis was partially impaired due to prion infection; suggesting that prion infection may contribute to neuronal dysfunction and neurodegeneration (Roffe *et al.*, 2010).

Likewise, PrP^C also associates with several proteins on the neuronal cell surface to promote neural development. One of these molecules is the vesicle-associated protein synapsin Ib (Spielhaupter and Schatzl, 2001). Another is the neural cell adhesion molecule (NCAM) (Santuccione *et al.*, 2005). PrP has been identified in a complex with NCAM by chemical cross-linking (Schmitt-Ulms *et al.*, 2001). In primary neuronal cultures it was shown that NCAM undergoes PrP^C-mediated recruitment in lipid rafts to activate the p59 fyn kinase pathway (Bodrikov *et al.*, 2008) which induces neuritogenesis, neural development and synaptic plasticity (Ditlevsen *et al.*, 2008). NCAM also employs signalling molecules involved in cell adhesion; a process in which PrP^C may also plays a role. Subversion of PrP^C interactions with various membrane proteins has been suggested to promote neurotoxic signaling cascades in prion-induced toxicity (Hernandez-Rapp *et al.*, 2014).

Among the mebrane proteins interacting with PrP^C are glutamate receptors. N-methyl-D-aspartate receptors (NMDAR) are crucial regulators of glutamatergic transmission, and loss of both synapses and neurons has been attributed to inappropriate NMDAR activation (Khosravani *et al.*, 2008). The group-I metabotropic glutamate receptors (group I mGluRs), mGluR1 and mGluR5, can both associate with PrP^C and induce similar intracellular pathways (Beraldo *et al.*, 2011). Metabotropic glutamate receptors (mGluRs) were also reported to play a role in prion diseases. Impairment of the mGluR1/1-phosphatidylinositol 4,5-bisphosphate phosphodiesterase 1 (PLC1)/protein kinase C (PKC) signaling pathway has been observed in a murine model of BSE; abnormal mGluR1 signaling correlated with PrP^{Sc} deposition, histological changes, and clinical scores (Rodriguez *et al.*, 2006).

A role for group-I mGluRs is emerging in a multitude of CNS disorders including Fragile X syndrome, ischemia, multiple sclerosis, amyotrophic lateral sclerosis, Huntington's, and Parkinson's disease (Aguilar-Valles *et al.*, 2015; Caraci *et al.*, 2012; Dinamarca *et al.*, 2012; Dolen and Bear, 2008; Michalon *et al.*, 2014; Milanese *et al.*, 2014; Scharf *et al.*, 2015). In AD, PrP^C and mGluR5 may directly contribute to disease manifestation and toxicity of Amyloid β (Aβ) aggregates. Aβ oligomers can bind to PrP^C at the cell surface (Lauren *et al.*, 2009) and form complexes that contain mGluR5 receptors (Haas *et al.*, 2014). These receptors couple to G-proteins and trigger subcellular events that ultimately result in elevated intracellular Ca^{2+} levels.

In a mouse model of Aβ deposition, cognitive decline and synaptic alterations were rescued by mGluR5 inhibition (Um *et al.*, 2013).

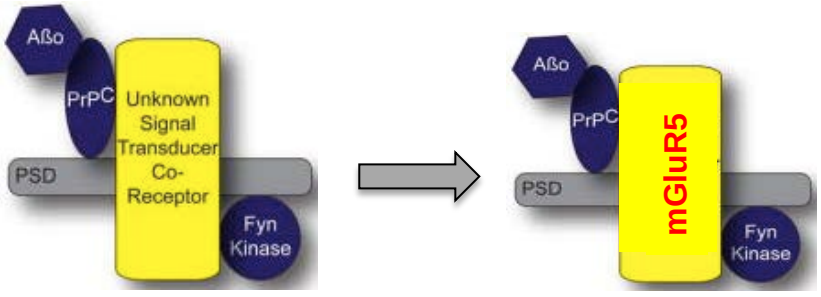

Figure 1.15. mGluR5 acts as a co-receptor which couples A [illegible]PrP^C to intracellular Fyn kinase.

Schematics which depict the Aβo in complex with PrP^C at post synaptic densities (PSD). The first schematic proposes that an unknown signal transducer is required to activate Fyn kinase signalling. The mGluR5 was identified as the unknown receptor [modified by (Um *et al.*, 2013)].

Furthermore, PrP^C-mGluR5 coupling was involved in Aβ-mediated inhibition of LTP and Aβ-facilitated LTD *in vivo* (Hu *et al.*, 2014). Also, genetic ablation of mGluR5 reversed disease-related memory deficits in a murine model of AD (APPswe/PS1ΔE9) (Hamilton A. *et al.*, 2014). In another study, exposure of cortical APPswe/PS1ΔE9 neuronal cultures to Aβ oligomers upregulated mGluR1 and PrP^C α-cleavage, whereas activation of group-I mGluRs increased PrP^C shedding from the membrane (Ostapchenko *et al.*, 2013). In primary hippocampal neurons, membrane-bound Aβ oligomers induce toxicity by promoting clustering of mGluR5 in synapses, resulting in elevated intracellular calcium and synaptic failure (Renner *et al.*, 2010). All these studies speak in favor of an role of group-I mGluRs in the pathogenesis of AD. On the other hand, others have reported that neither PrP^C ablation nor overexpression had any effect on neurotoxicity in AD models (Balducci *et al.*, 2010; Calella *et al.*, 2010; Cisse *et al.*, 2011; Kessels *et al.*, 2010). As a possible explanation for these discrepancies, it has been suggested that only a defined oligomeric fraction of Aβ (Kostylev et al., 2015) interacts with mGluR5 (Haas *et al.*, 2016).

In prion diseases, changes in mGluR1 expression levels, leading to reduced expression levels of phospholipases, were observed in the cerebral cortex of Creutzfeldt-Jakob disease (CJD) patients (Rodriguez *et al.*, 2005).

Collectivelly, group I mGluRs have emerged as potential targets for drug therapy in Parkinson's disease, Alzheimer's disease (Gasparini *et al.*, 2013), Fragile X syndrome (Dolen and Bear, 2009), schizophrenia (Vinson and Conn, 2012) and major depressive disorder (Deschwanden *et al.*, 2011), and finally prion diseases (Rodriguez *et al.*, 2005). The role of group I mGluR-PrP^C interaction as well as the aberrant group I mGluR signaling in prion- and prion-mimetic antibody-mediated toxicity is of utmost importance to the current study, as it will be defined in the aim of the study. Before this, the molecular and cellular pathways that lead to synaptic pathology will be discussed in detail.

1.15. Molecular and cellular pathways leading to neurodegeneration and synaptic pathology in prion diseases

Neuronal loss is a common feature in prion diseases and could account for some of the other observed pathologies such as astrogliosis and vacuolation. However, the identity of the misfolded, toxic PrP species and the pathways that induce neurodegeneration in prion disease are still elusive.

Given the relative lack of classical immunological response in TSE-affected brain (Brown, 1990), neurodegeneration in prion diseases was expected to follow a programmed cell death (PCD) and not necrotic pathway. Events that may lead to neuronal apoptosis include oxidative stress, dysfunction of endosomal-lysosomal systems, endoplasmic reticulum stress, synaptic alterations and dendritic atrophy, and microglial activation.

1.15.1. Apoptotic and authophagic cell death

Apoptosis is a process of programmed cell death, characterized by cell shrinkage, DNA fragmentation, condensation of chromatin and formation of apoptotic bodies (Liberski *et al.*, 2008).

The first observations of apoptotic cell death in prion diseases were made in the brains of patients with sporadic CJD and mice with experimental scrapie. Exposure to PrP^{Sc} resulted in cells with fragmented nuclei, DNA laddering and caspase activation (mainly caspase 3) (Ferrer, 2002; Siso *et al.*, 2002). Apoptosis was also reported in the cerebellum of Tg(PG14) mice (Chiesa *et al.*, 2000). The morphological aspects of apoptosis were also detected in GT1 hypothalamic cells, following infection with scrapie prions (Schatzl *et al.*, 1997). The same features were observed upon prion infection of primary cultured neurons and astrocytes (Cronier *et al.*, 2004). Apoptotic changes were also induced by the neurotoxic synthetic peptide PrP106–126 (Forloni *et al.*, 1993) as well as by mature amyloid fibrils produced from full-length recombinant mammalian prion protein (rPrP) in cultured cells and primary hippocampal and cerebellar neurons (Novitskaya *et al.*, 2006).

Autophagy, a process of orderly degragation and recycling of cellular components, could also be involved in prion diseases. Autophagic vacuoles were described in experimentally induced scrapie, CJD, GSS disease, and FFI (Liberski *et al.*, 2004); represented by membrane sequestration, by concentric arrays of double membranes and formation of autophagic vacuoles in all parts of the neuron including synaptic endings. Intraneuronal accumulation of PrP^{Sc}, which overload the catabolic machinery, is suggested as the culprit of the observed phenotype. Autophagy could also participate in the spongiform changes (Liberski *et al.*, 2004). At the molecular level, autophagic cell death correlated with the upregulation of the scrapie regulated gene 1 (Scrg1), which encodes a protein associated with the Golgi apparatus, as well as with autophagic vacuoles of degenerative neurons (Dron *et al.*, 2006).

1.15.2. Oxidative stress

Oxidative stress refers to the inability of a biological system to readily remove abundand reactive intermediates or to repair the damage caused by their accumulation.

Immunohistochemical studies in prion infected mouse brains showed the presence of nitrotyrosine, eme-oxygenase 1, and lipid oxidation markers; suggesting that oxidative stress may play a role in the prion pathology (Brown, 2005). In CJD brains, oxidative nucleic acid damage correlated with disease duration but not with PrP^{Sc} deposition (Guentchev *et al*., 2002). Also, cells infected with scrapie or treated with the neurotoxic PrP106–126 peptide showed decreased levels of antioxidants and oxidative damage (Brown, 2005). In bioaminergic neuronal cells treatment with the PrP106-126 peptide causes oxidative stress by activating a PrP^{C}-caveolin-Fyn signalling pathway and thus stimulating NADPH-oxidase activity (Pietri *et al.*, 2006; Schneider *et al.*, 2003b). *In vivo*, NOX2, an important NADPH oxidase, was markendly upregulated in microglia of CJD patients. Also, prion-infected, NOX2-deficient mice showed delayed onset of motor deficits and increased survival (Sorce *et al.*, 2014).

1.15.3. The endosomal-lysosomal system

In cell cultures, it was reported that the endosomal-lysosomal system is involved in the processing of both PrP^{C} and exogenous PrP^{Sc} (Campana *et al.*, 2005; Peters *et al.*, 2003; Taraboulos *et al.*, 1992); suggesting a role of these compartments in the PrP^{C} to PrP^{Sc} transformation (Caughey and Baron, 2006). It has also been proposed that pathogenic PrP oligomers could be directly released from host cells into the extracellular space by endosomal recycling and/or by exosome secretion (Fevrier *et al.*, 2004; Marijanovic *et al.*, 2009). Additionally, cysteine protease (lysosomal protease) inhibitors have been shown to inhibit PrP^{Sc} accumulation (Doh-Ura *et al.*, 2000; Fournier *et al.*, 2000; Laszlo *et al.*, 1992). Moreover, degenerating neurons showed an increased volume of cathepsin-D-immunoreactive lysosomes; suggesting an overloading of the endosomal-lysosomal system (Kovacs *et al.*, 2007).

1.15.4. Endoplasmic reticulum stress

Endoplasmic reticulum (ER) stress has been proposed as a potential mechanism of neuronal death in prion diseases. ER responds to cellular stress by activating adaptive pathways, termed unfolded protein response (UPR). This leads to reduced translation, induction of ER chaperones and

degradation of misfolded proteins (Bonifacino and Weissman, 1998). Prolonged ER stress results in alteraction of Ca^{2+} homeostasis and the cell death. Upregulation of several ER-related chaperones and activation of the ER-related caspase-12 have been reported in models of prion disease (Hetz *et al.*, 2007; Hetz *et al.*, 2003). ER stress induced by PrP peptides has also been linked to changes in Ca^{2+} homeostasis (Ferreiro *et al.*, 2004). ER stress has been also shown to induce the generation of a misfolded PrP formsthat (Hetz *et al.*, 2007); suggesting that ER stress could accelerates prion replication. However, genetic ablation of caspase or the X-box-binding protein-1 (XBP-1), a key effector of UPR, had no effect on prion infected mice (Hetz *et al.*, 2008; Steele *et al.*, 2007).

1.15.5. Astroglial and microglial activation

Activation of microglia and astrocytes is an early event in prion diseases (Prusiner, 1994). Astrocytic enzymes such as glial fibrillary acidic protein (GFAP) are up-regulated, following an increase in PrP^{Sc}, before the development of neuropathological lesions; suggesting a potential role of astrocytic activation in tissue damage (Liberski *et al.*, 2004). *In vitro*, addition of the toxic PrP82-146 peptide induced astrocyte proliferation (Fioriti *et al.*, 2007).

Microglia activation is generally confined to regions with spongiform change and PrP^{Sc} deposition (Brown, 2001a). Activated microglia, the resident immune cells of the CNS, respond to neuronal damage by rapid up-regulation or *de novo* expression of a variety of cytokines, chemokines and cell surface antigens (Perry and Gordon, 1988). Microglia activation is an early event in murine prion disease (Betmouni *et al.*, 1996; Cunningham *et al.*, 2003a; Cunningham *et al.*, 2005); sensitive to changes in neuronal homeostasis and early synaptic damage. For example, anti-inflammatory response of microglia, following neurodegeneration in synaptic boutons, has been reported in mice infected with the ME7 prion strain at the early stages of the disease (Boche *et al.*, 2006). However, chronic microglial activation induces neuronal damage, associated with induction of proinflammatory cytokines, ROS, proteases, and complement proteins (Chiarini *et al.*, 2006). Microglia recruitment close to PrP aggregates is regulated by chemokines, acting through the activation of specific G-protein-coupled receptors. Moreover, PrP^{Sc} accumulation triggered the up-regulation of the chemokine RANTES, through the activation MAPK/ERK1/2 pathways (Marella and Chabry, 2004). A role of microglia in the propagation of oxidative stress in prion diseases has also been hypothesized. Addition of the toxic PrP106-126 peptide to neuron/glia co-cultures elicited an over-production of the

pro-inflammatory cytokines IL-1β and IL-6 by microglial cells (Peyrin *et al.*, 1999). Microglial cells exacerbated the toxic effect of PrP106-126 peptide on neuronal cultures by producing ROS (Brown *et al.*, 1996). *In vivo*, NOX2 levels were significantly increased in microglia of CJD patients. Also, prion-infected, NOX2-deficient mice showed delayed onset of motor deficits and increased survival (Sorce *et al.*, 2014).

1.15.6. Synaptic and dendritic *p*athology

Several immunohistochemical studies showed accumulation of PrP^{Sc} at the synaptic terminals; suggesting synaptic pathology as a primary event in prion diseases. Indeed, in rodent models of prion disease synaptic accumulation of PrP^{Sc} and prominent synaptic degeneration was detected at the early stages of the disease process, before any overt signs of neuronal death (Bouzamondo-Bernstein *et al.*, 2004; Cunningham *et al.*, 2003a; Gray *et al.*, 2009; Jeffrey *et al.*, 2000). Disruption of presynaptic boutons and degeneration of axon terminals did not strictly correlate with PrP^{Sc} deposition. This suggested that other toxic intermediates, likely soluble and PK-sensitive oligomeric species of abnormal PrP, also injured synapses (Gray *et al.*, 2009; Jeffrey *et al.*, 2001) and compromised synaptic function before PrP^{Sc} deposition could be detected (Cunningham *et al.*, 2003a; Mallucci *et al.*, 2007). In brain samples from CJD patients, PrP^{Sc} deposition at the presynapstic terminals has been reported (Kovacs *et al.*, 2005; Siso *et al.*, 2002). PrP^{Sc} deposition was associated with reduced level of presynaptic proteins such as synaptophysin, synapsin I, SNAP-25 (Ferrer *et al.*, 2000).

Another prominent feature of prion diseases is dendritic atrophy (Jamieson *et al.*, 2001); characterized by distorted dendritic arborization and dendritic atrophy in CJD brains. The associated molecular mechanism involved activation of Notch (a known regulator of dendritic growth and maturation). Indeed, in the neocortex of infected mice, higher level of *Notch-1* mRNA and nuclear translocation of Notch-1 intracellular domain (NICD), correlated with PrP^{Sc} accumulation. In vitro, in N2a neuroblastoma cells, the expression of NICD was also increased following scrapie infection. Morphologically, N2a cells showed synaptic abnormalities, such as shorter dendritic processes (Ishikura, 2007; Ishikura *et al.*, 2005).

The role of synaptic pathology in neuronal degeneration is still elusive. It has been proposed that accumulation of PrP^{Sc} at the synapse directly affects the synaptic function by altering the balance

between excitatory and inhibitory transmission. Indeed, enhanced glutamatergic excitatory transmission (through NMDARs) as well as impairment of inhibitory GABAergic signalling, has been described in both mouse and human models of prion diseases (Bouzamondo-Bernstein *et al.*, 2004; Ratte *et al.*, 2008).

1.15.7. Ca^{2+} deregulation and prion pathophysiology

So far, conclusive evidence about the exact pathogenic mechanism of prion toxicity is still missing. Moreover, the physiological function of PrP^{C} as well as its role in prion pathogenesis remains largerly unknown. Nonetheless, latest evidence propose that the loss of PrP^{C} function per se, and not the effect of PrP^{Sc} formation alone, contributes to the observed neurodegeneration. It is suggested that PrP^{C} acts by regulating crucial cellular processes - determining both the life and the death of a cell- such as Ca^{2+} homeostasis. Indeed, Ca^{2+} is a key regulator of multiple intracellular processes that are crucial for cell survival. However, if not finely regulated, Ca^{2+} is also known to switch into a threat for the cell. If this were true, Ca^{2+} could turn out to be the common denominator for the multiple roles ascribed to PrP^{C}. Yet, it is worth underlying that PrP^{C} faces the extracellular milieu and cannot directly influence calcium signaling. Accordingly, there are two possible mechanism of action. The first one suggests that PrP^{C} interacts with transmembrane molecular systems involved in Ca^{2+} homeostasis (such as Ca^{2+} channels, metabotropic glutamate receptors). The second one postulates that PrP^{C}, as member of membrane multicomponent signalling complexes, controls downstream signaling events that coordinate the expression of Ca^{2+}-related proteins (Peggion *et al.*, 2011).

Several findings suggested a link between prion pathology and impaired Ca^{2+} control. For example pioneer work in neuronal cell lines exhibited reduced Ca^{2+} responses following prion infection (Kristensson et al., 1993; Wong et al., 1996). Also, treatment of cells and neurons with prions or the fibrillogenic and neurotoxic peptide encompassing PrP amino acid residues 106–126 (PrP (106–126)), induced the downregulation of N-type voltage-gated Ca^{2+} channels (VGCCs) (Florio *et al.*, 1998; Forloni *et al.*, 1993; Sandberg *et al.*, 2004; Thellung *et al.*, 2000). Mechanistically, however, it is still unknown whether prions or PrP (106–126), acted directly on VGCC and modulated their activity or prion toxicity indirectly caused an alteration in Ca^{2+} homeostasis. Furthermore, electrophysiologic and morphologic synaptic abnormalities, such as alterations of presynaptic/postsynaptic potentials, neuronal depolarization leading to increased excitability, loss of slow after hyperpolarization (AHP),

impaired generation and maintenance of long-term potentiation (LTP), and loss of dendritic spines with abnormal dendritic morphology (Cunningham *et al.*, 2003b; Johnston *et al.*, 1997; Johnston *et al.*, 1998a; Johnston *et al.*, 1998b) have been reported in prion infected brains and/or cultured neurons. These pathologies could be attributed to changes in Ca^{2+} homeostasis.

In support of the first hypothesis, a number of intracellular effectors of PrP^{C}-mediated signaling, including $p59^{fyn}$, mitogen-activated kinases (MAPKs) Erk1/2, PI3K/Akt, and cyclic adenosine monophosphate (cAMP)-dependent protein kinase A (PKA) have been reported (Sorgato *et al.*, 2009). The interaction of PrP^{C} and glutamate receptors also seems to be critical for Ca^{2+} regulation. Zamponi and coworkers have reported that blocking NMDAR activity can reverse the increased excitability of $Prnp^{-/-}$ hippocampal neurons. From a molecular point of view, this observation was explained by the ability of PrP^{C} to interact and selectively inhibit the NR2D subunit of the NMDAR (Khosravani *et al.*, 2008). Laminin γ1 chain-PrP^{C} interaction was reported to activate group I mGluRs. This triggers Ca^{2+} release from $InsP_3$ -sensitive ER stores and the subsequent cytosolic Ca^{2+}. The latter promotes PKC-mediated neuritogenesis (Beraldo *et al.*, 2011). However, in an AD disease model this interaction has also been shown to be the effector of neurodegeneration (Um *et al.*, 2013). A similar mechanism has been described for the interaction between PrP^{C} and STI1. In this case, PrP^{C}-STI1 interaction promotes coupling of PrP^{C} with the a7 nicotinic acetylcholine receptor (a7nAChR) and activation of the latter. The resulting increase of cytosolic Ca^{2+} would then trigger either neuronal differentiation or survival, depending on downstream activated pathways, one MAPK Erk1/2 or PKA, respectively (Beraldo *et al.*, 2010; Lopes *et al.*, 2005).

In support of the second hypothesis, Lazzari *et al.* showed a direct role of PrP^{C} in the regulation of local Ca^{2+} movements in cerebellar granular neurons. More specifically, primary cerebellar granular neurons (CGNs) were prepared from both wt and $Prnp^{-/-}$ mice. Both preparations were transduced with an aequorin (AEQ) lentiviral vector. The use of a plasma membrane (PM)-targeted AEQ allowed monitoring of Ca^{2+} flunctuations in the cytosolic domains close to the plasma membrane. Intracellular store depletion or membrane depolarizations were used to trigger the entry of Ca^{2+} ions into the cell. $Prnp^{-/-}$ primary CGNs exhibited much higher Ca^{2+} peak transients in PM subdomains compared to their wt counterparts. Also, the absence of PrP^{C} strongly delayed the re-establishment of basal Ca^{2+} levels, due to the reduced number of PM and ER Ca^{2+} -ATPases. Importantly, addition of PrP^{C}

restored the physiological PrP^C levels and reversed the aforementioned phenotype (Lazzari *et al.*, 2011). Because both the infection by prions and the absence of PrP^C mainly affect the CA1 region of the hippocampus, several studies have analyzed the electrophysiological features of this region in acute hippocampal slices. They reported a significantly reduced slow AHP in $Prnp^{-/-}$ CA1 cells and pyramidal neurons compared to their wt counterparts (Asante *et al.*, 2004; Colling *et al.*, 1996; Fuhrmann *et al.*, 2006; Mallucci *et al.*, 2002; Powell *et al.*, 2008); mediated by Ca^{2+}-activated K^+ currents (Sah and Davies, 2000). This impairment has been attributed to either reduced Ca^{2+} influx through L-type VGCC (Fuhrmann *et al.*, 2006) or to increased activity of the sarco-ER Ca^{2+}-ATPase (SERCA) and cell Ca^{2+}-buffering capacity (Powell *et al.*, 2008), both phenomena resulting in decreased cytosolic Ca^{2+} levels. Interestingly, decreased depolarization-induced Ca^{2+} rise and reduced Ca^{2+}-activated K^+ currents were also observed in $Prnp^{-/-}$ cerebellar Purkinje cells (Herms *et al.*, 2001).

From what reported so far, it seems that deregulation of processes carefully orchestrated by Ca^{2+} signalling is common to both AD and prion disease, and that Aβ fragments and (the good and bad) PrP isoforms as well as PrP^C per se or through its interactions significant roles in the Ca^{2+}-based cell network. The exact mechanism of these interactions remains to be elucidated.

1.16. Aims of the thesis

Prion diseases are fatal neurological disorders, characterized by accumulation of aggregated, misfolded proteins and progressive neurological dysfunction and neurodegeneration. The decisive event in the pathogenesis of prion diseases is the conversion of the normal cellular prion protein (PrP^C) into an aggregated conformational variant called PrP^{Sc}. However the molecular mechanisms of the disease progression are largerly unknown. It is proposed that this process is partially mediated by PrP^C interaction partner. Key interactors are group I metabotropic glutamate receptors (mGluRs). Group I mGluRs couple with PrP^C and laminin γ chain (PrP^C-Ln γ1) and promote neuronal differentiation (Graner et al., 2000). Beraldo and colleagues further showed that upon formation of the group I mGluRs -PrP^C -Ln γ1 complex, group I mGluRs are activated and transduce signals for neuritogenesis (Beraldo *et al.*, 2011). However, this interaction does not always promote development.

Recent studies in AD shed light into "the dark side" of PrP^C-group I mGluRs interaction. Aβ oligomers can bind to PrP^C at the cell surface (Lauren *et al.*, 2009) and form complexes that contain mGluR5 (Haas *et al.*, 2014). Inhibition of mGluR5, *in vivo*, rescued cognitive decline and synaptic alterations caused by exposure to Aβ-aggregates (Um *et al.*, 2013). Furthermore, PrP^C-mGluR5 coupling is involved in Aβ-mediated inhibition of LTP and Aβ-facilitated LTD *in vivo* (Hu *et al.*, 2014), and genetic ablation of mGluR5 reverses disease-related memory deficits in a murine model of AD (APPswe/PS1ΔE9) (Hamilton A. *et al.*, 2014). Exposure of cortical APPswe/PS1ΔE9 neuronal cultures to Aβ oligomers upregulated mGluR1 and PrP^C α-cleavage, whereas activation of group-I mGluRs increased PrP^C shedding from the membrane (Ostapchenko *et al.*, 2013). All these studies speak in favor of an involvement of group-I mGluRs in the pathogenesis of AD. On the other hand, others have reported that neither PrP^C ablation nor overexpression had any effect on neurotoxicity in AD models (Balducci *et al.*, 2010; Calella *et al.*, 2010; Cisse *et al.*, 2011; Kessels *et al.*, 2010). As a possible explanation for these discrepancies, it has been suggested that only a defined oligomeric fraction of Aβ (Kostylev *et al.*, 2015) interacts with mGluR5 (Haas *et al.*, 2016). Evidence exists that PrP^C-group I mGluRs interaction also plays a role in prion disease. Changes in mGluR1, leading to reduced expression levels of phospholipases, were observed in the cerebral cortex of Creutzfeldt-Jakob disease (CJD) patients (Rodriguez *et al.*, 2005). Also, impairment of the mGluR1/1-phosphatidylinositol 4,5-bisphosphate phosphodiesterase 1 (PLC1)/protein kinase C (PKC) signaling pathway has been observed in a murine model of BSE; abnormal mGluR1 signaling correlated with PrP^{Sc} deposition, histological changes, and clinical scores (Rodriguez *et al.*, 2006). The aim of the current thesis was to study the role of mGluR1 and mGluR5 in prion diseases and to elucidate the mechanisms involved in this process.

First, we tested whether toxicity induced by prion infection (RML6 prion strain) (Falsig *et al.*, 2012) or prion mimetic anti-PrP^C antibodies (Sonati *et al.*, 2013), namely globular domain ligands (GDLs), could be rescued in cerebellar and hippocampal organotypic cultured slices (COCS and HOCS, respectively) upon pharmacological inhibition of either mGluR5 or mGluR1 (treatment with MPEP and YM202074 respectively). Dose-dependent treatment potential of the pharmacological inhibitors was also performed. Rescue was defined by morphometric assessment of the area of the cerebellar granule cell layer (CGL) or pyramidal hippocampal neurons immunoreactive to antibodies against the

neuronal NeuN antigen.

Second, so as to evaluate the specificity of the therapeutic potential of group I mGluR inhibitors a group of cerebellar slices was also treated with the selective agonist of group III (L-AP4)) and the potent antagonist of group II and group III (CPPG) metabotropic glutamate.

Third, we sought to evaluate whether there exists a specific interaction of PrPC with all members of the mGluR superfamily. Brain homogenate from wt and $Prnp^{-/-}$ mice was subjected to immunoprecipitation by POM1 (monoclonal anti-PrP^C antibody) followed by immunobloting using polyclonal antibodies against the different mGlu receptors and PrP^C. Control conditions such as unconjugated beads, IgG bound beads and POM1 blocked by recombinant PrP^C were run in parallel to ensure the specificity of the selected antibodies.

Forth, after verifying the specificity of the interaction with group I mGluRs pharmacologically we decided to move on with the genetic model. We tested whether toxicity induced by prion infection (RML6 prion strain) or prion mimetic anti-PrP^C antibodies could be rescued in cerebellar and hippocampal slices (COCS and HOCS) upon genetic deletion of mGluR5 (groups included in the study and compared in parallel are: $Grm5^{-/-}$, $Grm5^{+/-}$ and control wt littermates). Rescue was defined by morphometric assessment of the area of the cerebellar granule cell layer (CGL) or pyramidal hippocampal neurons immunoreactive to antibodies against the neuronal NeuN antigen.

Fifth, we probed mouse brain homogenate derived from transgenic amino-proximal deletion mutants of PrP^C to define **(a)** the type of interaction-direct or indirect, and **(b)** where the region of interaction between mGluR1-PrP^C and mGluR5-PrP^C may lie. Towards this end, a series of transgenic mouse lines that express variants of full length PP^C, possessing an intact globular domain (GD) but extensive deletions in the flexible tail (FT) region of PrP^C, were utilized (Figure 1.16.). Also known as amino-proximal deletion mutants (ΔC, ΔCC, ΔF, ΔOR), these truncated variants induce pathological features in $Prnp^{-/-}$ background that can be rescued by introduction of full-length PrP^C [reviewed in (Aguzzi *et al.*, 2008)]

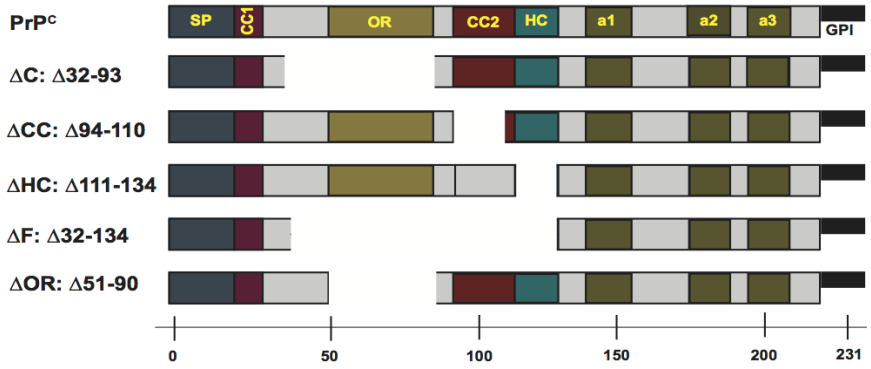

Figure 1.16. Schematic representation of the PrP^C deletion mutants utilized in this study

Sixth, we sought to assess a possible therapeutic effect of MPEP on prion pathogenesis *in vivo*. C57BL/6J male mice were inoculated intracerebrally with 3 or 5 log LD_{50} units of RML6 prions as previously described (Kranich *et al.*, 2010), and chronically treated with MPEP. Control mice were inoculated with NBH. In order to record the neurological deficits associated with prion disease, we utilized the rotarod behavioral test which measures a combination of motor performance, coordination, and balance (Brooks and Dunnett, 2009). At the terminal stage of the disease mice were sacrifized and brain samples (whole brain as well as specific brain regions, such as cortex, hippocampus and cerebellum) were collected and further processed. Immunohistochemical staining (Iba1, GFAP, SAF84) of brain sections was performed and analysis included: vacuole area and number counting, percentage of reactive astrogliosis, percentage of microglia activation and PrP^{Sc} accumulation respectively.

Seventh, after verifying the therapeutic potential of pharmacological inhibition of mGluR5 we decided to test the genetic inhibition model. We tested whether toxicity induced by prion infection (RML6 prion strain) upon genetic deletion of mGluR5 (groups included in the study and compared in parallel are: $Grm5^{-/-}$, $Grm5^{+/-}$ and control wt littermates). In order to record the neurological deficits associated with prion disease, we utilized the rotarod behavioral test which measures a combination of motor performance, coordination, and balance (Brooks and Dunnett, 2009). At the terminal stage of the disease mice were sacrifized and brain samples (whole brain as well as specific brain regions, such as cortex, hippocampus and cerebellum) were collected. Unfortunately, no significant therapeutic effect was observed upon deletion of Grm5 *in vivo*. However, this observation led us to examine the

potential for epistasis between mGlu1 and mGlu5 receptors.

Eight, we sought to the mechanism of the observed toxicity (GDL-induced toxicity) and how this is mediated through PrP^C-mGluR5 interaction. In AD, it has been reported that clusters of mGluR5s accumulate around excitatory synapses, and increase the size of synaptic mGluR5s clusters. This increase is associated with toxic calcium influx (Renner *et al.*, 2010; Shrivastava *et al.*, 2013; Um *et al.*, 2013). Therefore, we sought to identify whether the prion-mimetic POM1 antibody altered the clustering of mGluR5s or the fluorescent intensity of mGluR5s in dendritic spines. Immunofluorescent analysis of mGluR5s clusters was performed on primary hippocampal neurons following exposure to the anti-PrP^C $F(ab)_1$ antibody fragments, toxic POM1 and control POM2, and POM3 (Sonati *et al.*, 2013). Also, the fluorescence level of mGluR5s in dendritic spines of neurons expressing mGluR5-pHluorin was quantified. Furthermore, in order to assess the specificity of the interaction for mGluR5 (and not other excitatory glutamate receptors) after exposure of the primary hippocampal cultures to toxic POM1 antibodies, the cluster size and the fluorescent intensity of NMDA and AMPA receptors were also assessed. The membrane clustering of mGluR5s following exposure to toxic POM1 antibodies was further assessed by cell surface biotinylation experiments.

Nine, with the aim to assess changes in Ca^{2+} homeostasis in prion diseases novel transgenic mice expressing the potent Ca^{2+} reporter (RCamp1.07) were generated. In brief, embryonic stem (ES) cell culture and gene targeting of the RCaMP1.07 reporter gene into the TIGRE locus were carried out and the targeted ES cells were microinjected into B6N-Tyrc blastocysts. Chimeras were tested for transgene expression and inheritance by Southern blotting using specific 5' and 3' external probes. Transgenic mice were further crossbred with R26phiC31o mice (Raymond and Soriano, 2007) for removal of the *AttB*/*AttP*-flanked hygro-TK cassette. Following removal of the cassette, mice were mated with either Camk2a-tTA (Mayford *et al.*, 1996) or ROSA:LNL:tTA (Wang *et al.*, 2008) transgenic mice to allow for the generation of compound mutant mice in which expression of the reporter gene can be defined by the chosen Cre-recombinase and turned off by the addition of tetracycline (or its analog doxycycline). Expression of the transgene was evaluated both in fixed brain sections as well as in organotypic slice cultures.

In summary, our results demonstrate that pharmacological inhibition of mGluR1 and mGluR5 antagonizes dose-dependently the neurotoxicity triggered by prion infection and by exposure to prion-mimetic anti-PrP^C antibodies in organotypic brain slices. Prion-mimetic antibodies increase mGluR5 clustering around dendritic spines mimicking a mechanism of toxicity documented for Aβ oligomers, whereas prion-protective antibodies reduce mGluR5 clustering. Treatment with the protective antibodies reduces mGluR5 clustering. Interestingly, pre-blocking of the toxic POM1 antibodies with the protective POM1 antibodies significantly reduces the cluster size; similar to MPEP treatment. Although genetic deletion of mGluR5 was not protective against prion infections *in vivo*, oral treatment with the mGluR5 pharmacological inhibitor MPEP, delayed the onset of motor deficits and prolonged survival of prion-infected mice. Group-I mGluR inhibition was not curative, yet these results suggest that it may have the potential to alleviate the neurological dysfunctions induced by prion diseases.

Chapter 2: MATERIALS AND METHODS

2.1. Mice

Prnp$^{-/-}$ *(or Prnp*$^{o/o}$*)* and *Prnp*$^{o/o}$; *tga20*$^{+/+}$ (*Tga20*), were on a mixed 129Sv/BL6 background (Fischer *et al.*, 1996). Transgenic mice expressing mutated PrP^{C} were utilized for immunoprecipitation experiments. The production and relevance to disease phenotype of the transgenic mice expressing N-terminal deletion mutants of PrP^{C} (termed ΔC, ΔCC, ΔF, ΔOR and ΔHC) PrP^{C} has been previously reported (Baumann *et al.*, 2007a; Bremer *et al.*, 2010; Flechsig *et al.*, 2000; Shmerling *et al.*, 1998). *Grm5*$^{+/-}$ embryos (Jia et al., 1998; Lu et al., 1997) were acquired from Dr. Gasparini and were revitalized at the transgenics facility of the University Hospital of Zurich. *GRM5* null mice were derived from breeding of these mice.

2.2. Transgenic mice generation

Embryonic stem (ES) cell culture and gene targeting of the RCaMP1.07 reporter gene into the TIGRE locus were carried out as previously described (Madisen *et al.*, 2015; Madisen *et al.*, 2010). Targeted ES cells were microinjected into B6N-Tyrc blastocysts and chimeras were bred with C57BL/6J mice. DNA was extracted from the biopsied tails of mouse pups and the F1 generation was identified by Southern blotting using the following 5' and 3' external probes. The former was generated by PCR using a primer pair of 5'-tagggaagcactggccaaaggaa-3' and 5'-tcacggtaaccgcggcataaaac-3', and the latter by 5'-cgaactgcccgctgttctgc-3' and 5'- gtagcgcgtctgctgctcca-3'. Transgenic mice were further crossbred with R26phiC31o mice (Raymond and Soriano, 2007) for removal of the *AttB*/*AttP*-flanked hygro-TK cassette. Following removal of the cassette, mice were mated with either Camk2a-tTA (Mayford et al., 1996) or ROSA:LNL:tTA (Wang *et al.*, 2008) transgenic mice to allow for the generation of compound mutant mice in which expression of the reporter gene can be defined by the chosen Cre-recombinase and turned off by the addition of tetracycline (or its analog doxycycline).

2.3. Organotypic slice culture preparation

Organotypic cerebellar cultured slices, 350 µm thick, were prepared from 9–12 day-old pups according to a previously published protocol (Falsig *et al.*, 2008). Organotypic hippocampal cultured slices, 350 µm thick, were prepared from 4–6 day-old pups according to a previously published protocol (Gogolla *et al.*, 2006). Cultures were kept in a standard cell incubator (37 °C, 5% CO_2, 95% humidity) and the culture medium was changed three times per week.

2.4. Prion inoculation and GDLs treatment

Inoculations were performed with either infectious brain lysate (RML6) or non-infectious brain homogenate (NBH). Slices were inoculated (as free-floating sections for 1 h at 4°C) with 100μg brain homogenate per 10 slices. After washing in GBSSK, they were cultured on a 6-well Millicell-CM Biopore PTFE membrane insert (Millipore) according to previously published protocol (Falsig *et al.*, 2012). Drug-treated *tga20* slices were maintained until 45 dpi, fixed and analyzed by NeuN morphometry (analySIS vc5.0 software). Neurotoxicity was defined as significant $NeuN^{+}$ neuronal layer loss over NBH treatment. Slices prepared from *Grm5*$^{-/-}$, *Grm5*$^{+/-}$ and *Grm5*$^{+/+}$ littermates were maintained until 60 dpi, fixed and analyzed by NeuN morphometry (analySIS vc5.0 software). Neurotoxicity was defined as significant $NeuN^{+}$ neuronal layer loss over NBH treatment. For globular domain ligand (*GDL*) treatment, toxicity in slices was induced by exposure to ligands, toxic anti- PrP^{C} antibodies targeting the globular domain, such as full length POM1 antibody and/or (sc)POM1 mini-antibody, after a 14-day recovery period; allowing the initial gliosis induced by tissue preparation to subside, according to previously published protocol (Sonati *et al.*, 2013). *Tga20* COCS were exposed to POM1 (67 nM, 14 dpe)/ scPOM1 (200 nM, 8 dpe), or to control treatment (67 nM POM1/140nM recPrP, 14 dpe)/ (200 nM scPOM1/210nM recPrP, 8 dpe), immunostained for the neuronal marker NeuN and counterstained with DAPI. Slices were imaged and analysed as previously described. Antibody treatment was randomly assigned to individual wells.

2.5. Pharmacological treatment of slices

Treatment with the specific inhibitors 2-Methyl-6-(phenylethynyl)-pyridine (MPEP) (Gasparini *et al.*, 1999) or N-cyclohexyl-6-N- methylthiazolo[3,2-a]benzimidazole-2-carboxamide (YM202074) (Kohara *et al.*, 2008) was initiated at the time of GDL addition (14dpe) for the GDL toxicity model (treated slices were maintained until 28 dpe for POM1 treatment and until 22dpe for scPOM1 treatment) (Sonati *et al.*, 2013) and at 21 days post-inoculation (dpi) for prion infected slices, when PrP^{Sc} accumulation was already discernible (Falsig *et al.*, 2008). Drug treatments were re-added at every media change (Gasparini *et al.*, 1999). Post-treatment slices were fixed

in 4% paraformaldehyde (PFA), immunostained for the neuronal marker NeuN and counterstained with DAPI. Slices were imaged at 4x magnification on a fluorescence microscope (BX-61, Olympus) analyzed by NeuN morphometry (analySIS vc5.0 software). Neuroprotection was defined as significant neuronal layer rescue over toxic-antibody treated, non-drug treated slices.

2.6. Prion Inoculations

Inoculum of the RML6 strain of mouse-adapted scrapie prion was prepared from pooled 10% w/v brain homogenates of RML6 terminally sick CD1 mice. C57BL/6J mice were inoculated with serial dilutions (10^{-3} and 10^{-5}) of the RML6 inoculum. C57BL/6J mice were injected intracerebrally with 30□l of brain homogenate prepared in a solution of PBS/5% BSA, containing 3log LD_{50} units or 5log LD_{50} units of the RML6 strain. Control mice received 30μl of NBH derived from healthy CD1 mice. Scrapie was diagnosed according to clinical criteria (ataxia, kyphosis, priapism, and hind leg paresis). Mice were sacrificed on the day of onset of terminal clinical signs of scrapie. The operator was blinded to drug treatment.

2.7. Rotarod

The rotarod test was used to assess motor coordination and endurance at defined timepoints after prion inoculations. A rotarod machine (Ugo Basile) with five cylinders (3cm diameter) separated by dividers (25cm diameter) in five lanes, each 57mm wide, was utilized. Before the training sessions, the mice were habituated to stay on the rotating rod (4rpm lowest speed) for 3 sessions lasting 1-2 minutes each and separated by 10' intervals. Test phase started 30 minutes after the last habituation session and consisted of 3 trials separated by 1 inter-trial intervals. For each test session the mouse was placed on a rotating rod, which accelerated from 5 to 40 rpm. Each test session lasted a maximum of 5min. Latency to fall was assessed when the mouse was no longer capable of riding on the accelerating rod, due to slipping from the drum or clinging to the rod and rotating with it. Test sessions were always performed at the same time of the day, mice were tested in a randomized manner and the operator was blind to drug treatment.

2.8. Brain Homogenization and Immunoprecipitation experiments

Adult mice *Prnp*$^{o/o}$, *Prnp*$^{o/o}$, *tga20*$^{+/+}$ (*Tga20*) and C57BL/6J mice were euthanized and brain was dissected. Brain samples were snap frozen in liquid nitrogen. Samples were subsequently homogenized in ice cold Lysis Buffer (50 mM Tris-Cl, 1% Igepal (NP-40), 75 mM NaCl, pH 7.4) supplemented with protease (EDTA-free) and phosphatase inhibitor cocktail mix (Roche). Protein concentration was determined using the bicinchoninic acid assay (Pierce). Following immunoprecipitation of PrP^{C} with a specific anti-PrP monoclonal antibody (POM1) and addition of dynabeads (Life Technologies), samples were prepared in loading buffer (NuPAGE, Invitrogen) and boiled at 95 °C for 5 min. The samples were migrated on 4-12% NuPage gels and transfered onto the Polyvinylidene difluoride (PVDF) membrane**.**

2.9. Whole-genome single nucleotide polymorphisms analysis

Tail biopsies from *Grm5*$^{-/-}$, *Grm5*$^{+/-}$ and *Grm5*$^{+/+}$ littermates were collected and sent to Taconic Laboratories so as to perform whole-genome SNP analysis, using the Illumina Mouse MD Linkage Panel array. Results were compared with data from reference strains (129S6/SvEvTac, C57BL/6JBomTac).

2.10. Antibodies and Chemicals

All compounds were purchased from Sigma-Aldrich unless otherwise stated. Monoclonal anti PrP antibody POM1 (1:5000) was generated as described previously (Polymenidou et al., 2008). Anti-mGluRs antibodies against representative receptors of each group, targeting the N-terminal domain were utilized: anti-mGluR5 #ab53090 (AbCam) or AB5675 (Millipore), anti-mGluR1 [EPR13540] (ab183712) (AbCam), anti-mGluR2+3 #ab6438 (AbCam) and anti-mGluR6 #AGC-026 (Alomone labs). Secondary antibodies were horseradish peroxidase (HRP)- conjugated rabbit anti–mouse IgG_1 (1:10,000, Zymed) and goat anti-rabbit IgG_1 (1:10,000, Zymed). Blots were developed using SuperSignal West Pico chemiluminescent substrate (Pierce) and visualized using the VersaDoc system (model 3000, Bio-Rad). Rocky Mountain Laboratory strain (RML; passage #6) prions (RML6) were amplified in CD1 mice by intracerebral inoculation into the lateral forebrain of 30 µl of 1% (wt/vol) brain homogenate. The mGluR5 antagonist MPEP was a gift from Novartis. The mGluR1 antagonist YM202074 was purchased from Tocris Bioscience

(Ellisville, USA).

2.11. Immunohistochemistry and NeuN morphometry

Immunohistochemistry of fixed organotypic slices and subsequent NeuN morphometric analysis was performed according to previously published protocols (Falsig *et al.*, 2012; Sonati *et al.*, 2013).

2.12. Histology and immunohistochemistry

Stainings were performed on sections from brain tissues fixed in formalin and treated with concentrated formic acid to inactivate prions. Partially protease-resistant prion protein deposits, astrogliosis and microglia deposition were visualized by staining brain sections with the SAF84 antibody (1:200, SPI bio), GFAP (1:1000, Millipore) and IBA1 (1:2500, WAKO) respectively on a NEXES immunohistochemistry robot (Ventana instruments) using an IVIEW DAB Detection Kit (Ventana), after preceding incubation with protease 1 (Ventana). Images of DAB stained sections were acquired using the NanoZoomer scanner (Hamamatsu Photonics) and NanoZoomer digital pathology software (NDPview; Hamamatsu Photonics). Quantifications of IBA1, GFAP staining and vacuoles in mouse sections were performed on acquired image regions of interest were drawn on a Digital Image Hub (Leica Biosystems) and analyzed as previously described (Sorce *et al.*, 2014).

2.13. Primary neuron culture

Hippocampal neurons were prepared from embryonic day 18 (E18) C57/BL6 mice (Janvier Labs, France). Freshly dissociated (trypsin) cells were plated (80,000 cells per 18 mm coverslip per ml) in neuronal attachment media consisting of 10% horse serum, 1 mM sodium pyruvate, and 2 mM glutamine in MEM for 3h. The attachment medium was replaced and cells were maintained in serum-free neurobasal medium supplemented with B27 (1X) and glutamine (2 mM). 300 µl of fresh medium was added once a week.

2.14. Plasmids and Transfection

mGluR5-pHllorin construct was generated and kindly provided by Lili Wang and Christian Specht. Dendra2 was inserted between residues Q222 and A223 of mouse prion protein. GluN2A-GFP

was kindly provided by Andrea Yao and Pierre Paoletti. Transfection was performed on DIV 17-18 neurons using Lipofectamine® as described recently (Shrivastava et al., 2015). Transfection medium (TM) was composed of 1 mM sodium pyruvate and 2 mM glutamine in nerobasal medium (Invitrogen). 0.5 µg of plasmid and 2 µl of lipofectamine- 2000 reagent were used for each coverslip. Experiments were performed on DIV 21-22.

2.15. Immunocytochemistry and Image Analysis

Immunocytochemistry of mGluR5 (rabbit polyclonal, Millipore, AB5675, 1:200 dilution) or GluR2-AMPA receptor (rabbit polyclonal, Synaptic System, 182103, 1:400 dilution) was performed following methanol fixation/permeabilization (10 min at -20ºC; methanol pre-stored at -20º). Image thresholding using wavelet decomposition to identify fluorescent clusters (mGluR5 and GluR2-AMPA immunoreactivity or GluN2-GFP fluorescence) has been described in previous studies (Shrivastava *et al.*, 2015; Renner *et al.*, 2010). Images were acquired using Leica Inverted Spinning Disk microscope (DM5000B, Coolsnap HQ2 camera, Cobolt lasers) using 100X objective (field of view = 1392 x 1040 pixels) and a pixel size of 60.5nm. For estimation of mGluR5 fluorescence within dendritic spines, ratio of fluorescence within a circular region of fixed size (6 pixel) on spine head to the shaft below was measured using ImageJ program.

Chapter 3: RESULTS

3.1. Pharmacological inhibition of group-I mGluRs rescues prion-induced neurotoxicity in organotypic slice cultures

Cerebellar and hippocampal organotypic cultured slices (COCS and HOCS, respectively) (Falsig *et al.*, 2008; Gogolla *et al.*, 2006) prepared from PrP^C overexpressing (*tga20)* mice can be efficiently infected with the Rocky Mountain Laboratory (RML) strain of prions and undergo neurodegeneration after ca. 5 weeks (Falsig *et al.*, 2008). The time course and extent of neurodegeneration can be reliably measured by morphometric assessment of the area of the cerebellar granule cell layer (CGL) immunoreactive to antibodies against the neuronal NeuN antigen. We therefore inoculated COCS and HOCS with brain homogenate from CD1 mice infected with RML prions (passage #6, henceforth called RML6). For control, slices were inoculated with non-infectious brain homogenate (NBH) derived from healthy CD1 mice. Starting at 21 days post infection, slices were treated with a range of concentrations of either N-cyclohexyl-6-N-methylthiazolo[3,2-a]benzimidazole-2-carboxamide (YM202074) (Kohara *et al.*, 2008) or 2-methyl-6-(phenylethynyl)-pyridine (MPEP) (Gasparini *et al.*, 1999) which specifically inhibit mGluR1 and mGluR5, respectively. Morphometry revealed that MPEP and YM202074 significantly prevented CGL loss in treated COCS at concentrations as low as 10 nM (**Figure 3.1.A-B**) and 500 nM (**Figure 3.1.C-D**), respectively. Higher MPEP concentrations (3-10 μM) were not intrinsically toxic (**Figure 3.2.A**), as previously reported (Gasparini et al., 1999), but failed to protect against prion toxicity (**Figure 3.2.B**). Expression levels of mGluR5 in COCS were assessed (**Figure 3.2.C-D**). MGluR5 expression in the cerebellum was comparable to that of hippocampus and cortex. Results were in accordance with previous studies reporting high mGluR5 levels at early developmental stages (Romano et al., 1996a). Also in HOCS, prepared from 4-6 days old *tga20* mice, MPEP significantly suppressed neuronal loss after prion infection at concentrations as low as 36 nM (**Figure 3.1.E-F**).

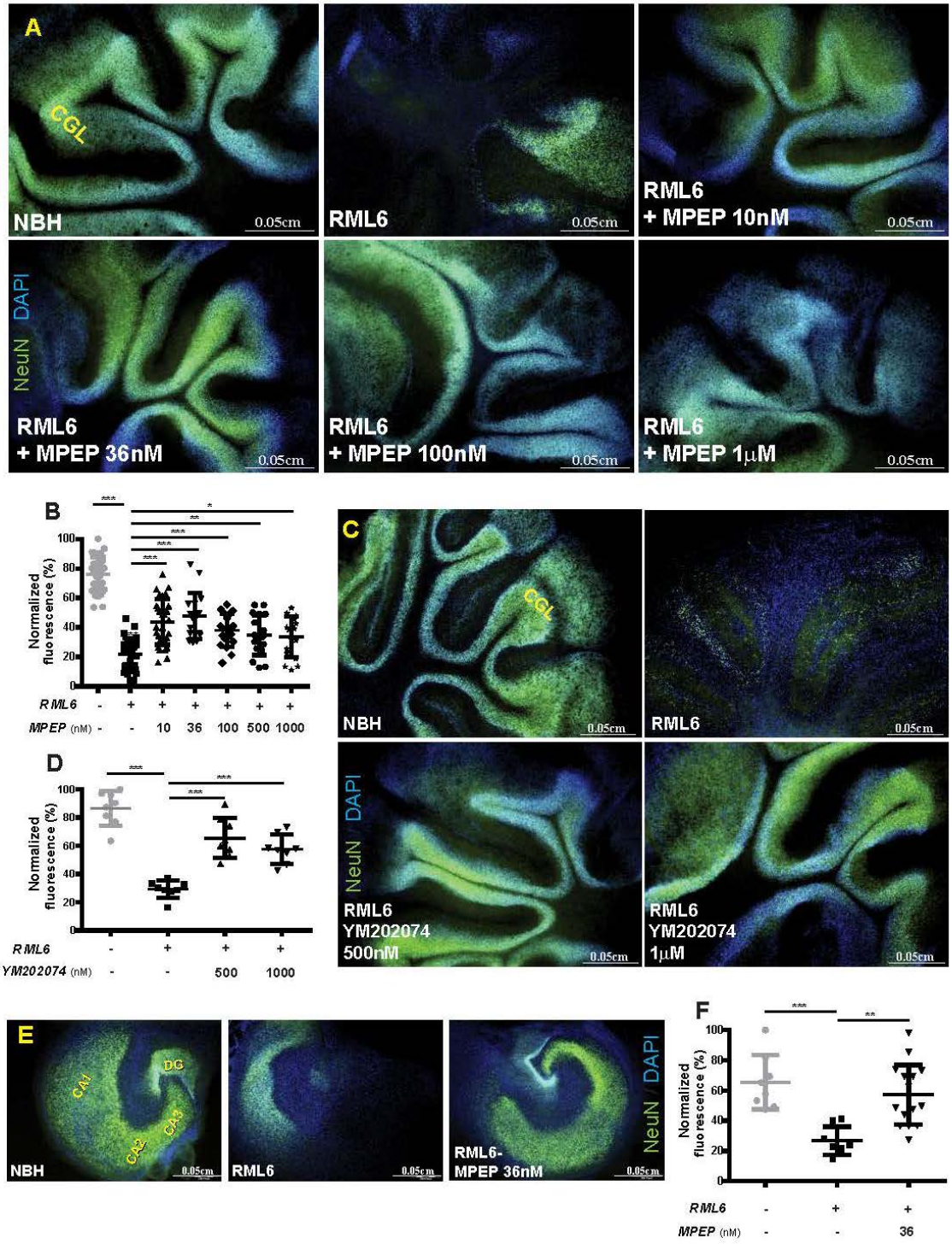

Figure 3.1. Group-I mGluR inhibition rescues prion neurotoxicity in organotypic slice cultures

(A-B) Treatment with the mGluR5 inhibitor (MPEP) rescued neurodegeneration in *tga20* RML6-treated COCS. **(A)** Fluorescence micrographs of *tga20* COCS, showing ablation of the cerebellar granular layer (CGL) induced by RML6 infection, that is significantly ameliorated by addition of MPEP,

the mGluR5 inhibitor, (C=10nM-1μM). **(B)** Graphical representation of NeuN morphometry of *tga20* COCS exposed to RML6 or NBH and treated with MPEP from 21–42 days post inoculation (dpi). **(C-D)** Treatment with the mGluR1 inhibitor (YM202074) rescued neurodegeneration in *tga20* RML6-treated COCS. **(C)** Fluorescence micrographs of *tga20* COCS, showing ablation of the cerebellar granular layer (CGL) induced by RML6 infection, that is significantly ameliorated by addition of YM202074, the mGluR1 inhibitor, (C=500nM-1μM). **(D)** Graphical representation of NeuN morphometry of *tga20* COCS exposed to RML6 or NBH and treated with YM202074 from 21–42 dpi. **(E-F)** Treatment with the mGluR5 inhibitor (MPEP) rescued neurodegeneration in *tga20* RML6-treated HOCS. **(E)** Fluorescence micrographs of *tga20* HOCS, showing ablation of the hippocampal neuronal layer induced by RML6 infection (middle), that is significantly ameliorated by addition of the IC50 concentration of MPEP (C=36nM) (right). **(F)** Graphical representation of NeuN morphometry of *tga20* HOCS exposed to RML6 or NBH and treated with MPEP from 21–42 dpi.

For **(B)**, **(D)** and **(F)** panels: Scatter dot plots represent NeuN relative signal intensity as percentage of NBH samples; each dot corresponds to a pool of 7-10 cerebellar slices or 4-6 hippocampal slices cultured in the same well; Data are presented as mean ± s.d.; One-way ANOVA followed by Dunnet's post-hoc test. **Panel (B):** (NBH, n=30 pools; RML6, n=30 pools; RML6+10nM MPEP, n=31 pools; RML6+36nM MPEP, n=18 pools; RML6+100nM MPEP, n=18 pools; RML6+500nM MPEP, n=18 pools; RML6+1μM MPEP, n=17 pools; *: P < 0.05, **: P < 0.01, ***: P < 0.001. **Panel (D):** (NBH, n=8 pools; RML6, n=8 pools; RML6+500nM YM202074, n=8 pools; RML6+1μM YM202074, n=8 pools); ***: P < 0.001. **Panel (F):** (NBH, n=7 pools; RML6, n= 8 pools; RML6+36nM MPEP, n=15 pools); **: P < 0.01, ***: P < 0.001.

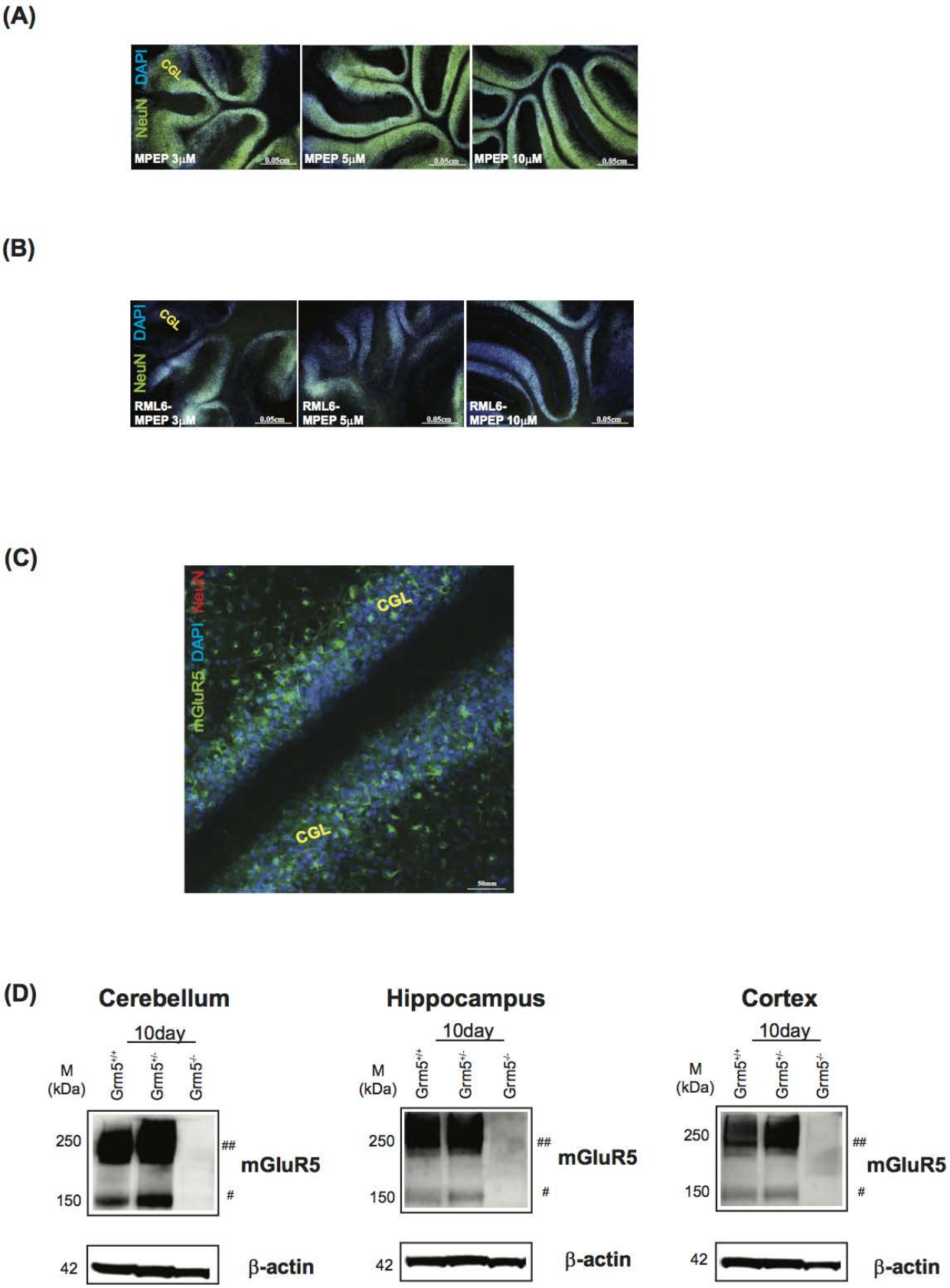
(A)
DAPI
NeuN
CGL
MPEP 3μM
MPEP 5μM
MPEP 10μM
(B)
RML6-
MPEP 3μM
RML6-
MPEP 5μM
RML6-
MPEP 10μM
(C)
mGluR5 DAPI NeuN
CGL
CGL
(D)
Cerebellum
Hippocampus
Cortex
10day
M
(kDa)
Grm5+/+
Grm5+/-
Grm5-/-
250
150
42
##
#
mGluR5
β-actin

Figure 3.2. Assessment of mGluR5 expression levels and the effect of high concentrations of the mGluR5 inhibitor (MPEP) in cerebellar organotypic cultured slices (COCS)

(A) Fluorescence micrographs of COCS, showing no toxicity on slices treated with high concentrations (C=3-10μM) of MPEP. **(B)** Fluorescent micrographs of COCS, infected with RML6 and treated with high concentrations (C=3-10μM) of MPEP. High concentrations of MPEP are not protective against prion infection. **(C)** MGluR5 localization in *Tga20* COCS. MGluR5 (green) is highly expressed in neuronal and non- neuronal cell populations in the cerebellar slices. Neurons were stained with an antibody against NeuN (red), nuclei were counterstained with DAPI (blue). Granular cell layer was imaged by confocal microscopy. **(D)** Cerebellar extracts from *Grm5*$^{-/-}$, *Grm5*$^{+/-}$ and *Grm5*$^{+/+}$ mice, collected at postnatal day 10 (comparable with the organotypic slices), were subjected to western blot analysis to control for endogenous levels of mGluR5. MGluR5 expression in the cerebellum was comparable to that of hippocampus and cortex.

3.2. MPEP alleviates the clinical signs of prion disease in mice

The beneficial effects of mGluR5 inhibition *ex vivo* encouraged us to assess a possible therapeutic effect of MPEP on prion pathogenesis *in vivo*. C57BL/6J male mice were inoculated intracerebrally with 3 or 5 log LD_{50} units of RML6 prions as previously described (Kranich *et al.*, 2010), and chronically treated with MPEP. Control mice were inoculated with NBH. In order to record the neurological deficits associated with prion disease, we utilized the rotarod behavioral test which measures a combination of motor performance, coordination, and balance (Brooks and Dunnett, 2009). Rotarod performance was similar in RML6- and NBH (control)-inoculated mice until 18 weeks following prion inoculation. Starting from 19 weeks post inoculation, mice receiving control food showed a progressive decline in rotarod performance, whereas the performance of MPEP-treated mice declined significantly less. This improvement was lasting and detectable until the very late

stages of the disease (22-23 weeks post inoculation; **Figure 3.3.A-B**), suggesting that the progression of the disease was delayed by MPEP.

At very late time points, the general health status of all mice deteriorated to an extent that made it impossible to accurately measure their rotarod performance. Nevertheless, MPEP-treated mice showed a modest, though significant, prolongation of survival (**Figure 3.3.C-D**). The median survival for untreated vs MPEP-treated RML6-inoculated C57BL/6J mice was, respectively, 183 vs 190 days post inoculation (dpi) after injection with 3 log LD_{50} units of prions and 188 vs 195 dpi after inoculation with 5 log LD_{50} units (P=0.0008 and 0.0231 respectively; log-rank test). Control mice injected with NBH and treated with MPEP exhibited stable rotarod performance during the entire test period, up to 23 weeks post-injection (**Figure 3.4.A**). No significant changes in average food and water consumption were observed between control and treatment groups during the experiment (**Figure 3.4.B**). So as to determine the exposure of the brain to MPEP, mice treated with control and MPEP food were sacrificed in two different timepoints, corresponding to the active and the inactive phase of the mice across the circadian circle. Average brain to blood ratio for the MPEP concentration was measured to be around 1, suggesting good access of MPEP to the brain (**Figure 3.4.C**).

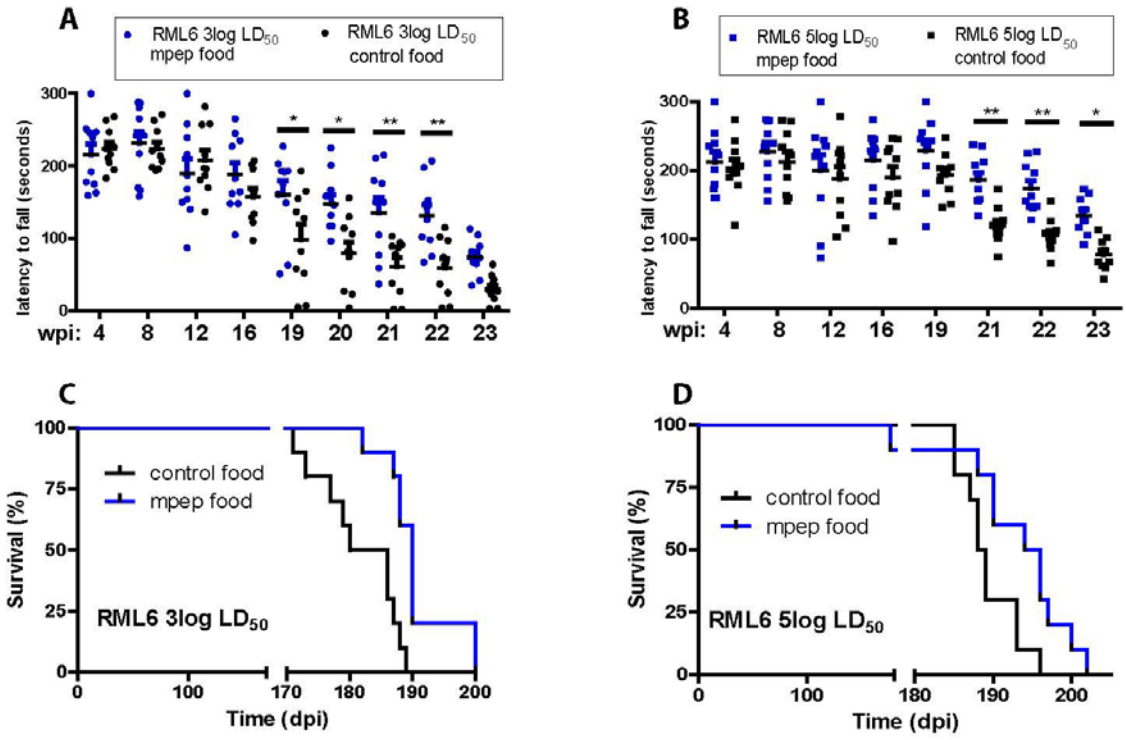

Figure 3.3. mGluR5 inhibition delays clinical manifestation of prion disease in wt mice

(A-B) mGluR5 pharmacological inhibition (MPEP treatment) significantly improves motor performance in mouse models of prion disease. Motor abilities of MPEP treated and MPEP untreated C57BL/6J males were assessed with the rotarod test at specified time points after i.c. inoculation with 3log LD_{50} **(A)** and 5log LD_{50} **(B)** units of RML6 prions respectively. Scatter dot plots show the time spent by each mouse on the rotating rod (latency to fall) expressed in seconds (s). Each dot corresponds to a mouse. Two-way ANOVA per each time point revealed a significant difference between MPEP treated and MPEP untreated groups at 19-22wpi (*: $P < 0.05$ and **: $P < 0.01$) for mice injected with 3log LD_{50} RML6 units and at 21-23wpi (*: $P < 0.05$ and **: $P < 0.001$) for mice injected with 5log LD_{50} RML6 units respectively, n=10 mice per group. **(C-D)** mGluR5 inhibition (MPEP treatment) significantly prolongs survival in mouse models of prion disease. Survival curves of MPEP treated and MPEP untreated C57BL/6J males, inoculated i.c. with 3log LD_{50} and 5log LD_{50} units of RML6 prions respectively. **(C)** Mice inoculated with 3log LD_{50} RML6 units: MPEP untreated group, n=10, median incubation time 183 days post inoculation (dpi). MPEP treated group, n=10, median incubation time 190dpi; P=0.0008; log-rank test. **(D)** Mice inoculated with 5log LD_{50} RML6 units: MPEP untreated group, n=10, median incubation time: 188.5 dpi, P=0.0008; MPEP treated group, n=10, median incubation time: 195dpi, P=0.0231; log-rank test.

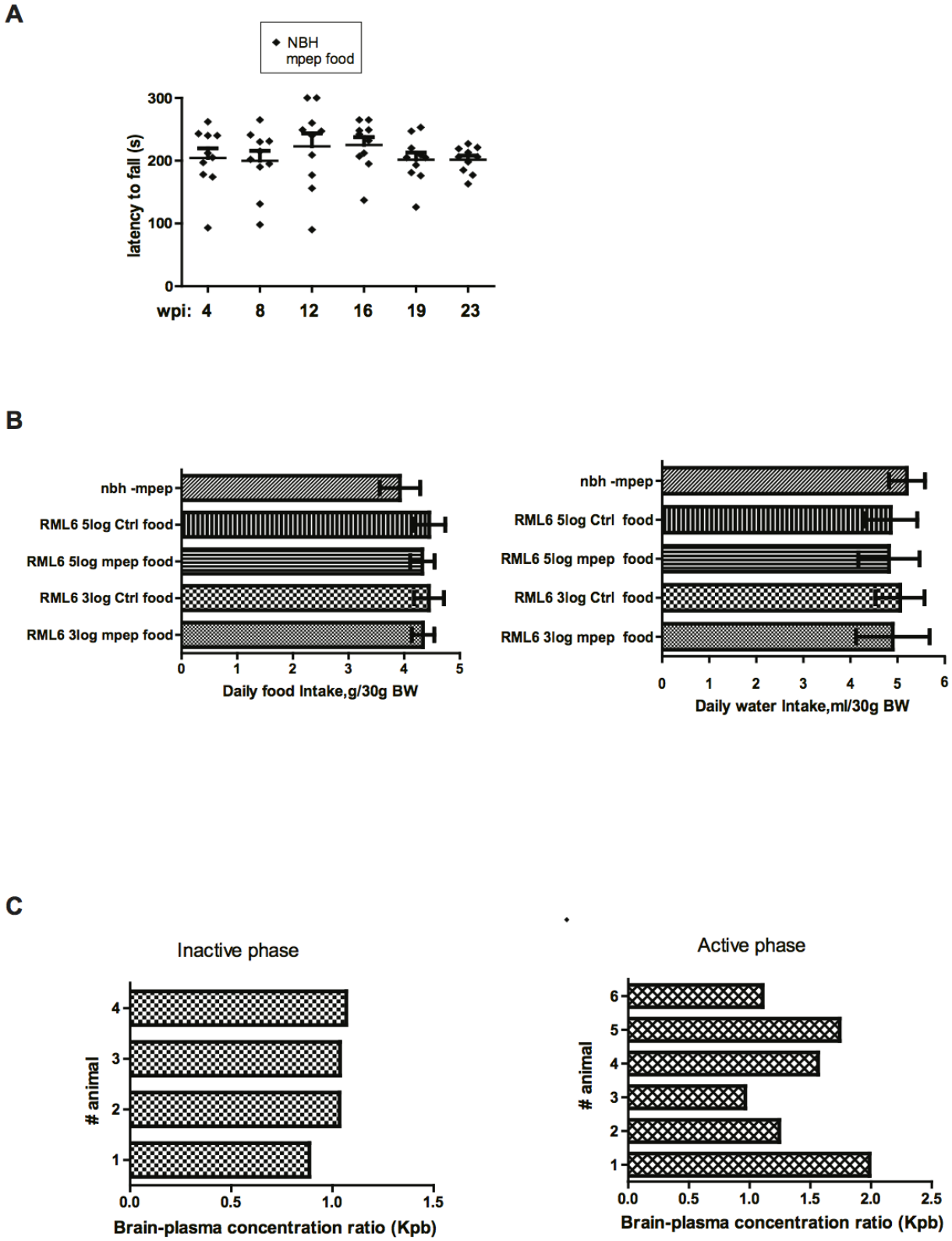
A
NBH
mpep food
latency to fall (s)
300
200
100
0
wpi: 4 8 12 16 19 23
B
nbh -mpep
RML6 5log Ctrl food
RML6 5log mpep food
RML6 3log Ctrl food
RML6 3log mpep food
0 1 2 3 4 5
Daily food Intake,g/30g BW
nbh -mpep
RML6 5log Ctrl food
RML6 5log mpep food
RML6 3log Ctrl food
RML6 3log mpep food
0 1 2 3 4 5 6
Daily water Intake,ml/30g BW
C
Inactive phase
animal
4
3
2
1
0.0 0.5 1.0 1.5
Brain-plasma concentration ratio (Kpb)
Active phase
animal
6
5
4
3
2
1
0.0 0.5 1.0 1.5 2.0 2.5
Brain-plasma concentration ratio (Kpb)

Figure 3.4. MPEP is effectively delivered to the brain, does not induce changes in food and water consumption and rotarod performance of non-infectious brain homogenate (NBH) inoculated mice

(A) Control mice injected with NBH and treated with MPEP exhibited stable rotarod performance during the entire test period, up to 23 weeks post-injection. Each dot corresponds to a mouse. Two-way ANOVA per each time point revealed no significant difference in the latency to fall of NBH-injected, MPEP treated mice during the course of the study. **(B)** No significant changes in average food and water consumption were observed between control and treatment (MPEP) groups during the experiment; Data are presented as mean ± s.d.; One-way ANOVA followed by Dunnet's post-hoc test. **(C)** Mice treated with control and MPEP food were sacrificed in two different timepoints, corresponding to the active and the inactive phase of the mice across the circadian circle to determine the exposure of the brain to MPEP. The results indicated the average brain to blood ratio for the MPEP concentration to be around 1; suggesting that the current treatment scheme allows good exposure of the brain to MPEP.

3.3. mGluR5 and mGluR1 inhibitors protects against prion-mimetic antibodies

Antibody-derived molecules targeting the globular domain (GD) of PrP^C (termed GDLs) are acutely neurotoxic (Sonati et al., 2013) and activate similar cascades as bona fide prion infection (Herrmann *et al.*, 2015). To investigate if pharmacological inhibition of mGluR1 and mGluR5 rescues *GDL* toxicity, we exposed *tga20* COCS to the *GDL* agent POM1, followed by YM202074 and MPEP treatments. Treatment with POM1 led to almost complete CGL loss within 14 days of treatment. No CGL loss occurred in control treatment where POM1 was blocked by pre-incubation with a molar excess of recombinant PrP (recPrP). Treatment with MPEP significantly reduced CGL loss in POM1-treated slices. As with prion infections, MPEP treatment (at concentrations as low as 10 nM) was sufficient to rescue the loss of CGL, whereas high concentrations (≥1μM) did not show protective activity (**Figure 3.5.A-B**).

Single chain POM1 miniantibodies (scPOM1), fusion proteins containing only the variable regions of the heavy (V_H) and light chains (V_L) of the antibody connected with a short linker peptide, were previously shown to be sufficient to induce toxicity in COCS (Sonati *et al.*, 2013). The toxicity of

scPOM1 was also significantly reduced in the presence of the specific mGluR1 inhibitor (YM202074), with protective concentrations as low as 200nM (**Figure 3.5.A-B**) as well as in the presence of the specific mGluR5 inhibitor MPEP (C=36nM) (**Figure 3.6.A**). No protection was observed upon treatment with the selective agonist of group III (L-2-amino-4-phosphonobutyrate (L-AP4)) (Tones et al., 1995) and the potent antagonist of group II and group III ((*RS*)-α-Cyclopropyl-4-phosphonophenyl glycine (CPPG)) (Toms et al., 1996) metabotropic glutamate receptors (**Figure 3.6.C-D**).

Similarly to COCS, HOCS treated with scPOM1 exhibited conspicuous toxicity after 8 days of treatment. As in previous experiments, we observed somewhat stronger toxicity of the single-chain version of the *GDL* (scPOM1), perhaps because of its smaller size leading to improved tissue penetration. Neuronal loss was monitored by morphometric analysis of NeuN immunofluorescence, and was readily visible in *GDL*-treated samples. In comparison, the survival of hippocampal neurons exposed to scPOM1 (**Figure 3.5.E-F**) was greatly increased by treatment with MPEP. We conclude that toxicity of both infectious prions and prion-mimetic GDLs was prevented by pharmacological inhibition of mGluR1 or mGluR5.

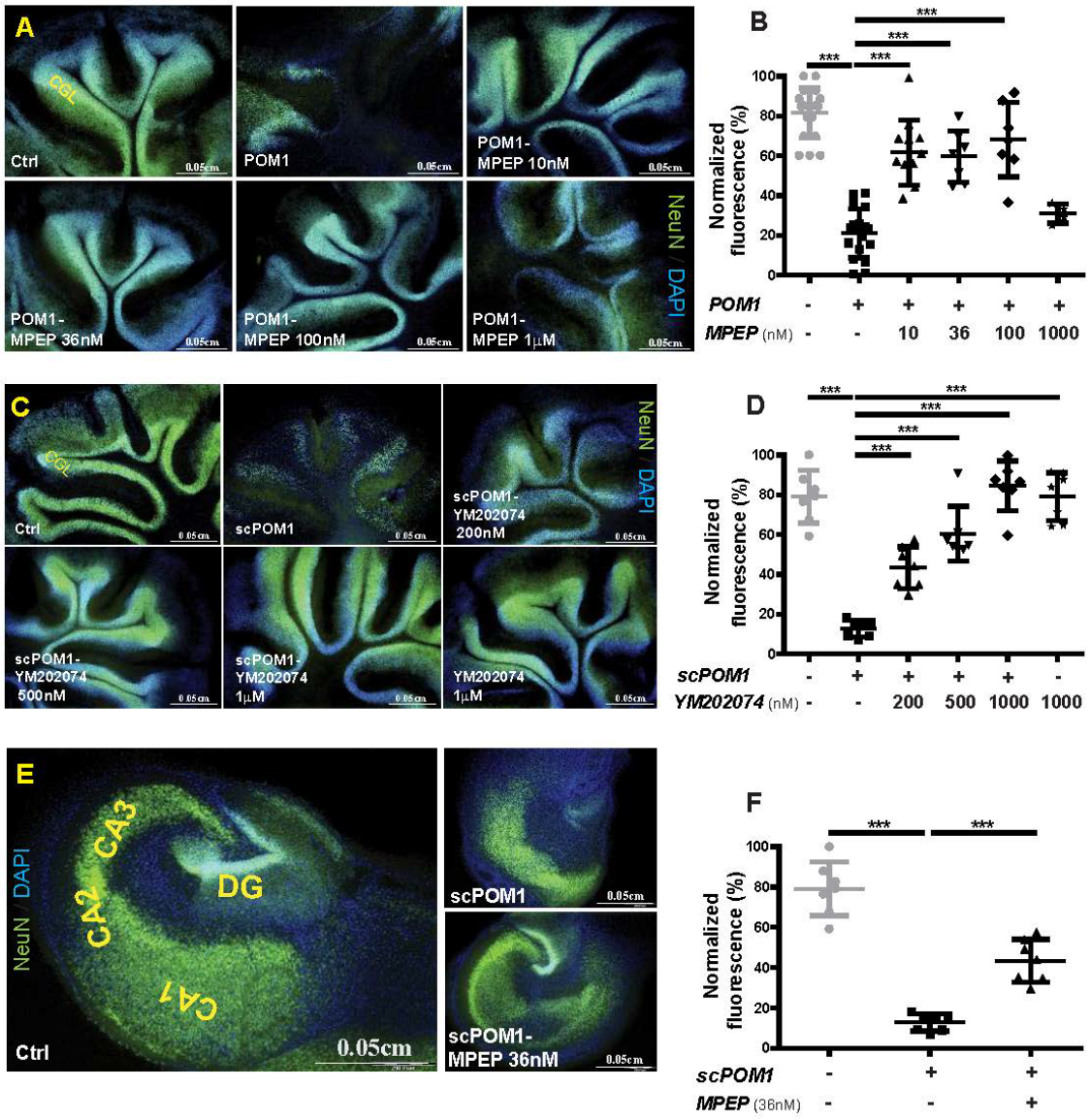

Figure 3.5. Group-I mGluR inhibition protects against GDL toxicity in organotypic slice cultures

(A-B) Treatment with the mGluR5 inhibitor (MPEP) rescued neurodegeneration in *tga20* POM1-treated COCS. **(A)** Representative images of *tga20* COCS, showing ablation of the cerebellar granular layer (CGL) induced by exposure to toxic POM1 antibody, that is significantly ameliorated by addition of low concentrations of MPEP (C=10nM-100nM). Higher concentrations of MPEP (C=1μM) did not rescue POM1 toxicity. **(B)** Graphical representation of NeuN morphometry of *tga20* slices exposed to POM1 or control (POM1 blocked with recPrP) and treated with MPEP from 14–28 days post exposure (dpe). **(C-D)** Treatment with the mGluR1 inhibitor (YM202074) rescued neurodegeneration in *tga20* scPOM1-treated COCS. **(C)** Representative images of COCS, showing

ablation of the cerebellar granular layer (CGL) induced by exposure to toxic POM1 antibody, that is significantly ameliorated by addition of low concentrations of YM202074 (C=200nM-1μM). **(D)** Graphical representation of NeuN morphometry of *tga20* slices exposed to scPOM1 or control scPOM1 blocked with recPrP and treated with MPEP from 14–22 dpe. **(E-F)** Treatment with MPEP rescued neurodegeneration in *tga20* scPOM1-treated COCS. **(E)** Representative images of HOCS, showing ablation of the hippocampal neuronal layer induced by exposure to toxic scPOM1 antibody (middle), that is significantly ameliorated by addition of MPEP (C=36nM). **(F)** Graphical representation of NeuN morphometry of *tga20* slices exposed to scPOM1 or control (scPOM1 blocked with recPrP) and treated with MPEP from 14–22 dpe. For **(B)**, **(D)** and **(F)** panels: Scatter dot plots represent NeuN relative signal intensity as percentage of POM1+recPrP or scPOM1+recPrP control samples; each dot corresponds to a pool of 7-10 cerebellar slices or 4-6 hippocampal slices cultured in the same well; Data are presented as mean ± s.d.; One-way ANOVA followed by Dunnet's post-hoc test. **Panel (B):** (Ctrl (POM1+recPrP), $n=18$ pools; POM1, $n=18$ pools; POM1+10nM MPEP, $n=12$ pools; RML6+36nM MPEP, $n=7$ pools; RML6+100nM MPEP, $n=7$ pools; RML6+1μM MPEP, $n=4$ pools; ***: $P < 0.001$. **Panel (D):** (Ctrl (scPOM1+recPrP), $n=7$ pools; scPOM1, $n=7$ pools; scPOM1+200nM YM202074, $n=7$ pools; scPOM1+500nM YM202074, $n=7$ pools; RML6+1μM YM202074, $n=7$ pools; 1μM YM202074, $n=7$ pools); ***: $P < 0.001$. **Panel (F):** (Ctrl (scPOM1+recPrP), $n=7$ pools; scPOM1, $n= 7$ pools; scPOM1+36nM MPEP, $n=7$ pools); ***: $P < 0.001$.

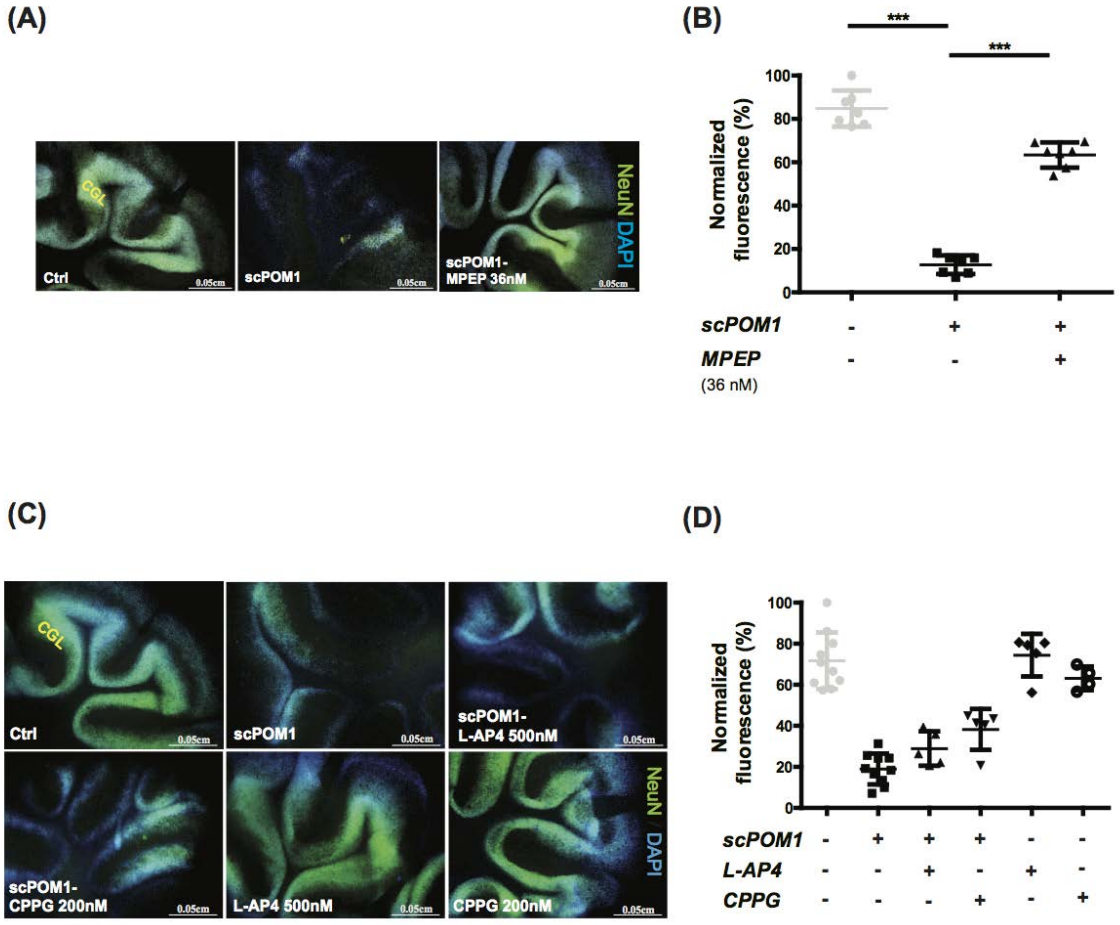

Figure 3.6. Treatment with MPEP, but not L-AP4 and CPPG rescues GDL toxicity in cerebellar organotypic cultures slices

(A-B) Treatment with the mGluR5 inhibitor (MPEP) rescued neurodegeneration in *Tga20* scPOM1-treated COCS. **(A)** Representative images of *Tga20* COCS, showing ablation of the cerebellar granular layer (CGL) induced by exposure to toxic scPOM1 antibody, that is significantly ameliorated by addition MPEP (C=36nM). **(B)** Graphical representation of NeuN morphometry of *Tga20* slices exposed to scPOM1 or control (POM1 blocked with recPrP) and treated with MPEP from 14–24 days post exposure (dpe). **(C-D)** Treatment with the selective agonist of group III (L-AP4)) and the potent antagonist of group II and group III (CPPG) metabotropic glutamate receptors did not rescue neurodegeneration in *Tga20* scPOM1-treated COCS. **(A)** Representative images of *Tga20* COCS, showing ablation of the cerebellar granular layer (CGL) induced by exposure to toxic scPOM1 antibody, that is not ameliorated by addition of L-AP4 (C=500nM) or CPPG (C=200nM). **(B)** Graphical representation of NeuN morphometry of *Tga20* slices exposed to scPOM1 or control (POM1 blocked with recPrP) and treated with L-AP4 or CPPG from 14–24 dpe.

For panels (B) and (D): Scatter dot plots represent NeuN relative signal intensity as percentage of POM1+recPrP or scPOM1+recPrP control samples; each dot corresponds to a pool of 7-10 cerebellar slices in the same well; Data are presented as mean ± s.d.; One-way ANOVA followed by Dunnet's post-hoc test. **Panel (B):** (Ctrl (scPOM1+recPrP), *n*=8 pools; POM1, *n*=7 pools; RML6+36nM MPEP, *n*=7 pools; ***: P < 0.001. **Panel (D):** (Ctrl (scPOM1+recPrP), *n*=12 pools; scPOM1, *n*=10 pools; scPOM1+500nM L-AP4, *n*=5 pools; scPOM1+200nM CPPG, *n*=5 pools; 500nM L-AP4, *n*=5 pools; 200nM CPPG, *n*=4 pools.

3.4. Toxicity of prions and prion-mimetic antibodies in Grm5$^{-/-}$ mice

Cerebellar organotypic slice cultures from *Grm5*$^{-/-}$, *Grm5*$^{+/-}$ and *Grm5*$^{+/+}$ littermates were treated with the anti-GD antibody POM1 (Polymenidou *et al.*, 2008), which acts as a prion-mimetic compound. Exposure to POM1 led to the loss of cerebellar granular layer (CGL) neurons in *Grm5*$^{+/+}$ slices, but not in *Grm5*$^{-/-}$ and *Grm5*$^{+/-}$ slices (**Figure 3.7.A-B**). Cerebellar and hippocampal organotypic slice cultures from *Grm5*$^{-/-}$, *Grm5*$^{+/-}$ and *Grm5*$^{+/+}$ littermates were then inoculated with brain homogenate from CD1 mice infected with RML prions (RML6) or control NBH homogenate. In both COCS and HOCS, genetic ablation of mGluR5 was protective against prion induced toxicity (**Figures 3.7.C-D** and **4.7.E-F**).

To assess the role of mGluR5 in prion infections *in vivo*, we infected *Grm5*$^{-/-}$, *Grm5*$^{+/-}$, and control *Grm*$^{+/+}$ littermates with RML6 prions (5 log LD_{50}). Again, we utilized the rotarod test. All RML6 inoculated mice showed similar rotarod performance during monitoring; with *Grm5*$^{-/-}$ mice showing a tendency towards better motor performance in general (**Figure 3.7.G**). However, no significant difference in survival was observed between *Grm5*$^{-/-}$, *Grm5*$^{+/-}$ and *Grm5*$^{+/+}$ mice (**Figure 3.8.A**).

The group-I metabotropic glutamate receptors, mGluR1 and mGluR5, can both associate with PrP^{C} and induce similar intracellular pathways (Beraldo et al., 2011) suggesting functional redundancy between these two receptors. In order to detect any epistasis between mGluR1 and mGluR5, we assessed mGluR1 and mGluR5 protein levels in hippocampus and cerebellum of *Grm5*$^{-/-}$, *Grm5*$^{+/-}$ and *Grm5*$^{+/+}$ mice. Expression decreased in all brain regions with increasing age. In hippocampi we observed increased expression of the mGluR1 in samples from *Grm5*$^{-/-}$ mice at 10-day and 53-d old, compared to heterozygous and wild type control littermates. (**Figure 3.8.D** right panel, lanes 3 and 9).

We additionally analyzed whole-brain lysates to control for mGluR1 and mGluR5 level changes between young and old mice. Samples from 44-day old *Grm5*$^{-/-}$ mice show higher expression levels of mGluR1 to heterozygous and wt control littermates. At later time points expression levels of mGluR1 were similar between samples (**Figure 3.8.F**). These results point to compensatory mechanisms between mGluR1 and mGluR5. We further sought to evaluate whether treatment with MPEP has a similar effect on the expression of mGluR1. MGluR1 expression levels were assessed in whole-brain lysates from 1-year old control wt mice, NBH-inoculated wt mice, and NBH-inoculated wt mice that received MPEP food. No differences were observed in the mGluR1 expression levels between the samples (**Figure 3.8.B**).

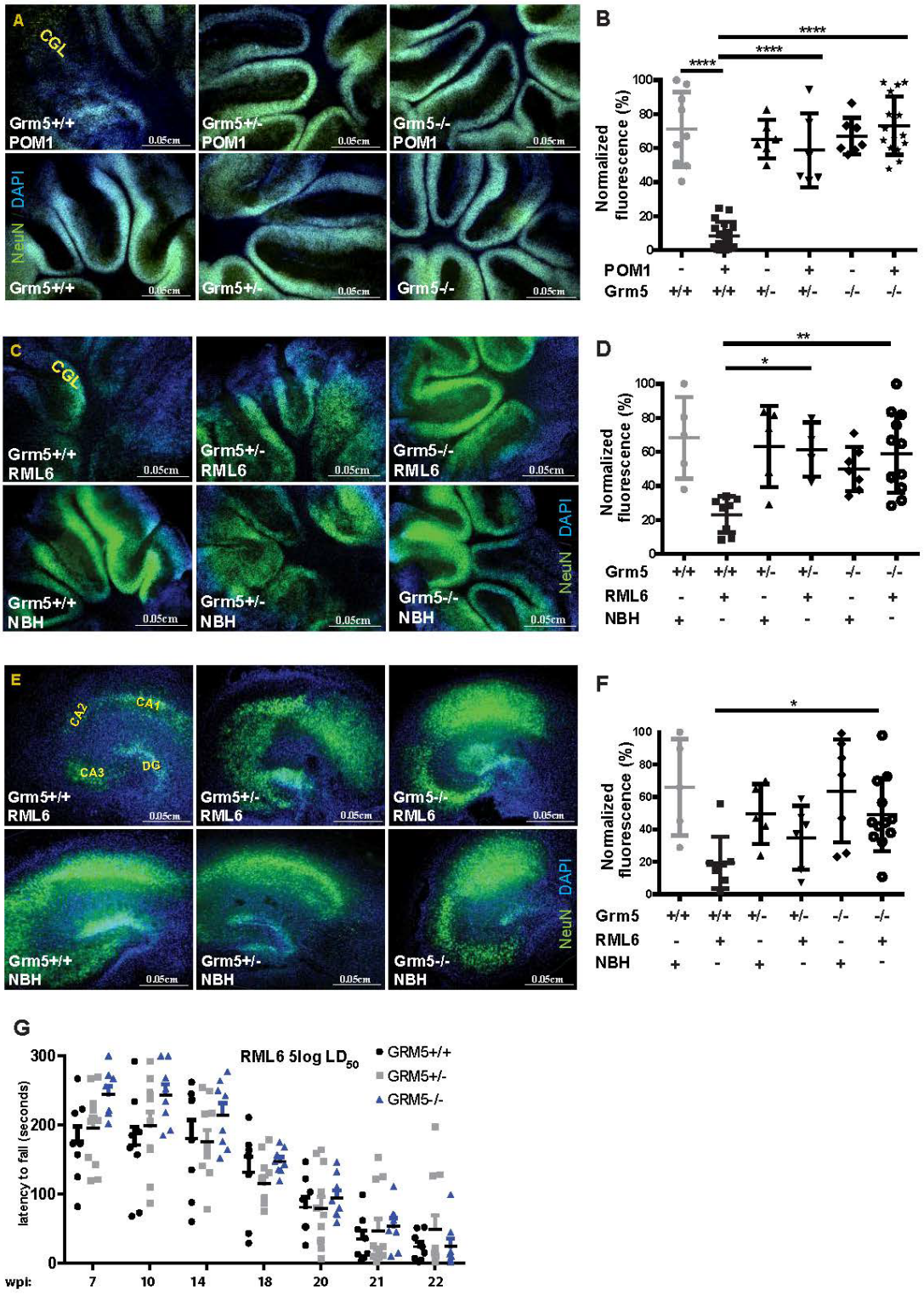

Figure 3.7. Grm5 ablation protects against GDL and prion-induced neurotoxicity in slice cultures but does not prolong survival *in vivo*

(A-B) Genetic ablation of Grm5 rescued *GDL*-induced neurodegeneration in COCS. **(A)** Representative images of COCS, showing ablation of the cerebellar granular layer (CGL) induced by

exposure to 67nM of toxic POM1 antibody in control *GRM5*$^{+/+}$ slices, that is significantly ameliorated by the genetic deletion of *GRM5* (*GRM5*$^{+/-}$ and *GRM5*$^{-/-}$ slices). **(B)** Graphical representation of NeuN morphometry of *GRM5*$^{+/-}$ and *GRM5*$^{-/-}$ and *GRM5*$^{+/+}$ slices exposed to POM1 or control (POM1 blocked with recPrP) from 14–42 dpe.

(C-D) Genetic ablation of Grm5 rescued prion-induced neurodegeneration in COCS. **(C)** Representative images of COCS, showing ablation of the cerebellar granular layer (CGL) induced by RML6 infection in control *GRM5*$^{+/+}$ slices, that is significantly ameliorated by the genetic deletion of *GRM5* (*GRM5*$^{+/-}$ and *GRM5*$^{-/-}$ slices). Slices were maintained in culture for 60dpi. **(D)** Graphical representation of NeuN morphometry of *GRM5*$^{+/-}$ and *GRM5*$^{-/-}$ and *GRM5*$^{+/+}$ slices exposed to RML6 or NBH. **(E-F)** Genetic ablation of Grm5 rescued prion-induced neurodegeneration in HOCS. **(E)** Representative images of HOCS, showing ablation of the hippocampal neuronal layer induced by RML6 infection in control *GRM5*$^{+/+}$ slices, that is significantly ameliorated by the genetic deletion of *GRM5* (*GRM5*$^{-/-}$ slices). Slices were maintained in culture for 60dpi. **(F)** Graphical representation of NeuN morphometry of *GRM5*$^{+/-}$ and *GRM5*$^{-/-}$ and *GRM5*$^{+/+}$ slices exposed to RML6 or NBH. RML6-induced neurodegeneration is rescued in the *GRM5*$^{+/-}$ and *GRM5*$^{-/-}$ HOCS.

For **(B)**, **(D)** and **(F)** panels: Scatter dot plots represent NeuN relative signal intensity as percentage of control samples (Grm5$^{+/+}$, NBH or POM1+recPrP) ; each dot corresponds to a pool of 7-10 cerebellar slices or 4-6 hippocampal slices cultured in the same well; Data are presented as mean ± s.d.; One-way ANOVA followed by Dunnet's post-hoc test. **Panel (B):** (Ctrl (Grm5$^{+/+}$, POM1+recPrP), *n*=8 pools; Grm5$^{+/+}$, POM1, *n*=18 pools; Grm5$^{+/-}$, POM1+recPrP, *n*=6 pools; Grm5$^{+/-}$, POM1, *n*=6 pools; Grm5$^{-/-}$, POM1+recPrP, *n*=7 pools; Grm5$^{-/-}$, POM1, *n*=15 pools; ****: P < 0.0001. **Panel (D):** (Ctrl (Grm5$^{+/+}$, NBH), *n*=5 pools; Grm5$^{+/+}$, RML6, *n*=8 pools; Grm5$^{+/-}$, NBH, *n*=5 pools; Grm5$^{+/-}$, RML6, *n*=4 pools; Grm5$^{-/-}$, NBH, *n*=7 pools; Grm5$^{-/-}$, RML6, *n*=11 pools; *: P < 0.05, **: P < 0.01. **Panel (F):** (Ctrl (Grm5$^{+/+}$, NBH), *n*=5 pools; Grm5$^{+/+}$, RML6, *n*=7 pools; Grm5$^{+/-}$, NBH, *n*=5 pools; Grm5$^{+/-}$, RML6, *n*=6 pools; Grm5$^{-/-}$, NBH, *n*=7 pools; Grm5$^{-/-}$, RML6, *n*=12 pools; *: P < 0.05. **(G)** MGluR5 genetic deletion does not significantly improve motor performance in mouse models of prion disease. Motor abilities of *GRM5*$^{+/+}$, *GRM5*$^{+/-}$ and *GRM5*$^{-/-}$ mice were assessed with the rotarod test at specified time points after i.c. inoculation with 5log LD_{50} units of RML6 prions. Scatter dot plots show the time spent by each mouse on the rotating rod (latency to fall) expressed in seconds (s). Each dot corresponds to a mouse. Two-way ANOVA per each time point revealed a non-significant difference

(ns: P>0.05) between *GRM5*$^{+/+}$, *GRM5*$^{+/-}$ and *GRM5*$^{-/-}$ groups at 7-22wpi for mice injected with 5log LD_{50} RML6 units respectively, n=7-13 mice per group.

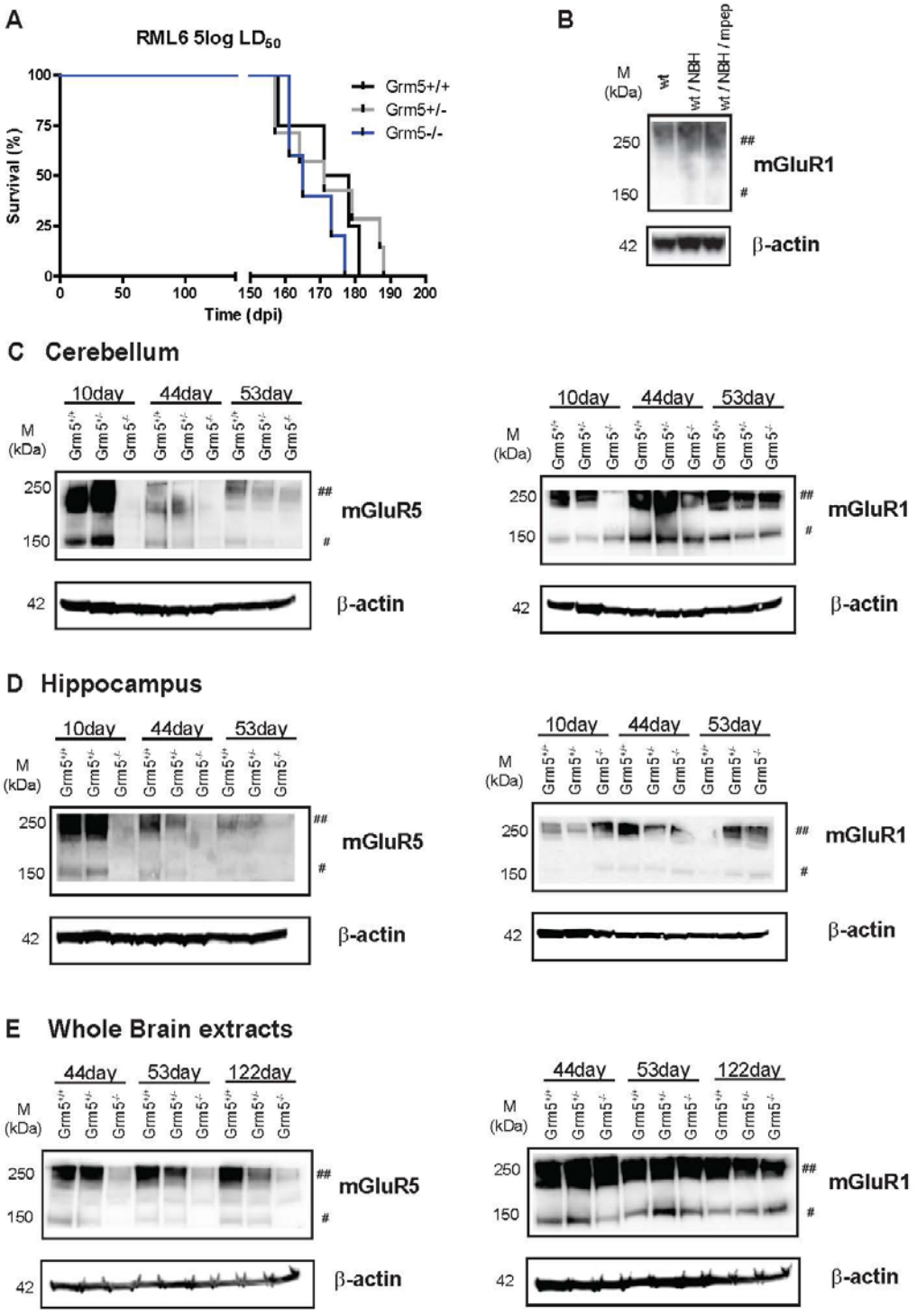

Figure 3.8. Grm5 genetic deletion does not significantly prolong survival of prion-infected mice - a compensatory mechanism between mGlu1 and mGlu5 receptors

(A) Survival curves of *GRM5*$^{+/+}$, *GRM5*$^{+/-}$ and *GRM5*$^{-/-}$ groups, inoculated i.c. with 5log LD_{50} units of RML6, n=4-6 males per group. Each dot corresponds to a mouse. Two-way ANOVA per each time point revealed a non-significant difference between *GRM5*$^{+/+}$, *GRM5*$^{+/-}$ and *GRM5*$^{-/-}$ groups. **(B)** Total brain extracts from mice inoculated with NBH and received control or mpep foods, as well as control wt brain lysates, were subjected to western blot analysis to evaluate whether mpep treatment changes the expression of mGlu1 receptor. No differences were observed in the mGluR1 expression levels between the samples. **(C-D)** Epistatic expression of mGlu1 and mGlu5 receptors. Total brain extracts from different brain regions - cerebellum **(C)**, hippocampus **(D)** - were subjected to western blot analysis to control for endogenous levels of both mGluR1 (right panel) and mGluR5 (left panel) in samples collected from different age groups (10day, 44day, 53day) of *Grm5*$^{-/-}$, *Grm5*$^{+/-}$ and *Grm5*$^{+/+}$ mice. At postnatal day 10 (comparable with the organotypic slices), mGluR5 expression in the cerebellum is similar to that of hippocampus. Over time, expression decreases in both brain regions. In hippocampi we observed increased expression of the mGluR1 in samples from *Grm5*$^{-/-}$ mice at 10-day and 53-d old, compared to heterozygous and wild type control littermates. (figure 3.8.D: right panel, lanes 3 and 9). **(E)** Total brain extracts from 44day, 53day and 122 days old *Grm5*$^{-/-}$, *Grm5*$^{+/-}$ and *Grm5*$^{+/+}$ were in parallel subjected to western blot analysis to control for endogenous levels of mGluR1 and mGluR5 in young and old mice. Samples from 44-day old *Grm5*$^{-/-}$ mice show higher expression levels of mGluR1 to heterozygous and wild type control littermates. In the later time points expression levels of mGlur1 are comparable between the samples. #: band corresponds to the mGluR1 or mGluR5 monomer. ##: band corresponds to the mGluR1 or mGluR5 dimer.

3.5. PrP^C interacts with mGluR1 and mGluR5 *in vivo*

PrP^C has been reported to interact with mGluR1 and mGluR5 (Beraldo *et al.*, 2011; Um *et al.*, 2013). To test whether PrP^C interacts with group-I mGluRs *in vivo*, brain homogenates from wild-type (C57BL/6J) or *Prnp* knockout mice (*Prnp*$^{o/o}$) were subjected to immunoprecipitation using antibody POM1 against PrP^C, followed by western blotting with antibodies to mGluR1 and mGluR5. The group-I mGlu receptors, which migrate as functionally active oligomers at 250kDa (Romano *et al.*, 1996b), were found to co-precipitate with PrP^C (**Figure 3.9.A** left and right panels, lanes 5). For control, we

performed immunoprecipitations in the presence of non-specific pooled immunoglobulins (IgG) and blocked the antigen-recognition domain of POM1 with recombinant PrP. Under neither condition did we observe mGluR1 and mGluR5 co-immunoprecipitating with PrP (**Figure 3.10.A** left and right panels, lanes 3 and 4). Western blots from the total brain lysates (TEs) did not reveal any changes in the concentration of mGluR1 and mGluR5 protein between wild-type and *Prnp*$^{o/o}$ homogenates (**Figure 3.10.A**, lanes 7-8). Other mGluRs (mGluR6, mGluR2/3) did not co-precipitate, confirming the specificity of the interaction (**Figure 3.10.B**).

The PrP^{C} residues 91-153 participate to the interaction with mGluR5 (Haas *et al.*, 2014).We sought to confirm these findings and to identify the domain of PrP^{C} mediating its interaction with mGluR1. We studied a panel of transgenic mice expressing variants of PrP^{C} bearing deletions in the flexible tail (FT) regions, designated ΔC, ΔCC, ΔF, ΔOR, and ΔHC (**Figure 3.10.C**). The relevance of these mutants to prion disease was previously reported (Baumann *et al.*, 2007a; Bremer *et al.*, 2010; Flechsig *et al.*, 2000; Shmerling *et al.*, 1998; Weissmann *et al.*, 1998). As expected, mGluR1 and mGluR5 co-precipitated with PrP^{C}. Deletions affecting residues 32-110 (as in the transgenic lines □¢ and □¢C, lacking the central domain and the charge cluster regions of PrP^{C}, respectively) reduced the interaction of PrP^{C} with mGluR5 (**Figure 3.9.B**, lanes 3 and 5). Deletions extending from residues 51 to 90, as in the transgenic line ΔOR, (**Figure 3.9.B**, lane 4) increased the interaction with mGluR5, yet reduced the interaction with mGluR1 (**Figure 3.9.C**, lane 4). These results suggest that the interaction domain between PrP^{C} and mGluR5 is larger than previously inferred, with residues 32-110 participating to the *in vivo* interaction.

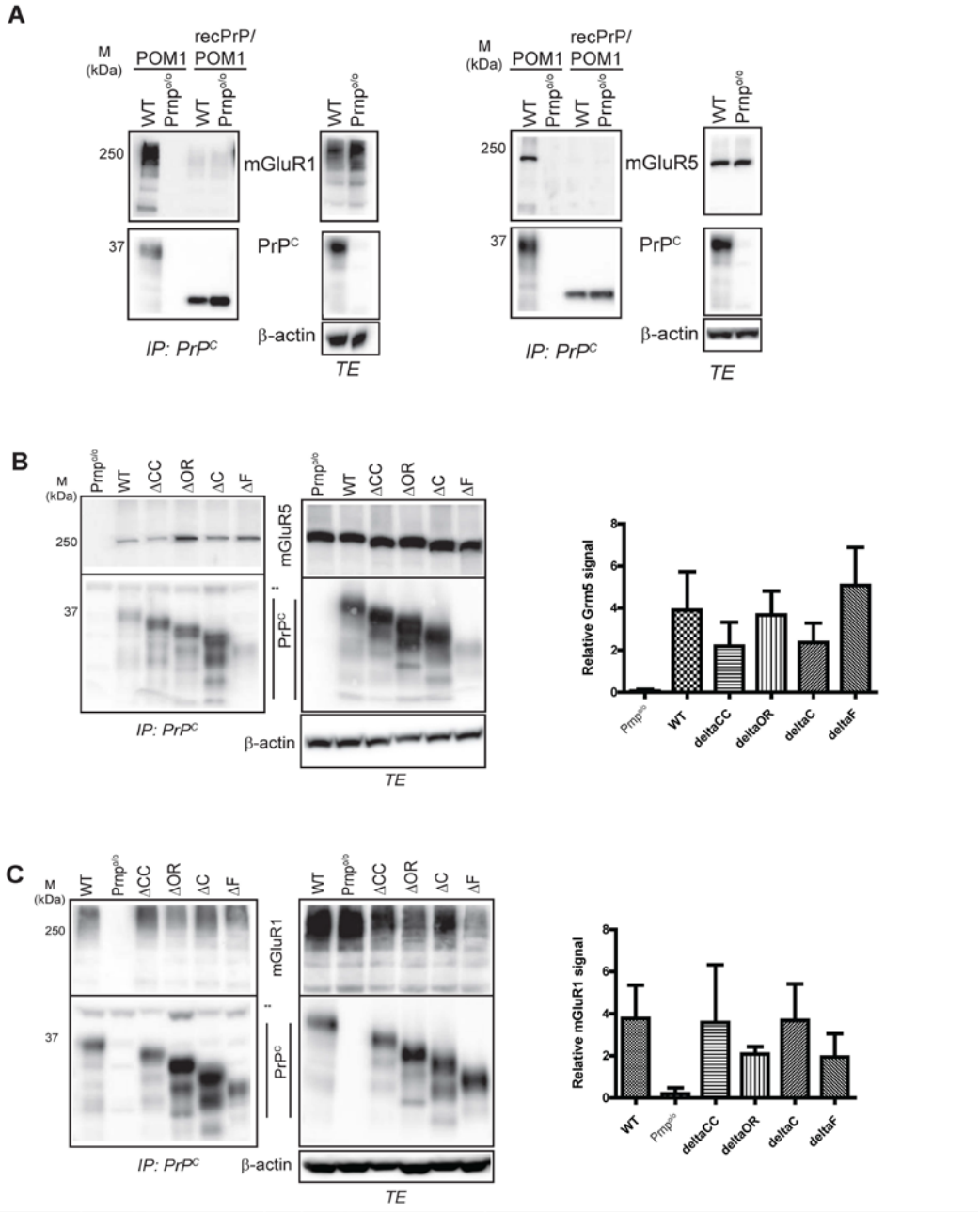

Figure 3.9. Mapping the mGluR1 and mGluR5 interacting regions on PrP^C

(A) PrP^C interacts with group I metabotropic glutamate receptors. Brain homogenate from wild-type (C57BL/6J) and *Prnp*$^{o/o}$ mice was subjected to immunoprecipitation by POM1 (monoclonal anti-PrP^C antibody) followed by immunobloting using polyclonal anti-mGluR5 (right panel) or anti-mGluR1 (left panel) and anti-PrP^C antibodies to detect mGluR5/mGluR1 and PrP^C respectively. Control conditions (POM1 blocked by recombinant PrP^C) were run in parallel to ensure the specificity of the selected mGluR5/mGluR1 antibodies. A specific band of 250kDa was detected in wild-type immunoprecipitates only when immunoblotting with the specific mGluR5 antibody. Specific bands of 250kDa and 150kDa

(corresponding to the dimer and monomer of the receptor) were detected in wild-type immunoprecipitates only when immunoblotting with the specific mGluR1 antibody. Total brain extracts were in parallel subjected to Western blot analysis to control for endogenous levels of mGluR5/1 and PrP^C. **(B-C)** Mapping the mGluR1 and mGluR5 interacting domains on PrP^C. Brain homogenate from wild-type and *Prnp*$^{o/o}$ and aminoterminal deletion mutants was subjected to immunoprecipitation by POM1, followed by immunobloting using polyclonal anti-mGluR5 **(B)** or anti-mGluR1 **(C)** and anti-PrP^C antibodies to detect mGluR5/1 and PrP^C respectively. Deletions extending from residues 32-93 and 94 to 110- corresponding to the ΔC (deletion of the central domain) and the ΔCC (deletion of the charged cluster region of PrP^C), reduced the interaction with mGluR5, whereas deletions extending from residues 51 to 90, corresponding to the ΔOR (deletion of the octarepeat region on PrP^C), decreased the interaction with mGluR1. Total brain extracts (TEs) were subjected to Western blot analysis to control for endogenous levels of mGluR5/1 and PrP^C. Densitometric quantitation of mGluR1 or mGluR5 signal from the immunoprecipitation was normalized over the ration of Grm/Actin signal in TEs. Graph bars represents mGluR1 or mGluR5 relative signal intensity; N=3-5; One-way ANOVA followed by Tukey's post-hoc test; ns: P>0.05.

*: band corresponds to the light chain of the POM1 antibody. **: band corresponds to recombinant PrP. #: band corresponds to the mGluR1 monomer. ##: band corresponds to the mGluR1 dimer.

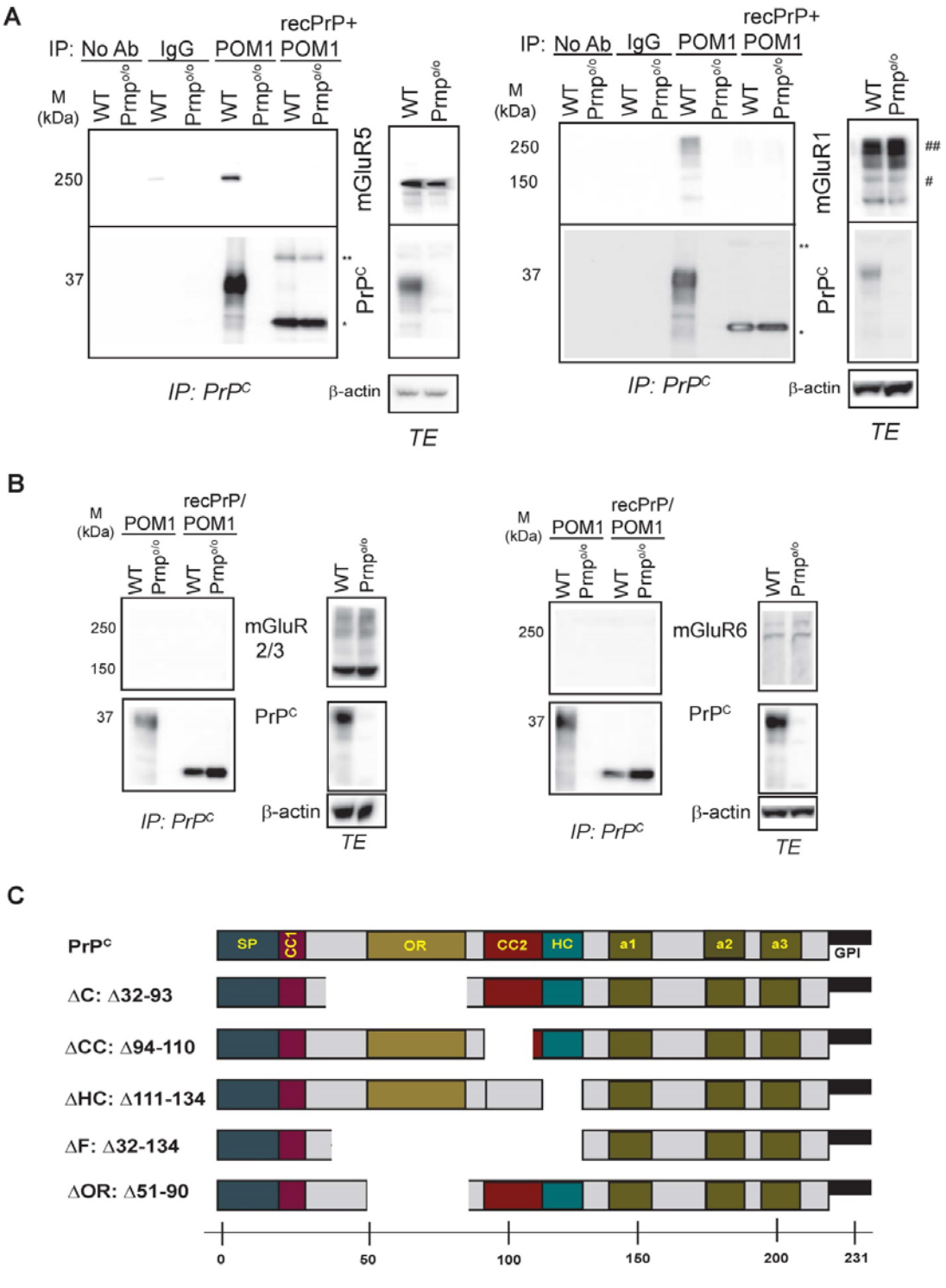

Figure 3.10. PrP^C specifically interacts with mGluR1/5 and not with group II and III mGluRs

(A) Brain homogenate from (C57BL/6J) and *Prnp$^{o/o}$* mice was subjected to immunoprecipitation by POM1 (monoclonal anti-PrP^C antibody) followed by immunobloting using polyclonal anti-mGluR5

(left panel) or anti-mGluR1 (right panel) and anti-PrP^C antibodies to detect mGluR5/mGluR1 and PrP^C respectively. Control conditions (unconjugated beads, IgG bound beads and POM1 blocked by recombinant PrP^C) were run in parallel to ensure the specificity of the selected mGluR5/mGluR1 antibodies. A specific band of 250kDa was detected in wild-type immunoprecipitates only when immunoblotting with the specific mGluR5 antibody. Specific bands of 250kDa and 150kDa (corresponding to the dimer and monomer of the receptor) were detected in wild-type immunoprecipitates only when immunoblotting with the specific mGluR1 antibody. Total brain extracts were in parallel subjected to Western blot analysis to control for endogenous levels of mGluR5/1 and PrP^C. *: band corresponds to the light chain of the POM1 antibody. **: band corresponds to the recombinant PrP. #: band corresponds to the mGluR1 monomer. ##: band corresponds to the mGluR1 dimer. **(B)** Brain homogenate from wild-type (C57BL/6J) and *Prnp*$^{o/o}$ mice was subjected to immunoprecipitation by POM1 (monoclonal, anti-PrP^C antibody) followed by immunoblotting using polyclonal anti-mGluR2/3and anti-mGluR6, or anti-PrP^C antibodies to detect group II and III glutamate receptors and PrP^C, respectively. Group II and III receptors (mGluR2/3 and mGluR6) were not associated with PrP^C, indicating a specificity of this interaction for group-I mGluRs. **(C)** Schematic representation of PrP^C deletion mutants.

3.6. MPEP treatment reduces vacuole size and astrogliosis in prion-infected mice

PrP^{Sc} deposition is accompanied by neurodegeneration, vacuole formation and activation of microglia and astrocytes (Brown and Sassoon, 2004). MPEP treatment did not affect the accumulation of PrP^{Sc} in prion-infected mice and slices (**Figure 3.12.A-B**). However, it did affect vacuole formation. We analyzed the extent of vacuolation in the granular layer of the cerebellum (CGL) and in the hippocampus. Although the numbers of vacuoles in control and MPEP treated groups were similar, vacuole size was significantly reduced in cerebella and hippocampi of MPEP-treated mice (**Figure 3.11.A-B**). Astrogliosis, assessed by immunohistochemistry for glial fibrillary acidic protein (GFAP), was prominent at the terminal stage of prion infected mice but not in NBH-inoculated mice. Astrogliosis was unaltered by MPEP in the cerebellar granule cell layer (**Figure 3.12.C**), but was markedly reduced in the hippocampus of MPEP-treated, RML6-infected (3 log) group (**Figure 3.10.C**).

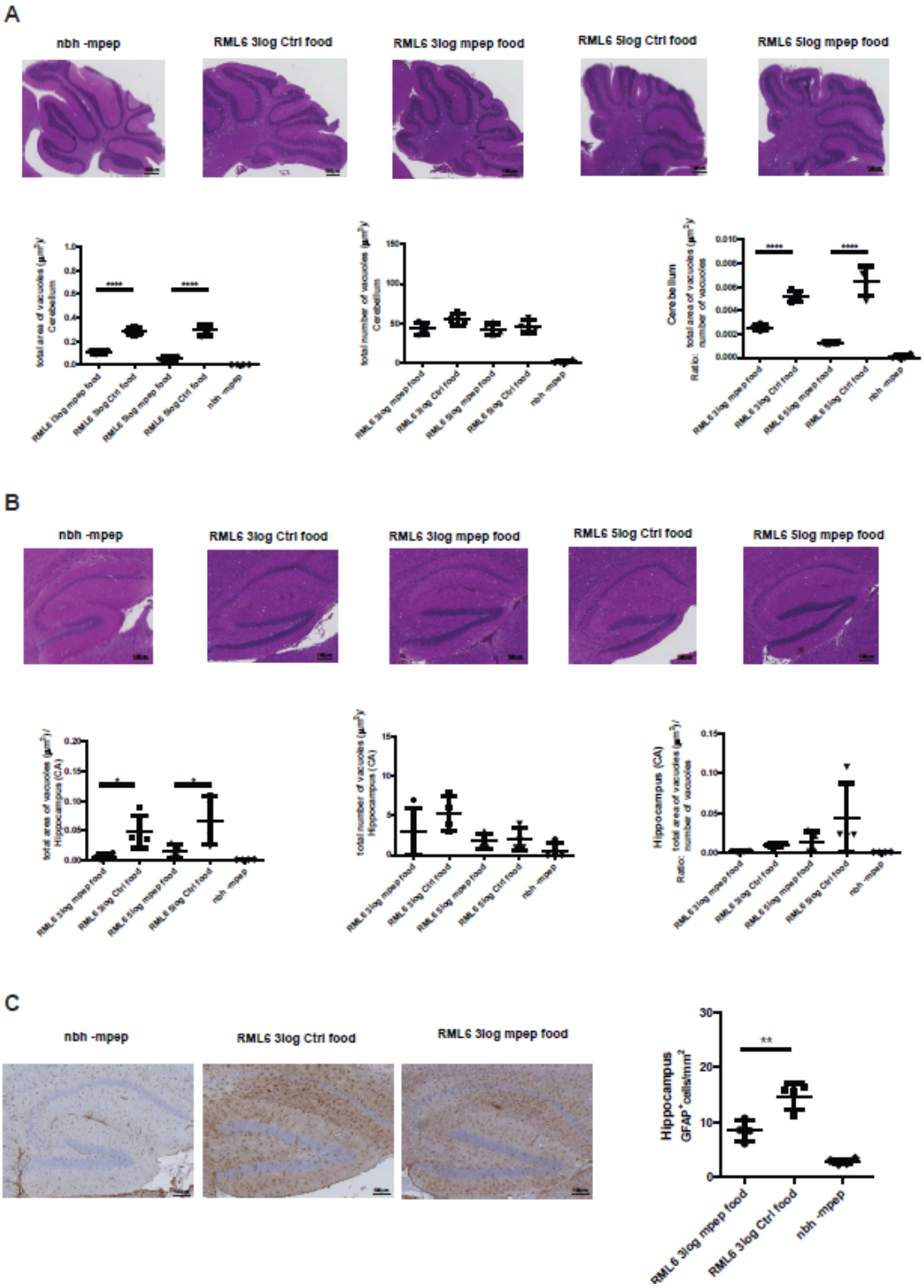

Figure 3.11. MPEP treatment reduces vacuole size and astrogliosis in prion-infected mice

(A-B) Representative images of hematoxylin and eosin-stained cerebellar and hippocampal sections from *C57BL/6J* mice injected i.c. with NBH or RML6 prions and treated with control or MPEP-

containing food respectively. Number of spongiform vacuoles was quantified in cerebellar cortex and hippocampal CA (Cornu Ammonis) areas. Cerebellum: control-food treated animals: vacuole area (0.4□m^2), MPEP-food treated animals: vacuole area (0.1μm^2), Hippocampus: control-food treated animals: vacuole area (0.18μm^2), MPEP-food treated animals: vacuole area (0.03μm^2). Each graph corresponds to a treatment group. 10 regions of interest per slice, 4 slices per mouse and 4 mice per treatment group were used for quantification. **(C)** Astrocyte proliferation was analyzed by immunohistochemistry with the GFAP antibody in paraffin-embedded sections of hippocampal areas from *C57BL/6J* mice injected i.c. with NBH or RML6 prions and treated with control or MPEP-containing food respectively. Number of GFAP$^+$ cells was quantified in the hippocampus. Each graph corresponds to a treatment group. GFAP staining was markedly reduced in the MPEP-treated, RML6 3log group. Dot blots represent mean ± SD GFAP expression, quantified as the percentage of the surface occupied by the GFAP staining over the total measured area; 10 regions of interest per slice, 4 slices per mouse and 4 mice per treatment group were used for quantification. ***P<0.0001; two-way ANOVA followed by Bonferroni's *post-hoc* test.

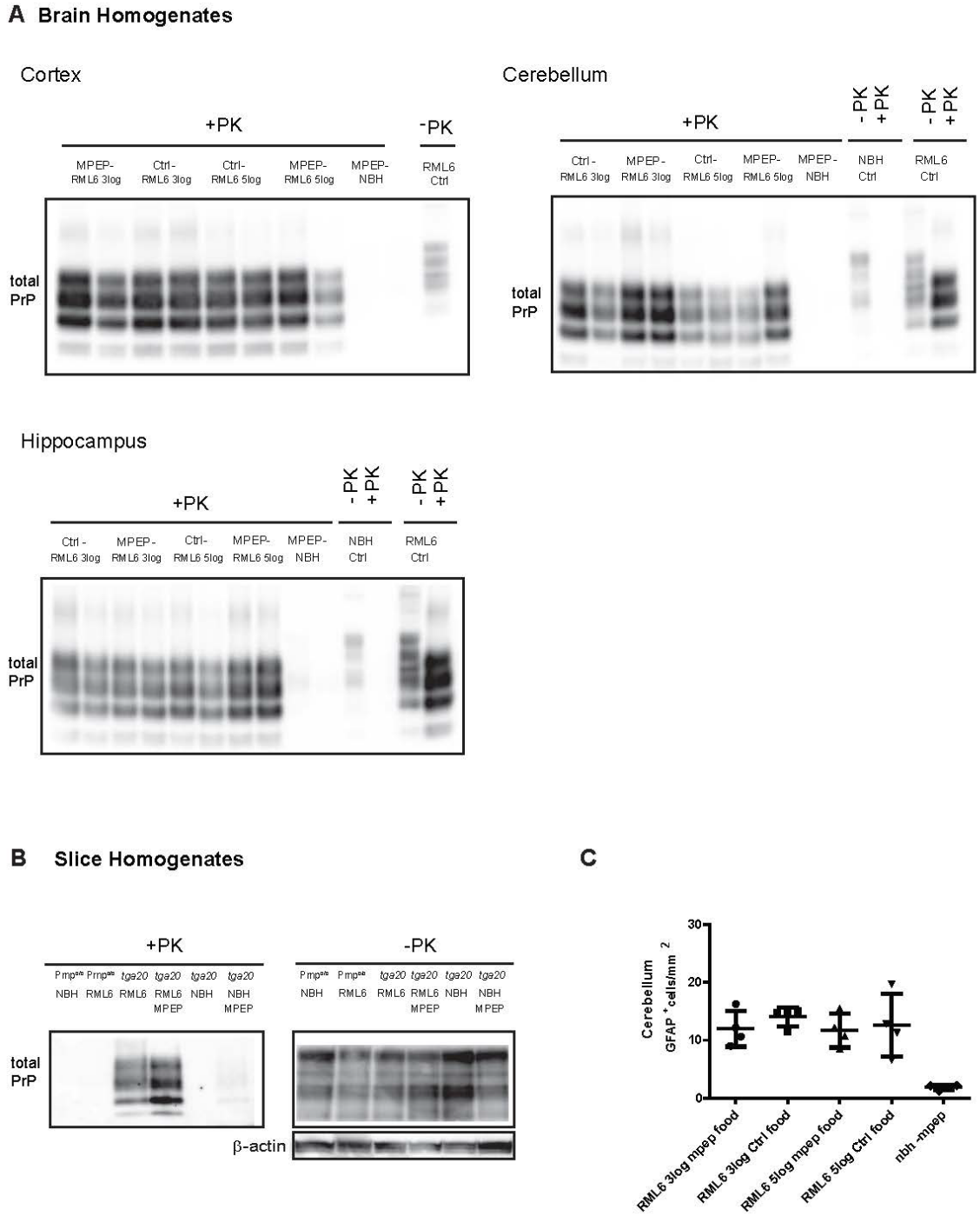

Figure 3.12. PrP^{Sc} accumulation in prion-infected slices or in the brain of prion-infected mice is not altered by MPEP treatment

(A) Total PrP and PrP^{Sc} levels (detected by addition of proteinase K (PK)) in homogenates from different brain regions (cortex, hippocampus, and cerebellum) of terminal C57BL/6J mice injected i.c. with NBH or RML6 prions and treated with control or MPEP-containing food respectively. Control NBH and RML6 samples, with or without addition of PK were run in parallel.

(B) Total PrP and PrP^{Sc} levels (detected by addition of proteinase K (PK)) in homogenates from RML6 infected cerebellar slices prepared from *Tga20* or $PrP^{o/o}$ mice. Cerebellar slices infected with RML6 prions were also treated with MPEP according to the previously described protocol. Control NBH samples, with or without addition of PK were run in parallel. **(C)** Astrocyte proliferation was analyzed by immunohistochemistry with the GFAP antibody on cerebellar sections from *C57BL/6J* mice injected i.c. with NBH or RML6 prions and treated with control or MPEP-containing food respectively. Number of $GFAP^{+}$ cells was quantified in the cerebellar granular layer (CGL). Dot blots represent mean ± SD GFAP expression, quantified as the percentage of the surface occupied by the GFAP staining over the total measured area; 10 regions of interest per slice, 4 slices per mouse and 4 mice per treatment group were used for quantification; two-way ANOVA followed by Bonferroni's *post-hoc* test.

3.7. Prion-mimetic antibodies increase mGluR5 and PrP^{C} translocation to dendritic spines

Clusters of mGluR5s accumulate around excitatory synapses, and increased size of synaptic mGluR5s clusters is associated with toxic calcium influx (Renner *et al.*, 2010; Shrivastava *et al.*, 2013; Um *et al.*, 2013). Therefore, we asked whether the prion-mimetic POM1 antibody altered the clustering of mGluR5s. Immunofluorescent analysis of mGluR5s clusters was performed on primary hippocampal neurons following exposure to the anti-PrP^{C} $F(ab)_1$ antibody fragments, POM1, POM2, and POM3 (Sonati *et al.*, 2013). Exposure of cultures to POM1, but not to POM2 or POM3, increased the fluorescence intensity of mGluR5s clusters (**Figure 3.13.A-B**). In contrast, the cluster size of NMDA and AMPA receptors was not modified by anti-PrP antibodies (**Figure 3.14.**). Next, we quantified the fluorescence level of mGluR5s in dendritic spines of neurons expressing mGluR5-pHluorin. We observed increased accumulation of mGluR5s in dendritic spines following exposure to POM1, but not to POM2 or POM3 (**Figure 3.13.C-D**).

Both mGluR5 and PrP^{C} are enriched in postsynaptic densities (PSD) (Um *et al.*, 2013). In order to assess if the changes in mGluR5s level in spines correlated with PrP^{C} level in spines, we performed photo-activated localization microscopy (PALM) on neurons expressing a PrP^{C}-Dendra fusion protein (**Figure 3.13.E**). PALM images were obtained from single-molecule detection events rendered with a pixel size of 20 nm. The PrP^{C}-Dendra fluorescence patterns showed both clustered and diffuse

staining (**Figure 3.13.E**, control); we observed increased enrichment within dendrites spines following POM1 but not POM1+2 exposure (**Figure 3.13. E-F**). Furthermore, exposure to Fab_1-POM2, which was previously found to protect against POM1 toxicity (Sonati et al., 2013), induced a subtle but significant reduction in PrP^C enrichment within dendritic spines. Therefore, Fab_1-POM1 and Fab_1-POM2 have opposite effects on the topology and size of mGluR5 clusters, with POM1 inducing abnormal accumulation and translocation to dendritic spines.

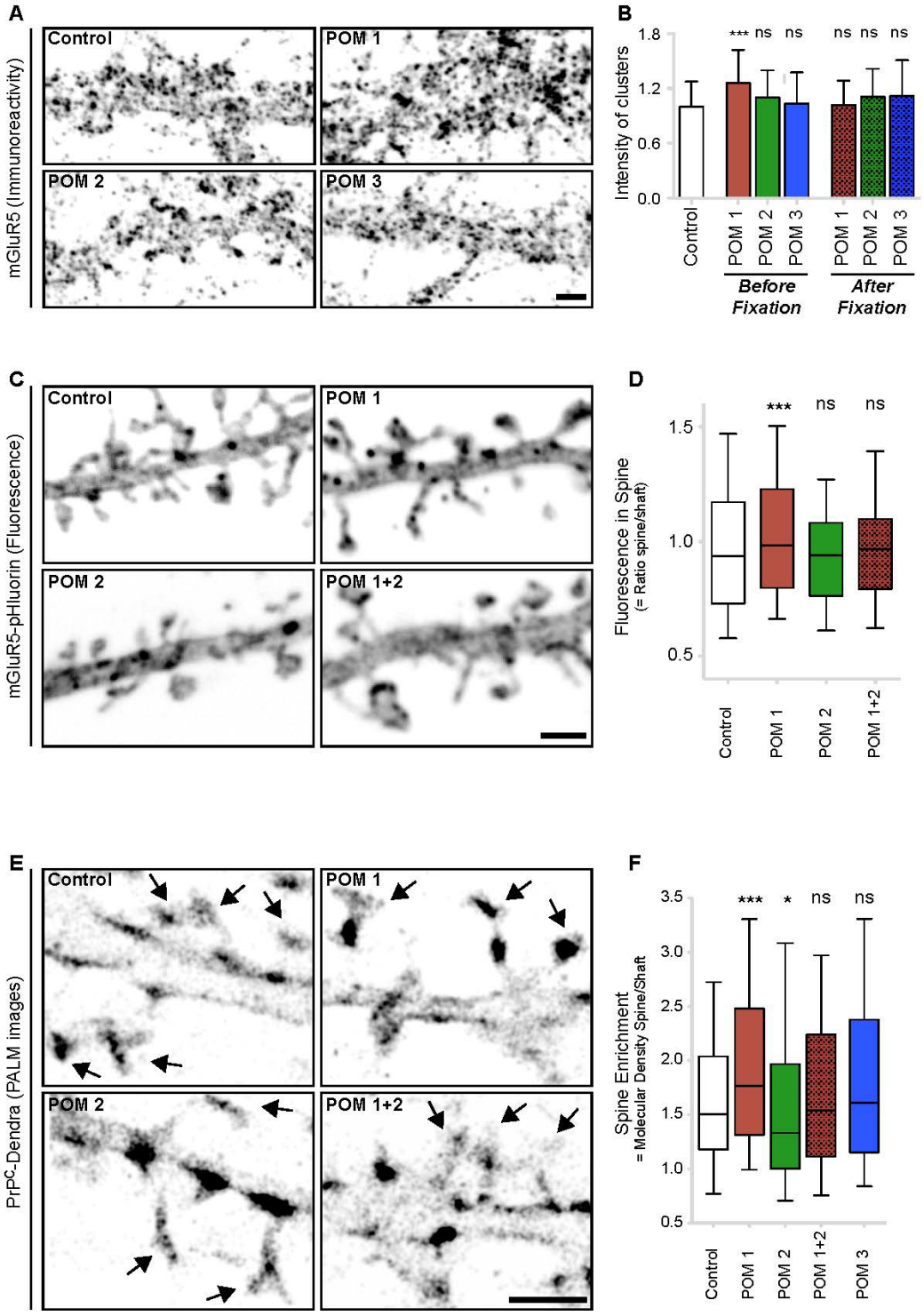

Figure 3.13. Exposure to Fab_1-POM1 increases mGluR5 and PrP^C translocation to dendritic spines

(A-B) mGluR5 immunoreactivity following Fab_1-POM1 administration to live neurons. Quantification of fluorescence intensity **(B)** showed increased size of mGluR5 clusters following exposure of live

neurons to Fab_1-POM1, but not to Fab_1-POM2 or Fab_1-POM3. "*ex vivo*": antibody administration to live neurons; "*post mortem*": administration to fixed neurons. One-way ANOVA with Dunnett's post-hoc test relative to control. The number of fields-of-view analyzed was: 88 (control), 90 (POM1/live), 59 (POM2/live), 60 (POM3/live), and 30 (POM1/fixed; POM2/fixed; POM3). Results were pooled from three independent experiments. **(C-D)** Increased mGluR5s immunoreactivity in dendritic spines following Fab_1-POM1 exposure. **(C)** Representative images showing the expression of mGluR5-pHluorin in untreated and Fab_1-POM1-treated neurons (1 μg, 1 h). **(D)** Fluorescence ratio (spine/shaft) emphasizing the increase in mGluR5-pHluorin level in spines following exposure to Fab_1-POM1, but not to Fab_1-POM2 or a mixture of Fab_1-POM1 and Fab_1-POM2. Number of spines analyzed (n): 1070 (control), 1190 (Fab_1-POM1), 1082 (Fab_1-POM2), 908 (Fab_1-POM1+2). Mann-Whitney test on data from three independent experiments. (**E-F**) Spine enrichment of PrP^C following exposure to Fab_1-POM1. (**E**) Single-molecule detection of PrP^C-Dendra by photoactivated localization microscopy (PALM) on dendritic spines and shafts. Aantibody treatment: 1μg, 1h. (**F**) Ratio of molecular density in spine versus dendritic shaft emphasizing spine-enrichment of PrP^C-Dendra following exposure to Fab_1-POM1 but not to other antibodies. Number of spines analyzed (n): 318 (control), 328 (POM1), 364 (POM2), 331 (POM1+2), 416 (POM3). Mann-Whitney test; *p<0.05, ***p<0.001, ns= non-significant. Scale bars: 2μm.

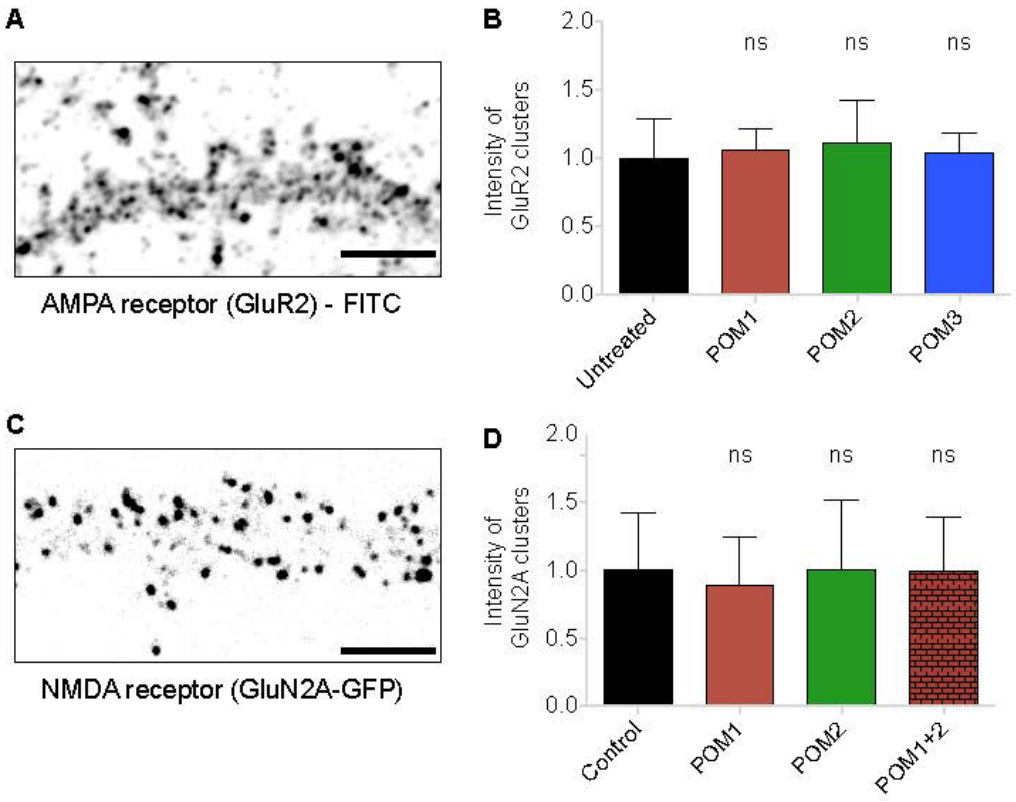

Figure 3.14. POM antibodies do not alter AMPA and NMDA receptor clustering

(A) Representative image (control condition) showing the immunoreactivity of GluR2 subunit of AMPA receptor following methanol fixation / permeabilization. **(B)** Quantification of the fluorescence intensity indicates that cluster size was not modified following POM antibodies application **(**One-way ANOVA with Dunnett's post-hoc test relative to control; field of view (n): Control-22, POM1-22, POM2-22, POM3-22 from 2 independent experiments**).** **(C)** Representative image (control condition) showing the fluorescence of GluN2A-GFP subunit of NMDA receptor ~48 h after transfection and paraformaldehyde fixation. (D) Quantification of fluorescence intensity indicate that the cluster size was not modified following POM antibodies application **(**One-way ANOVA with Dunnett's post-hoc test relative to control; field of view (n): Control-22, POM1-22, POM2-22, POM3-20 from 2-independent experiments**).** Scale bar: 2μm.

3.8. Prion-mimetic antibodies increase the cell surface expression of mGluR5 and PrP^C

A number of different mechanisms and signalling pathways, such as Ca^{2+}/CaMKIIa and PLC, regulate the processes of activation and internalization of mGlu5 receptor and thus its signalling. Seeking to investigate the effect of toxic versus protective POM antibodies and the group I mGluR5 antagonist, MPEP, on mGluR5 activation/desensitization in cerebellar organotypic slice cultures we used cell surface biotinylation with a cell impermeable reagent. Single chain POM1 miniantibodies (scPOM1), fusion proteins containing only the variable regions of the heavy (V_H) and light chains (V_L) of the antibody connected with a short linker peptide, were previously shown to be sufficient to induce toxicity in COCS (Sonati *et al.*, 2013). At 2h after addition of the toxic scPOM1 antibody, we observed an increase in the surface mGluR5 levels (quantified as a surface/total; mGluR5 ratios). Exposure to scPOM2 antibody yielded surface mGluR5s ratios more similar to untreated, scPOM1/recPrP or MPEP controls. Interestingly, pre-blocking of scPOM1 with the scPOM2 or combined POM1/MPEP treatment significantly reduced the cell surface expression of mGluR5s. The observed increase in the surface/total mGluR5 ratios after POM1 addition may represent capturing of the receptors in stable complexes as previously descibed in AD upon exposure to Aβ-oligomers (Renner *et al.*, 2010; Um and Strittmatter, 2013).

To conclude, exposure to toxic scPOM1 antibodies seems to induce an increase in the cell surface expression of mGluR5s. Interestingly, blocking of toxic scPOM1 with protective scPOM2 significantly reduces the mGluRs surface expression slightly similar to treatment with the specific mGluR5 inhibitor MPEP. These results support our previous observations showing increase of mGluR5 clusters in dendritic spines after addition of toxic POM1 antibodies.

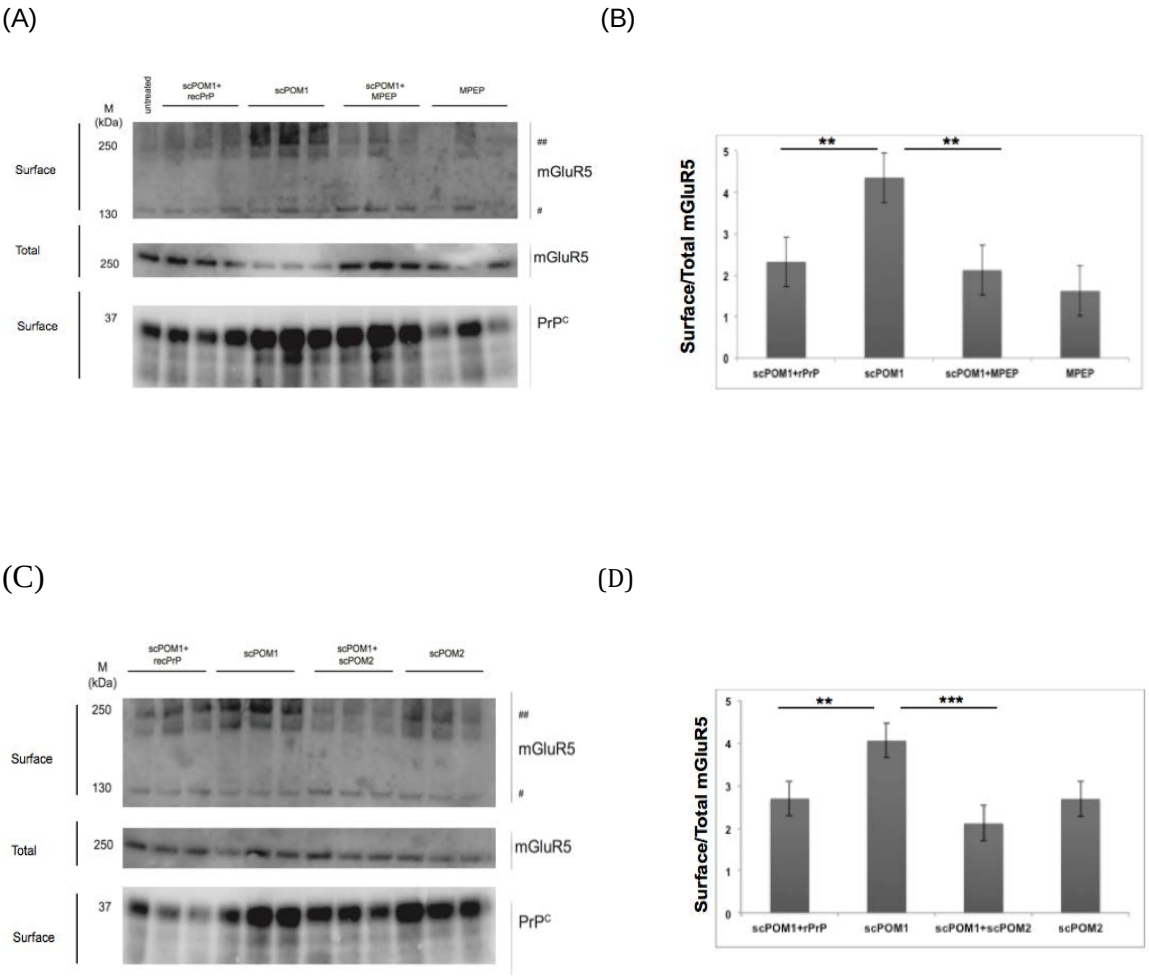

Figure 3.15. POM1 antibodies increase the cell surface expression of mGlu5 receptors

(A) Representatives images of cerebellar organotypic slice cultures from *Tga20* mice untreated or treated with 400nM scPOM1 blocked with rPrP *or* 400nM scPOM1 *or* 400nM scPOM1 with 500nM MPEP *or* 500nM MPEP for 2h. Subsequently, cell surface proteins were biotinylated and then isolated with NeutrAvidin conjugated beads. Isolated cell surface and total lysate proteins were assessed by anti-mGluR5 (upper panel: mGluR5 pull down, lower panel: mGluR5 lysate) and anti-PrP immunoblot. **(B)** Quantification of surface expression of mGluR5 normalized to total mGluR5 level after 2h treatment in *Tga20* COCS **(**n=3, Mean ± SE, unpaired t-test, P values: i. scPOM1+recPrP vs scPOM1, P=0.0057/ ii. scPOM1 vs scPOM1+MPEP, P=0.0043/ iii. scPOM1+MPEP vs MPEP, P=0.3824). **(C)** Representatives images of cerebellar organotypic slice cultures from *Tga20* mice treated with 400nM scPOM1 blocked with rPrP *or* 400nM scPOM1 *or* 400nM scPOM1 blocked with 400nM scPOM2 *or* 400nM scPOM2 for 2h. Subsequently, cell surface

proteins were biotinylated and then isolated with NeutrAvidin conjugated beads. Isolated cell surface and total lysate proteins were assessed by anti-mGluR5 (upper panel: mGluR5 pull down, lower panel: mGluR5 lysate) and anti-PrP immunoblot **(D)** Quantification of surface expression of mGluR5 normalized to total mGluR5 level after 2h treatment in *Tga20* COCS **(**n=3, Mean ± SE, unpaired t-test, P-values: i. scPOM1+recPrP vs scPOM1, P=0.0311/ ii. scPOM1 vs scPOM1+scPOM2, P=0.0099/iii. scPOM1+scPOM2 vs scPOM2, P=0.087/ iv. scPOM1 vs scPOM2, P=0.0317)

3.9. Characterization of novel transgenic mice expressing the RCaMP1.07 calcium indicator

Aiming to assess changes in Ca^{2+} homeostasis in prion diseases novel transgenic mice expressing the potent Ca2+ reporter (RCamp1.07) were generated. In brief, embryonic stem (ES) cell culture and gene targeting of the RCaMP1.07 reporter gene into the TIGRE locus were carried out and the targeted ES cells were microinjected into B6N-Tyrc blastocysts. Chimeras were tested for transgene expression and inheritance by Southern blotting using specific 5' and 3' external probes. Transgenic mice were further crossbred with R26phiC31o mice (Raymond and Soriano, 2007) for removal of the *AttB*/*AttP*-flanked hygro-TK cassette. Following removal of the cassette, mice were mated with either Camk2a-tTA (Mayford et al., 1996) or ROSA:LNL:tTA (Wang *et al.*, 2008) transgenic mice to allow for the generation of compound mutant mice in which expression of the reporter gene can be defined by the chosen Cre-recombinase and turned off by the addition of tetracycline (or its analog doxycycline). Expression of the transgene was evaluated both in fixed brain sections as well as in organotypic slice cultures (as indicated in the figure below).

(A)


Vibratome - Coronal brain sections
Mice
- CamK2a;TITL-RC;Syn1Cre pos
- CamK2a;TITL-RC;Syn1Cre neg
Brain Dissection
4% PFA fixation
Vibratome sectioning
30μm coronal
brain sections

(B)

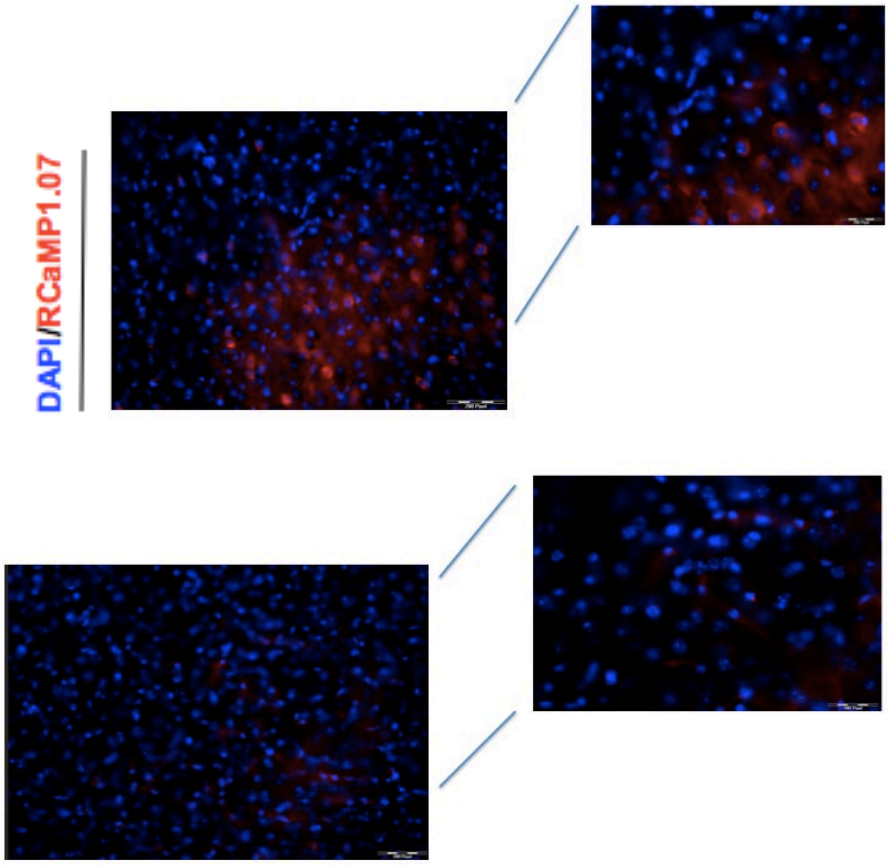
DAPI/RCaMP1.07

(C)

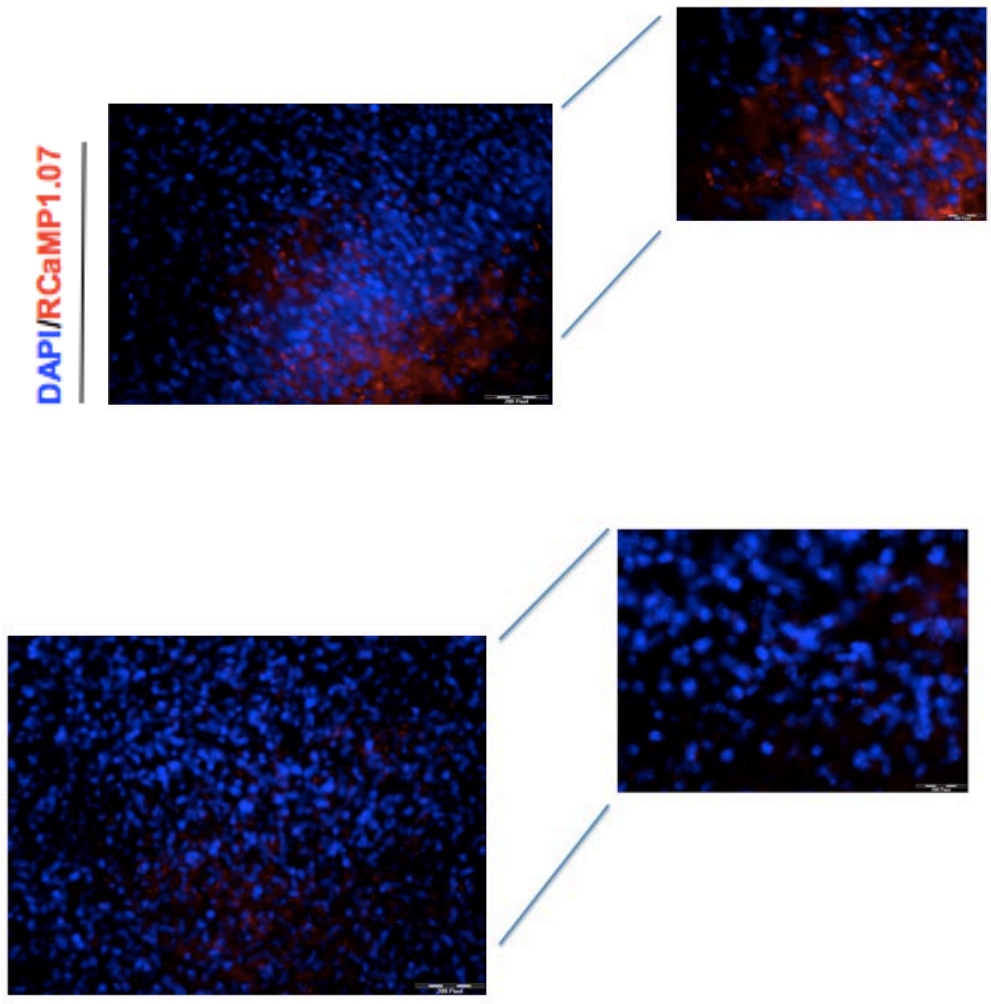

Figure 3.16. Evaluating the expression of RCaMP1.07 fixed brain section and HOCS prepated from the CaMK2a-TITL-RCaMP-Syn Cre mice

(A) Schematic representation of the preparation of coronal brain sections

(B) Expression of the RCamp1.07 reporter in coronal brain sections from CaMK2a-TITL-RCaMP-Syn Cre positive mice (upper panel). Control sections from CaMK2a-TITL-RCaMP-Syn Cre negative mice were run in parallel. Red: internal expression of RCaMP1.07 reporter, Blue: DAPI counterstaining post fixation. Left panel (upper and lower): coronal brain section 20x magnification, Right panel (upper and lower): coronal brain section 40x magnification

(C) Expression of the RCamp1.07 reporter in hippocampal organotypic cultured slices (HOCS) from CaMK2a-TITL-RCaMP-Syn Cre positive mice (upper panel). Slices from CaMK2a-TITL-RCaMP-Syn Cre negative mice were run in parallel. Red: internal expression of RCaMP1.07 reporter, Blue: DAPI counterstaining post fixation. Left panel (upper and lower): coronal brain section 20x magnification, Right panel (upper and lower): coronal brain section 40x magnification.

Chapter 4: DISCUSSION

4.1. Summary

The aim of the present study was to ascertain both the physical and functional relevance of PrP^C and group I mGluRs in prion (RML6) and GDL-induced (POM1) toxicity as well as the role of this interaction in disease both *in vitro* (primary neuronal cultures and organotypic slices cultures) and *in vivo* (mouse models of prion diseases). Upon validation of a specific interaction between group I mGluRs and PrP^C in brain homogenates, the region of PrP^C necessary for its interaction with group I mGluRs was examined utilizing a series of amino-proximal deletion mutants of PrP^C. The suggested site of interaction between PrP^C and mGluR1 spans amino acid residues 51 to 90; the suggested site of interaction between PrP^C and mGluR5 spans amino acids 32 to 134. Although the definitive causality of this relationship has yet to be identified, association of group I mGluRs with PrP^C has been suggested in multiple processes, such as developmental processes, synaptic transmission, synaptic plasticity as well as neurotoxic signaling cascades (Bruno *et al.*, 1995; Lopez-Bendito *et al.*, 2002; Salinska and Stafiej, 2003). Also, it has been reported that clusters of mGluR5s accumulate around excitatory synapses, and increased size of synaptic mGluR5s clusters is associated with toxic calcium influx in Alzheimer's disease (AD) (Renner *et al.*, 2010; Shrivastava *et al.*, 2013; *Um et al.*, 2013). Aiming to shed light into the mechanistic angles of this interaction in prion toxicity we performed cell surface biotinylation experiments on organotypic slice cultures and live cell imaging of primary hippocampal neurons after exposure to the toxic prion –mimetic POM1 antibody. Immunofluorescent analysis of mGluR5s-PrP clusters following exposure to the anti-PrP^C $F(ab)_1$ antibody fragments, POM1, POM2, and POM3 (Sonati *et al.*, 2013), showed that exposure of cultures to POM1, but not to POM2 or POM3, increased the number of mGluR5s clusters as well as the fluorescent intensity of mGluR5s in dendritic spines of neurons. In contrast, the cluster size of NMDA and AMPA receptors was not modified by anti-PrP antibodies. Likewise, exposure of cerebellar organotypic slice cultures to toxic scPOM1 antibodies induced an increase in the surface/total mGluR5 ratios. Interestingly, blocking of toxic scPOM1 with protective scPOM2 significantly reduces the mGluRs surface expression slightly similar to treatment with the specific mGluR5 inhibitor MPEP. These results most probably represent capturing of the receptors in stable, immobile complexes at the neck of the dendritic spines upon prion-mimetic antibody induced toxicity and resemble a toxicity mechanism previously descibed in AD upon exposure to Aβ-oligomers (Renner *et al.*, 2010; Um and Strittmatter, 2013).

Having identified a specific interaction between group I mGluRs and PrP^C and its potential role in protein toxicity *in vitro*, we sought and further examine the contribution of group I mGluRs in prion and GDL-induced toxicity *ex vivo* and *in vivo*. To observe the effects of mGluR1 and mGluR5, cerebellar and hippocampal organotypic slice cultures (COCS and HOCS respectively) were subjected to prion (RML6) and GDL (POM1, scPOM1)-induced toxicity and concomitant pharmacological inhibition of the respective receptor (addition of MPEP and YM202074 for mGluR5 and mGluR1 inhibition respectively). We demonstrated that dose-dependent treatment with specific pharmacological inhibitors of group I mGluRs rescues cerebellar granule or pyramidal hippocampal neurons immunoreactive to antibodies against the neuronal NeuN antigen in slices (COCS and HOCS). In contrast, treatment of cerebellar slices with the selective agonist of group III (L-AP4)) and the potent antagonist of group II and group III (CPPG) metabotropic glutamate did not rescue the observed granular cell layer (GCL) ablation. We additionally identified the therapeutic effect of Grm5 gene ablation in rescuing prion and GDP-induced neuronal death, by utilizing $Grm5^{-/-}$, $Grm5^{+/-}$ and wt littermates as controls. After identifying the protective effect of the pharmacological inhibition of mGluR5 (MPEP treatment) *ex vivo* we sought to assess a possible therapeutic effect of MPEP treatment on prion pathogenesis *in vivo*. C57BL/6J male mice were inoculated intracerebrally with two different concentrations 3 or 5 log LD_{50} units of RML6 prions as previously described (Kranich et al., 2010), and chronically treated with MPEP (MPEP-containing food). Control mice were inoculated with NBH. In order to record the neurological deficits associated with prion disease, we utilized the rotarod behavioral test which measures a combination of motor performance, coordination, and balance (Brooks and Dunnett, 2009). At the terminal stage of the disease mice were sacrifized and brain samples (whole brain as well as specific brain regions, such as cortex, hippocampus and cerebellum) were collected and further processed. Immunohistochemical staining (Iba1, GFAP, SAF84) of brain sections was performed and analysis included: vacuole area and number counting, percentage of reactive astrogliosis, percentage of reactive microgliosis and PrP^{Sc} accumulation. After verifying the therapeutic potential of pharmacological inhibition of mGluR5 we decided to test the genetic inhibition model. We tested whether toxicity induced by prion infection (RML6 prion strain) upon genetic deletion of mGluR5 (groups included in the study and compared in parallel are: $Grm5^{-/-}$, $Grm5^{+/-}$ and control wt littermates). In order to record the neurological deficits associated with prion disease, we utilized the rotarod behavioral test At the terminal stage of the disease mice were sacrifized and brain

samples (whole brain as well as specific brain regions, such as cortex, hippocampus and cerebellum) were collected. Unfortunately, no significant therapeutic effect was observed upon deletion of Grm5 *in vivo*. However, this observation led us to examine the potential for epistasis between mGlu1 and mGlu5 receptors. Indeed, we could see an increase in the expression levels of mGluR1 in the $Grm5^{-/-}$ and $Grm5^{+/-}$ mice.

In conclusion, this study provides insights into the interaction of PrP^C with group I mGluRs and its effect in *in vitro*, *ex vivo* and *in vivo* models of prion diseases. The above data suggest that group-I mGluRs inhibition may attenuate dysfunctions associated with prion diseases, for which there are no disease-modifying therapies. MGluR5 antagonists were expected to have only a moderate effect on survival, since this therapeutic modality is likely to affect downstream consequences of prion toxicity. However, given the fact that they are well-tolerated and have high bioavailability and blood-brain-barrier penetration (Gasparini *et al.*, 2013; Pop *et al.*, 2014; Schaefer *et al.*, 2015), mGluR5 antagonists may be considered for enhancing the quality of life of prion patients.

4.2. Specific Interaction of PrP^C with group I mGluRs

Protein-protein interactions at defined regions of the post-synaptic membrane-surface, namely at microdomains referred to as post-synaptic densities (PSDs), are a critical site for the examination of localized proteins such as PrP^C. Group I mGluRs are also situated within PSDs and modulate neuronal activity by interacting with multiple partners (Baundry M. *et al.*, 2012). Group I mGluRs and PrP^C co-localization in PSDs and participation in neuritogenesis (through the additional interaction with laminin) (Beraldo *et al.*, 2011) provided the necessary grounds to further examine their potential interaction in disease.

While PSDs were not isolated in this study, brain homogenates from wt and $Prnp^{-/-}$ mice were subjected to immunoprecipitation using antibody POM1 against PrP^C, followed by western blotting with antibodies to mGluR1 and mGluR5. The group-I mGlu receptors, which migrate as functionally active oligomers at 250kDa (Romano *et al.*, 1996b), were found to co-precipitate with PrP^C. In addition upon control immunoprecipitation conditions we did we observe mGluR1 and mGluR5 co-immunoprecipitating with PrP. Furthermore, western blots from the total brain lysates (TEs) did not reveal any changes in the concentration of mGluR1 and mGluR5 protein between wild-type and

Prnp$^{o/o}$ homogenates. Last but not least, mGlu receptors from the group II and III subtypes (mGluR6, mGluR2/3) did not co-precipitate with PrP^C, confirming the specificity of the interaction. These results are in accordance with previous reports showing specific interaction of PrP^C with group I mGluRs (Beraldo *et al.*, 2011; Um *et al.*, 2013). Additional experiments were performed in order to map the interaction between PrP^C and group I mGluRs onto PrP^C. The PrP^C residues 91-153 were previously reported to participate to the interaction with mGluR5. This interaction was shown to promote Aβ-induced toxicity in an experimental model of AD (Haas *et al.*, 2014). With regards to this, recent reports utilizing both *in vitro* and *in vivo* models highlighted the role of mGluR5 as a co-receptor of PrP^C and Aβ oligomers and the effector of Aβ and Aβ oligomers toxicity (Renner *et al.*, 2010). As group I mGluRs are also reported to contribute to prion pathophysiology (Rodriguez *et al.*, 2005; Rodriguez *et al.*, 2006), we sought to identify which region of PrP^C may be critical for the binding of group I mGluRs. We used a panel of transgenic mice expressing variants of PrP^C bearing deletions in the flexible tail (FT) regions, designated ΔC, ΔCC, ΔF, ΔOR, and ΔHC. The relevance of these mutants to prion disease was previously reported (Baumann *et al.*, 2007a; Bremer *et al.*, 2010; Flechsig *et al.*, 2000; Shmerling *et al.*, 1998; Weissmann *et al.*, 1998). As expected, mGluR1 and mGluR5 co-precipitated with PrP^C. Deletions affecting residues 32-110 (as in the transgenic lines ΔC and ΔCC, lacking the central domain and the charge cluster regions of PrP^C, respectively) reduced the interaction of PrP^C with mGluR5. Conversely, deletions extending from residues 51 to 90, as in the transgenic line ΔOR, increased the interaction with mGluR5, yet reduced the interaction with mGluR1. These results suggest that the interaction domain between PrP^C and mGluR5 is larger than previously inferred, with residues 32-110 participating to the *in vivo* interaction.

4.3. Pharmacological Inhibition of group I mGluRs rescues prion and GDL-induced toxicity in organotypic slices from *Tga20* mice

So as to identify the effect of group I mGluR pharmacological inhibition, we utilized an *ex vivo* model of prion diseases. More specifically, COCS and HOCS were inoculated with brain homogenate from CD1 mice infected with RML prions. For control, slices were inoculated with non-infectious brain

homogenate (NBH) derived from healthy CD1 mice. Infected slices were treated with a range of concentrations of either YM202074 (Kohara *et al.*, 2008) or MPEP (Gasparini *et al.*, 1999) which specifically inhibit mGluR1 and mGluR5, respectively. Following treatment, slices were collected and stained for the specific neuronal marker NeuN. Morphometric analysis of NeuN revealed that MPEP and YM202074 significantly prevented CGL loss, in a dose-dependent manner, in treated COCS and HOCS at concentrations as low as 36 nM and 500 nM, respectively.

We further sought to identify the effect of group I mGluR pharmacological inhibition in our GDL-induced toxicity model. GDLs are antibody-derived molecules targeting the globular domain (GD) of PrP^{C} (termed GDLs) are acutely neurotoxic (Sonati *et al.*, 2013) that activate similar cascades as bona fide prion infection (Herrmann *et al.*, 2015). To investigate if pharmacological inhibition of mGluR1 and mGluR5 rescues *GDL* toxicity, we exposed *tga20* COCS to the *GDL* agent POM1, followed by YM202074 and MPEP treatments. Treatment with POM1 led to almost complete CGL loss within 14 days of treatment, whereas treatment with MPEP or YM202074 significantly reduced CGL loss in POM1-treated slices. As with prion infections, MPEP treatment was sufficient to rescue the loss of CGL. So, how do group I mGluRs inhibition rescues prion (RML6)- or prion-mimetic antibody-induced toxicity? We hypothesize that group I mGluRs inhibition reduces glutamatergic signaling and calcium overload in prion-infected cells (Falsig *et al.*, 2012), similarly to models of Alzheimer's disease (Ostapchenko *et al*., 2013; Renner *et al.*, 2010; Um *et al.*, 2013). Conversely, no protection was observed upon treatment with the selective agonist of group III (L-2-amino-4-phosphonobutyrate (L-AP4)) (Tones *et al.*, 1995) and the potent antagonist of group II and group III ((*RS*)-α-Cyclopropyl-4-phosphonophenylglycine (CPPG)) (Toms *et al.*, 1996) metabotropic glutamate receptors; despite reportrs of group III mGluR association with prion diseases (Sanchez-Juan *et al.*, 2014). The latter, suggest a specific role of group I mGluRs in prion toxicity.

4.4. Pharmacological Inhibition of mGluR5 rescues prion-induced toxicity *in vivo*

The beneficial effects of mGluR5 inhibition *ex vivo* encouraged us to assess a possible therapeutic effect of MPEP on prion pathogenesis *in vivo*. C57BL/6J male mice were inoculated intracerebrally with 3 or 5 log LD_{50} units of RML6 prions as previously described (Kranich *et al.*, 2010), and chronically treated with MPEP. Control mice were inoculated with NBH. In order to record the

neurological deficits associated with prion disease, we utilized the rotarod behavioral test. Rotarod performance was similar in RML6- and NBH (control)-inoculated mice until 18 weeks following prion inoculation. Starting from 19 weeks post inoculation, the rotarod performance of mice receiving control food declined, whereas the performance of MPEP-treated mice declined significantly less. This improvement was lasting and detectable until the very late stages of the disease (22-23 weeks post inoculation); suggesting that the progression of the disease was delayed by MPEP. In contrast, control mice injected with NBH and treated with MPEP exhibited stable rotarod performance during the entire test period, up to 23 weeks post-injection. Treatment with MPEP also has a positive effect on the survival of prion infected mice, as MPEP-treated mice showed a modest, though significant, prolongation of survival. The selected *in vivo* MPEP dose (30mg/ml) has been previously reported to have analgesic effects even in mGluR5$^{-/-}$ mice and MPEP has been reported to have a short plasma half-life (Montana et al., 2009). In order to control for brain and plasma exposure to MPEP, receptor occupancy, MPEP activity and mGluR5-independent actions, mice treated with control and MPEP food were sacrificed in two different timepoints, corresponding to the active and the inactive phase of the mice across the circadian circle. Pharmacokinetic and pharmakodynamic analysis showed a good delivery of MPEP to the brain (brain to plasma ratios above 1), without induction of changes in food and water consumption or rotarod performance of treated mice. PK analysis showed that the MPEP levels in the brain are around 150nM during the inactive phase and around 260nM during the active phase of the mice life cycle. The values are 8 times above the IC50 (during the active phase) suggesting that the likelihood of completely inhibiting the receptor is very high. Even during the inactive phase values are far above the IC50. In addition, the values detected in this study are far below any reported off-target effect. Therefore we conclude that the brain and plasma exposure to MPEP is adequate to induce mGluR5-specific effects. Detailed information about the exact levels of MPEP both in the brain and plasma of all animals involved in the study are provided in tables at the appendix section.

Still the effect of the MPEP-treatment in the disease phenotype remained unclear. It has been previously reported that upregulation of mGluR5 can go along with glial activation (D'Antoni *et al.*, 2008; Shelton and McCarthy, 1999; Shrivastava *et al.*, 2013). Indeed, we observed reactive astrogliosis (measured as GFAP immunoreactivity) in the hippocampi of prion-infected animals. Interestingly, treatment with MPEP resulted in a decrease of GFAP immunoreactivity in the

hippocampi of prion-infected mice. Conversely, MPEP was unable to suppress glial activation in adult cerebella where mGluR5 expression is low. Taken together, these results suggest that dampened neuroinflammation was overall beneficial. Although an effect on microgliosis was not observed, a significant effect on vacuolation was identified. Vacuolation per se was not halted; the number of vacuoles was the same between the MPEP-treated versus control animals. However, the area of vacuoles was significantly reduced.

Although mGluR5 inhibition delayed neurological deterioration, survival was only modestly (though significantly) improved. These findings support the concept that mGluR5 inhibition alleviates the symptoms of the disease whereas prion replication progresses unabated.

4.5. Genetic ablation of mGluR5 rescues prion and GDL-induced toxicity in cerebellar and hippocampal organotypic slices but not *in vivo*

To further assess the role of mGluR5 in prion toxicity, cerebellar organotypic slice cultures from *Grm5*$^{-/-}$, *Grm5*$^{+/-}$ and *Grm5*$^{+/+}$ littermates were treated with the anti-GD antibody POM1 (Polymenidou *et al.*, 2008), a prion-mimetic compound. Exposure to POM1 led to the loss of cerebellar granular layer (CGL) neurons in *Grm5*$^{+/+}$ slices, but not in *Grm5*$^{-/-}$ and *Grm5*$^{+/-}$ slices. Cerebellar and hippocampal organotypic slice cultures from *Grm5*$^{-/-}$, *Grm5*$^{+/-}$ and *Grm5*$^{+/+}$ littermates were further inoculated with brain homogenate from CD1 mice infected with RML prions (RML6) or control NBH homogenate. In both COCS and HOCS, genetic ablation of Grm5 was protective against prion induced toxicity; further supporting a primary role of mGluR5 in prion toxicity.

To assess the role of mGluR5 ablation in prion infections *in vivo*, we infected *Grm5*$^{-/-}$, *Grm5*$^{+/-}$, and control *Grm5*$^{+/+}$ littermates with RML6 prions (5 log LD_{50}). Again, we utilized the rotarod test. All RML6 inoculated mice showed similar rotarod performance during monitoring; with *Grm5*$^{-/-}$ mice showing a tendency towards better motor performance in general. Moreover, no significant difference in survival was observed between *Grm5*$^{-/-}$, *Grm5*$^{+/-}$ and *Grm5*$^{+/+}$ mice.

MPEP treatment rescued prion-induced neuronal loss in slices, delayed neurological deterioration and modestly improved survival in mice. Genetic ablation of Grm5 rescued prion-induced neuronal loss in slices but was not protective against prion-induced toxicity in mice. It could be hypothesized that the prion load may exert neurotoxicity through mGluR5-independent mechanisms (including mGluR1 activation). Indeed, not all neurons express mGluR5 (Boer *et al.*, 2010; Lopez-Bendito *et al.*, 2002). It

could be hypothesized that neurons essential for survival are mGluR5^{-} (and possibly mGluR1^{+}) and are therefore not influenced by mGluR5 ablation.

In order to investigate a potential epistasis between mGluR1 and mGluR5, we analyzed whole-brain lysates to control for mGluR1 and mGluR5 level changes between young and old mice. We observed higher expression levels of mGluR1 in samples from 44-day old *Grm5*$^{-/-}$ mice compared to heterozygous and wt control littermates. At later time points expression levels of mGluR1 were similar between samples. These results point to compensatory mechanisms between mGluR1 and mGluR5 at least at certain developmental stages. We further sought to evaluate whether treatment with MPEP has a similar effect on the expression of mGluR1. mGluR1 expression levels were assessed in whole-brain lysates from 1-year old control wt mice, NBH-inoculated wt mice, and NBH-inoculated wt mice that received MPEP food. No differences were observed in the mGluR1 expression levels between the samples: suggesting that pharmacological inhibition of mGluR5 does not influence the expression levels of mGluR1.

4.6. Exposure to toxic POM1 antibodies increases cell surface expression of mGluR5 and PrP^{C}-mGluR5 cluster formation at dendritic spines

Early features of prion diseases include synaptic degeneration and dendritic atrophy. In rodent models of prion disease synaptic accumulation of PrP^{Sc} and prominent synaptic degeneration was detected at the early stages of the disease process, before any overt signs of neuronal death (Bouzamondo-Bernstein *et al.*, 2004; Cunningham *et al.*, 2003a; Gray *et al.*, 2009; Jeffrey *et al.*, 2000). Disruption of presynaptic boutons and degeneration of axon terminals did not strictly correlate with PrP^{Sc} deposition. Also, in brain samples from CJD patients, PrP^{Sc} deposition at the presynapstic terminals has been reported (Kovacs *et al.*, 2005; Siso *et al.*, 2002). PrP^{Sc} deposition was associated with reduced level of presynaptic proteins such as synaptophysin, synapsin I, SNAP-25 (Ferrer *et al.*, 2000). Another prominent feature of prion diseases is dendritic atrophy (Jamieson *et al.*, 2001); characterized by distorted dendritic arborization and dendritic atrophy in CJD brains. In the neocortex of infected mice, higher level of *Notch-1* mRNA and nuclear translocation of Notch-1 intracellular domain (NICD), correlated with PrP^{Sc} accumulation; suggesting a role of Notch signalling. *In vitro*, in N2a neuroblastoma cells, the expression of NICD was also increased following scrapie infection.

Morphologically, N2a cells showed synaptic abnormalities, such as shorter dendritic processes (Ishikura, 2007; Ishikura *et al.*, 2005).

Prion toxicity is mediated by unfolded-protein responses (Moreno *et al.*, 2013; Moreno *et al.*, 2012), yet it is unclear how these are triggered by extracellular PrP^{Sc}. We identified a specific group I mGluR interaction with PrP^{C} and a therapeutic effect of mGluR5 inhibition in *ex vivo* and *in vivo* models of prion diseases. However, the mechanism of the observed protection was still missing.We reasoned that group-I metabotropic glutamate receptors mGluR5 and mGluR1, G-protein coupled receptors that interact with PrP^{C} (Lauren *et al.*, 2009; Renner *et al.*, 2010; Um *et al.*, 2013), may represent one such link. We hypothesized that if prion toxicity depends on the direct interaction of PrP^{C} to group-I mGluRs, it may modify the subcellular distribution of mGluR5. To investigate this we used both toxic and protective anti-PrP^{C} antibodies (Polymenidou *et al.*, 2008; Sonati *et al.*, 2013).

Toxic anti-PrP^{C} antibodies induce damage by stimulating pathways similar to *bona fide* prion infections, such as activation of calpains and PERK pathway and production of reactive oxygen species (Doolan and Colby, 2015; Falsig *et al.*, 2012; Herrmann *et al.*, 2015; Sonati *et al.*, 2013). The proposed mechanism of action postulates that the amino-terminal, flexible tail of PrP^{C} mediates the toxicity of antiprion antibodies by binding to the globular domain of PrP^{C} (Sonati *et al.*, 2013). Indeed, exposure of primary hippocampal cultures to prion-mimetic antibodies selectivelly increased clustering of mGluR5 (but not of AMPA and NMDA receptors) in dendritic spine heads, thus bringing them closer to synaptic glutamate. Prion mimetics also increased the level of PrP^{C} in spines, reinforcing the notion that mGluR5 and PrP^{C} are part of the same complex whose accumulation at excitatory synapses instigates neurotoxicity in prion diseases. Increased cell surface clustering may also slow down endocytosis, thereby increasing the amount of functional mGluR5s at the cell surface (Casley *et al.*, 2009; Hamilton A. *et al.*, 2014; Um *et al.*, 2013). Indeed, 2h exposure of cerebellar organotypic slice cultures to high concentrations of toxic scPOM1 antibodies induced an increase in the cell surface expression of mGluR5s. Interestingly, parallel treatment with the specific mGluR5 inhibitor MPEP reduced the mGluRs surface expression. These results support our hypothesis that mGluR5 clustering at synapses may amplify responses to glutamate, thereby inducing Ca^{2+} influx and spine loss, a primary event in prion diseases (Fuhrmann *et al.*, 2007).

The POM2 antibody (Polymenidou *et al.*, 2008) against the Flexible Tail (FT) of PrP is neuroprotective *in vivo* and *in vitro* (Reimann *et al.*, 2016; Sonati *et al.*, 2013). If mGluR5 is instrumental to POM1

toxicity, its clustering may be relieved by POM2. Indeed, exposure of primary cultures to POM2 prevented mGluR5 clustering and spine translocation. We observed reduced mGluR5 and PrP^C enrichment in spines even after exposure to POM2 alone. More importantly, in cell surface biotinylation experiments performed in COCS, exposure to scPOM2 did not significantly increase the surface expression of mGluR5s in COCS. Also blocking of scPOM1 toxicity with addition of scPOM2 resulted in significant reduction of the mGluR5s surface expression. Hence prion-mimetic and protective antibodies have opposite effects on the mGluR5-PrP^C complex, with anti-GD antibodies promoting spine translocation and anti-FT antibodies inhibiting it. Since both POM2 and mGluR5 bind to the N-terminus of PrP^C, binding of mGluR5 to PrP^C may facilitate its activation whereas POM2 may compete for PrP^C binding. The hypothesized mechanism of action is summarized in the figure below (**Figure 4.1.**)

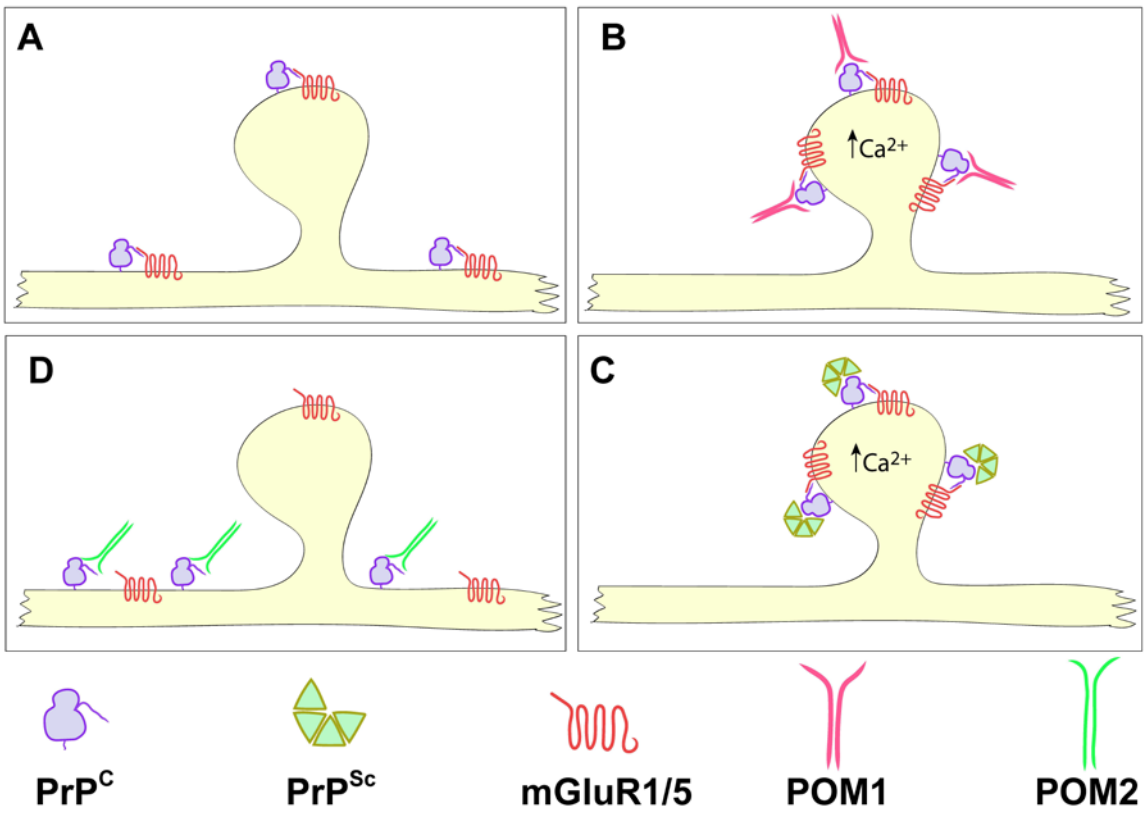

Figure 4.1. Model of the interactions between mGluR5, PrP^C, and anti-PrP antibodies

(**A**) In untreated neurons, mGluR5-PrP^C complexes are distributed within and outside spines. Upon exposure to prion-mimetic antibodies (**B**), mGluR5 translocates to the spine, where it may enhance neurotoxicity by contributing to a Ca^{2+} overload. (**C**) Exposure to POM2, in contrast, engages the N-

terminal “flexible tail” of PrP^C, thereby making it unavailable to mGluR5. Consequently, mGluR5-PrP^C (and possibly also mGluR1-PrP^C) complexes do not translocate to spines. As a result, POM2 affords functional neuroprotection similarly to mGluR5 antagonists. (**D**) We speculate that prion infection may trigger topological rearrangements similar to those observed after POM1 exposure.

4.7. Conclusion

The above data propose that group-I mGluRs interaction is crucial for the propagation of prion-induced toxicity in the synaptic level. Indeed, we showed that exposure to toxic, prion-mimetic anti-PrP^C antibodies (GD ligands) increases the clustering of mGluR5s on dendritic spines as well as the mGluR5s cell surface expression. Conversely, exposure to protective anti-PrP^C antibodies (FT ligands) reduced clustering of mGluR5s on dendritic spines as well as the mGluR5s cell surface expression. Interestingly, we observed the same protection upon exposure of prion-infected models to MPEP treatment. We additionally need to identify the intracellular, downstream pathways that are activated upon prion-induced toxicity and how MPEP treatment conveys protection. In AD, it has been reported that Aβo-mGluR5-PrP^C complexes at the neuronal surface mobilize mGluR5 to activating cytoplasmic Fyn kinase and trigger eEF2 phosphorylation; increasing intracellular calcium signaling and inducing dendritic spine loss *(Um et al., 2013). We are currently examining whether a similar mechanism is triggered upon formation of stable PrP^{Sc}-mGluR5-PrP^C complexes on the neuronal surface. This work is ongoing.*

Our results further propose that inhibition may improve the phenotypic dysfunctions associated with prion diseases, for which there are currently no disease-modifying therapies. MGluR5 antagonists have only a moderate effect on survival, mainly due to the fact that they are probably affecting downstream pathways of prion toxicity rather than the formation and propagation of PrP^{Sc} per se. However, the fact that well-tolerated, with high bioavailability and blood-brain-barrier penetration (Gasparini et al., 2013; Pop et al., 2014; Schaefer et al., 2015) mGluR5 antagonists exist gives promise for their use in enhancing the quality of life of prion patients - a legitimate aim even if the overall life expectancy may not be dramatically improved.

REFERENCES

Abe, T., H. Sugihara, H. Nawa, R. Shigemoto, N. Mizuno, and S. Nakanishi. 1992. Molecular Characterization of a Novel Metabotropic Glutamate Receptor Mglur5 Coupled to Inositol Phosphate/Ca2+ Signal Transduction. *J Biol Chem* 267:13361-13368.

Aguilar-Valles, A., E. Matta-Camacho, A. Khoutorsky, C. Gkogkas, K. Nader, J.C. Lacaille, and N. Sonenberg. 2015. Inhibition of Group I Metabotropic Glutamate Receptors Reverses Autistic-Like Phenotypes Caused by Deficiency of the Translation Repressor eIF4E Binding Protein 2. *J Neurosci* 35:11125-11132.

Aguzzi, A., F. Baumann, and J. Bremer. 2008. The prion's elusive reason for being. *Annu Rev Neurosci* 31:439-477.

Aguzzi, A., and A.M. Calella. 2009. Prions: Protein Aggregation and Infectious Diseases. *Physiol Rev* 89:1105-1152.

Aguzzi, A., and M. Heikenwalder. 2006. Pathogenesis of prion diseases: current status and future outlook. *Nat Rev Microbiol* 4:765-775.

Aguzzi, A., and T. O'Connor. 2010. Protein aggregation diseases: pathogenicity and therapeutic perspectives. *Nat Rev Drug Discov* 9:237-248.

Aguzzi, A., and M. Polymenidou. 2004. Mammalian prion biology: one century of evolving concepts. *Cell* 116:313-327.

Aguzzi, A., and C. Weissmann. 1996. Spongiform encephalopathies: a suspicious signature. *Nature* 383:666-667.

Aiba, A., M. Kano, C. Chen, M.E. Stanton, G.D. Fox, K. Herrup, T.A. Zwingman, and S. Tonegawa. 1994. Deficient cerebellar long-term depression and impaired motor learning in mGluR1 mutant mice. *Cell* 79:377-388.

Albin, R.L., and J.T. Greenamyre. 1992. Alternative excitotoxic hypotheses. *Neurology* 42:733-738.

Alper, T., W. Cramp, D. Haig, and M. Clarke. 1967. Does the agent of scrapie replicate without nucleid acid? *Nature* 214:764-766.

Araneda, R.C., R.S. Zukin, and M.V.L. Bennett. 1993. Effects of Polyamines on Nmda-Induced Currents in Rat Hippocampal-Neurons - a Whole-Cell and Single-Channel Study. *Neurosci Lett* 152:107-112.

Armentero, M.T., R. Fancellu, G. Nappi, P. Bramanti, and F. Blandini. 2006. Prolonged blockade of NMDA or mGluR5 glutamate receptors reduces nigrostriatal degeneration while inducing selective metabolic changes in the basal ganglia circuitry in a rodent model of Parkinson's disease. *Neurobiology of disease* 22:1-9.

Asante, E.A., Y.G. Li, I. Gowland, J.G. Jefferys, and J. Collinge. 2004. Pathogenic human prion protein rescues PrP null phenotype in transgenic mice. *Neurosci Lett* 360:33-36.

Attucci, S., V. Carla, G. Mannaioni, and F. Moroni. 2001. Activation of type 5 metabotropic glutamate receptors enhances NMDA responses in mice cortical wedges. *Brit J Pharmacol* 132:799-806.

Ayalon, G., and Y. Stern-Bach. 2001. Functional assembly of AMPA and kainate receptors is mediated by several discrete protein-protein interactions. *Neuron* 31:103-113.

Babic, T. 1999. The cholinergic hypothesis of Alzheimer's disease: a review of progress. *J Neurol Neurosurg Psychiatry* 67:558.

Balazs, R., S. Miller, C. Romano, A. deVries, Y. Chun, and C.W. Cotman. 1997. Metabotropic glutamate receptor mGluR5 in astrocytes: Pharmacological properties and agonist regulation. *J Neurochem* 69:151-163.

Balducci, C., M. Beeg, M. Stravalaci, A. Bastone, A. Sclip, E. Biasini, L. Tapella, L. Colombo, C. Manzoni, T. Borsello, R. Chiesa, M. Gobbi, M. Salmona, and G. Forloni. 2010.

Synthetic amyloid-beta oligomers impair long-term memory independently of cellular prion protein. *Proc Natl Acad Sci U S A* 107:2295-2300.

Balschun, D., D. Manahan-Vaughan, T. Wagner, T. Behnisch, K.G. Reymann, and W. Wetzel. 1999. A specific role for group I mGluRs in hippocampal LTP and hippocampus-dependent spatial learning. *Learning & memory* 6:138-152.

Barria, M.A., A. Mukherjee, D. Gonzalez-Romero, R. Morales, and C. Soto. 2009. De novo generation of infectious prions in vitro produces a new disease phenotype. *PLoS Pathog* 5:e1000421.

Basler, K., B. Oesch, M. Scott, D. Westaway, M. Walchli, D.F. Groth, M.P. Mckinley, S.B. Prusiner, and C. Weissmann. 1986. Scrapie and Cellular Prp Isoforms Are Encoded by the Same Chromosomal Gene. *Cell* 46:417-428.

Battaglia, G., V. Bruno, A. Pisani, D. Centonze, M.V. Catania, P. Calabresi, and F. Nicoletti. 2001. Selective blockade of type-1 metabotropic glutamate receptors induces neuroprotection by enhancing gabaergic transmission. *Mol Cell Neurosci* 17:1071-1083.

Battaglia, G., C.L. Busceti, G. Molinaro, F. Biagioni, M. Storto, F. Fornai, F. Nicoletti, and V. Bruno. 2004. Endogenous activation of mGlu5 metabotropic glutamate receptors contributes to the development of nigro-striatal damage induced by 1-methyl-4-phenyl-1,2,3,6-tetrahydropyridine in mice. *J Neurosci* 24:828-835.

Baude, A., Z. Nusser, J.D.B. Roberts, E. Mulvihill, R.A.J. Mcilhinney, and P. Somogyi. 1993. The Metabotropic Glutamate-Receptor (Mglur1-Alpha) Is Concentrated at Perisynaptic Membrane of Neuronal Subpopulations as Detected by Immunogold Reaction. *Neuron* 11:771-787.

Baumann, F., M. Tolnay, C. Brabeck, J. Pahnke, U. Kloz, H.H. Niemann, M. Heikenwalder, T. Rulicke, A. Burkle, and A. Aguzzi. 2007a. Lethal recessive myelin toxicity of prion protein lacking its central domain. *Embo J* 26:538-547.

Baumann, F., M. Tolnay, C. Brabeck, J. Pahnke, U. Kloz, H.H. Niemann, M. Heikenwalder, T. Rulicke, A. Burkle, and A. Aguzzi. 2007b. Lethal recessive myelin toxicity of prion protein lacking its central domain. *Embo J* 26:538-547.

Baundry M., Greget R., Pernot F., Bouteiller JM., and Bi X. 2012. Roles of group I metabotropic glutamate receptors under physiological conditions and in neurodegeneration. *Wiley Interdisciplinary Reviews: Membrane Transport and Signaling* 1:523-532.

Bear, M. 2005. The mGluR theory of fragile X mental retardation. *Neuropsychopharmacol* 30:S59-S59.

Beneyto, M., and J.H. Meador-Woodruff. 2004. Expression of transcripts encoding AMPA receptor subunits and associated postsynaptic proteins in the macaque brain. *J Comp Neurol* 468:530-554.

Beraldo, F.H., C.P. Arantes, T.G. Santos, C.F. Machado, M. Roffe, G.N. Hajj, K.S. Lee, A.C. Magalhaes, F.A. Caetano, G.L. Mancini, M.H. Lopes, T.A. Americo, M.H. Magdesian, S.S.G. Ferguson, R. Linden, M.A.M. Prado, and V.R. Martins. 2011. Metabotropic glutamate receptors transduce signals for neurite outgrowth after binding of the prion protein to laminin gamma 1 chain. *Faseb J* 25:265-279.

Beraldo, F.H., C.P. Arantes, T.G. Santos, N.G. Queiroz, K. Young, R.J. Rylett, R.P. Markus, M.A. Prado, and V.R. Martins. 2010. Role of alpha7 nicotinic acetylcholine receptor in calcium signaling induced by prion protein interaction with stress-inducible protein 1. *J Biol Chem* 285:36542-36550.

Bessen, R.A., D.A. Kocisko, G.J. Raymond, S. Nandan, P.T. Lansbury, and B. Caughey. 1995. Non-genetic propagation of strain-specific properties of scrapie prion protein [see comments]. *Nature* 375:698-700.

Betmouni, S., V.H. Perry, and J.L. Gordon. 1996. Evidence For an Early Inflammatory Response In the Central Nervous System Of Mice With Scrapie. *Neuroscience* 74:1-5.

Bhave, G., F. Karim, S.M. Carlton, and R.W.t. Gereau. 2001. Peripheral group I metabotropic glutamate receptors modulate nociception in mice. *Nature neuroscience* 4:417-423.

Black, Y.D., D.Q. Xiao, D. Pellegrino, A. Kachroo, A.L. Brownell, and M.A. Schwarzschild. 2010. Protective effect of metabotropic glutamate mGluR5 receptor elimination in a 6-hydroxydopamine model of Parkinson's disease. *Neurosci Lett* 486:161-165.

Boche, D., C. Cunningham, F. Docagne, H. Scott, and V.H. Perry. 2006. TGFbeta1 regulates the inflammatory response during chronic neurodegeneration. *Neurobiol Dis* 22:638-650.

Bodrikov, V., V. Sytnyk, I. Leshchyns'ka, J. den Hertog, and M. Schachner. 2008. NCAM induces CaMKIIalpha-mediated RPTPalpha phosphorylation to enhance its catalytic activity and neurite outgrowth. *J Cell Biol* 182:1185-1200.

Boer, K., F. Encha-Razavi, M. Sinico, and E. Aronica. 2010. Differential distribution of group I metabotropic glutamate receptors in developing human cortex. *Brain research* 1324:24-33.

Bolton, D.C., M.P. McKinley, and S.B. Prusiner. 1984. Molecular characteristics of the major scrapie prion protein. *Biochemistry* 23:5898-5906.

Bonifacino, J.S., and A.M. Weissman. 1998. Ubiquitin and the control of protein fate in the secretory and endocytic pathways. *Annu Rev Cell Dev Biol* 14:19-57.

Borchelt, D.R., V.E. Koliatsos, M. Guarnieri, C.A. Pardo, S.S. Sisodia, and D.L. Price. 1994. Rapid anterograde axonal transport of the cellular prion glycoprotein in the peripheral and central nervous systems. *J Biol Chem* 269:14711-14714.

Borchelt, D.R., M. Rogers, N. Stahl, G. Telling, and S.B. Prusiner. 1993. Release of the cellular prion protein from cultured cells after loss of its glycoinositol phospholipid anchor. *Glycobiology* 3:319-329.

Bosque, P., G. Telling, D. Hanahan, and S.B. Pruisiner. 1995. Ectopic Expression of the Prion Protein Directed by the Insulin Gene Promoter to the Pancreas of Transgenic Mice. *Neurology* 45:A308-A308.

Bouzamondo-Bernstein, E., S.D. Hopkins, P. Spilman, J. Uyehara-Lock, C. Deering, J. Safar, S.B. Prusiner, H.J. Ralston, 3rd, and S.J. DeArmond. 2004. The neurodegeneration sequence in prion diseases: evidence from functional, morphological and ultrastructural studies of the GABAergic system. *J Neuropathol Exp Neurol* 63:882-899.

Boxall, A.R. 2000. GABAergic mIPSCs in rat cerebellar Purkinje cells are modulated by TrkB and mGluR1-mediated stimulation of Src. *J Physiol-London* 524:677-684.

Bremer, J., F. Baumann, C. Tiberi, C. Wessig, H. Fischer, P. Schwarz, A.D. Steele, K.V. Toyka, K.A. Nave, J. Weis, and A. Aguzzi. 2010. Axonal prion protein is required for peripheral myelin maintenance. *Nat Neurosci* 13:310-U319.

Brooks, S.P., and S.B. Dunnett. 2009. Tests to assess motor phenotype in mice: a user's guide. *Nat Rev Neurosci* 10:519-529.

Brown, D., and J. Sassoon. 2004. Role of glia in prion disease. In Adv Mol Cell Biol. L. Hertz, editor Gulf Professional Publishing, 1085-1104.

Brown, D.R. 2001a. Microglia and prion disease. *Microscopy research and technique* 54:71-80.

Brown, D.R. 2001b. Prion and prejudice: normal protein and the synapse. *Trends Neurosci* 24:85-90.

Brown, D.R. 2005. Neurodegeneration and oxidative stress: prion disease results from loss of antioxidant defence. *Folia Neuropathol* 43:229-243.

Brown, D.R., and A. Besinger. 1998. Prion protein expression and superoxide dismutase activity. *Biochem J* 334 (Pt 2):423-429.

Brown, D.R., C. Clive, and S.J. Haswell. 2001. Antioxidant activity related to copper binding of native prion protein. *J Neurochem* 76:69-76.

Brown, D.R., F. Hafiz, L.L. Glasssmith, B.S. Wong, I.M. Jones, C. Clive, and S.J. Haswell. 2000. Consequences of manganese replacement of copper for prion protein function and proteinase resistance. *The EMBO journal* 19:1180-1186.

Brown, D.R., R.S.J. Nicholas, and L. Canevari. 2002. Lack of prion protein expression results in a neuronal phenotype sensitive to stress. *J Neurosci Res* 67:211-224.

Brown, D.R., K. Qin, J.W. Herms, A. Madlung, J. Manson, R. Strome, P.E. Fraser, T. Kruck, A. Von Bohlen, and H. Kretzschmar. 1997a. The cellular prion protein binds copper in vivo. *Nature* 390:684-687.

Brown, D.R., K. Qin, J.W. Herms, A. Madlung, J. Manson, R. Strome, P.E. Fraser, T. Kruck, A. von Bohlen, W. Schulz-Schaeffer, A. Giese, D. Westaway, and H. Kretzschmar. 1997b. The cellular prion protein binds copper in vivo. *Nature* 390:684-687.

Brown, D.R., B. Schmidt, and H.A. Kretzschmar. 1996. Role of microglia and host prion protein in neurotoxicity of a prion protein fragment. *Nature* 380:345-347.

Brown, D.R., B. Schmidt, and H.A. Kretzschmar. 1998. Prion protein fragment interacts with PrP-deficient cells. *J Neurosci Res* 52:260-267.

Brown, D.R., W.J. SchulzSchaeffer, B. Schmidt, and H.A. Kretzschmar. 1997c. Prion protein-deficient cells show altered response to oxidative stress due to decreased SOD-1 activity. *Experimental Neurology* 146:104-112.

Brown, D.R., B.S. Wong, F. Hafiz, C. Clive, S.J. Haswell, and I.M. Jones. 1999. Normal prion protein has an activity like that of superoxide dismutase. *Biochem J* 344 Pt 1:1-5.

Brown, L.R., and D.A. Harris. 2003. Copper and zinc cause delivery of the prion protein from the plasma membrane to a subset of early endosomes and the Golgi. *J Neurochem* 87:353-363.

Brown, P. 1990. The phantasmagoric immunology of transmissible spongiform encephalopathy. [Review] [77 refs]. *Research Publications Association for Research in Nervous & Mental Disease* 68:305-313.

Bruno, V., G. Battaglia, A. Copani, M. D'Onofrio, P. Di Iorio, A. De Blasi, D. Melchiorri, P.J. Flor, and F. Nicoletti. 2001. Metabotropic glutamate receptor subtypes as targets for neuroprotective drugs. *J Cerebr Blood F Met* 21:1013-1033.

Bruno, V., A. Copani, T. Knopfel, R. Kuhn, G. Casabona, P. Dell'Albani, D.F. Condorelli, and F. Nicoletti. 1995. Activation of metabotropic glutamate receptors coupled to inositol phospholipid hydrolysis amplifies NMDA-induced neuronal degeneration in cultured cortical cells. *Neuropharmacology* 34:1089-1098.

Bueler, H., A. Aguzzi, A. Sailer, R.A. Greiner, P. Autenried, M. Aguet, and C. Weissmann. 1993. Mice Devoid of Prp Are Resistant to Scrapie. *Cell* 73:1339-1347.

Bueler, H., M. Fischer, Y. Lang, H. Bluethmann, H.P. Lipp, S.J. DeArmond, S.B. Prusiner, M. Aguet, and C. Weissmann. 1992. Normal development and behaviour of mice lacking the neuronal cell-surface PrP protein. *Nature* 356:577-582.

Calella, A.M., M. Farinelli, M. Nuvolone, O. Mirante, R. Moos, J. Falsig, I.M. Mansuy, and A. Aguzzi. 2010. Prion protein and Abeta-related synaptic toxicity impairment. *EMBO molecular medicine* 2:306-314.

Campana, V., D. Sarnataro, and C. Zurzolo. 2005. The highways and byways of prion protein trafficking. *Trends Cell Biol* 15:102-111.

Caraci, F., G. Battaglia, M.A. Sortino, S. Spampinato, G. Molinaro, A. Copani, F. Nicoletti, and V. Bruno. 2012. Metabotropic glutamate receptors in neurodegeneration/neuroprotection: still a hot topic? *Neurochem Int* 61:559-565.

Carleton, A., P. Tremblay, J.D. Vincent, and P.M. Lledo. 2001. Dose-dependent, prion protein (PrP)-mediated facilitation of excitatory synaptic transmission in the mouse hippocampus. *Pflugers Arch* 442:223-229.

Casley, C.S., V. Lakics, H.G. Lee, L.M. Broad, T.A. Day, T. Cluett, M.A. Smith, M.J. O'Neill, and A.E. Kingston. 2009. Up-regulation of astrocyte metabotropic glutamate receptor 5 by amyloid-beta peptide. *Brain research* 1260:65-75.

Castilla, J., D. Gonzalez-Romero, P. Saa, R. Morales, J. De Castro, and C. Soto. 2008. Crossing the species barrier by PrP(Sc) replication in vitro generates unique infectious prions. *Cell* 134:757-768.

Castilla, J., P. Saa, C. Hetz, and C. Soto. 2005. In vitro generation of infectious scrapie prions. *Cell* 121:195-206.

Castilla, J., P. Saa, R. Morales, K. Abid, K. Maundrell, and C. Soto. 2006. Protein misfolding cyclic amplification for diagnosis and prion propagation studies. *Methods Enzymol* 412:3-21.

Castillo, P.E., R.C. Malenka, and R.A. Nicoll. 1997. Kainate receptors mediate a slow postsynaptic current in hippocampal CA3 neurons. *Nature* 388:182-186.

Catania, M.V., G.B. Landwehrmeyer, C.M. Testa, D.G. Standaert, J.B. Penney, and A.B. Young. 1994. Metabotropic Glutamate Receptors Are Differentially Regulated during Development. *Neuroscience* 61:481-495.

Caughey, B., and G.S. Baron. 2006. Prions and their partners in crime. *Nature* 443:803-810.

Caughey, B., G.S. Baron, B. Chesebro, and M. Jeffrey. 2009. Getting a grip on prions: oligomers, amyloids, and pathological membrane interactions. *Annu Rev Biochem* 78:177-204.

Caughey, B., D.A. Kocisko, G.J. Raymond, and P.T. Lansbury. 1995. Aggregates Of Scrapie-Associated Prion Protein Induce the Cell-Free Conversion Of Protease-Sensitive Prion Protein to the Protease-Resistant State. *Chemistry & Biology* 2:807-817.

Caughey, B., and P.T. Lansbury. 2003. Protofibrils, pores, fibrils, and neurodegeneration: separating the responsible protein aggregates from the innocent bystanders. *Annu Rev Neurosci* 26:267-298.

Caughey, B., R.E. Race, D. Ernst, M.J. Buchmeier, and B. Chesebro. 1989. Prion protein biosynthesis in scrapie-infected and uninfected neuroblastoma cells. *J Virol* 63:175-181.

Caughey, B.W., A. Dong, K.S. Bhat, D. Ernst, S.F. Hayes, and W.S. Caughey. 1991. Secondary structure analysis of the scrapie-associated protein PrP 27-30 in water by infrared spectroscopy. *Biochemistry* 30:7672-7680.

Chaffin, K.E., C.R. Beals, T.M. Wilkie, K.A. Forbush, M.I. Simon, and R.M. Perlmutter. 1990. Dissection of Thymocyte Signaling Pathways by Invivo Expression of Pertussis Toxin Adp-Ribosyltransferase. *Embo Journal* 9:3821-3829.

Chen, G.Q., C.H. Cui, M.L. Mayer, and E. Gouaux. 1999. Functional characterization of a potassium-selective prokaryotic glutamate receptor. *Nature* 402:817-821.

Chen, S.Z., A. Mange, L. Dong, S. Lehmann, and M. Schachner. 2003. Prion protein as trans-interacting partner for neurons is involved in neurite outgrowth and neuronal survival. *Mol Cell Neurosci* 22:227-233.

Chiarini, A., I. Dal Pra, J.F. Whitfield, and U. Armato. 2006. The killing of neurons by beta-amyloid peptides, prions, and pro-inflammatory cytokines. *Ital J Anat Embryol* 111:221-246.

Chiesa, R., B. Drisaldi, E. Quaglio, A. Migheli, P. Piccardo, B. Ghetti, and D.A. Harris. 2000. Accumulation of protease-resistant prion protein (PrP) and apoptosis of cerebellar granule cells in transgenic mice expressing a PrP insertional mutation [In Process Citation]. *Proc Natl Acad Sci U S A* 97:5574-5579.

Choi, D.W. 1992. Excitotoxic cell death. *Journal of neurobiology* 23:1261-1276.

Cisse, M., P.E. Sanchez, D.H. Kim, K. Ho, G.Q. Yu, and L. Mucke. 2011. Ablation of cellular prion protein does not ameliorate abnormal neural network activity or cognitive dysfunction in the J20 line of human amyloid precursor protein transgenic mice. *J Neurosci* 31:10427-10431.

Clark, B.A., M. Farrant, and S.G. CullCandy. 1997. A direct comparison of the single-channel properties of synaptic and extrasynaptic NMDA receptors. *J Neurosci* 17:107-116.

Cohen, F.E. 1999. Protein misfolding and prion diseases. *J Mol Biol* 293:313-320.

Coitinho, A.S., M.H. Lopes, G.N. Hajj, J.I. Rossato, A.R. Freitas, C.C. Castro, M. Cammarota, R.R. Brentani, I. Izquierdo, and V.R. Martins. 2007. Short-term memory formation and long-term memory consolidation are enhanced by cellular prion association to stress-inducible protein 1. *Neurobiol Dis* 26:282-290.

Colby, D.W., and S.B. Prusiner. 2011. Prions. *Csh Perspect Biol* 3:

Collett, V.J., and G.L. Collingridge. 2004. Interactions between NMDA receptors and mGlu(5) receptors expressed in HEK293 cells. *Brit J Pharmacol* 142:991-1001.

Colling, S.B., J. Collinge, and J.G. Jefferys. 1996. Hippocampal slices from prion protein null mice: disrupted Ca(2+)-activated K+ currents. *Neurosci Lett* 209:49-52.

Colling, S.B., M. Khana, J. Collinge, and J.G.R. Jefferys. 1997. Mossy Fibre Reorganization In the Hippocampus Of Prion Protein Null Mice. *Brain Research* 755:28-35.

Collinge, J. 2001. Prion diseases of humans and animals: Their causes and molecular basis. *Annu Rev Neurosci* 24:519-550.

Collinge, J., and A.R. Clarke. 2007. A general model of prion strains and their pathogenicity. *Science* 318:930-936.

Collinge, J., M.A. Whittington, K.C. Sidle, C.J. Smith, M.S. Palmer, A.R. Clarke, and J.G. Jefferys. 1994. Prion protein is necessary for normal synaptic function. *Nature* 370:295-297.

Collingridge, G.L., and T.V.P. Bliss. 1995. Memories of Nmda Receptors and Ltp. *Trends Neurosci* 18:54-56.

Collingridge, G.L., and R.A. Lester. 1989. Excitatory amino acid receptors in the vertebrate central nervous system. *Pharmacological reviews* 41:143-210.

Conn, P.J., and J.P. Pin. 1997. Pharmacology and functions of metabotropic glutamate receptors. *Annu Rev Pharmacol* 37:205-237.

Conti, V., A. Aghaie, M. Cilli, N. Martin, G. Caridi, L. Musante, G. Candiano, M. Castagna, A. Fairen, R. Ravazzolo, J.L. Guenet, and A. Puliti. 2006. crv4, a mouse model for human ataxia associated with kyphoscoliosis caused by an mRNA splicing mutation of the metabotropic glutamate receptor 1 (Grm1). *Int J Mol Med* 18:593-600.

Cotto, E., M. Andre, J. Forgue, H.J. Fleury, and P.J. Babin. 2005. Molecular characterization, phylogenetic relationships, and developmental expression patterns of prion genes in zebrafish (Danio rerio). *Febs J* 272:500-513.

Coutinho, V., and T. Knopfel. 2002. Metabotropic glutamate receptors: Electrical and chemical signaling properties. *Neuroscientist* 8:551-561.

Cozzi, A., E. Meli, V. Carla, R. Pellicciari, F. Moroni, and D.E. Pellegrini-Giampietro. 2002. Metabotropic glutamate 1 (mGlu1) receptor antagonists enhance GABAergic neurotransmission: a mechanism for the attenuation of post-ischemic injury and epileptiform activity? *Neuropharmacology* 43:119-130.

Crepel, V., L. Aniksztejn, Y. Ben-Ari, and C. Hammond. 1994. Glutamate metabotropic receptors increase a Ca(2+)-activated nonspecific cationic current in CA1 hippocampal neurons. *Journal of neurophysiology* 72:1561-1569.

Cronier, S., H. Laude, and J.M. Peyrin. 2004. Prions can infect primary cultured neurons and astrocytes and promote neuronal cell death. *Proc Natl Acad Sci U S A* 101:12271-12276.

Cunningham, C., R. Deacon, H. Wells, D. Boche, S. Waters, C.P. Diniz, H. Scott, J.N. Rawlins, and V.H. Perry. 2003a. Synaptic changes characterize early behavioural signs in the ME7 model of murine prion disease. *Eur J Neurosci* 17:2147-2155.

Cunningham, C., R. Deacon, H. Wells, D. Boche, S. Waters, C.P. Diniz, H. Scott, J.N.P. Rawlins, and V.H. Perry. 2003b. Synaptic changes characterize early behavioural signs in the ME7 model of murine prion disease. *Eur J Neurosci* 17:2147-2155.

Cunningham, C., R.M. Deacon, K. Chan, D. Boche, J.N. Rawlins, and V.H. Perry. 2005. Neuropathologically distinct prion strains give rise to similar temporal profiles of behavioral deficits. *Neurobiol Dis* 18:258-269.

Curtis, J., M. Errington, T. Bliss, K. Voss, and N. MacLeod. 2003. Age-dependent loss of PTP and LTP in the hippocampus of PrP-null mice. *Neurobiol Dis* 13:55-62.

Czuczwar, S.J. 2000. Perspectives for the use of excitatory amino acid ionotropic receptor antagonists as antiepileptic drugs. *Pol J Pharmacol* 52:67-70.

D'Antoni, S., A. Berretta, C.M. Bonaccorso, V. Bruno, E. Aronica, F. Nicoletti, and M.V. Catania. 2008. Metabotropic glutamate receptors in glial cells. *Neurochem Res* 33:2436-2443.

D'Antoni, S., A. Berretta, G. Seminara, P. Longone, A.M. Giuffrida-Stella, G. Battaglia, M.A. Sortino, F. Nicoletti, and M.V. Catania. 2011. A prolonged pharmacological blockade of type-5 metabotropic glutamate receptors protects cultured spinal cord motor neurons against excitotoxic death. *Neurobiology of disease* 42:252-264.

Dale, L.B., M. Bhattacharya, P.H. Anborgh, B. Murdoch, M. Bhatia, S. Nakanishi, and S.S. Ferguson. 2000. G protein-coupled receptor kinase-mediated desensitization of metabotropic glutamate receptor 1A protects against cell death. *J Biol Chem* 275:38213-38220.

Degos, V., S. Peineau, C. Nijboer, A.M. Kaindl, S. Sigaut, G. Favrais, Plaisant F., Teissier N., Gouadon E., Lombet A., Saliba E., G.L. Collingridge, Maze M., Nocoletti F., C.J. Heijnen, Mantz J., A. Kavelaars, and P. Gressens. 2013. GRK2 and group I mGluR mediate inflammation-induced sensitization to excitotoxic neurodegeneration *Ann Neurol* 73:

Deleault, N.R., B.T. Harris, J.R. Rees, and S. Supattapone. 2007. Formation of native prions from minimal components in vitro. *Proc Natl Acad Sci U S A* 104:9741-9746.

Deschwanden, A., B. Karolewicz, A.M. Feyissa, V. Treyer, S.M. Ametamey, A. Johayem, C. Burger, Y.P. Auberson, J. Sovago, C.A. Stockmeier, A. Buck, and G. Hasler. 2011. Reduced metabotropic glutamate receptor 5 density in major depression determined by [(11)C]ABP688 PET and postmortem study. *The American journal of psychiatry* 168:727-734.

Dinamarca, M.C., J.A. Rios, and N.C. Inestrosa. 2012. Postsynaptic Receptors for Amyloid-beta Oligomers as Mediators of Neuronal Damage in Alzheimer's Disease. *Frontiers in physiology* 3:464.

Ditlevsen, D.K., G.K. Povlsen, V. Berezin, and E. Bock. 2008. NCAM-induced intracellular signaling revisited. *J Neurosci Res* 86:727-743.

Doh-Ura, K., T. Iwaki, and B. Caughey. 2000. Lysosomotropic agents and cysteine protease inhibitors inhibit scrapie-associated prion protein accumulation. *J Virol* 74:4894-4897.

Doherty, A.J., M.J. Palmer, J.M. Henley, G.L. Collingridge, and D.E. Jane. 1997. (RS)-2-chloro-5-hydroxyphenylglycine (CHPG) activates mGlu(5), but not mGlu(1), receptors expressed in CHO cells and potentiates NMDA responses in the hippocampus. *Neuropharmacology* 36:265-267.

Dolen, G., and M.F. Bear. 2008. Role for metabotropic glutamate receptor 5 (mGluR5) in the pathogenesis of fragile X syndrome. *The Journal of physiology* 586:1503-1508.

Dolen, G., and M.F. Bear. 2009. A role for metabotropic glutamate receptor 5 (mGluR5) in the pathogenesis of fragile X syndrome. *Neurosci Res* 65:S27-S27.

Dong, X.X., Y. Wang, and Z.H. Qin. 2009. Molecular mechanisms of excitotoxicity and their relevance to pathogenesis of neurodegenerative diseases. *Acta Pharmacol Sin* 30:379-387.

Doolan, K.M., and D.W. Colby. 2015. Conformation-dependent epitopes recognized by prion protein antibodies probed using mutational scanning and deep sequencing. *Journal of molecular biology* 427:328-340.

Dron, M., Y. Bailly, V. Beringue, A.M. Haeberle, B. Griffond, P.Y. Risold, M.G. Tovey, H. Laude, and F. Dandoy-Dron. 2006. SCRG1, a potential marker of autophagy in transmissible spongiform encephalopathies. *Autophagy* 2:58-60.

Duncan, R.S., S.Y. Hwang, and P. Koulen. 2005. Effects of Vesl/Homer proteins on intracellular signaling. *Experimental biology and medicine* 230:527-535.

Emery, A.C., H. Hathaway, S. Pshenichkin, G.R. Takoudjou, J.O. DiRaddo, E. Grajkowska, R.P. Yasuda, B.B. Wolfe, and J.T. Wroblewski. 2011. Ligand Bias at mGlu1

Receptors Reveals a Second Binding Site and New Endogenous Agonists. *Current neuropharmacology* 9:18-18.

Emery, A.C., S. Pshenichkin, G.R. Takoudjou, E. Grajkowska, B.B. Wolfe, and J.T. Wroblewski. 2010. The Protective Signaling of Metabotropic Glutamate Receptor 1 Is Mediated by Sustained, beta-Arrestin-1-dependent ERK Phosphorylation. *J Biol Chem* 285:26041-26048.

Fairman, W.A., and S.G. Amara. 1999. Functional diversity of excitatory amino acid transporters: ion channel and transport modes. *The American journal of physiology* 277:F481-486.

Falsig, J., C. Julius, I. Margalith, P. Schwarz, F.L. Heppner, and A. Aguzzi. 2008. A versatile prion replication assay in organotypic brain slices. *Nat Neurosci* 11:109-117.

Falsig, J., T. Sonati, U.S. Herrmann, D. Saban, B. Li, K. Arroyo, B. Ballmer, P.P. Liberski, and A. Aguzzi. 2012. Prion pathogenesis is faithfully reproduced in cerebellar organotypic slice cultures. *PLoS pathogens* 8:e1002985.

Farlow, M.R., R.D. Yee, S.R. Dlouhy, P.M. Conneally, B. Azzarelli, and B. Ghetti. 1989. Gerstmann-Straussler-Scheinker disease. I. Extending the clinical spectrum. *Neurology* 39:1446-1452.

Fernaeus, S., J. Halldin, L. Bedecs, and T. Land. 2005a. Changed iron regulation in scrapie-infected neuroblastoma cells. *Mol Brain Res* 133:266-273.

Fernaeus, S., and T. Land. 2005. Increased iron-induced oxidative stress and toxicity in scrapie-infected neuroblastoma cells. *Neurosci Lett* 382:217-220.

Fernaeus, S., K. Reis, K. Bedecs, and T. Land. 2005b. Increased susceptibility to oxidative stress in scrapie-infected neuroblastoma cells is associated with intracellular iron status. *Neurosci Lett* 389:133-136.

Ferraguti, F., L. Crepaldi, and F. Nicoletti. 2008. Metabotropic Glutamate 1 Receptor: Current Concepts and Perspectives. *Pharmacological reviews* 60:536-581.

Ferreiro, E., C.R. Oliveira, and C. Pereira. 2004. Involvement of endoplasmic reticulum Ca2+ release through ryanodine and inositol 1,4,5-triphosphate receptors in the neurotoxic effects induced by the amyloid-beta peptide. *J Neurosci Res* 76:872-880.

Ferrer, I. 2002. Synaptic pathology and cell death in the cerebellum in Creutzfeldt-Jakob disease. *Cerebellum* 1:213-222.

Ferrer, I., B. Puig, R. Blanco, and E. Marti. 2000. Prion protein deposition and abnormal synaptic protein expression in the cerebellum in Creutzfeldt-Jakob disease. *Neuroscience* 97:715-726.

Fevrier, B., D. Vilette, F. Archer, D. Loew, W. Faigle, M. Vidal, H. Laude, and G. Raposo. 2004. Cells release prions in association with exosomes. *Proc Natl Acad Sci U S A* 101:9683-9688.

Fioriti, L., N. Angeretti, L. Colombo, A. De Luigi, A. Colombo, C. Manzoni, M. Morbin, F. Tagliavini, M. Salmona, R. Chiesa, and G. Forloni. 2007. Neurotoxic and gliotrophic activity of a synthetic peptide homologous to Gerstmann-Straussler-Scheinker disease amyloid protein. *J Neurosci* 27:1576-1583.

Fischer, M., T. Rulicke, A. Raeber, A. Sailer, M. Moser, B. Oesch, S. Brandner, A. Aguzzi, and C. Weissmann. 1996. Prion protein (PrP) with amino-proximal deletions restoring susceptibility of PrP knockout mice to scrapie. *Embo J* 15:1255-1264.

Flechsig, E., I. Hegyi, R. Leimeroth, A. Zuniga, D. Rossi, A. Cozzio, P. Schwarz, T. Rulicke, J. Gotz, A. Aguzzi, and C. Weissmann. 2003. Expression of truncated PrP targeted to Purkinje cells of PrP knockout mice causes Purkinje cell death and ataxia. *EMBO J* 22:3095-3101.

Flechsig, E., D. Shmerling, I. Hegyi, A.J. Raeber, M. Fischer, A. Cozzio, C. von Mering, A. Aguzzi, and C. Weissmann. 2000. Prion protein devoid of the octapeptide repeat region restores susceptibility to scrapie in PrP knockout mice. *Neuron* 27:399-408.

Florio, T., S. Thellung, C. Amico, M. Robello, M. Salmona, O. Bugiani, F. Tagliavini, G. Forloni, and G. Schettini. 1998. Prion protein fragment 106-126 induces apoptotic cell

death and impairment of L-type voltage-sensitive calcium channel activity in the GH3 cell line. *J Neurosci Res* 54:341-352.
Ford, M.J., L.J. Burton, R.J. Morris, and S.M. Hall. 2002. Selective expression of prion protein in peripheral tissues of the adult mouse. *Neuroscience* 113:177-192.
Forloni, G., N. Angeretti, R. Chiesa, E. Monzani, M. Salmona, O. Bugiani, and F. Tagliavini. 1993. Neurotoxicity of a prion protein fragment. *Nature* 362:543-546.
Fotuhi, M., D.G. Standaert, C.M. Testa, J.B. Penney, and A.B. Young. 1994. Differential Expression of Metabotropic Glutamate Receptors in the Hippocampus and Entorhinal Cortex of the Rat. *Mol Brain Res* 21:283-292.
Fournier, J.G., F. Escaig-Haye, and V. Grigoriev. 2000. Ultrastructural localization of prion proteins: physiological and pathological implications. *Microsc Res Tech* 50:76-88.
Francesconi, A., and R.M. Duvoisin. 2004. Divalent cations modulate the activity of metabotropic glutamate receptors. *J Neurosci Res* 75:472-479.
Frigo, M., M.G. Cogo, M.L. Fusco, M. Gardinetti, and B. Frigeni. 2012. Glutamate and Multiple Sclerosis. *Curr Med Chem* 19:1295-1299.
Fuhrmann, M., T. Bittner, G. Mitteregger, N. Haider, S. Moosmang, H. Kretzschmar, and J. Herms. 2006. Loss of the cellular prion protein affects the Ca2+ homeostasis in hippocampal CA1 neurons. *J Neurochem* 98:1876-1885.
Fuhrmann, M., G. Mitteregger, H. Kretzschmar, and J. Herms. 2007. Dendritic pathology in prion disease starts at the synaptic spine. *J Neurosci* 27:6224-6233.
Gasparini, F., T. Di Paolo, and B. Gomez-Mancilla. 2013. Metabotropic glutamate receptors for Parkinson's disease therapy. *Parkinson's disease* 2013:196028.
Gasparini, F., K. Lingenhohl, N. Stoehr, P.J. Flor, M. Heinrich, I. Vranesic, M. Biollaz, H. Allgeier, R. Heckendorn, S. Urwyler, M.A. Varney, E.C. Johnson, S.D. Hess, S.P. Rao, A.I. Sacaan, E.M. Santori, G. Velicelebi, and R. Kuhn. 1999. 2-Methyl-6-(phenylethynyl)-pyridine (MPEP), a potent, selective and systemically active mGlu5 receptor antagonist. *Neuropharmacology* 38:1493-1503.
Ghani, A.C., C.A. Donnelly, N.M. Ferguson, and R.M. Anderson. 2002. The transmission dynamics of BSE and vCJD. *C R Biol* 325:37-47.
Giese, A., M. Buchholz, J. Herms, and H.A. Kretzschmar. 2005. Mouse brain synaptosomes accumulate copper-67 efficiently by two distinct processes independent of cellular prion protein. *J Mol Neurosci* 27:347-354.
Goda, Y., and G.W. Davis. 2003. Mechanisms of synapse assembly and disassembly. *Neuron* 40:243-264.
Gogolla, N., I. Galimberti, V. DePaola, and P. Caroni. 2006. Preparation of organotypic hippocampal slice cultures for long-term live imaging. *Nat Protoc* 1:1165-1171.
Gouaux, E. 2004. Structure and function of AMPA receptors. *J Physiol-London* 554:249-253.
Govaerts, C., H. Wille, S.B. Prusiner, and F.E. Cohen. 2004. Evidence for assembly of prions with left-handed beta 3-helices into trimers. *P Natl Acad Sci USA* 101:8342-8347.
Graner, E., A.F. Mercadante, S.M. Zanata, O.V. Forlenza, A.L. Cabral, S.S. Veiga, M.A. Juliano, R. Roesler, R. Walz, A. Minetti, I. Izquierdo, V.R. Martins, and R.R. Brentani. 2000. Cellular prion protein binds laminin and mediates neuritogenesis. *Brain Res Mol Brain Res* 76:85-92.
Graveland, G.A., R.S. Williams, and M. DiFiglia. 1985. Evidence for degenerative and regenerative changes in neostriatal spiny neurons in Huntington's disease. *Science* 227:770-773.
Gray, B.C., Z. Siskova, V.H. Perry, and V. O'Connor. 2009. Selective presynaptic degeneration in the synaptopathy associated with ME7-induced hippocampal pathology. *Neurobiol Dis* 35:63-74.
Grewal, S.S., R.D. York, and P.J.S. Stork. 1999. Extracellular-signal-regulated kinase signalling in neurons. *Curr Opin Neurobiol* 9:544-553.
Griffith, J.S. 1967. Self-Replication and Scrapie. *Nature* 215:1043-&.

Grosskreutz, J., L. Van Den Bosch, and B.U. Keller. 2010. Calcium dysregulation in amyotrophic lateral sclerosis. *Cell Calcium* 47:165-174.

Gubellini, P., E. Saulle, D. Centonze, C. Costa, D. Tropepi, G. Bernardi, F. Conquet, and P. Calabresi. 2003. Corticostriatal LTP requires combined mGluR1 and mGluR5 activation. *Neuropharmacology* 44:8-16.

Guentchev, M., S.L. Siedlak, C. Jarius, F. Tagliavini, R.J. Castellani, G. Perry, M.A. Smith, and H. Budka. 2002. Oxidative damage to nucleic acids in human prion disease. *Neurobiol Dis* 9:275-281.

Guerineau, N.C., B.H. Gahwiler, and U. Gerber. 1994. Reduction of Resting K+ Current by Metabotropic Glutamate and Muscarinic Receptors in Rat Ca3 Cells - Mediation by G-Proteins. *J Physiol-London* 474:27-33.

Haas, L.T., M.A. Kostylev, and S.M. Strittmatter. 2014. Therapeutic molecules and endogenous ligands regulate the interaction between brain cellular prion protein (PrPC) and metabotropic glutamate receptor 5 (mGluR5). *J Biol Chem* 289:28460-28477.

Haas, L.T., S.V. Salazar, M.A. Kostylev, J.W. Um, A.C. Kaufman, and S.M. Strittmatter. 2016. Metabotropic glutamate receptor 5 couples cellular prion protein to intracellular signalling in Alzheimer's disease. *Brain : a journal of neurology* 139:526-546.

Haeberle, A.M., C. Ribaut-Barassin, G. Bombarde, J. Mariani, G. Hunsmann, J. Grassi, and Y. Bailly. 2000. Synaptic prion protein immuno-reactivity in the rodent cerebellum. *Microsc Res Tech* 50:66-75.

Hajj, G.N., M.H. Lopes, A.F. Mercadante, S.S. Veiga, R.B. da Silveira, T.G. Santos, K.C. Ribeiro, M.A. Juliano, S.G. Jacchieri, S.M. Zanata, and V.R. Martins. 2007. Cellular prion protein interaction with vitronectin supports axonal growth and is compensated by integrins. *J Cell Sci* 120:1915-1926.

Hajj, G.N., T.G. Santos, Z.S. Cook, and V.R. Martins. 2009. Developmental expression of prion protein and its ligands stress-inducible protein 1 and vitronectin. *J Comp Neurol* 517:371-384.

Hamilton A., Esseltine JL., DeVries RA., Cregan SP., and Fergusson SS. 2014. Metabotropic glutamate receptor 5 knockout reduces cognitive impairment and pathogenesis in a mouse model of Alzheimer's disease. *Mol. Brain* 29:

Hannan, A.J., C. Blakemore, A. Katsnelson, T. Vitalis, K.M. Huber, M. Bear, J. Roder, D. Kim, H.S. Shin, and P.C. Kind. 2001. PLC-beta1, activated via mGluRs, mediates activity-dependent differentiation in cerebral cortex. *Nature neuroscience* 4:282-288.

Harris, D.A. 1999. Cellular biology of prion diseases. *Clin Microbiol Rev* 12:429-444.

Harris, D.A., M.T. Huber, P. van Dijken, S.L. Shyng, B.T. Chait, and R. Wang. 1993a. Processing of a cellular prion protein: identification of N- and C-terminal cleavage sites. *Biochemistry* 32:1009-1016.

Harris, D.A., P. Lele, and W.D. Snider. 1993b. Localization of the mRNA for a chicken prion protein by in situ hybridization. *Proc Natl Acad Sci U S A* 90:4309-4313.

Hegde, R.S., J.A. Mastrianni, M.R. Scott, K.A. DeFea, P. Tremblay, M. Torchia, S.J. DeArmond, S.B. Prusiner, and V.R. Lingappa. 1998. A transmembrane form of the prion protein in neurodegenerative disease. *Science* 279:827-834.

Henley, J.M., E.A. Barker, and O.O. Glebov. 2011. Routes, destinations and delays: recent advances in AMPA receptor trafficking. *Trends Neurosci* 34:258-268.

Heppner, F.L., C. Musahl, I. Arrighi, M.A. Klein, T. Rulicke, B. Oesch, R.M. Zinkernagel, U. Kalinke, and A. Aguzzi. 2001. Prevention of scrapie pathogenesis by transgenic expression of anti-prion protein antibodies. *Science* 294:178-182.

Hermans, E., and R.A.J. Challiss. 2001. Structural, signalling and regulatory properties of the group I metabotropic glutamate receptors: prototypic family C G-protein-coupled receptors. *Biochem J* 359:465-484.

Herms, J., T. Tings, S. Gall, A. Madlung, A. Giese, H. Siebert, P. Schurmann, O. Windl, N. Brose, and H. Kretzschmar. 1999. Evidence of presynaptic location and function of the prion protein. *J Neurosci* 19:8866-8875.

Herms, J.W., S. Korte, S. Gall, I. Schneider, S. Dunker, and H.A. Kretzschmar. 2000. Altered intracellular calcium homeostasis in cerebellar granule cells of prion protein-deficient mice. *J Neurochem* 75:1487-1492.

Herms, J.W., H.A. Kretzschmar, S. Titz, and B.U. Keller. 1995. Patch-Clamp Analysis Of Synaptic Transmission to Cerebellar Purkinje Cells Of Prion Protein Knockout Mice. *European Journal of Neuroscience* 7:2508-2512.

Herms, J.W., T. Tings, S. Dunker, and H.A. Kretzschmar. 2001. Prion protein affects Ca2+-activated K+ currents in cerebellar purkinje cells. *Neurobiol Dis* 8:324-330.

Hernandez-Rapp, J., S. Martin-Lanneree, T.Z. Hirsch, J.M. Launay, and S. Mouillet-Richard. 2014. Hijacking PrPc-dependent signal transduction: when prions impair A beta clearance. *Front Aging Neurosci* 6:

Herrero, I., M.T. Miras-Portugal, and J. Sanchez-Prieto. 1998. Functional switch from facilitation to inhibition in the control of glutamate release by metabotropic glutamate receptors. *J Biol Chem* 273:1951-1958.

Herrmann, U.S., T. Sonati, J. Falsig, R.R. Reimann, P. Dametto, T. O'Connor, B. Li, A. Lau, S. Hornemann, S. Sorce, U. Wagner, D. Sanoudou, and A. Aguzzi. 2015. Prion infections and anti-PrP antibodies trigger converging neurotoxic pathways. *PLoS pathogens* 11:e1004662.

Hetz, C., J. Castilla, and C. Soto. 2007. Perturbation of endoplasmic reticulum homeostasis facilitates prion replication. *J Biol Chem* 282:12725-12733.

Hetz, C., A.H. Lee, D. Gonzalez-Romero, P. Thielen, J. Castilla, C. Soto, and L.H. Glimcher. 2008. Unfolded protein response transcription factor XBP-1 does not influence prion replication or pathogenesis. *Proc Natl Acad Sci U S A* 105:757-762.

Hetz, C., M. Russelakis-Carneiro, K. Maundrell, J. Castilla, and C. Soto. 2003. Caspase-12 and endoplasmic reticulum stress mediate neurotoxicity of pathological prion protein. *Embo J* 22:5435-5445.

Hill, A.F., S. Joiner, J. Linehan, M. Desbruslais, P.L. Lantos, and J. Collinge. 2000. Species-barrier-independent prion replication in apparently resistant species. *Proc Natl Acad Sci U S A* 97:10248-10253.

Hollmann, M., and S. Heinemann. 1994. Cloned Glutamate Receptors. *Annu Rev Neurosci* 17:31-108.

Hollmann, M., B. Keller, M. Blaschke, R. Rivosecchi, A. Konnerth, and S. Heinemann. 1993. Structural and Functional-Properties of Cloned Glutamate Receptors. *J Neurochem* 61:S261-S261.

Hollmann, M., A. Osheagreenfield, S.W. Rogers, and S. Heinemann. 1989. Cloning by Functional Expression of a Member of the Glutamate Receptor Family. *Nature* 342:643-648.

Hooper, N.M. 2005. Roles of proteolysis and lipid rafts in the processing of the amyloid precursor protein and prion protein. *Biochem Soc Trans* 33:335-338.

Hornshaw, M.P., J.R. McDermott, J.M. Candy, and J.H. Lakey. 1995. Copper binding to the N-terminal tandem repeat region of mammalian and avian prion protein: structural studies using synthetic peptides. *Biochem Biophys Res Commun* 214:993-999.

Houamed, K.M., J.L. Kuijper, T.L. Gilbert, B.A. Haldeman, P.J. Ohara, E.R. Mulvihill, W. Almers, and F.S. Hagen. 1991. Cloning, Expression, and Gene Structure of a G-Protein-Coupled Glutamate Receptor from Rat-Brain. *Science* 252:1318-1321.

Hsiao, K.K., M. Scott, D. Foster, D.F. Groth, S.J. DeArmond, and S.B. Prusiner. 1990. Spontaneous neurodegeneration in transgenic mice with mutant prion protein [see comments]. *Science* 250:1587-1590.

Hu, N.W., A.J. Nicoll, D. Zhang, A.J. Mably, T. O'Malley, S.A. Purro, C. Terry, J. Collinge, D.M. Walsh, and M.J. Rowan. 2014. mGlu5 receptors and cellular prion protein mediate amyloid-beta-facilitated synaptic long-term depression in vivo. *Nature communications* 5:3374.

Huber, K.M., S.M. Gallagher, S.T. Warren, and M.F. Bear. 2002. Altered synaptic plasticity in a mouse model of fragile X mental retardation. *Proceedings of the National Academy of Sciences of the United States of America* 99:7746-7750.

Hundt, C., J.M. Peyrin, S. Haik, S. Gauczynski, C. Leucht, R. Rieger, M.L. Riley, J.P. Deslys, D. Dormont, C.I. Lasmezas, and S. Weiss. 2001. Identification of interaction domains of the prion protein with its 37-kDa/67-kDa laminin receptor. *Embo J* 20:5876-5886.

Hutter, G., F.L. Heppner, and A. Aguzzi. 2003. No superoxide dismutase activity of cellular prion protein in vivo. *Biol Chem* 384:1279-1285.

Hynd, M.R., H.L. Scott, and P.R. Dodd. 2004. Glutamate-mediated excitotoxicity and neurodegeneration in Alzheimer's disease. *Neurochem Int* 45:583-595.

Ishikura, N. 2007. [Notch-1 is involved in neurodegeneration in prion diseases]. *Nippon Rinsho* 65:1397-1400.

Ishikura, N., J.L. Clever, E. Bouzamondo-Bernstein, E. Samayoa, S.B. Prusiner, E.J. Huang, and S.J. DeArmond. 2005. Notch-1 activation and dendritic atrophy in prion disease. *Proc Natl Acad Sci U S A* 102:886-891.

Jackson, G.S., I. Murray, L.L.P. Hosszu, N. Gibbs, J.P. Waltho, A.R. Clarke, and J. Collinge. 2001. Location and properties of metal-binding sites on the human prion protein. *P Natl Acad Sci USA* 98:8531-8535.

Jackson, W.S., A.W. Borkowski, H. Faas, A.D. Steele, O.D. King, N. Watson, A. Jasanoff, and S. Lindquist. 2009. Spontaneous generation of prion infectivity in fatal familial insomnia knockin mice. *Neuron* 63:438-450.

Jamieson, E., M. Jeffrey, J.W. Ironside, and J.R. Fraser. 2001. Apoptosis and dendritic dysfunction precede prion protein accumulation in 87V scrapie. *Neuroreport* 12:2147-2153.

Jantzie, L.L., D.M. Talos, D.B. Selip, L. An, M.C. Jackson, R.D. Folkerth, W.B. Deng, and F.E. Jensen. 2010. Developmental regulation of group I metabotropic glutamate receptors in the premature brain and their protective role in a rodent model of periventricular leukomalacia. *Neuron Glia Biol* 6:277-288.

Jarrett, J.T., and P.T. Lansbury, Jr. 1993. Seeding "one-dimensional crystallization" of amyloid: a pathogenic mechanism in Alzheimer's disease and scrapie?. [Review]. *Cell* 73:1055-1058.

Jeffrey, M., W.G. Halliday, J. Bell, A.R. Johnston, N.K. MacLeod, C. Ingham, A.R. Sayers, D.A. Brown, and J.R. Fraser. 2000. Synapse loss associated with abnormal PrP precedes neuronal degeneration in the scrapie-infected murine hippocampus. *Neuropathol Appl Neurobiol* 26:41-54.

Jeffrey, M., S. Martin, J. Barr, A. Chong, and J.R. Fraser. 2001. Onset of accumulation of PrPres in murine ME7 scrapie in relation to pathological and PrP immunohistochemical changes. *J Comp Pathol* 124:20-28.

Jia, Z.P., Y.M. Lu, J. Henderson, F. Taverna, C. Romano, W. Abramow-Newerly, J.M. Wojtowicz, and J. Roder. 1998. Selective abolition of the NMDA component of long-term potentiation in mice lacking mGluR5. *Learn Memory* 5:331-343.

Jin, D.Z., M.L. Guo, B. Xue, L.M. Mao, and J.Q. Wang. 2013. Differential regulation of CaMKIIalpha interactions with mGluR5 and NMDA receptors by Ca(2+) in neurons. *J Neurochem* 127:620-631.

Jingami, H., S. Nakanishi, and K. Morikawa. 2003. Structure of the metabotropic glutamate receptor. *Curr Opin Neurobiol* 13:271-278.

Jobling, M.F., X.D. Huang, L.R. Stewart, K.J. Barnham, C. Curtain, I. Volitakis, M. Perugini, A.R. White, R.A. Cherny, C.L. Masters, C.J. Barrow, S.J. Collins, A.I. Bush, and R. Cappai. 2001. Copper and zinc binding modulates the aggregation and neurotoxic properties of the prion peptide PrP106-126. *Biochemistry-Us* 40:8073-8084.

Johnston, A.R., C. Black, J. Fraser, and N. MacLeod. 1997. Scrapie infection alters the membrane and synaptic properties of mouse hippocampal CA1 pyramidal neurones. *The Journal of physiology* 500 (Pt 1):1-15.

Johnston, A.R., J.R. Fraser, M. Jeffrey, and N. MacLeod. 1998a. Alterations in potassium currents may trigger neurodegeneration in murine scrapie. *Exp Neurol* 151:326-333.
Johnston, A.R., J.R. Fraser, M. Jeffrey, and N. MacLeod. 1998b. Synaptic plasticity in the CA1 area of the hippocampus of scrapie-infected mice. *Neurobiology of disease* 5:188-195.
Julio-Pieper, M., P.J. Flor, T.G. Dinan, and J.F. Cryan. 2011. Exciting times beyond the brain: metabotropic glutamate receptors in peripheral and non-neural tissues. *Pharmacological reviews* 63:35-58.
Kammermeier, P.J., and J. Yun. 2005. Activation of metabotropic glutamate receptor 1 dimers requires glutamate binding in both subunits. *J Pharmacol Exp Ther* 312:502-508.
Kasahara, K., K. Watanabe, T. Yamamoto, and Y. Sanai. 1999. Regulation of GPI-Anchored neuronal cell adhesion molecule TAG-1 signaling via Src-family tyrosine kinase Lyn by glycosphingolipids in lipid rafts. *Mol Biol Cell* 10:306a-306a.
Katamine, S., N. Nishida, T. Sugimoto, T. Noda, S. Sakaguchi, K. Shigematsu, Y. Kataoka, A. Nakatani, S. Hasegawa, R. Moriuchi, and T. Miyamoto. 1998. Impaired motor coordination in mice lacking prion protein. *Cell Mol Neurobiol* 18:731-742.
Kessels, H.W., and R. Malinow. 2009. Synaptic AMPA Receptor Plasticity and Behavior. *Neuron* 61:340-350.
Kessels, H.W., L.N. Nguyen, S. Nabavi, and R. Malinow. 2010. The prion protein as a receptor for amyloid-beta. *Nature* 466:E3-E4.
Khosravani, H., Y. Zhang, S. Tsutsui, S. Hameed, C. Altier, J. Hamid, L. Chen, M. Villemaire, Z. Ali, F.R. Jirik, and G.W. Zamponi. 2008. Prion protein attenuates excitotoxicity by inhibiting NMDA receptors. *J Gen Physiol* 131:i5.
Kim, C.K., A. Sakudo, Y. Taniuchi, K. Shigematsu, C.B. Kang, K. Saeki, Y. Matsumoto, S. Sakaguchi, S. Itohara, and T. Onodera. 2007. Late-onset olfactory deficits and mitral cell loss in mice lacking prion protein with ectopic expression of Doppel. *Int J Mol Med* 20:169-176.
Kim, N.H., J.K. Choi, B.H. Jeong, J.I. Kim, M.S. Kwon, R.I. Carp, and Y.S. Kim. 2005. Effect of transition metals (Mn, Cu, Fe) and deoxycholic acid (DA) on the conversion of PrPC to PrPres. *Faseb J* 19:783-785.
Klamt, F., F. Dal-Pizzol, M.L. Conte da Frota, Jr., R. Walz, M.E. Andrades, E.G. da Silva, R.R. Brentani, I. Izquierdo, and J.C. Fonseca Moreira. 2001. Imbalance of antioxidant defense in mice lacking cellular prion protein. *Free Radic Biol Med* 30:1137-1144.
Klohn, P.C., M. Farmer, J.M. Linehan, C. O'Malley, M. Fernandez de Marco, W. Taylor, M. Farrow, A. Khalili-Shirazi, S. Brandner, and J. Collinge. 2012. PrP antibodies do not trigger mouse hippocampal neuron apoptosis. *Science* 335:52.
Ko, S.J., K. Isozaki, I. Kim, J.H. Lee, H.J. Cho, S.Y. Sohn, S.R. Oh, S. Park, D.G. Kim, C.H. Kim, and K.W. Roche. 2012. PKC phosphorylation regulates mGluR5 trafficking by enhancing binding of Siah-1A. *J Neurosci* 32:16391-16401.
Kocisko, D.A., J.H. Come, S.A. Priola, B. Chesebro, G.J. Raymond, P.T. Lansbury, and B. Caughey. 1994. Cell-free formation of protease-resistant prion protein [see comments]. *Nature* 370:471-474.
Kohara, A., M. Takahashi, S. Yatsugi, S. Tamura, Y. Shitaka, S. Hayashibe, S. Kawabata, and M. Okada. 2008. Neuroprotective effects of the selective type 1 metabotropic glutamate receptor antagonist YM-202074 in rat stroke models. *Brain research* 1191:168-179.
Kostylev, M.A., A.C. Kaufman, H.B. Nygaard, P. Patel, L.T. Haas, E.C. Gunther, A. Vortmeyer, and S.M. Strittmatter. 2015. Prion-Protein-interacting Amyloid-beta Oligomers of High Molecular Weight Are Tightly Correlated with Memory Impairment in Multiple Alzheimer Mouse Models. *J Biol Chem* 290:17415-17438.
Kovacs, G.G., E. Gelpi, T. Strobel, G. Ricken, J.R. Nyengaard, H. Bernheimer, and H. Budka. 2007. Involvement of the endosomal-lysosomal system correlates with

regional pathology in Creutzfeldt-Jakob disease. *J Neuropathol Exp Neurol* 66:628-636.

Kovacs, G.G., M. Preusser, M. Strohschneider, and H. Budka. 2005. Subcellular localization of disease-associated prion protein in the human brain. *Am J Pathol* 166:287-294.

Kranich, J., N.J. Krautler, J. Falsig, B. Ballmer, S. Li, G. Hutter, P. Schwarz, R. Moos, C. Julius, G. Miele, and A. Aguzzi. 2010. Engulfment of cerebral apoptotic bodies controls the course of prion disease in a mouse strain-dependent manner. *The Journal of experimental medicine* 207:2271-2281.

Kristensson, K., B. Feuerstein, A. Taraboulos, W.C. Hyun, S.B. Prusiner, and S.J. DeArmond. 1993. Scrapie prions alter receptor-mediated calcium responses in cultured cells. *Neurology* 43:2335-2341.

Krueger, D.D., and M.F. Bear. 2011. Toward Fulfilling the Promise of Molecular Medicine in Fragile X Syndrome. *Annu Rev Med* 62:411-429.

Kubler, E., B. Oesch, and A.J. Raeber. 2003. Diagnosis of prion diseases. *British medical bulletin* 66:267-279.

Kubo, Y., T. Miyashita, and Y. Murata. 1998. Structural basis for a Ca2+-sensing function of the metabotropic glutamate receptors. *Science* 279:1722-1725.

Kuffer, A., A.K. Lakkaraju, A. Mogha, S.C. Petersen, K. Airich, C. Doucerain, R. Marpakwar, P. Bakirci, A. Senatore, A. Monnard, C. Schiavi, M. Nuvolone, B. Grosshans, S. Hornemann, F. Bassilana, K.R. Monk, and A. Aguzzi. 2016. The prion protein is an agonistic ligand of the G protein-coupled receptor Adgrg6. *Nature*

Kunishima, N., Y. Shimada, Y. Tsuji, T. Sato, M. Yamamoto, T. Kumasaka, S. Nakanishi, H. Jingami, and K. Morikawa. 2000. Structural basis of glutamate recognition by a dimeric metabotropic glutamate receptor. *Nature* 407:971-977.

Kuwahara, C., A.M. Takeuchi, T. Nishimura, K. Haraguchi, A. Kubosaki, Y. Matsumoto, K. Saeki, T. Yokoyama, S. Itohara, and T. Onodera. 1999. Prions prevent neuronal cell-line death. *Nature* 400:225-226.

Ladogana, A., M. Puopolo, E.A. Croes, H. Budka, C. Jarius, S. Collins, G.M. Klug, T. Sutcliffe, A. Giulivi, A. Alperovitch, N. Delasnerie-Laupretre, J.P. Brandel, S. Poser, H. Kretzschmar, I. Rietveld, E. Mitrova, P. Cuesta Jde, P. Martinez-Martin, M. Glatzel, A. Aguzzi, R. Knight, H. Ward, M. Pocchiari, C.M. van Duijn, R.G. Will, and I. Zerr. 2005. Mortality from Creutzfeldt-Jakob disease and related disorders in Europe, Australia, and Canada. *Neurology* 64:1586-1591.

Lanore, F., V.F. Labrousse, Z. Szabo, E. Normand, C. Blanchet, and C. Mulle. 2012. Deficits in Morphofunctional Maturation of Hippocampal Mossy Fiber Synapses in a Mouse Model of Intellectual Disability. *J Neurosci* 32:17882-17893.

Lapointe, V., F. Morin, S. Ratte, A. Croce, F. Conquet, and J.C. Lacaille. 2004. Synapse-specific mGluR1-dependent long-term potentiation in interneurones regulates mouse hippocampal inhibition. *J Physiol* 555:125-135.

Lasmezas, C.I., J.P. Deslys, O. Robain, A. Jaegly, V. Beringue, J.M. Peyrin, J.G. Fournier, J.J. Hauw, J. Rossier, and D. Dormont. 1997. Transmission Of the Bse Agent to Mice In the Absence Of Detectable Abnormal Prion Protein. *Science* 275:402-405.

Laszlo, L., J. Lowe, T. Self, N. Kenward, M. Landon, T. McBride, C. Farquhar, I. McConnell, J. Brown, J. Hope, and et al. 1992. Lysosomes as key organelles in the pathogenesis of prion encephalopathies. *J Pathol* 166:333-341.

Lauren, J., D.A. Gimbel, H.B. Nygaard, J.W. Gilbert, and S.M. Strittmatter. 2009. Cellular prion protein mediates impairment of synaptic plasticity by amyloid-beta oligomers. *Nature* 457:1128-1132.

Lazzari, C., C. Peggion, R. Stella, M.L. Massimino, D. Lim, A. Bertoli, and M.C. Sorgato. 2011. Cellular prion protein is implicated in the regulation of local Ca2+ movements in cerebellar granule neurons. *J Neurochem* 116:881-890.

Le Duigou, C., and D.M. Kullmann. 2011. Group I mGluR Agonist-Evoked Long-Term Potentiation in Hippocampal Oriens Interneurons. *J Neurosci* 31:5777-5781.

Lee, I.Y., D. Westaway, A.F. Smit, K. Wang, J. Seto, L. Chen, C. Acharya, M. Ankener, D. Baskin, C. Cooper, H. Yao, S.B. Prusiner, and L.E. Hood. 1998. Complete genomic sequence and analysis of the prion protein gene region from three mammalian species. *Genome Res* 8:1022-1037.

Lefebvre-Roque, M., E. Kremmer, S. Gilch, W.Q. Zou, C. Feraudet, C.M. Gilles, N. Sales, J. Grassi, P. Gambetti, T. Baron, H. Schatzl, and C.I. Lasmezas. 2007. Toxic effects of intracerebral PrP antibody administration during the course of BSE infection in mice. *Prion* 1:198-206.

Legname, G., I.V. Baskakov, H.O. Nguyen, D. Riesner, F.E. Cohen, S.J. DeArmond, and S.B. Prusiner. 2004. Synthetic mammalian prions. *Science* 305:673-676.

Lerma, J., and J.M. Marques. 2013. Kainate Receptors in Health and Disease. *Neuron* 80:292-311.

Levenes, C., H. Daniel, D. Jaillard, F. Conquet, and F. Crepel. 1997. Incomplete regression of multiple climbing fibre innervation of cerebellar Purkinje cells in mGLuR1 mutant mice. *Neuroreport* 8:571-574.

Li, A., H.M. Christensen, L.R. Stewart, K.A. Roth, R. Chiesa, and D.A. Harris. 2007. Neonatal lethality in transgenic mice expressing prion protein with a deletion of residues 105-125. *Embo J* 26:548-558.

Li, A., S. Sakaguchi, R. Atarashi, B.C. Roy, R. Nakaoke, K. Arima, N. Okimura, J. Kopacek, and K. Shigematsu. 2000. Identification of a novel gene encoding a PrP-like protein expressed as chimeric transcripts fused to PrP exon 1/2 in ataxic mouse line with a disrupted PrP gene. *Cell Mol Neurobiol* 20:553-567.

Liberski, P.P., D.R. Brown, B. Sikorska, B. Caughey, and P. Brown. 2008. Cell death and autophagy in prion diseases (transmissible spongiform encephalopathies). *Folia Neuropathol* 46:1-25.

Liberski, P.P., B. Sikorska, J. Bratosiewicz-Wasik, D.C. Gajdusek, and P. Brown. 2004. Neuronal cell death in transmissible spongiform encephalopathies (prion diseases) revisited: from apoptosis to autophagy. *Int J Biochem Cell Biol* 36:2473-2490.

Lima, F.R., C.P. Arantes, A.G. Muras, R. Nomizo, R.R. Brentani, and V.R. Martins. 2007. Cellular prion protein expression in astrocytes modulates neuronal survival and differentiation. *J Neurochem* 103:2164-2176.

Linden, R., V.R. Martins, M.A. Prado, M. Cammarota, I. Izquierdo, and R.R. Brentani. 2008. Physiology of the prion protein. *Physiol Rev* 88:673-728.

Lipton, S.A. 2007. Pathologically activated therapeutics for neuroprotection. *Nat Rev Neurosci* 8:803-808.

Liu, J.F., P. Rondard, and J.P. Pin. 2006. Coupling of agonist binding to effector domain activation in metabotropic glutamate-like receptors. *Acta Pharmacol Sin* 27:396-396.

Lledo, P.M., P. Tremblay, S.J. Dearmond, S.B. Prusiner, and R.A. Nicoll. 1996. Mice Deficient For Prion Protein Exhibit Normal Neuronal Excitability and Synaptic Transmission In the Hippocampus. *Proceedings of the National Academy of Sciences of the United States of America* 93:2403-2407.

Locht, C., B. Chesebro, R. Race, and J.M. Keith. 1986. Molecular cloning and complete sequence of prion protein cDNA from mouse brain infected with the scrapie agent. *Proc Natl Acad Sci U S A* 83:6372-6376.

Lopes, M.H., G.N. Hajj, A.G. Muras, G.L. Mancini, R.M. Castro, K.C. Ribeiro, R.R. Brentani, R. Linden, and V.R. Martins. 2005. Interaction of cellular prion and stress-inducible protein 1 promotes neuritogenesis and neuroprotection by distinct signaling pathways. *J Neurosci* 25:11330-11339.

Lopez-Bendito, G., R. Shigemoto, A. Fairen, and R. Lujan. 2002. Differential distribution of group I metabotropic glutamate receptors during rat cortical development. *Cereb Cortex* 12:625-638.

Lorenz, H., O. Windl, and H.A. Kretzschmar. 2002. Cellular phenotyping of secretory and nuclear prion proteins associated with inherited prion diseases. *J Biol Chem* 277:8508-8516.

Lu, W., Y. Shi, A.C. Jackson, K. Bjorgan, M.J. During, R. Sprengel, P.H. Seeburg, and R.A. Nicoll. 2009. Subunit Composition of Synaptic AMPA Receptors Revealed by a Single-Cell Genetic Approach. *Neuron* 62:254-268.

Lu, Y.M., Z.P. Jia, C. Janus, J.T. Henderson, R. Gerlai, J.M. Wojtowicz, and J.C. Roder. 1997. Mice lacking metabotropic glutamate receptor 5 show impaired learning and reduced CA1 long-term potentiation (LTP) but normal CA3 LTP. *J Neurosci* 17:5196-5205.

Lujan, R., Z. Nusser, J.D.B. Roberts, R. Shigemoto, and P. Somogyi. 1996. Perisynaptic location of metabotropic glutamate receptors mGluR1 and mGluR5 on dendrites and dendritic spines in the rat hippocampus. *Eur J Neurosci* 8:1488-1500.

Luo, P., F. Fei, L. Zhang, Y. Qu, and Z. Fei. 2011. The role of glutamate receptors in traumatic brain injury: Implications for postsynaptic density in pathophysiology. *Brain Res Bull* 85:313-320.

Luscher, C., and K.M. Huber. 2010. Group 1 mGluR-dependent synaptic long-term depression: mechanisms and implications for circuitry and disease. *Neuron* 65:445-459.

Maas, E., M. Geissen, M.H. Groschup, R. Rost, T. Onodera, H. Schatzl, and I.M. Vorberg. 2007. Scrapie infection of prion protein-deficient cell line upon ectopic expression of mutant prion proteins. *J Biol Chem* 282:18702-18710.

Madisen, L., A.R. Garner, D. Shimaoka, A.S. Chuong, N.C. Klapoetke, L. Li, A. van der Bourg, Y. Niino, L. Egolf, C. Monetti, H. Gu, M. Mills, A. Cheng, B. Tasic, T.N. Nguyen, S.M. Sunkin, A. Benucci, A. Nagy, A. Miyawaki, F. Helmchen, R.M. Empson, T. Knopfel, E.S. Boyden, R.C. Reid, M. Carandini, and H. Zeng. 2015. Transgenic mice for intersectional targeting of neural sensors and effectors with high specificity and performance. *Neuron* 85:942-958.

Madisen, L., T.A. Zwingman, S.M. Sunkin, S.W. Oh, H.A. Zariwala, H. Gu, L.L. Ng, R.D. Palmiter, M.J. Hawrylycz, A.R. Jones, E.S. Lein, and H. Zeng. 2010. A robust and high-throughput Cre reporting and characterization system for the whole mouse brain. *Nat Neurosci* 13:133-140.

Maejima, T., T. Ohno-Shosaku, and M. Kano. 2001. Endogenous cannabinoid as a retrograde messenger from depolarized postsynaptic neurons to presynaptic terminals. *Neurosci Res* 40:205-210.

Maglio, L.E., M.F. Perez, V.R. Martins, R.R. Brentani, and O.A. Ramirez. 2004. Hippocampal synaptic plasticity in mice devoid of cellular prion protein. *Brain Res Mol Brain Res* 131:58-64.

Magri, G., M. Clerici, P. Dall'Ara, M. Biasin, M. Caramelli, C. Casalone, M.L. Giannino, R. Longhi, L. Piacentini, S. Della Bella, P. Gazzuola, P.A. Martino, S. Della Bella, C. Pollera, M. Puricelli, F. Servida, I. Crescio, A. Boasso, W. Ponti, and G. Poli. 2005. Decrease in pathology and progression of scrapie after immunisation with synthetic prion protein peptides in hamsters. *Vaccine* 23:2862-2868.

Makarava, N., G.G. Kovacs, O. Bocharova, R. Savtchenko, I. Alexeeva, H. Budka, R.G. Rohwer, and I.V. Baskakov. 2010. Recombinant prion protein induces a new transmissible prion disease in wild-type animals. *Acta Neuropathol* 119:177-187.

Malaga-Trillo, E., G.P. Solis, Y. Schrock, C. Geiss, L. Luncz, V. Thomanetz, and C.A. Stuermer. 2009. Regulation of embryonic cell adhesion by the prion protein. *PLoS Biol* 7:e55.

Malenka, R.C., and R.A. Nicoll. 1999. Neuroscience - Long-term potentiation - A decade of progress? *Science* 285:1870-1874.

Mallucci, G., and J. Collinge. 2005. Rational targeting for prion therapeutics. *Nat Rev Neurosci* 6:23-34.

Mallucci, G.R., S. Ratte, E.A. Asante, J. Linehan, I. Gowland, J.G. Jefferys, and J. Collinge. 2002. Post-natal knockout of prion protein alters hippocampal CA1 properties, but does not result in neurodegeneration. *The EMBO journal* 21:202-210.

Mallucci, G.R., M.D. White, M. Farmer, A. Dickinson, H. Khatun, A.D. Powell, S. Brandner, J.G. Jefferys, and J. Collinge. 2007. Targeting cellular prion protein reverses early cognitive deficits and neurophysiological dysfunction in prion-infected mice. *Neuron* 53:325-335.

Mameli, M., B. Halbout, C. Creton, D. Engblom, J.R. Parkitna, R. Spanagel, and C. Luscher. 2009. Cocaine-evoked synaptic plasticity: persistence in the VTA triggers adaptations in the NAc. *Nature neuroscience* 12:1036-U1108.

Mange, A., F. Beranger, K. Peoc'h, T. Onodera, Y. Frobert, and S. Lehmann. 2004. Alpha- and beta- cleavages of the amino-terminus of the cellular prion protein. *Biol Cell* 96:125-132.

Mannaioni, G., M.J. Marino, O. Valenti, S.F. Traynelis, and P.J. Conn. 2001. Metabotropic glutamate receptors 1 and 5 differentially regulate CA1 pyramidal cell function. *J Neurosci* 21:5925-5934.

Manson, J., J.D. West, V. Thomson, P. McBride, M.H. Kaufman, and J. Hope. 1992. The prion protein gene: a role in mouse embryogenesis? *Development* 115:117-122.

Manson, J.C., A.R. Clarke, M.L. Hooper, L. Aitchison, I. Mcconnell, and J. Hope. 1994. 129/Ola Mice Carrying a Null Mutation in Prp That Abolishes Messenger-Rna Production Are Developmentally Normal. *Mol Neurobiol* 8:121-127.

Manson, J.C., J. Hope, A.R. Clarke, A. Johnston, C. Black, and N. MacLeod. 1995. PrP gene dosage and long term potentiation [letter]. *Neurodegeneration* 4:113-114.

Manuelidis, L. 2003. Transmissible encephalopathies: speculations and realities. *Viral Immunol* 16:123-139.

Marella, M., and J. Chabry. 2004. Neurons and astrocytes respond to prion infection by inducing microglia recruitment. *J Neurosci* 24:620-627.

Marijanovic, Z., A. Caputo, V. Campana, and C. Zurzolo. 2009. Identification of an intracellular site of prion conversion. *PLoS Pathog* 5:e1000426.

Martin, J.B. 1999. Molecular basis of the neurodegenerative disorders. *N Engl J Med* 340:1970-1980.

Masilamoni, G.J., J.W. Bogenpohl, D. Alagille, K. Delevich, G. Tamagnan, J.R. Votaw, T. Wichmann, and Y. Smith. 2011. Metabotropic glutamate receptor 5 antagonist protects dopaminergic and noradrenergic neurons from degeneration in MPTP-treated monkeys. *Brain : a journal of neurology* 134:2057-2073.

Masu, M., Y. Tanabe, K. Tsuchida, R. Shigemoto, and S. Nakanishi. 1991. Sequence and Expression of a Metabotropic Glutamate Receptor. *Nature* 349:760-765.

Matsuzaki, M., N. Honkura, G.C.R. Ellis-Davies, and H. Kasai. 2004. Structural basis of long-term potentiation in single dendritic spines. *Nature* 429:761-766.

Mayer, M.L. 2006. Glutamate receptors at atomic resolution. *Nature* 440:456-462.

Mayford, M., M.E. Bach, Y.Y. Huang, L. Wang, R.D. Hawkins, and E.R. Kandel. 1996. Control of memory formation through regulated expression of a CaMKII transgene. *Science* 274:1678-1683.

McKinley, M.P., R.K. Meyer, L. Kenaga, F. Rahbar, R. Cotter, A. Serban, and S.B. Prusiner. 1991. Scrapie prion rod formation in vitro requires both detergent extraction and limited proteolysis. *J Virol* 65:1340-1351.

Medrano, A.Z., S.J. Barmada, E. Biasini, and D.A. Harris. 2008. GFP-tagged mutant prion protein forms intra-axonal aggregates in transgenic mice. *Neurobiol Dis* 31:20-32.

Meldrum, B.S. 2000. Glutamate as a neurotransmitter in the brain: Review of physiology and pathology. *J Nutr* 130:1007S-1015S.

Mermelstein, P.G. 2009. Membrane-localised oestrogen receptor alpha and beta influence neuronal activity through activation of metabotropic glutamate receptors. *Journal of neuroendocrinology* 21:257-262.

Meyer, R.K., M.P. Mckinley, K.A. Bowman, M.B. Braunfeld, R.A. Barry, and S.B. Prusiner. 1986. Separation and Properties of Cellular and Scrapie Prion Proteins. *P Natl Acad Sci USA* 83:2310-2314.

Micevych, P.E., and P.G. Mermelstein. 2008. Membrane estrogen receptors acting through metabotropic glutamate receptors: An emerging mechanism of estrogen action in brain. *Mol Neurobiol* 38:66-77.

Michalon, A., A. Bruns, C. Risterucci, M. Honer, T.M. Ballard, L. Ozmen, G. Jaeschke, J.G. Wettstein, M. von Kienlin, B. Kunnecke, and L. Lindemann. 2014. Chronic Metabotropic Glutamate Receptor 5 Inhibition Corrects Local Alterations of Brain Activity and Improves Cognitive Performance in Fragile X Mice. *Biol Psychiat* 75:189-197.

Milanese, M., F. Giribaldi, M. Melone, T. Bonifacino, I. Musante, E. Carminati, P.I.A. Rossi, L. Vergani, A. Voci, F. Conti, A. Puliti, and G. Bonanno. 2014. Knocking down metabotropic glutamate receptor 1 improves survival and disease progression in the SOD1(G93A) mouse model of amyotrophic lateral sclerosis(star). *Neurobiol Dis* 64:48-59.

Miller, S., C. Romano, and C.W. Cotman. 1995. Growth factor upregulation of a phosphoinositide-coupled metabotropic glutamate receptor in cortical astrocytes. *J Neurosci* 15:6103-6109.

Miller, S., N. Sehati, C. Romano, and C.W. Cotman. 1996. Exposure of astrocytes to thrombin reduces levels of the metabotropic glutamate receptor mGluR5. *J Neurochem* 67:1435-1447.

Mironov, A., Jr., D. Latawiec, H. Wille, E. Bouzamondo-Bernstein, G. Legname, R.A. Williamson, D. Burton, S.J. DeArmond, S.B. Prusiner, and P.J. Peters. 2003. Cytosolic prion protein in neurons. *J Neurosci* 23:7183-7193.

Montana, M.C., L.F. Cavallone, K.K. Stubbert, A.D. Stefanescu, E.D. Kharasch, and R.W.t. Gereau. 2009. The metabotropic glutamate receptor subtype 5 antagonist fenobam is analgesic and has improved in vivo selectivity compared with the prototypical antagonist 2-methyl-6-(phenylethynyl)-pyridine. *J Pharmacol Exp Ther* 330:834-843.

Montrasio, F., R. Frigg, M. Glatzel, M.A. Klein, F. Mackay, A. Aguzzi, and C. Weissmann. 2000. Impaired prion replication in spleens of mice lacking functional follicular dendritic cells. *Science* 288:1257-1259.

Moore, R.C., I.Y. Lee, G.L. Silverman, P.M. Harrison, R. Strome, C. Heinrich, A. Karunaratne, S.H. Pasternak, M.A. Chishti, Y. Liang, P. Mastrangelo, K. Wang, A.F. Smit, S. Katamine, G.A. Carlson, F.E. Cohen, S.B. Prusiner, D.W. Melton, P. Tremblay, L.E. Hood, and D. Westaway. 1999. Ataxia in prion protein (PrP)-deficient mice is associated with upregulation of the novel PrP-like protein doppel. *J Mol Biol* 292:797-817.

Moore, R.C., P. Mastrangelo, E. Bouzamondo, C. Heinrich, G. Legname, S.B. Prusiner, L. Hood, D. Westaway, S.J. DeArmond, and P. Tremblay. 2001. Doppel-induced cerebellar degeneration in transgenic mice. *Proc Natl Acad Sci U S A* 98:15288-15293.

Moreno, J.A., M. Halliday, C. Molloy, H. Radford, N. Verity, J.M. Axten, C.A. Ortori, A.E. Willis, P.M. Fischer, D.A. Barrett, and G.R. Mallucci. 2013. Oral treatment targeting the unfolded protein response prevents neurodegeneration and clinical disease in prion-infected mice. *Sci Transl Med* 5:206ra138.

Moreno, J.A., H. Radford, D. Peretti, J.R. Steinert, N. Verity, M.G. Martin, M. Halliday, J. Morgan, D. Dinsdale, C.A. Ortori, D.A. Barrett, P. Tsaytler, A. Bertolotti, A.E. Willis, M. Bushell, and G.R. Mallucci. 2012. Sustained translational repression by eIF2 alpha-P mediates prion neurodegeneration. *Nature* 485:507-U119.

Moser, M., R.J. Colello, U. Pott, and B. Oesch. 1995. Developmental expression of the prion protein gene in glial cells. *Neuron* 14:509-517.

Mouillet-Richard, S., M. Ermonval, C. Chebassier, J.L. Laplanche, S. Lehmann, J.M. Launay, and O. Kellermann. 2000. Signal transduction through prion protein. *Science* 289:1925-1928.

Moya, K.L., R. Hassig, C. Creminon, I. Laffont, and L. Di Giamberardino. 2004. Enhanced detection and retrograde axonal transport of PrPc in peripheral nerve. *J Neurochem* 88:155-160.

Muramoto, T., S.J. Dearmond, M. Scott, G.C. Telling, F.E. Cohen, and S.B. Prusiner. 1997. Heritable Disorder Resembling Neuronal Storage Disease In Mice Expressing Prion Protein With Deletion Of an Alpha-Helix. *Nature Medicine* 3:750-755.

Muto, T., D. Tsuchiya, K. Morikawa, and H. Jingami. 2007. Structures of the extracellular regions of the group II/III metabotropic glutamate receptors. *Proceedings of the National Academy of Sciences of the United States of America* 104:3759-3764.

Nakanishi, S., and M. Masu. 1994. Molecular Diversity and Functions of Glutamate Receptors. *Annu Rev Bioph Biom* 23:319-348.

Naslavsky, N., R. Stein, A. Yanai, G. Friedlander, and A. Taraboulos. 1997. Characterization Of Detergent-Insoluble Complexes Containing the Cellular Prion Protein and Its Scrapie Isoform. *Journal of Biological Chemistry* 272:6324-6331.

Nazor, K.E., F. Kuhn, T. Seward, M. Green, D. Zwald, M. Purro, J. Schmid, K. Biffiger, A.M. Power, B. Oesch, A.J. Raeber, and G.C. Telling. 2005. Immunodetection of disease-associated mutant PrP, which accelerates disease in GSS transgenic mice. *Embo J* 24:2472-2480.

Nelson, R., M.R. Sawaya, M. Balbirnie, A.O. Madsen, C. Riekel, R. Grothe, and D. Eisenberg. 2005. Structure of the cross-beta spine of amyloid-like fibrils. *Nature* 435:773-778.

Nicoletti, F., J. Bockaert, G.L. Collingridge, P.J. Conn, F. Ferraguti, D.D. Schoepp, J.T. Wroblewski, and J.P. Pin. 2011. Metabotropic glutamate receptors: from the workbench to the bedside. *Neuropharmacology* 60:1017-1041.

Nishida, N., P. Tremblay, T. Sugimoto, K. Shigematsu, S. Shirabe, C. Petromilli, S.P. Erpel, R. Nakaoke, R. Atarashi, T. Houtani, M. Torchia, S. Sakaguchi, S.J. DeArmond, S.B. Prusiner, and S. Katamine. 1999. A mouse prion protein transgene rescues mice deficient for the prion protein gene from purkinje cell degeneration and demyelination. *Lab Invest* 79:689-697.

Niswender, C.M., and P.J. Conn. 2010. Metabotropic glutamate receptors: physiology, pharmacology, and disease. *Annual review of pharmacology and toxicology* 50:295-322.

Novitskaya, V., O.V. Bocharova, I. Bronstein, and I.V. Baskakov. 2006. Amyloid fibrils of mammalian prion protein are highly toxic to cultured cells and primary neurons. *J Biol Chem* 281:13828-13836.

Nuvolone, M., M. Hermann, S. Sorce, G. Russo, C. Tiberi, P. Schwarz, E. Minikel, D. Sanoudou, P. Pelczar, and A. Aguzzi. 2016. Strictly co-isogenic C57BL/6J-Prnp(-/-) mice: A rigorous resource for prion science. *J Exp Med* 213:313-327.

Oesch, B., D.B. Teplow, N. Stahl, D. Serban, L.E. Hood, and S.B. Prusiner. 1990. Identification of cellular proteins binding to the scrapie prion protein. *Biochemistry* 29:5848-5855.

Ohsawa, N., C.H. Song, A. Suzuki, H. Furuoka, R. Hasebe, and M. Horiuchi. 2013. Therapeutic effect of peripheral administration of an anti-prion protein antibody on mice infected with prions. *Microbiol Immunol* 57:288-297.

Olney, J.W. 1989. Excitotoxicity and N-Methyl-D-Aspartate Receptors. *Drug Develop Res* 17:299-319.

Olney, J.W., M.T. Price, L. Samson, and J. Labruyere. 1986. The Role of Specific Ions in Glutamate Neurotoxicity. *Neurosci Lett* 65:65-71.

Olney, J.W., C.F. Zorumski, G.R. Stewart, M.T. Price, G.J. Wang, and J. Labruyere. 1990. Excitotoxicity of L-Dopa and 6-Oh-Dopa - Implications for Parkinsons and Huntingtons Diseases. *Exp Neurol* 108:269-272.

Ostapchenko, V.G., F.H. Beraldo, A.L. Guimaraes, S. Mishra, M. Guzman, J. Fan, V.R. Martins, V.F. Prado, and M.A. Prado. 2013. Increased prion protein processing and

expression of metabotropic glutamate receptor 1 in a mouse model of Alzheimer's disease. *Journal of neurochemistry* 127:415-425.

Pan, K.M., M. Baldwin, J. Nguyen, M. Gasset, A. Serban, D. Groth, I. Mehlhorn, Z.W. Huang, R.J. Fletterick, F.E. Cohen, and S.B. Prusiner. 1993. Conversion of Alpha-Helices into Beta-Sheets Features in the Formation of the Scrapie Prion Proteins. *P Natl Acad Sci USA* 90:10962-10966.

Paoletti, P., C. Bellone, and Q. Zhou. 2013. NMDA receptor subunit diversity: impact on receptor properties, synaptic plasticity and disease. *Nat Rev Neurosci* 14:383-400.

Parkin, E.T., N.T. Watt, A.J. Turner, and N.M. Hooper. 2004. Dual mechanisms for shedding of the cellular prion protein. *J Biol Chem* 279:11170-11178.

Peggion, C., A. Bertoli, and M.C. Sorgato. 2011. Possible role for Ca2+ in the pathophysiology of the prion protein? *BioFactors* 37:241-249.

Perry, V.H., and S. Gordon. 1988. Macrophages and microglia in the nervous system. *Trends Neurosci* 11:273-277.

Peters, P.J., A. Mironov, Jr., D. Peretz, E. van Donselaar, E. Leclerc, S. Erpel, S.J. DeArmond, D.R. Burton, R.A. Williamson, M. Vey, and S.B. Prusiner. 2003. Trafficking of prion proteins through a caveolae-mediated endosomal pathway. *J Cell Biol* 162:703-717.

Petralia, R.S., Y.X. Wang, and R.J. Wenthold. 1994a. The Nmda Receptor Subunits Nr2a and Nr2b Show Histological and Ultrastructural-Localization Patterns Similar to Those of Nr1. *J Neurosci* 14:6102-6120.

Petralia, R.S., N. Yokotani, and R.J. Wenthold. 1994b. Light and Electron-Microscope Distribution of the Nmda Receptor Subunit Nmdar1 in the Rat Nervous-System Using a Selective Antipeptide Antibody. *J Neurosci* 14:667-696.

Peyrin, J.M., C.I. Lasmezas, S. Haik, F. Tagliavini, M. Salmona, A. Williams, D. Richie, J.P. Deslys, and D. Dormont. 1999. Microglial cells respond to amyloidogenic PrP peptide by the production of inflammatory cytokines. *Neuroreport* 10:723-729.

Pietri, M., A. Caprini, S. Mouillet-Richard, E. Pradines, M. Ermonval, J. Grassi, O. Kellermann, and B. Schneider. 2006. Overstimulation of PrPC signaling pathways by prion peptide 106-126 causes oxidative injury of bioaminergic neuronal cells. *J Biol Chem* 281:28470-28479.

Pin, J.P., T. Galvez, and L. Prezeau. 2003. Evolution, structure, and activation mechanism of family 3/C G-protein-coupled receptors. *Pharmacol Therapeut* 98:325-354.

Pinheiro, P.S., F. Lanore, J. Veran, J. Artinian, C. Blanchet, V. Crepel, D. Perrais, and C. Mulle. 2013. Selective Block of Postsynaptic Kainate Receptors Reveals Their Function at Hippocampal Mossy Fiber Synapses. *Cereb Cortex* 23:323-331.

Pisani, A., P. Gubellini, P. Bonsi, F. Conquet, B. Picconi, D. Centonze, G. Bernardi, and P. Calabresi. 2001. Metabotropic glutamate receptor 5 mediates the potentiation of N-methyl-D-aspartate responses in medium spiny striatal neurons. *Neuroscience* 106:579-587.

Polymenidou, M., F.L. Heppner, E.C. Pellicioli, E. Urich, G. Miele, N. Braun, F. Wopfner, H.M. Schatzl, B. Becher, and A. Aguzzi. 2004. Humoral immune response to native eukaryotic prion protein correlates with anti-prion protection. *Proceedings of the National Academy of Sciences of the United States of America* 101:14670-14676.

Polymenidou, M., R. Moos, M. Scott, C. Sigurdson, Y.Z. Shi, B. Yajima, I. Hafner-Bratkovic, R. Jerala, S. Hornemann, K. Wuthrich, A. Bellon, M. Vey, G. Garen, M.N. James, N. Kav, and A. Aguzzi. 2008. The POM monoclonals: a comprehensive set of antibodies to non-overlapping prion protein epitopes. *PloS one* 3:e3872.

Pop, A.S., B. Gomez-Mancilla, G. Neri, R. Willemsen, and F. Gasparini. 2014. Fragile X syndrome: a preclinical review on metabotropic glutamate receptor 5 (mGluR5) antagonists and drug development. *Psychopharmacology* 231:1217-1226.

Portera-Cailliau, C. 2012. Which Comes First in Fragile X Syndrome, Dendritic Spine Dysgenesis or Defects in Circuit Plasticity? *Neuroscientist* 18:28-44.

Powell, A.D., E.C. Toescu, J. Collinge, and J.G. Jefferys. 2008. Alterations in Ca2+-buffering in prion-null mice: association with reduced afterhyperpolarizations in CA1 hippocampal neurons. *J Neurosci* 28:3877-3886.

Prestori, F., P. Rossi, B. Bearzatto, J. Laine, D. Necchi, S. Diwakar, S.N. Schiffmann, H. Axelrad, and E. D'Angelo. 2008. Altered neuron excitability and synaptic plasticity in the cerebellar granular layer of juvenile prion protein knock-out mice with impaired motor control. *J Neurosci* 28:7091-7103.

Price, D.L., E. Rockenstein, K. Ubhi, V. Phung, N. MacLean-Lewis, D. Askay, A. Cartier, B. Spencer, C. Patrick, P. Desplats, M.H. Ellisman, and E. Masliah. 2010. Alterations in mGluR5 expression and signaling in Lewy body disease and in transgenic models of alpha-synucleinopathy--implications for excitotoxicity. *Plos One* 5:e14020.

Prusiner, S.B. 1982. Novel proteinaceous infectious particles cause scrapie. *Science* 216:136-144.

Prusiner, S.B. 1994. Neurodegeneration in humans caused by prions. [Review] [114 refs]. *Western Journal of Medicine* 161:264-272.

Prusiner, S.B. 1998. Prions. *P Natl Acad Sci USA* 95:13363-13383.

Prusiner, S.B., D.C. Bolton, D.F. Groth, K.A. Bowman, S.P. Cochran, and M.P. Mckinley. 1982. Further Purification and Characterization of Scrapie Prions. *Biochemistry* 21:6942-6950.

Pshenichkin, S., M. Dolinska, M. Klauzinska, V. Luchenko, E. Grajkowska, and J.T. Wroblewski. 2008. Dual neurotoxic and neuroprotective role of metabotropic glutamate receptor 1 in conditions of trophic deprivation - Possible role as a dependence receptor. *Neuropharmacology* 55:500-508.

Pshenichkin, S., A.C. Emery, G.R. Takoudjou, J. DiRaddo, H. Hathaway, E. Grajkowska, B.B. Wolfe, and J.T. Wroblewski. 2011. Neuroprotective and Neurotoxic Signaling of mGlu1 Receptors. *Current neuropharmacology* 9:54-55.

Puckett, C., P. Concannon, C. Casey, and L. Hood. 1991a. Genomic Structure of the Human Prion Protein Gene. *Am J Hum Genet* 49:320-329.

Puckett, C., P. Concannon, C. Casey, and L. Hood. 1991b. Genomic structure of the human prion protein gene [see comments]. *Am J Hum Genet* 49:320-329.

Purgert, C.A., Y. Izumi, Y.J.I. Jong, V. Kumar, C.F. Zorumski, and K.L. O'Malley. 2014. Intracellular mGluR5 Can Mediate Synaptic Plasticity in the Hippocampus. *J Neurosci* 34:4589-4598.

Rachidi, W., D. Vilette, P. Guiraud, M. Arlotto, J. Riondel, H. Laude, S. Lehmann, and A. Favier. 2003. Expression of prion protein increases cellular copper binding and antioxidant enzyme activities but not copper delivery. *J Biol Chem* 278:9064-9072.

Radovanovic, I., N. Braun, O.T. Giger, K. Mertz, G. Miele, M. Prinz, B. Navarro, and A. Aguzzi. 2005. Truncated prion protein and Doppel are myelinotoxic in the absence of oligodendrocytic PrPC. *J Neurosci* 25:4879-4888.

Raeber, A.J., R.E. Race, S. Brandner, S.A. Priola, A. Sailer, R.A. Bessen, L. Mucke, J. Manson, A. Aguzzi, M.B. Oldstone, C. Weissmann, and B. Chesebro. 1997. Astrocyte-specific expression of hamster prion protein (PrP) renders PrP knockout mice susceptible to hamster scrapie. *The EMBO journal* 16:6057-6065.

Rangel, A., F. Burgaya, R. Gavin, E. Soriano, A. Aguzzi, and J.A. Del Rio. 2007. Enhanced susceptibility of Prnp-deficient mice to kainate-induced seizures, neuronal apoptosis, and death: Role of AMPA/kainate receptors. *J Neurosci Res* 85:2741-2755.

Rangel, A., N. Madronal, A. Gruart, R. Gavin, F. Llorens, L. Sumoy, J.M. Torres, J.M. Delgado-Garcia, and J.A. Del Rio. 2009. Regulation of GABA(A) and glutamate receptor expression, synaptic facilitation and long-term potentiation in the hippocampus of prion mutant mice. *PLoS One* 4:e7592.

Ratte, S., S.A. Prescott, J. Collinge, and J.G. Jefferys. 2008. Hippocampal bursts caused by changes in NMDA receptor-dependent excitation in a mouse model of variant CJD. *Neurobiol Dis* 32:96-104.

Raymond, C.S., and P. Soriano. 2007. High-efficiency FLP and PhiC31 site-specific recombination in mammalian cells. *PloS one* 2:e162.

Raymond, L.A., V.M. Andre, C. Cepeda, C.M. Gladding, A.J. Milnerwood, and M.S. Levine. 2011. Pathophysiology of Huntington's Disease: Time-Dependent Alterations in Synaptic and Receptor Function. *Neuroscience* 198:252-273.

Reder, A.T., A.S. Mednick, P. Brown, J.P. Spire, E. Van Cauter, R.L. Wollmann, L. Cervenakova, L.G. Goldfarb, A. Garay, F. Ovsiew, and et al. 1995. Clinical and genetic studies of fatal familial insomnia. *Neurology* 45:1068-1075.

Reimann, R.R., T. Sonati, S. Hornemann, U.S. Herrmann, M. Arand, S. Hawke, and A. Aguzzi. 2016. Differential Toxicity of Antibodies to the Prion Protein. *PLoS pathogens* 12:e1005401.

Renner, M., P.N. Lacor, P.T. Velasco, J.A. Xu, A. Contractor, W.L. Klein, and A. Triller. 2010. Deleterious Effects of Amyloid beta Oligomers Acting as an Extracellular Scaffold for mGluR5. *Neuron* 66:739-754.

Rieger, R., F. Edenhofer, C.I. Lasmezas, and S. Weiss. 1997. The human 37-kDa laminin receptor precursor interacts with the prion protein in eukaryotic cells. *Nat Med* 3:1383-1388.

Rockman, M., E. Troisi, and J. Hines. 2014. Ectopic expression studies of the J-protein Swa2 and its potential role in yeast prion propagation. *Faseb J* 28:

Rodriguez, A., M. Freixes, E. Dalfo, M. Martin, B. Puig, and I. Ferrer. 2005. Metabotropic glutamate receptor/phospholipase C pathway: a vulnerable target to Creutzfeldt-Jakob disease in the cerebral cortex. *Neuroscience* 131:825-832.

Rodriguez, A., M. Martin, J.L. Albasanz, M. Barrachina, J.C. Espinosa, J.M. Torres, and I. Ferrer. 2006. Group I mGluR signaling in BSE-infected bovine-PrP transgenic mice. *Neuroscience letters* 410:115-120.

Roffe, M., F.H. Beraldo, R. Bester, M. Nunziante, C. Bach, G. Mancini, S. Gilch, I. Vorberg, B.A. Castilho, V.R. Martins, and G.N. Hajj. 2010. Prion protein interaction with stress-inducible protein 1 enhances neuronal protein synthesis via mTOR. *Proc Natl Acad Sci U S A* 107:13147-13152.

Romano, C., A.N. van den Pol, and K.L. O'Malley. 1996a. Enhanced early developmental expression of the metabotropic glutamate receptor mGluR5 in rat brain: protein, mRNA splice variants, and regional distribution. *The Journal of comparative neurology* 367:403-412.

Romano, C., W.L. Yang, and K.L. OMalley. 1996b. Metabotropic glutamate receptor 5 is a disulfide-linked dimer. *J Biol Chem* 271:28612-28616.

Rondard, P., J.F. Liu, S.L. Huang, F. Malhaire, C. Vol, A. Pinault, G. Labesse, and J.P. Pin. 2006. Coupling of agonist binding to effector domain activation in metabotropic glutamate-like receptors. *J Biol Chem* 281:24653-24661.

Ronesi, J.A., and K.M. Huber. 2008. Homer interactions are necessary for metabotropic glutamate receptor-induced long-term depression and translational activation. *J Neurosci* 28:543-547.

Rong, R., J.Y. Ahn, H. Huang, E. Nagata, D. Kalman, J.A. Kapp, J. Tu, P.F. Worley, S.H. Snyder, and K. Ye. 2003. PI3 kinase enhancer-Homer complex couples mGluRI to PI3 kinase, preventing neuronal apoptosis. *Nature neuroscience* 6:1153-1161.

Rossi, D., L. Brambilla, C.F. Valori, C. Roncoroni, A. Crugnola, T. Yokota, D.E. Bredesen, and A. Volterra. 2008. Focal degeneration of astrocytes in amyotrophic lateral sclerosis. *Cell death and differentiation* 15:1691-1700.

Rossi, D., A. Cozzio, E. Flechsig, M.A. Klein, T. Rulicke, A. Aguzzi, and C. Weissmann. 2001. Onset of ataxia and Purkinje cell loss in PrP null mice inversely correlated with Dpl level in brain. *Embo J* 20:694-702.

Rothman, S.M., and J.W. Olney. 1995. Excitotoxicity and the Nmda Receptor - Still Lethal after 8 Years. *Trends Neurosci* 18:57-58.

Roucou, X., and A.C. LeBlanc. 2005. Cellular prion protein neuroprotective function: implications in prion diseases. *J Mol Med* 83:3-11.

Saborio, G.P., B. Permanne, and C. Soto. 2001. Sensitive detection of pathological prion protein by cyclic amplification of protein misfolding. *Nature* 411:810-813.

Sachs, A.J., J.K. Schwendinger, A.W. Yang, N.B. Haider, and A.M. Nystuen. 2007. The mouse mutants recoil wobbler and nmf373 represent a series of Grm1 mutations. *Mammalian genome : official journal of the International Mammalian Genome Society* 18:749-756.

Safar, J., H. Wille, V. Itri, D. Groth, H. Serban, M. Torchia, F.E. Cohen, and S.B. Prusiner. 1998. Eight prion strains have PrP(Sc) molecules with different conformations [see comments]. *Nat Med* 4:1157-1165.

Sah, P., and P. Davies. 2000. Calcium-activated potassium currents in mammalian neurons. *Clin Exp Pharmacol P* 27:657-663.

Sakaguchi, S., S. Katamine, N. Nishida, R. Moriuchi, K. Shigematsu, T. Sugimoto, A. Nakatani, Y. Kataoka, T. Houtani, S. Shirabe, H. Okada, S. Hasegawa, T. Miyamoto, and T. Noda. 1996. Loss of cerebellar Purkinje cells in aged mice homozygous for a disrupted Prp gene. *Nature* 380:528-531.

Sakurai-Yamashita, Y., S. Sakaguchi, D. Yoshikawa, N. Okimura, Y. Masuda, S. Katamine, and M. Niwa. 2005. Female-specific neuroprotection against transient brain ischemia observed in mice devoid of prion protein is abolished by ectopic expression of prion protein-like protein. *Neuroscience* 136:281-287.

Salinska, E., and A. Stafiej. 2003. Metabotropic glutamate receptors (mGluRs) are involved in early phase of memory formation: possible role of modulation of glutamate release. *Neurochem Int* 43:469-474.

Sanchez-Juan, P., M.T. Bishop, G.G. Kovacs, M. Calero, Y.S. Aulchenko, A. Ladogana, A. Boyd, V. Lewis, C. Ponto, O. Calero, A. Poleggi, A. Carracedo, S.J. van der Lee, T. Strobel, F. Rivadeneira, A. Hofman, S. Haik, O. Combarros, J. Berciano, A.G. Uitterlinden, S.J. Collins, H. Budka, J.P. Brandel, J.L. Laplanche, M. Pocchiari, I. Zerr, R.S. Knight, R.G. Will, and C.M. van Duijn. 2014. A genome wide association study links glutamate receptor pathway to sporadic creutzfeldt-jakob disease risk. *PloS one* 10:e0123654.

Sandberg, M.K., P. Wallen, M.A. Wikstrom, and K. Kristensson. 2004. Scrapie-infected GT1-1 cells show impaired function of voltage-gated N-type calcium channels (Ca-nu 2.2) which is ameliorated by quinacrine treatment. *Neurobiology of disease* 15:143-151.

Santuccione, A., V. Sytnyk, I. Leshchyns'ka, and M. Schachner. 2005. Prion protein recruits its neuronal receptor NCAM to lipid rafts to activate p59fyn and to enhance neurite outgrowth. *J Cell Biol* 169:341-354.

Scartabelli, T., E. Gerace, E. Landucci, F. Moroni, and D.E. Pellegrini-Giampietro. 2008. Neuroprotection by group I mGlu receptors in a rat hippocampal slice model of cerebral ischemia is associated with the PI3K-Akt signaling pathway: A novel postconditioning strategy? *Neuropharmacology* 55:509-516.

Schaefer, T.L., M.H. Davenport, and C.A. Erickson. 2015. Emerging pharmacologic treatment options for fragile X syndrome. *The application of clinical genetics* 8:75-93.

Scharf, S.H., G. Jaeschke, J.G. Wettsteinl, and L. Lindemann. 2015. Metabotropic glutamate receptor 5 as drug target for Fragile X syndrome. *Curr Opin Pharmacol* 20:124-134.

Schatzl, H.M., F. Wopfner, S. Gilch, A. Vonbrunn, and G. Jager. 1997. Is Codon 129 Of Prion Protein Polymorphic In Human Beings But Not In Animals. *Lancet* 349:1603-1604.

Schmitt-Ulms, G., G. Legname, M.A. Baldwin, H.L. Ball, N. Bradon, P.J. Bosque, K.L. Crossin, G.M. Edelman, S.J. DeArmond, F.E. Cohen, and S.B. Prusiner. 2001. Binding of neural cell adhesion molecules (N-CAMs) to the cellular prion protein. *Journal of molecular biology* 314:1209-1225.

Schneider, B., V. Mutel, M. Pietri, M. Ermonval, S. Mouillet-Richard, and O. Kellermann. 2003a. NADPH oxidase and extracellular regulated kinases 1/2 are targets of prion protein signaling in neuronal and nonneuronal cells. *Proceedings of the National Academy of Sciences of the United States of America* 100:13326-13331.

Schneider, B., V. Mutel, M. Pietri, M. Ermonval, S. Mouillet-Richard, and O. Kellermann. 2003b. NADPH oxidase and extracellular regulated kinases 1/2 are targets of prion protein signaling in neuronal and nonneuronal cells. *Proc Natl Acad Sci U S A* 100:13326-13331.

Seebahn, A., H. Sticht, and R. Enz. 2013. Expression, Purification, and Structural Analysis of Intracellular C-Termini from Metabotropic Glutamate Receptors. *Method Enzymol* 520:257-279.

Seeburg, P.H. 1993. The Tins Tips Lecture - the Molecular-Biology of Mammalian Glutamate-Receptor Channels. *Trends Neurosci* 16:359-365.

Senatore, A., S. Colleoni, C. Verderio, E. Restelli, R. Morini, S.B. Condliffe, I. Bertani, S. Mantovani, M. Canovi, E. Micotti, G. Forloni, A.C. Dolphin, M. Matteoli, M. Gobbi, and R. Chiesa. 2012. Mutant PrP suppresses glutamatergic neurotransmission in cerebellar granule neurons by impairing membrane delivery of VGCC alpha(2)delta-1 Subunit. *Neuron* 74:300-313.

Serio, T.R., A.G. Cashikar, A.S. Kowal, G.J. Sawicki, J.J. Moslehi, L. Serpell, M.F. Arnsdorf, and S.L. Lindquist. 2000. Nucleated conformational conversion and the replication of conformational information by a prion determinant. *Science* 289:1317-1321.

Shelton, M.K., and K.D. McCarthy. 1999. Mature hippocampal astrocytes exhibit functional metabotropic and ionotropic glutamate receptors in situ. *Glia* 26:1-11.

Shepherd, J.D., and R.L. Huganirl. 2007. The cell biology of synaptic plasticity: AMPA receptor trafficking. *Annu Rev Cell Dev Bi* 23:613-643.

Shigemoto, R., S. Nakanishi, and N. Mizuno. 1992. Distribution of the mRNA for a metabotropic glutamate receptor (mGluR1) in the central nervous system: an in situ hybridization study in adult and developing rat. *J Comp Neurol* 322:121-135.

Shiraishi, Y., A. Mizutani, S. Yuasa, K. Mikoshiba, and T. Furuichi. 2004. Differential expression of Homer family proteins in the developing mouse brain. *J Comp Neurol* 473:582-599.

Shmerling, D., I. Hegyi, M. Fischer, T. Blattler, S. Brandner, J. Gotz, T. Rulicke, E. Flechsig, A. Cozzio, C. von Mering, C. Hangartner, A. Aguzzi, and C. Weissmann. 1998. Expression of amino-terminally truncated PrP in the mouse leading to ataxia and specific cerebellar lesions. *Cell* 93:203-214.

Shrivastava, A.N., J.M. Kowalewski, M. Renner, L. Bousset, A. Koulakoff, R. Melki, C. Giaume, and A. Triller. 2013. beta-amyloid and ATP-induced diffusional trapping of astrocyte and neuronal metabotropic glutamate type-5 receptors. *Glia* 61:1673-1686.

Shrivastava, A.N., V. Redeker, N. Fritz, L. Pieri, L.G. Almeida, M. Spolidoro, T. Liebmann, L. Bousset, M. Renner, C. Lena, A. Aperia, R. Melki, and A. Triller. 2015. alpha-synuclein assemblies sequester neuronal alpha 3-Na+/K+-ATPase and impair Na+ gradient. *Embo J* 34:2408-2423.

Shyng, S.L., M.T. Huber, and D.A. Harris. 1993. A prion protein cycles between the cell surface and an endocytic compartment in cultured neuroblastoma cells. *J Biol Chem* 268:15922-15928.

Sigurdsson, E.M., M.S. Sy, R.L. Li, H. Scholtzova, R.J. Kascsak, R. Kascsak, R. Carp, H.C. Meeker, B. Frangione, and T. Wisniewski. 2003. Anti-prion antibodies for prophylaxis following prion exposure in mice. *Neurosci Lett* 336:185-187.

Silveira, J.R., G.J. Raymond, A.G. Hughson, R.E. Race, V.L. Sim, S.F. Hayes, and B. Caughey. 2005. The most infectious prion protein particles. *Nature* 437:257-261.

Simoneau, S., H. Rezaei, N. Sales, G. Kaiser-Schulz, M. Lefebvre-Roque, C. Vidal, J.G. Fournier, J. Comte, F. Wopfner, J. Grosclaude, H. Schatzl, and C.I. Lasmezas. 2007. In vitro and in vivo neurotoxicity of prion protein oligomers. *PLoS pathogens* 3:e125.

Simons, K., and D. Toomre. 2000. Lipid rafts and signal transduction. *Nat Rev Mol Cell Biol* 1:31-39.

Siso, S., B. Puig, R. Varea, E. Vidal, C. Acin, M. Prinz, F. Montrasio, J. Badiola, A. Aguzzi, M. Pumarola, and I. Ferrer. 2002. Abnormal synaptic protein expression and cell death in murine scrapie. *Acta Neuropathol* 103:615-626.

Sistiaga, A., and J. Sanchez-Prieto. 1998. Functional switch from facilitation to inhibition in the control of glutamate release by group I metabotropic glutamate receptors. *Eur J Neurosci* 10:174-174.

Solforosi, L., J.R. Criado, D.B. McGavern, S. Wirz, M. Sanchez-Alavez, S. Sugama, L.A. DeGiorgio, B.T. Volpe, E. Wiseman, G. Abalos, E. Masliah, D. Gilden, M.B. Oldstone, B. Conti, and R.A. Williamson. 2004. Cross-linking cellular prion protein triggers neuronal apoptosis in vivo. *Science* 303:1514-1516.

Sonati, T., R.R. Reimann, J. Falsig, P.K. Baral, T. O'Connor, S. Hornemann, S. Yaganoglu, B. Li, U.S. Herrmann, B. Wieland, M. Swayampakula, M.H. Rahman, D. Das, N. Kav, R. Riek, P.P. Liberski, M.N. James, and A. Aguzzi. 2013. The toxicity of antiprion antibodies is mediated by the flexible tail of the prion protein. *Nature* 501:102-106.

Song, C.H., H. Furuoka, C.L. Kim, M. Ogino, A. Suzuki, R. Hasebe, and M. Horiuchi. 2008. Effect of intraventricular infusion of anti-prion protein monoclonal antibodies on disease progression in prion-infected mice. *J Gen Virol* 89:1533-1544.

Sorce, S., M. Nuvolone, A. Keller, J. Falsig, A. Varol, P. Schwarz, M. Bieri, H. Budka, and A. Aguzzi. 2014. The Role of the NADPH Oxidase NOX2 in Prion Pathogenesis. *PLoS pathogens* 10:

Sorgato, M.C., C. Peggion, and A. Bertoli. 2009. Is, indeed, the prion protein a Harlequin servant of "many" masters? *Prion* 3:202-205.

Soto, C., and N. Satani. 2011. The intricate mechanisms of neurodegeneration in prion diseases. *Trends Mol Med* 17:14-24.

Spampinato, S.F., G. Molinaro, S. Merlo, L. Iacovelli, F. Caraci, G. Battaglia, F. Nicoletti, V. Bruno, and M.A. Sortino. 2012. Estrogen receptors and type 1 metabotropic glutamate receptors are interdependent in protecting cortical neurons against beta-amyloid toxicity. *Molecular pharmacology* 81:12-20.

Sparkes, R.S., M. Simon, V.H. Cohn, R.E.K. Fournier, J. Lem, I. Klisak, C. Heinzmann, C. Blatt, M. Lucero, T. Mohandas, S.J. Dearmond, D. Westaway, S.B. Prusiner, and L.P. Weiner. 1986. Assignment of the Human and Mouse Prion Protein Genes to Homologous Chromosomes. *P Natl Acad Sci USA* 83:7358-7362.

Spielhaupter, C., and H.M. Schatzl. 2001. PrPC directly interacts with proteins involved in signaling pathways. *J Biol Chem* 276:44604-44612.

Spudich, A., R. Frigg, E. Kilic, U. Kilic, B. Oesch, A. Raeber, C.L. Bassetti, and D.M. Hermann. 2005. Aggravation of ischemic brain injury by prion protein deficiency: role of ERK-1/-2 and STAT-1. *Neurobiol Dis* 20:442-449.

Stahl, N., M.A. Baldwin, D.B. Teplow, L. Hood, B.W. Gibson, A.L. Burlingame, and S.B. Prusiner. 1993. Structural Studies of the Scrapie Prion Protein Using Mass-Spectrometry and Amino-Acid Sequencing. *Biochemistry* 32:1991-2002.

Stahl, N., D.R. Borchelt, K. Hsiao, and S.B. Prusiner. 1987. Scrapie prion protein contains a phosphatidylinositol glycolipid. *Cell* 51:229-240.

Steele, A.D., C. Hetz, C.H. Yi, W.S. Jackson, A.W. Borkowski, J. Yuan, R.H. Wollmann, and S. Lindquist. 2007. Prion pathogenesis is independent of caspase-12. *Prion* 1:243-247.

Stewart, R.S., and D.A. Harris. 2001. Most pathogenic mutations do not alter the membrane topology of the prion protein. *J Biol Chem* 276:2212-2220.

Sulzer, D., and D.J. Surmeier. 2013. Neuronal vulnerability, pathogenesis, and Parkinson's disease. *Mov Disord* 28:715-724.

Surmeier, D.J., J.N. Guzman, J. Sanchez-Padilla, and J.A. Goldberg. 2010. What causes the death of dopaminergic neurons in Parkinson's disease? *Prog Brain Res* 183:59-77.

Taraboulos, A., A.J. Raeber, D.R. Borchelt, D. Serban, and S.B. Prusiner. 1992. Synthesis and trafficking of prion proteins in cultured cells. *Mol Biol Cell* 3:851-863.

Taraboulos, A., M. Scott, A. Semenov, D. Avrahami, L. Laszlo, S.B. Prusiner, and D. Avraham. 1995. Cholesterol depletion and modification of COOH-terminal targeting sequence of the prion protein inhibit formation of the scrapie isoform [published erratum appears in J Cell Biol 1995 Jul;130(2):501]. *J Cell Biol* 129:121-132.

Taylor, D.R., E.T. Parkin, S.L. Cocklin, J.R. Ault, A.E. Ashcroft, A.J. Turner, and N.M. Hooper. 2009. Role of ADAMs in the ectodomain shedding and conformational conversion of the prion protein. *J Biol Chem* 284:22590-22600.

Taylor, D.R., N.T. Watt, W.S. Perera, and N.M. Hooper. 2005. Assigning functions to distinct regions of the N-terminus of the prion protein that are involved in its copper-stimulated, clathrin-dependent endocytosis. *J Cell Sci* 118:5141-5153.

Telling, G.C., T. Haga, M. Torchia, P. Tremblay, S.J. Dearmond, and S.B. Prusiner. 1996. Interactions Between Wild-Type and Mutant Prion Proteins Modulate Neurodegeneration Transgenic Mice. *Genes & Development* 10:1736-1750.

Telling, G.C., M. Scott, J. Mastrianni, R. Gabizon, M. Torchia, F.E. Cohen, S.J. Dearmond, and S.B. Prusiner. 1995. Prion Propagation in Mice Expressing Human and Chimeric Prp Transgenes Implicates the Interaction of Cellular Prp with Another Protein. *Cell* 83:79-90.

Thackray, A.M., R. Knight, S.J. Haswell, R. Bujdoso, and D.R. Brown. 2002. Metal imbalance and compromised antioxidant function are early changes in prion disease. *Biochem J* 362:253-258.

Thellung, S., T. Florio, V. Villa, A. Corsaro, S. Arena, C. Amico, M. Robello, M. Salmona, G. Forloni, O. Bugiani, F. Tagliavini, and G. Schettini. 2000. Apoptotic cell death and impairment of L-type voltage-sensitive calcium channel activity in rat cerebellar granule cells treated with the prion protein fragment 106-126. *Neurobiology of disease* 7:299-309.

Toms, N.J., D.E. Jane, M.C. Kemp, J.S. Bedingfield, and P.J. Roberts. 1996. The effects of (RS)-alpha-cyclopropyl-4-phosphonophenylglycine ((RS)-CPPG), a potent and selective metabotropic glutamate receptor antagonist. *Brit J Pharmacol* 119:851-854.

Tones, M.A., H. Bendali, P.J. Flor, T. Knopfel, and R. Kuhn. 1995. The agonist selectivity of a class III metabotropic glutamate receptor, human mGluR4a, is determined by the N-terminal extracellular domain. *Neuroreport* 7:117-120.

Traynelis, S.F., L.P. Wollmuth, C.J. McBain, F.S. Menniti, K.M. Vance, K.K. Ogden, K.B. Hansen, H. Yuan, S.J. Myers, and R. Dingledine. 2010. Glutamate receptor ion channels: structure, regulation, and function. *Pharmacological reviews* 62:405-496.

Tsuchiya, D., N. Kunishima, N. Kamiya, H. Jingami, and K. Morikawa. 2002. Structural views of the ligand-binding cores of a metabotropic glutamate receptor complexed with an antagonist and both glutamate and Gd3+. *Proceedings of the National Academy of Sciences of the United States of America* 99:2660-2665.

Tu, J.C., B. Xiao, S. Naisbitt, J.P. Yuan, R.S. Petralia, P. Brakeman, A. Doan, V.K. Aakalu, A.A. Lanahan, M. Sheng, and P.F. Worley. 1999. Coupling of mGluR/Homer and PSD-95 complexes by the shank family of postsynaptic density proteins. *Neuron* 23:583-592.

Turk, E., D.B. Teplow, L.E. Hood, and S.B. Prusiner. 1988. Purification and properties of the cellular and scrapie hamster prion proteins. *Eur J Biochem* 176:21-30.

Tzu, J., and M.P. Marinkovich. 2008. Bridging structure with function: structural, regulatory, and developmental role of laminins. *Int J Biochem Cell Biol* 40:199-214.

Um, J.W., A.C. Kaufman, M. Kostylev, J.K. Heiss, M. Stagi, H. Takahashi, M.E. Kerrisk, A. Vortmeyer, T. Wisniewski, A.J. Koleske, E.C. Gunther, H.B. Nygaard, and S.M. Strittmatter. 2013. Metabotropic glutamate receptor 5 is a coreceptor for Alzheimer abeta oligomer bound to cellular prion protein. *Neuron* 79:887-902.

Um, J.W., and S.M. Strittmatter. 2013. Amyloid-beta induced signaling by cellular prion protein and Fyn kinase in Alzheimer disease. *Prion* 7:37-41.

Valenti, O., P.J. Conn, and M.J. Marino. 2002. Distinct physiological roles of the Gq-coupled metabotropic glutamate receptors Co-expressed in the same neuronal populations. *Journal of cellular physiology* 191:125-137.

Vassallo, N., and J. Herms. 2003. Cellular prion protein function in copper homeostasis and redox signalling at the synapse. *J Neurochem* 86:538-544.

Viles, J.H., F.E. Cohen, S.B. Prusiner, D.B. Goodin, P.E. Wright, and H.J. Dyson. 1999. Copper binding to the prion protein: structural implications of four identical cooperative binding sites. *Proc Natl Acad Sci U S A* 96:2042-2047.

Vincent, B., E. Paitel, P. Saftig, Y. Frobert, D. Hartmann, B. De Strooper, J. Grassi, E. Lopez-Perez, and F. Checler. 2001. The disintegrins ADAM10 and TACE contribute to the constitutive and phorbol ester-regulated normal cleavage of the cellular prion protein. *J Biol Chem* 276:37743-37746.

Vinson, P.N., and P.J. Conn. 2012. Metabotropic glutamate receptors as therapeutic targets for schizophrenia. *Neuropharmacology* 62:1461-1472.

Waggoner, D.J., T.B. Bartnikas, and J.D. Gitlin. 1999. The role of copper in neurodegenerative disease. *Neurobiology of disease* 6:221-230.

Waggoner, D.J., B. Drisaldi, T.B. Bartnikas, R.L. Casareno, J.R. Prohaska, J.D. Gitlin, and D.A. Harris. 2000. Brain copper content and cuproenzyme activity do not vary with prion protein expression level. *J Biol Chem* 275:7455-7458.

Walmsley, A.R., N.T. Watt, D.R. Taylor, W.S. Perera, and N.M. Hooper. 2009. alpha-cleavage of the prion protein occurs in a late compartment of the secretory pathway and is independent of lipid rafts. *Mol Cell Neurosci* 40:242-248.

Walz, R., O.B. Amaral, I.C. Rockenbach, R. Roesler, I. Izquierdo, E.A. Cavalheiro, V.R. Martins, and R.R. Brentani. 1999. Increased sensitivity to seizures in mice lacking cellular prion protein. *Epilepsia* 40:1679-1682.

Wang, F., X. Wang, C.G. Yuan, and J. Ma. 2010. Generating a prion with bacterially expressed recombinant prion protein. *Science* 327:1132-1135.

Wang, L., K. Sharma, H.X. Deng, T. Siddique, G. Grisotti, E. Liu, and R.P. Roos. 2008. Restricted expression of mutant SOD1 in spinal motor neurons and interneurons induces motor neuron pathology. *Neurobiol Dis* 29:400-408.

Warner, R.G., C. Hundt, S. Weiss, and J.E. Turnbull. 2002. Identification of the heparan sulfate binding sites in the cellular prion protein. *J Biol Chem* 277:18421-18430.

Watt, N.T., D.R. Taylor, A. Gillott, D.A. Thomas, W.S. Perera, and N.M. Hooper. 2005. Reactive oxygen species-mediated beta-cleavage of the prion protein in the cellular response to oxidative stress. *J Biol Chem* 280:35914-35921.

Weiler, I.J., S.A. Irwin, A.Y. Klintsova, C.M. Spencer, A.D. Brazelton, K. Miyashiro, T.A. Comery, B. Patel, J. Eberwine, and W.T. Greenough. 1997. Fragile X mental retardation protein is translated near synapses in response to neurotransmitter activation. *Proceedings of the National Academy of Sciences of the United States of America* 94:5395-5400.

Weissmann, C. 2005. Birth of a prion: spontaneous generation revisited. *Cell* 122:165-168.

Weissmann, C., and A. Aguzzi. 1999. Perspectives: neurobiology. PrP's double causes trouble. *Science* 286:914-915.

Weissmann, C., M. Fischer, A. Raeber, H. Bueler, A. Sailer, D. Shmerling, T. Rulicke, S. Brandner, and A. Aguzzi. 1996. The Use Of Transgenic Mice In the Investigation Of Transmissible Spongiform Encephalopathies. *International Journal of Experimental Pathology* 77:283-293.

Weissmann, C., M. Fischer, A. Raeber, H. Bueler, A. Sailer, D. Shmerling, T. Rulicke, S. Brandner, and A. Aguzzi. 1998. The use of transgenic mice in the investigation of transmissible spongiform encephalopathies. *Rev Sci Tech* 17:278-290.

Werner, C.G., T. Scartabelli, T. Pancani, E. Landucci, F. Moroni, and D.E. Pellegrini-Giampietro. 2007. Differential role of mGlu1 and mGlu5 receptors in rat hippocampal slice models of ischemic tolerance. *Eur J Neurosci* 25:3597-3604.

Whetsell, W.O., and N.A. Shapira. 1993. Biology of Disease - Neuroexcitation, Excitotoxicity and Human Neurological Disease. *Lab Invest* 68:372-387.

White, A.R., S.J. Collins, F. Maher, M.F. Jobling, L.R. Stewart, J.M. Thyer, K. Beyreuther, C.L. Masters, and R. Cappai. 1999. Prion protein-deficient neurons reveal lower glutathione reductase activity and increased susceptibility to hydrogen peroxide toxicity. *Am J Pathol* 155:1723-1730.

White, A.R., P. Enever, M. Tayebi, R. Mushens, J. Linehan, S. Brandner, D. Anstee, J. Collinge, and S. Hawke. 2003. Monoclonal antibodies inhibit prion replication and delay the development of prion disease. *Nature* 422:80-83.

Whittington, M.A., K.C. Sidle, I. Gowland, J. Meads, A.F. Hill, M.S. Palmer, J.G. Jefferys, and J. Collinge. 1995. Rescue of neurophysiological phenotype seen in PrP null mice by transgene encoding human prion protein [published erratum appears in Nat Genet 1995 Apr;9(4):451]. *Nat Genet* 9:197-201.

Willard, S.S., and S. Koochekpour. 2013. Glutamate, Glutamate Receptors, and Downstream Signaling Pathways. *Int J Biol Sci* 9:948-959.

Wille, H., M.D. Michelitsch, V. Guenebaut, S. Supattapone, A. Serban, F.E. Cohen, D.A. Agard, and S.B. Prusiner. 2002. Structural studies of the scrapie prion protein by electron crystallography. *Proc Natl Acad Sci U S A* 99:3563-3568.

Wisniewski, T., and A. Boutajangout. 2010. Immunotherapeutic approaches for Alzheimer's disease in transgenic mouse models. *Brain Struct Funct* 214:201-218.

Wisniewski, T., and F. Goni. 2015. Immunotherapeutic Approaches for Alzheimer's Disease. *Neuron* 85:1162-1176.

Wong, B.S., T. Liu, R. Li, T. Pan, R.B. Petersen, M.A. Smith, P. Gambetti, G. Perry, J.C. Manson, D.R. Brown, and M.S. Sy. 2001. Increased levels of oxidative stress markers detected in the brains of mice devoid of prion protein. *J Neurochem* 76:565-572.

Wong, K., Y. Qiu, W. Hyun, R. Nixon, J. VanCleff, J. Sanchez-Salazar, S.B. Prusiner, and S.J. DeArmond. 1996. Decreased receptor-mediated calcium response in prion-infected cells correlates with decreased membrane fluidity and IP3 release. *Neurology* 47:741-750.

Woods, N.K., and J. Padmanabhan. 2012. Neuronal Calcium Signaling and Alzheimer's Disease. *Adv Exp Med Biol* 740:1193-1217.

Wopfner, F., G. Weidenhofer, R. Schneider, A. von Brunn, S. Gilch, T.F. Schwarz, T. Werner, and H.M. Schatzl. 1999. Analysis of 27 mammalian and 9 avian PrPs reveals high conservation of flexible regions of the prion protein. *J Mol Biol* 289:1163-1178.

Xiao, B., J.C. Tu, R.S. Petralia, J.P. Yuan, A. Doan, C.D. Breder, A. Ruggiero, A.A. Lanahan, R.J. Wenthold, and P.F. Worley. 1998. Homer regulates the association of group 1 metabotropic glutamate receptors with multivalent complexes of homer-related, synaptic proteins. *Neuron* 21:707-716.

Xiao, M.Y., B. Gustafsson, and Y.P. Niu. 2006. Metabotropic glutamate receptors in the trafficking of ionotropic glutamate and GABA(A) receptors at central synapses. *Current neuropharmacology* 4:77-86.

Xu, W., T.P. Wong, N. Chery, T. Gaertner, Y.T. Wang, and M. Baudry. 2007. Calpain-mediated mGluR1alpha truncation: a key step in excitotoxicity. *Neuron* 53:399-412.

Yuan, J., and B.A. Yankner. 2000. Apoptosis in the nervous system. *Nature* 407:802-809.

Zahn, R., A.Z. Liu, T. Luhrs, R. Riek, C. von Schroetter, F.L. Garcia, M. Billeter, L. Calzolai, G. Wider, and K. Wuthrich. 2000. NMR solution structure of the human prion protein. *P Natl Acad Sci USA* 97:145-150.

Zanata, S.M., M.H. Lopes, A.F. Mercadante, G.N.M. Hajj, L.B. Chiarini, R. Nomizo, A.R.O. Freitas, A.L.B. Cabral, K.S. Lee, M.A. Juliano, E. de Oliveira, S.G. Jachieri, A. Burlingame, L. Huang, R. Linden, R.R. Brentani, and V.R. Martins. 2002. Stress-inducible protein 1 is a cell surface ligand for cellular prion that triggers neuroprotection. *Embo Journal* 21:3307-3316.

Zanusso, G., R.B. Petersen, T. Jin, Y. Jing, R. Kanoush, S. Ferrari, P. Gambetti, and N. Singh. 1999. Proteasomal degradation and N-terminal protease resistance of the codon 145 mutant prion protein. *J Biol Chem* 274:23396-23404.

Zhang, Z., Y. Zhang, F. Wang, X. Wang, Y. Xu, H. Yang, G. Yu, C. Yuan, and J. Ma. 2013. De novo generation of infectious prions with bacterially expressed recombinant prion protein. *Faseb J* 27:4768-4775.

Zhou, M., W. Xu, G. Liao, X. Bi, and M. Baudry. 2009. Neuroprotection against neonatal hypoxia/ischemia-induced cerebral cell death by prevention of calpain-mediated mGluR1alpha truncation. *Exp Neurol* 218:75-82.

Zundorf, G., and G. Reiser. 2011. Calcium Dysregulation and Homeostasis of Neural Calcium in the Molecular Mechanisms of Neurodegenerative Diseases Provide Multiple Targets for Neuroprotection. *Antioxid Redox Sign* 14:1275-1288.

APPENDICES

Synopsis of POM antibodies

	Domain*	Epitope*		Toxicity#	GD protection	Affinity (nM)		
		sequence	location			Holo-Ab	$F(ab)_1$	scFv
POM2	FT	GQPHGGG/SW	57-64, 64-72, 72-80, 80-88	-	+	<0.1*	2.5	20*
POM11	FT	GQPHGGSW	64-72, 72-80	-	+		-	-
POM12	FT	GQPHGGG/SW	57-64, 64-72, 72-80,80-88	-			-	-
POM3	HR	HNQWNK	95-100	+/-	+		-	-
POM1	GD	β1-α1 loop, α1 and α3	138-147; 204/208/212	+		0.58*	2.5	800
POM4	GD	β1 and α3	121-134 and 218-221	+			-	-
POM5	GD	β2-α2 loop, α2	168-174	-			16	-
POM6	GD	β1-α1 loop, α1 β2-α2 loop, α2	140/145; 158/177; 170/174	-			-	-
POM7	GD	β1-α1 loop, α1 β2-α2 loop, α2	140/145; 158/177; 170/174	-			-	-
POM8	GD	β1-α1 loop, α1 β2-α2 loop, α2	140/145; 170/174	+			-	-
POM9	GD	β1-α1 loop, α1 β2-α2 loop, α2	140/145; 170/174	+			-	-
POM10	GD	β1 and α3	121-134 and 218-221	+			-	
POM13	GD	α1		+/-			-	
POM15	GD	β1-α1 loop, α1	140/145	-			5	
POM17	GD	β1-α1 loop, α1	140/145	+			6.6	
POM19	GD	β1 and α3	121-134 and 218-221	+		0.87*	0.4	

[modified by (Sonati et al., 2013)]

Pharmacokinetic (PK) analysis of MPEP- treated mouse samples

Brain levels of CGP79775A/MPEP (Mouse PKPD MPEP)

brain	ng/g	pmol/g
LLOQ:	2.4	12.4
ULOQ:	7,500.0	38,819.9

Sample Number	Sample Identifier	Amount [ng/g]	Amount [pmol/g]	Remarks	Compound administered or analyzed	Vehicle	Dosage Form	Dose [mg/kg]	Administration Route	Administration frequency	Collection Time
11	H922_S011_brn_po_mm1_30_MPEP_0H	12.3	63.4		MPEP	Water	Pellets	30mg/kg	p.o.	continuous	Light (inactive) Phase
12	H922_S012_brn_po_mm2_30_MPEP_0H	4.3	22.4		MPEP	Water	Pellets	30mg/kg	p.o.	continuous	Light (inactive) Phase
13	H922_S013_brn_po_mm3_30_MPEP_0H	62.5	323.7		MPEP	Water	Pellets	30mg/kg	p.o.	continuous	Light (inactive) Phase
14	H922_S014_brn_po_mm4_30_MPEP_0H			BQL	MPEP	Water	Pellets	30mg/kg	p.o.	continuous	Light (inactive) Phase
15	H922_S015_brn_po_mm5_30_MPEP_0H	36.2	187.5		MPEP	Water	Pellets	30mg/kg	p.o.	continuous	Light (inactive) Phase
16	H922_S016_brn_po_mm6_30_MPEP_0H			BQL	MPEP	Water	Pellets	30mg/kg	p.o.	continuous	Light (inactive) Phase
17	H922_S017_brn_po_mm7_0_MPEP_0H			BQL	CONTROL	Water	Pellets	30mg/kg	p.o.	continuous	Light (inactive) Phase
18	H922_S018_brn_po_mm8_0_MPEP_0H			BQL	CONTROL	Water	Pellets	30mg/kg	p.o.	continuous	Light (inactive) Phase
19	H922_S019_brn_po_mm9_0_MPEP_0H			BQL	CONTROL	Water	Pellets	30mg/kg	p.o.	continuous	Light (inactive) Phase
20	H922_S020_brn_po_mm10_0_MPEP_0H			BQL	CONTROL	Water	Pellets	30mg/kg	p.o.	continuous	Light (inactive) Phase

Sample Number	Sample Identifier	Amount [ng/g]	Amount [pmol/g]	Remarks	Compound administered or analyzed	Vehicle	Dosage Form	Dose [mg/kg]	Administration Route	Administration frequency	Collection Time
31	H922_S031_brn_po_mm11_30_MPEP_0H	75.8	392.3		MPEP	Water	Pellets	30mg/kg	p.o.	continuous	Dark (active) Phase
32	H922_S032_brn_po_mm12_30_MPEP_0H	28.8	149.2		MPEP	Water	Pellets	30mg/kg	p.o.	continuous	Dark (active) Phase
33	H922_S033_brn_po_mm13_30_MPEP_0H	22.3	115.4		MPEP	Water	Pellets	30mg/kg	p.o.	continuous	Dark (active) Phase
34	H922_S034_brn_po_mm14_30_MPEP_0H	55.2	285.6		MPEP	Water	Pellets	30mg/kg	p.o.	continuous	Dark (active) Phase
35	H922_S035_brn_po_mm15_30_MPEP_0H	67.5	349.4		MPEP	Water	Pellets	30mg/kg	p.o.	continuous	Dark (active) Phase
36	H922_S036_brn_po_mm16_30_MPEP_0H	60.6	313.5		MPEP	Water	Pellets	30mg/kg	p.o.	continuous	Dark (active) Phase
37	H922_S037_brn_po_mm17_0_MPEP_0H			BQL	CONTROL	Water	Pellets	30mg/kg	p.o.	continuous	Dark (active) Phase
38	H922_S038_brn_po_mm18_0_MPEP_0H			BQL	CONTROL	Water	Pellets	30mg/kg	p.o.	continuous	Dark (active) Phase
39	H922_S039_brn_po_mm19_0_MPEP_0H			BQL	CONTROL	Water	Pellets	30mg/kg	p.o.	continuous	Dark (active) Phase
40	H922_S040_brn_po_mm20_0_MPEP_0H			BQL	CONTROL	Water	Pellets	30mg/kg	p.o.	continuous	Dark (active) Phase

Blood levels of CGP79775A/MPEP (Mouse PKPD MPEP)

blood	ng/mL	nM
LLOQ:	0.8	4.1
ULOQ:	2,500.0	12,940.0

Sample Number	Sample Identifier	Amount [ng/g]	Amount [pmol/g]	Remarks	Compound administered or analyzed	Vehicle	Dosage Form	Dose [mg/kg]	Administration Route	Administration frequency	Collection Time
1	H922_S001_bld_po_mm1_30_MPEP_0H	10.9	56.2		MPEP	Water	Pellets	30mg/kg	p.o.	continuous	Light (inactive) Phase
2	H922_S002_bld_po_mm2_30_MPEP_0H	4.5	23.2		MPEP	Water	Pellets	30mg/kg	p.o.	continuous	Light (inactive) Phase
3	H922_S003_bld_po_mm3_30_MPEP_0H	64.9	335.9		MPEP	Water	Pellets	30mg/kg	p.o.	continuous	Light (inactive) Phase
4	H922_S004_bld_po_mm4_30_MPEP_0H	1.9	9.6		MPEP	Water	Pellets	30mg/kg	p.o.	continuous	Light (inactive) Phase
5	H922_S005_bld_po_mm5_30_MPEP_0H	38.7	200.4		MPEP	Water	Pellets	30mg/kg	p.o.	continuous	Light (inactive) Phase
6	H922_S006_bld_po_mm6_30_MPEP_0H	0.9	4.7		MPEP	Water	Pellets	30mg/kg	p.o.	continuous	Light (inactive) Phase
7	H922_S007_bld_po_mm7_0_MPEP_0H			BQL	CONTROL	Water	Pellets	30mg/kg	p.o.	continuous	Light (inactive) Phase
8	H922_S008_bld_po_mm8_0_MPEP_0H			BQL	CONTROL	Water	Pellets	30mg/kg	p.o.	continuous	Light (inactive) Phase
9	H922_S009_bld_po_mm9_0_MPEP_0H			BQL	CONTROL	Water	Pellets	30mg/kg	p.o.	continuous	Light (inactive) Phase
10	H922_S010_bld_po_mm10_0_MPEP_0H			BQL	CONTROL	Water	Pellets	30mg/kg	p.o.	continuous	Light (inactive) Phase

Sample Number	Sample Identifier	Amount [ng/g]	Amount [pmol/g]	Remarks	Compound administered or analyzed	Vehicle	Dosage Form	Dose [mg/kg]	Administration Route	Administration frequency	Collection Time
21	H922_S021_bld_po_mm11_30_MPEP_0H	38.1	197.3		MPEP	Water	Pellets	30mg/kg	p.o.	continuous	Dark (active) Phase
22	H922_S022_bld_po_mm12_30_MPEP_0H	23.1	119.8		MPEP	Water	Pellets	30mg/kg	p.o.	continuous	Dark (active) Phase
23	H922_S023_bld_po_mm13_30_MPEP_0H	23.1	119.7		MPEP	Water	Pellets	30mg/kg	p.o.	continuous	Dark (active) Phase
24	H922_S024_bld_po_mm14_30_MPEP_0H	35.3	182.6		MPEP	Water	Pellets	30mg/kg	p.o.	continuous	Dark (active) Phase
25	H922_S025_bld_po_mm15_30_MPEP_0H	38.8	200.6		MPEP	Water	Pellets	30mg/kg	p.o.	continuous	Dark (active) Phase
26	H922_S026_bld_po_mm16_30_MPEP_0H	54.7	282.9		MPEP	Water	Pellets	30mg/kg	p.o.	continuous	Dark (active) Phase
27	H922_S027_bld_po_mm17_0_MPEP_0H			BQL	CONTROL	Water	Pellets	30mg/kg	p.o.	continuous	Dark (active) Phase
28	H922_S028_bld_po_mm18_0_MPEP_0H			BQL	CONTROL	Water	Pellets	30mg/kg	p.o.	continuous	Dark (active) Phase
29	H922_S029_bld_po_mm19_0_MPEP_0H			BQL	CONTROL	Water	Pellets	30mg/kg	p.o.	continuous	Dark (active) Phase
30	H922_S030_bld_po_mm20_0_MPEP_0H			BQL	CONTROL	Water	Pellets	30mg/kg	p.o.	continuous	Dark (active) Phase

Single Nucleotype Polymprphism (SNP) Analysis of $Grm5^{+/+}$ (WT), $Grm5^{+/-}$ (HET) and $Grm5^{-/-}$ (KO) mice

	WT	HET	KO
SNP's	867.5	868.5	862
Total SNPs	877	877	872
% C57BL/6JBomTac	98.92%	99.03%	98.85%

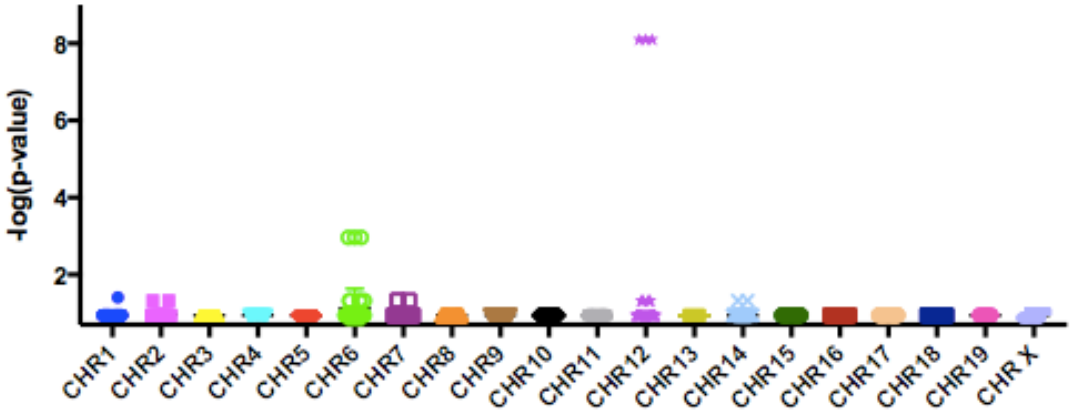

Curriculum Vitæ

Personal Data

Surname:	GONIOTAKI	**Nationality:**	Greek
First name:	DESPOINA	**Date of Birth:**	06/09/1987

Education

11/2011 - 10/ 2016	**University of Zurich**, CH, *Molecular Life Sciences Graduate Program (PhD candidate)*
10/2010 - 10/2011 *GPA: Merit*	**Imperial College London**, UK, *MRes in Experimental Neuroscience*
10/2005 - 11/2009 *GPA: 8.47/10*	**Democritus University of Thrace**, Gr, *Bachelor of Molecular Biology and Genetics (top of class)*
09/2002 - 09/2005 *GPA: 19.2/20*	**Zanneion Experimental Highschool of Piraeus**, Gr, *Highschool Diploma (Apolyterion)*

Scientific Experience

11/2011 – 10/2016	**PhD Project** "Inhibition of group I mGluRs is protective against prion-induced toxicity" , *Univeristy of Zurich*, CH, Thesis Supervisor: Prof. Dr Aguzzi Adriano
10/2010 - 10/2011	**MRes Rotation Projects,** Department of Medicine, *Imperial College London, UK* **1.** "The effect of neuroinflammation on the cholinergic signaling after renal transplantation", Thesis Supervisor: Dr. Ma Daqing **2.** "Cloning and production of a lentiviral vector encoding sequences that mediate chaperone-mediated autophagy and neuroprotection in models

of Huntington's disease", Thesis Supervisor: Prof. Mazarakis Nicholas

3. "Voxel-Lesion Symptom Mapping in Stroke: Attention and Global Recovery", Thesis Supervisor: Dr. Bentley Paul

09/2009 - 09/2010 **Internship** in "Molecular Neurobiology of Drosophila Melanogaster", Institute of Cellular and Developmental Biology, *BSRC 'Alexander Fleming', Athens,Gr*, Supervisor: Dr. Skoulakis Efthimios

01/2009 - 09/2009 **BSc Thesis** "Interaction of iron and ferritin with tau protein and its role in tauopathies in the model organism Drosophila Melanogaster", Institute of Molecular Biology and Genetics, *BSRC 'Alexander Fleming', Athens,Gr*, Thesis Supervisor: Dr. Skoulakis Efthimios

01/2008 - 07/2008 **Internship** in "Biochemical and Toxicological analysis of blood samples", Diagnostic Laboratory of Biochemistry and Pharmacology, *University Hospital, Alexandoupoli, Gr*, Supervisor: Dr. Manolopoulos Euaggelos

Publications

Peer-reviewed journal articles:

1. "*Inhibition of group I metabotropic glutamate receptors is protective against prion-induced toxicity*" (**Goniotaki *et al***, under review)
2. "*Triple dissociation of attention networks in stroke according to lesion location*" – Rinne P., Hassan M., **Goniotakis D.**, Chohan K., Sharma P., Langdon D., Soto D., Bentley P. Neurology. 2013; 81(9): 812-20. doi: 10.1212/WNL.0b013e3182a2ca34
3. "*Dose-dependent neuroprotection of $VEGF_{165}$ in Huntington's disease striatum*" – Ellison SM1, Trabalza A, Tisato V, Pazarentzos E, Lee S, Papadaki V, **Goniotaki D**, Morgan S, Mirzaei N, Mazarakis ND. Mol Ther. 2013; 21(10): 1862-75. doi: 10.1038/mt.2013.132.

Poster presentations: Ten (10) Poster Presentations – information available upon request

Oral Presentations:

1. **15th Day of Clinical Day:** "Inhibition of group I metabotropic glutamate receptors protects against prion-induced toxicity", *University Hospital Zurich, 03/2016*

2. **Departmental Talk, Title:** "Assessing the role of metabotropic glutamate receptor 5 in prion toxicity", *University Hospital Zurich, 11/2014*
3. **NEURINOX Summer School, Title:** "Role of metabotropic glutamate receptor 5 (mGluR5) in prion-induced toxicity", *BRFAA, Athens, Greece, 09/2014*

Honours & Awards

2012 - present	**Stiftung Neuropath Fellowship** (PhD grant, living costs & bench fees)
2010 - 2011	***Tuition fees scholarship***, Bodossakis foundation, "MRes in Experimental Neuroscience course, Imperial College London
2006 - 2007	***Performance excellence scholarship*** from the National Scholarship Foundation (IKY)
2005 - 2006	***Performance excellence scholarship & prize*** from the National Scholarship Foundation (IKY)